Characterisation of regulatory T cells during acute Friend retrovirus infection of mice.

Inaugural Dissertation

for

the Doctoral Degree of

Dr. rer. nat.

from the Faculty of Biology

University of Duisburg-Essen,

Germany

Submitted by

Jara Johanna Joedicke

from Dieburg, Germany

February 2014

Die der vorliegenden Arbeit zugrunde liegenden Experimente wurden am Institut für Virologie der Universität Duisburg-Essen durchgeführt.

1. Gutachter: Prof. Dr. rer. nat. Ulf Dittmer

2. Gutachter: Prof. Dr. med. Karl Lang

Vorsitzender des Prüfungsausschusses: Prof‘in. Dr. rer. nat. Astrid Westendorf

Tag der mündlichen Prüfung: 12.05.2014

Content

1. Introduction

The field of immunology deals with the study of the host organisms defence against invading pathogens or pathologic processes. There are various pathogens, like bacteria, viruses, fungi and small eukaryotic organisms, which can cause disease in all kinds of life. In contrast to these external infections, disease can also be caused by internal mechanisms (cancer and autoimmunity). The immune system seeks to provide protection against all kinds of disease development. Whereas invertebrates only possess an innate immune system, vertebrates have developed an additional system, the adaptive immune system, which can confer specific immunity against a pathogen and immunological memory for any subsequent encounters. (93, 211, 218)

1.1 The innate immune system

The innate immune system is the less specific component of the immune system and becomes immediately activated after invasion of an organism with a pathogen. The mechanisms of innate immune system action are not specific to a certain pathogen but recognise distinct molecular structures, called pathogen associated molecular patterns (PAMPs), and can therefore provide the first line of defence during formation of the adaptive immune response. The parts of the innate immune system are of varying natures including: molecular (antimicrobial compounds), cellular (macrophages and neutrophils) and more complex (skin). The innate immune system can be further subdivided into four types of defence: anatomical barriers, physiological barriers, phagocytosis and inflammation. (112)

PAMPs are recognised by pattern recognition receptors (PRRs) and these molecules can either be soluble or cell-associated. Examples of PRRs are the macrophage mannose receptor, complement, toll-like-receptors (TLRs) nucleotide-binding oligomerisation domain receptors, cytoplasmatic RNA sensors like RIG-I and MDA-5 (recognises dsRNA) and cytosolic DNA sensors like cGAS (recognises dsDNA) (288). These receptors trigger various responses, like phagocytosis, chemotaxis, up-regulation of co-stimulatory molecules or secretion of cytokines (112, 211).

One such group of cytokines are interferons (IFN), which can be induced as a result of PRR stimulation by its ligand resulting from different infections. Type I interferons

(IFNα and IFNβ) are important players in the immediate anti-viral response. Almost all cells express the interferon receptor. Upon binding of its ligand an anti-viral state is induced, which is characterised by the expression of hundreds of interferon-stimulated genes that are able to reduce viral replication and modulate immune cell responses. (211, 217)

Natural killer (NK) cells belong to the innate immune system, as they are able to respond to pathogens immediately in a non-specific manner. Once activated, they kill virus-infected or tumour cells by the release of cytotoxic granules, containing granzymes (Gzm) and perforin. This leads to the induction of apoptosis in the target cells. NK cells also express ligands for death receptors like TRAIL (tumour-necrosis-factor-related-apoptosis-inducing ligand) or FasL, which kill cells through binding their receptors on the target cells. (211, 217)

A further feature of the innate immune response is the mechanism of phagocytosis. This is carried out by specialised immune cells; macrophages/monocytes, dendritic cells (DCs) and granulocytes (especially neutrophils); which can engulf and destroy pathogens in phagosomes. Monocytes (in the blood) or macrophages (in tissues) are long-lived phagocytic cells which help to induce immune responses by secreting signalling proteins like cytokines and chemokines to attract other immune cells. In this capacity, activated macrophages initiate the process of inflammation. Additionally, DCs can take up large amounts of extracellular fluid and its content (macropinocytosis). Their main function is the recognition and degradation of invading pathogens. Resulting from this, DCs present antigens within the major histocompatibility complex (MHC) molecules on their surface to naïve T lymphocytes. The first encounter happens in peripheral lymphoid organs to initiate the adaptive immune response. DCs are also able to produce cytokines that influence the innate and adaptive immunity. The mechanism of antigen presentation provides the crucial connection between innate and adaptive immunity and is essential to initiate an effective immune response against a pathogen. (112, 211)

1.2 The adaptive immune system

While the innate immune response is activated within hours, it takes days to weeks for the adaptive immune system to develop its protective effects. Adaptive immunity is different to innate immunity in the way that it is pathogen specific, it takes time to

develop and a memory response can be launched at second encounter with an antigen. The adaptive immune system can be divided into the cellular (T and B cells) and humoral (antibodies) components.

Recognition of invading pathogens by DCs leads to their activation, causing the up-regulation of MHC class I and class II, as well as co-stimulatory molecules to initiate an effective T cell response. After migration to lymphoid organs, DCs present non-self-peptides bound to MHC molecules on their surface to naïve $CD4^+$ and $CD8^+$ T cells. $CD4^+$ T cells only interact with peptide bound to MHC class II and $CD8^+$ T cell only recognise peptides bound to MHC class I. Whereas almost all nucleated body cells express MHC class I, MHC class II is only present on professional antigen presenting cells (APCs), like DCs. There are two different pathways that lead to the presentation of a peptide on an MHC molecule. Peptides presented on MHC class I molecules are of cytosolic or endoplasmatic reticulum (ER) origin, whereas peptides presented on MHC class II molecules are derived from endosomes. All peptides are usually of pathogenic origin and the result from different routes of infection or pathogen encounter. (211)

For MHC class I loading endogenous antigens are generated. These are derived from misfolded proteins of cellular or pathogenic origin, or proteins produced within an infected cell. These proteins are cleaved into smaller peptides by the proteasome. The unloaded MHC class I molecule is initially located in the luminal side of the ER membrane. Therefore, peptides must be transported into the ER lumen via the transporter associated with antigen processing (TAP). TAP has the highest affinity for peptides with a length of 8 to 10 amino acids and with hydrophobic and basic carboxy-terminal amino acids, which present the optimal size and anchor charge for MHC class I binding. The process of MHC class I:peptide-complex assembly is highly chaperone guided. The fully assembled complex is then transported to the surface of the cell via the Golgi apparatus, where it can be recognised by specific $CD8^+$ T cells. (79, 112)

MHC class II loading occurs in a different process with peptides derived from exogenous antigens captured through phagocytosis or endocytosis. The internalised antigens become degraded in increasingly acidified compartments (early endosome – endolysosome – lysosome) containing hydrolytic enzymes. In this process oligopeptides with a length of 13 to 18 amino acids are produced, which are able to

bind to the peptide binding groove of the MHC class II complex. The assembly of the two chains of the MHC class II complex takes place in the ER, where an invariant chain blocks the peptide binding groove from binding endogenous peptides and stabilises the complex. After passing through the Golgi apparatus, the MHC class II:invariant chain-complex is included in the endosomal-lysomsomal pathway. The invariant chain is degraded, leaving only a small fragment blocking the peptide binding groove (CLIP, class II-associated invariant chain peptide). In a chaperon-mediated pathway, the CLIP is released and replaced by a peptide produced from the endosomal-lysosomal pathway. The MHC class II:peptide-complex is then presented on the surface of APCs, where it can be recognised by specific $CD4^+$ T cells. (79, 112)

B cells are APCs and thereby able to activate naive $CD4^+$ T cells. Their principle role is in the production of antibodies, as part of the humoral immune response to pathogens. B cells mature into antibody-producing plasma cells and memory B cells in an antigen-driven way. B cells can be activated in two different ways: by thymus-independent antigens and thymus-dependent antigens, which is mediated with the help of $CD4^+$ T cells. In response to stimulation, B cells produce antibodies and this process can be divided into primary and secondary responses. In the primary response, naïve B cells become activated to produce antibodies, whereas in the secondary response, plasma cells are activated to produce more specific antibodies of different classes. These antibodies from the secondary response are more specific because the B cells have undergone clonal selection, expansion and differentiation in germinal centres. Antibody production is important for specific pathogen recognition and elimination (complement activation, opsonisation and neutralisation of pathogens and phagocytosis of pathogens). (112)

1.2.1 Effector T cells

T cells are generated in the bone marrow. They mature in the thymus, where they are subject to positive and negative selection. The process of positive selection sorts for T cells that are able to recognise self-MHC molecules (self-restriction), whereas negative selection only protects T cells not recognising self-MHC:self-peptide-complexes (self-tolerance). These two processes provide a T cell repertoire capable of binding to self-MHC in combination with foreign antigens to mount a strong and

specific immune response upon encountering a pathogen. After thymic maturation, T cells leave the thymus as naïve $CD4^+$ or $CD8^+$ T cells. (112)

1.2.1.1 The activation of T cells

T cells become stimulated via the interaction of their T cell receptor (TCR)/CD3-complex binding to their specific antigen presented in the context of a self-MHC molecule, either MHC class I or MHC class II, which are also bound by the co-receptor CD8 or CD4, respectively, presented on the T cell (signal 1). This results in multiple intracellular signalling events leading to T cell activation, proliferation and differentiation into effector or memory cells. Moreover, the expression of various co-stimulatory molecules is also required (signal 2). This second signal is primarily provided by CD28 on T cells and molecules of the B7 family (B7-1 (CD80) and B7-2 (CD86)) on APCs. There are also inhibitory molecules, which can inhibit T cell activation. If the second signal does not follow the initial activation, anergy occurs, leading to unresponsive T cells. In addition to these signals, the T cell response is also shaped by various cytokines secreted by APCs, T cells and other activated cells (signal 3).

Activated T cells carry out different effector functions. Naïve $CD8^+$ T cells develop into cytotoxic $CD8^+$ T cells (CTLs) and naïve $CD4^+$ T cells differentiate into different helper T cell populations (Th), dependent on the cytokine milieu provided. Whereas CTLs primarily kill infected cells, Th cell populations are important for the recruitment and activation of other cells mediated through cytokine release, and providing assistance to B cells and $CD8^+$ T cells. However, under special conditions, Th cells are also able to kill infected or pathogenic (tumour) cells. The effector phase is followed by a down-phase in which most antigen-specific T cells are eliminated in a process called activation-induced cell death (AICD), leaving a smaller pool of memory T cells. (112, 211)

1.2.1.2 Common markers used for $CD4^+$ and $CD8^+$ T cell characterisation

Activation and homing markers

A whole host of molecules have been described as markers for T cell activation and homing. The markers mentioned in this section have been highlighted due to their widespread use and the fact that they have been utilised in this thesis. CD69, or very early activation antigen, is expressed on various leukocytes. Due to the activation of

T, B and NK cells, CD69 is up-regulated on the surface, which suggests a role in lymphocyte activation (335). CD43 (leukosialin or sialophorin) is expressed on peripheral T cells, thymocytes and early hematopoietic precursors in the bone marrow. It exists as different isoforms due to *O*-linked glycosylation and this is an effect of T cell activation. CD43 is involved in T cell mediated responses, co-stimulation, enhanced cytotoxicity of $CD8^+$ T cells and leukocyte adhesion (16, 276). CD11a, or integrin alpha L, is expressed on leukocytes and is an important adhesion molecule involved in T cell function and co-stimulation, which becomes up-regulated upon T cell stimulation (258). CD44 functions as an adhesion molecule and is involved in T cell activation. It is expressed on various hematopoietic and non-hematopoietic cells and peripheral B and T cells can up-regulate CD44 upon antigen encounter (191, 306).

CD62L is a member of the selectin family and is expressed on many different leukocytes. Its function is important for the rolling of lymphocytes on activated endothelium at the site of inflammation and homing to high endothelial venules of peripheral lymphoid tissues. Naïve and central memory T cells express CD62L, whereas its down-regulation indicates T cell activation (104). CD103 is the integrin alpha E and expressed on some DCs and a small subset of peripheral lymphocytes. CD103 is important for homing of T cells to the intestinal epithelium (176).

Co-stimulatory markers and inhibitory receptors

Co-stimulatory and inhibitory molecules are important for the activation of T cells through DCs. Many of these molecules have been identified and this section focuses on the ones that have been well characterised. The TCR-inducible co-stimulatory receptor (ICOS), homologous to CD28 and cytotoxic T lymphocyte antigen-4 (CTLA-4), interacts with its ligand on APCs thereby enhancing effector T cell responses (275). ICOS becomes up-regulated within 6 to 48 hours after stimulation on T cells and delivers a co-stimulatory signal to T cells. This enhances T cell dependent antibody production and cytokine secretion by $CD4^+$ T cells (49). The glucocorticoid-induced tumour necrosis factor receptor (TNFR) family related gene (GITR) is a co-stimulatory molecule expressed on T cells (250).

T cell immunoglobulin mucin 3 (TIM3) is usually expressed on Th1 and some $CD8^+$ T cells and acts as a negative regulator on these cells, inducing apoptosis. TIM3 is up-

regulated during a late stage of T cell differentiation and is expressed on dysfunctional or exhausted $CD8^+$ T cells (98, 220). Programmed cell death-1 (PD-1) is described to be a co-inhibitory receptor expressed on T cells and signalling through it attenuates TCR signalling and inhibits cytotoxic functions. Following TCR stimulation, PD-1 is expressed on T cells and binds members of the B7 family (PD-L1 (B7-H1) and PD-L2 (B7-DC)). Its ligand PD-L1 is up-regulated on hematopoietic and non-hematopoietic cells and its signalling down-regulates TCR signalling, inhibiting proliferation and cytokine secretion which promotes anergy and apoptosis, leading to immune suppression (99, 220). CTLA-4 is an inhibitory molecule and a homolog of the co-stimulatory molecule CD28. It has higher affinity than CD28 to the B7 family ligands CD80 and CD86. CTLA-4 becomes transiently up-regulated on T cells shortly after activation and interaction with its ligands prevents continuous T cell co-stimulation and activation (220). The lymphocyte-activation gene 3 (Lag3) is a CD4 homolog which binds MHC class II molecules with a higher affinity than CD4 (124). It is up-regulated on T cells after activation and negatively regulates T cell expansion and activation (127, 329).

Differentiation and proliferation markers

Different markers are described to indicate differentiation and proliferation of T cells and the most commonly used are described here. CD127 is the IL7 receptor α chain and is expressed at low levels on T cells in circulation. The down-regulation of CD127 indicates activation and differentiation of T cells, but also the transition to a memory T cell phenotype (284). The killer cell lectin-like receptor G1 (KLRG1) is expressed on some NK and T cells. KLRG1 has been described as a marker for terminally differentiated antigen-experienced T cells that lack proliferative capacity (311, 312).

Ki67 is a nuclear protein absent in resting cells (G0 phase) and present in the active stages of the cell cycle (G1, S, G2 and M phase) (109, 278). It can therefore be used to determine the proliferative potential of cell populations, although another technique to determine cell proliferation is to measure the incorporation of BrdU, a thymidine analogue, into the chromosomal DNA.

1.2.1.3 Mechanisms of $CD8^+$ T cell mediated killing

$CD8^+$ T cells are the main effector cells during the adaptive immune response to viral infections. $CD8^+$ T cells recognise virus-infected MHC class I presenting cells and

can kill them directly via a multitude of mechanisms involving Gzms, perforin and Fas-FasL interactions (Figure 1. 1). These cells are also able to secrete various cytokines, like IFNγ and tumour necrosis factor α (TNFα), and chemokines, like MIP-1α, MIP-1β (macrophage inflammatory protein) and RANTES (regulation on activation, normal T expressed and secreted). (211)

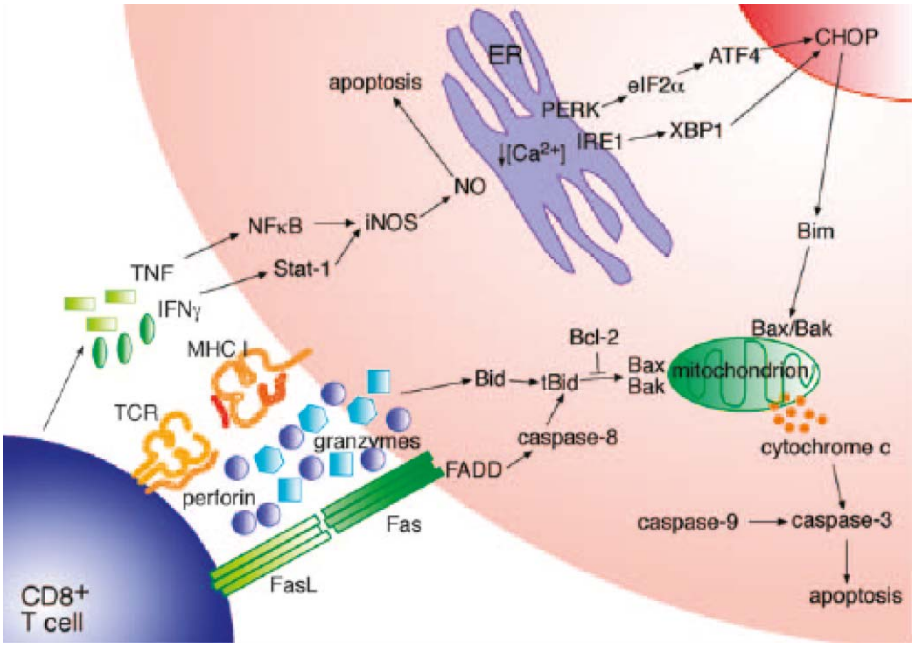

Figure 1. 1 **Pathways of CTL mediated killing of target cells.** The different mechanisms of CLTs – TNFα, IFNγ, granzyme/perforin and Fas-FasL – killing are displayed in this simplified schematic. (299)

Gzms are serine proteases that are stored in specialised lytic granules of CTLs and NK cells along with perforin. In mice, ten Gzms (A-G, M and gene duplications) and in humans five Gzms (A, B, H, K and M) have been described. When $CD8^+$ T cells become activated and recognise their antigen in an MHC class I context, these granules can be released and the Gzms can kill the target cell (Figure 1. 1). For the Gzms to enter the target cell, perforin pores are formed in the target cell membrane in a calcium dependent manner. It should be noted, however, that other attack mechanisms have been described (38, 209, 234). Upon entry into the target cell, Gzms induce proteolytic cleavage of caspases eventually leading to DNA fragmentation and cell apoptosis (232). In addition to activating caspases, Gzms can also activate caspase-independent mitochondrial collapse, resulting in the release of cytochrome c, a pro-apoptotic protein (21).

The Fas (CD95) – FasL (CD95L) pathway is another pathway through which CTLs can induce apoptosis in target cells (Figure 1. 1). Fas is a member of the TNFR family and contains an intracellular death domain to deliver an apoptotic signal upon FasL binding. Fas expression is induced by TNFα and IFNγ or the activation of lymphocytes and FasL is expressed after TCR engagement on $CD8^+$ T cells. The activation of the Fas – FasL pathway results in the activation of caspases causing apoptosis (168). The Fas – FasL pathway plays an important role in AICD to limit clonal T cell expansion after elimination of the antigen and to restrict auto-reactive T cells (318).

In addition to the above mechanisms, cytokines like IFNγ and TNFα are secreted by activated $CD8^+$ T cells. It should, however, be noted that these cytokines can be secreted by a variety of other immune cells as well (T cells, NK cells, APCs). IFNγ is the only member of the type II interferons and its functions have a wide range, including: leukocyte attraction, maturation and differentiation of many cell types, NK cell activity enhancing action and regulation of B cell functions and altering macrophage function during infections. IFNγ is also involved in the up-regulation of MHC class I and the immunoproteasome, therefore providing efficient recognition of virus-infected cells by CTLs. Furthermore, IFNγ also up-regulates factors involved in $CD4^+$ T cell recognition and induces further MHC class II expression on APCs and other cells. It also elicits direct antiviral effects by regulating antiviral proteins (induces an antiviral state) and has anti-proliferative and pro-apoptotic effects (free radical production and ER stress) (Figure 1. 1) (263, 299).

TNFα is a pleiotropic pro-inflammatory cytokine that exists as both a soluble (solTNFα) and a membrane-bound (mbTNFα) form, both of which are trimers. There are two receptors that bind TNFα: TNFRI and TNFRII. TNFRI is ubiquitously expressed at a low level on most cells and is associated with most TNFα-induced effects (37, 298). TNFRII is more restricted in its expression, and can mainly be found on cells of hematopoietic origin and endothelial cells (164, 187). TNFRI binds to both solTNFα and mbTNFα, whereas TNFRII only has high affinity for mbTNFα, which resulted from the observation that TNFRII can only be fully activated by mbTNFα (Figure 1. 2) (120, 121).

In contrast to TNFRI, which can mediate pro-apoptotic pathways (Figure 1. 1 and Figure 1. 2), TNFRII does not possess a death domain and mainly mediates anti-apoptotic pathways (313). mbTNFα is cleaved and released from the cell surface by the action of the metalloprotease TACE (TNFα convertase). The expression of TACE on hematopoietic cells is dependent on iRhom2, a rhomboid family member (5, 198, 273). TNFα was first described to exhibit anti-tumour activities and conferred resistance to certain infections, however TNFα has multiple functions (cell activation, proliferation, NK stimulation and cytokine production) and a variety of different signalling pathways are activated by its presence (211). The best described effect of TNFα is the induction of apoptosis upon binding to its receptor TNFRI (Figure 1. 1 and Figure 1. 2). TNFα induces a variety of responses like transcriptional activation, reactive oxygen or nitrogen radical production and activation of caspases via the intracellular death domain of TNFRI (142).

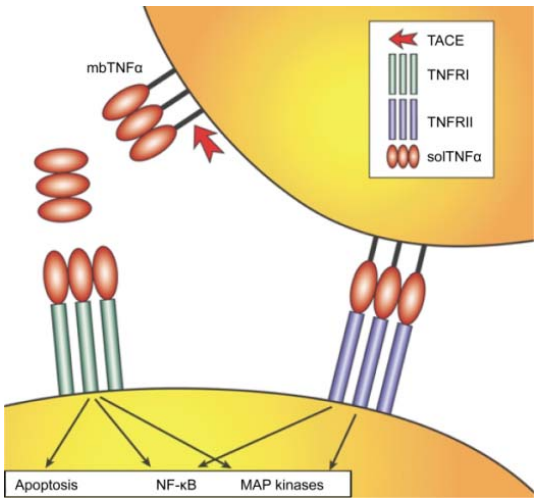

Figure 1. 2 **Interactions of TNFα with its receptors.** SolTNFα preferentially binds to TNFRI and TNFRII has the highest affinity for mbTNFα. Binding to the different receptors induces different pathways. NF- κB – nuclear factor κB. Adapted from (46).

A way to determine if cells recently de-granulated, is to analyse the surface expression of CD107a (lysosomal-associated membrane protein-1). CD107a is located on the surface of intracellular granules designated for exocytosis. Upon de-granulation of these intracellular bodies CD107a becomes exposed on the cell surface until it is recycled (26).

1.2.1.4 The different CD4$^+$ T cell subsets and their functions

Naïve CD4$^+$ T cells differentiate into various CD4$^+$ T helper subsets after activation and several rounds of division. The nature of the CD4$^+$ T cell response is dependent on the cytokine milieu, and differentiated CD4$^+$ T cell subsets have different functions and effector or helper mechanisms. The best described subsets are Th1 and Th2 cells, which are characterised by strong IFNγ or IL4 production, respectively. Whereas Th1 cells activate macrophages and drive inflammation, Th2 cells induce an effective humoral antibody-mediated immune response. In a viral infection, the Th cell response consists mainly of Th1 cells, where they are important for enhancing the CD8$^+$ T cell responses and memory cell development. Throughout the years different other Th subsets have been described, like T follicular helper cells (Tfh) (specialised B helper cells), Th17 (pro-inflammatory), Th9 (possibly involved in defence against parasitic helminth infections), Th22 (potentially involved in skin homeostasis and pathology), cytotoxic CD4$^+$ T cells (mediating direct killing) and induced regulatory T cells (iTreg) (immunosuppressive). Th cell subsets have a certain level of plasticity and can convert under special circumstances (change of cytokine milieu) into other Th subsets (150, 293). The different Th types are depicted in Figure 1. 3.

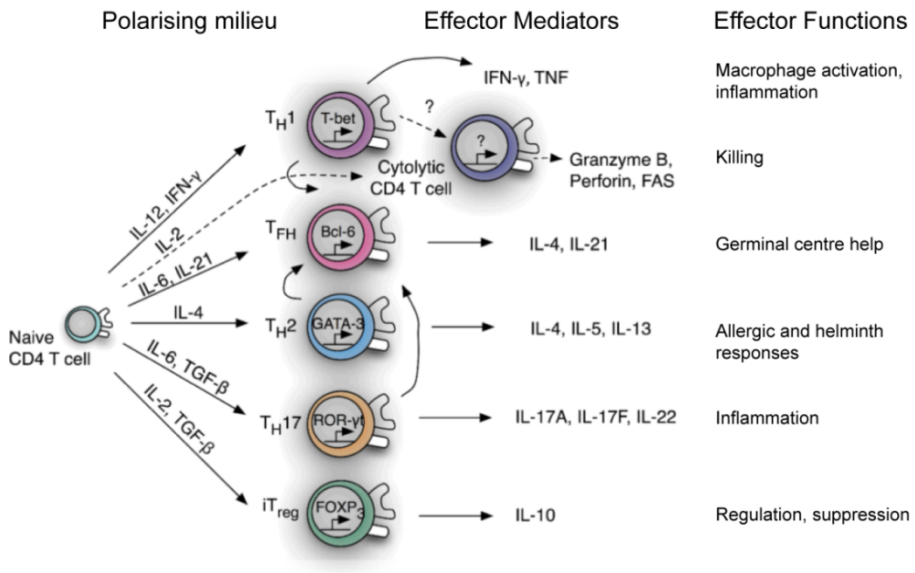

Figure 1. 3 **CD4$^+$ T cell subsets differentiating from naïve CD4$^+$ T cells.** Due to a different cytokine milieu (polarising milieu) in the periphery, naïve CD4$^+$ T cells differentiate into different T helper cell populations after activation. These Th cell populations secrete various molecules (effector mediators, mostly interleukins) thereby mediating specific effector functions dependent on infection or inflammation. The different transcription factors involved in Th cell differentiation are shown inside the cells. Adapted from (293).

1.2.2 Regulatory T cells

The concept of T cell-induced suppression of immune responses was first postulated in the early 1970s (110, 111, 196), but due to a lack of markers to identify a specific cell subset, the concept of suppressor T cells was dismissed in the 70's and 80's (134, 170, 279). However, in 1995 suppresser T cells were rediscovered and given a new name: regulatory T cells (Tregs). Sakaguchi *et al.* found that $CD4^+$ T cells, from which the $CD4^+CD25^+$ subset were removed, induced organ-specific autoimmunity after transfer into nude mice lacking endogenous T cells. These mice could be rescued by the transfer of additional $CD4^+CD25^+$ T cells in a dose-dependent manner. Furthermore, they could show that nude mice developed an immune response to allogenic skin transplants after the transfer of $CD4^+CD25^-$ T cells, whereas the reaction was quashed when additional $CD4^+CD25^+$ T cells were transferred (254).

Since then, the existence of Tregs has been widely accepted and studied in a variety of different models or disease. It is now established that Tregs constitute a major subset of immune suppressive T cells that mediate a balance between pro- and anti-inflammatory reactions (202). The function of Tregs is essential in the prevention of autoimmune diseases, maintaining peripheral tolerance and protection from immune response-mediated tissue damage during a variety of pathological situations (163, 202). In contrast to their beneficial role, Tregs can limit the immune responses during cancer or viral infections, preventing sterile immunity (202, 310, 317, 319).

CD25 expression has been found to be a hallmark of Tregs (254). CD25 represents the IL2 receptor α (IL2Rα) chain of the high affinity IL2-receptor. It is an important survival factor for Tregs and other T cells, but is not actually produced by Tregs (20, 96, 192, 261). The field of Treg biology made a great leap when the transcription factor forkhead box P3 (Foxp3) was discovered and determined to be the transcription factor regulating the development and the suppressive function of Tregs (95, 97, 136). For example, Foxp3 represses the expression of IL2 in Tregs and therefore renders them dependent on paracrine IL2 (108). Foxp3 was discovered by analysing the genetic defect of patients suffering from the X-linked diseases IPEX (immune dysregulation, polyendocrinopathy, enteropathy, X-linked syndrome) or XLAAD (X-linked autoimmunity-allergic dysregulation syndrome) or in scurfy mice,

displaying a similar phenotype of multiorgan autoimmune diseases (40, 52, 322). In mice, all T cells expressing Foxp3 are Tregs, whereas Foxp3 can also be a marker of activation in human T cells and is therefore not unique to Tregs (208, 249, 315). The use of CD25 and CD127 has been shown to be useful for the characterisation of human Tregs, as it was shown that there is a 90% correlation of $Foxp3^+$ expression with $CD4^+CD25^+CD127^{low}$ T cells (185, 264).

1.2.2.1 Treg subsets and their developmental origin

In the following section, the different Treg subsets will be described with a focus on $CD4^+$ Tregs. However, it should be noted that other regulatory cell populations do exist ($CD8^+$ Tregs, γδ $CD8^+$ T cells, NK and NKT cells, Bregs) (202). In general two subsets of $CD4^+$ Tregs exist, differing in their developmental origin, specificity, mechanisms and dependence on TCR and co-stimulatory signalling. These are classified as: natural Tregs (nTreg) or induced Tregs (iTreg) (Figure 1. 4).

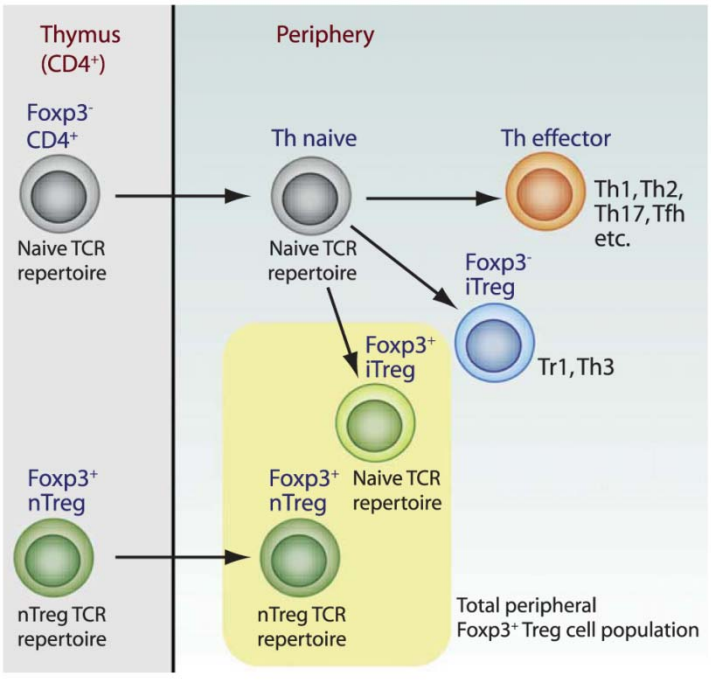

Figure 1. 4 **Developmental origin of the different Treg subsets.** $CD4^+$ T cells develop in the thymus and are present in the periphery as naïve $CD4^+$ T cells. With the appropriate cytokine and co-stimulatory milieu provided, these naïve $CD4^+$ T cells can then differentiate into various subsets of the T helper effector lineage (Th1, Th2, Th17, Tfh), into $Foxp3^-$ iTregs (Tr1 and Th3) and $Foxp3^+$ iTregs. nTregs develop in the thymus and leave into the periphery as pre-formed $Foxp3^+$ nTregs (76).

Natural Tregs

Natural Tregs are generated in the first few days of life in the thymus as $CD4^+$ T cells (254, 255) and undergo normal positive and negative selection before they are released into the periphery (Figure 1. 4). In the thymus, intermediate antigenic signals are required to generate nTregs (24, 332). In addition, co-stimulatory signals through CD28 might also be required for thymic selection of Tregs and peripheral maintenance (257). The absence of CD28 or CD80/CD86 has been shown to result in a substantial reduction of Tregs in lymphoid tissue or in the development of autoimmunity (178, 257). The antigen-specificity of these nTregs in not completely known, but it is presumed that they are a polyclonal population specific for multiple self-antigens of unknown nature (269). Furthermore, it has been shown that the TCR repertoire of Tregs has little overlap with the TCR repertoire of Tcon (92, 138, 229). nTregs survive in the periphery as a long-lived population and are important to maintain peripheral self-tolerance (30). Once exported into the periphery nTregs express high levels of CD25, CTLA-4, GITR and Foxp3 (257, 271). nTregs appear to conduct their suppressive mechanisms in a contact-dependent, cytokine-independent manner (30).

Since the discovery of nTregs, there has been a great search for nTreg specific markers. Two markers have gained importance in recent years for the characterisation of mouse nTregs, Helios and Neuropilin 1 (Nrp1). Helios belongs to the family of Ikaros transcription factors and is expressed during thymic development of T cells. It is up-regulated in Tregs but not in other T cell populations outside the thymus (17, 126). It has also been described as a marker able to distinguish nTregs from iTregs (286, 301). Recently it was shown that Helios can be induced in iTregs and has therefore been re-classed as an activation marker rather than a marker for nTregs (7, 117, 309). Nrp1, which was already described as a marker for Tregs (39), was shown to be able to distinguish between nTregs ($Nrp1^+$) and iTregs ($Nrp1^-$) (320, 331). However, the function of Nrp1 is not well understood, but it is thought to be involved in T cell activation and strengthens contacts between Tregs and APCs (39, 259).

Induced Tregs

Induced Tregs are generated from naïve $CD4^+$ T helper cells in the periphery. Both, effector and regulatory T cells can be generated from the same mature precursor,

leading to specificity for the same antigen (18, 149). It is thought that the development of iTregs depends on qualitative and/or quantitative differences in their antigen exposure (30). It was shown that some APCs are more efficient in inducing iTregs than others, for example skin langerin$^+$ DCs or pDCs at mucosal sites (141, 186). By *ex vivo* induction it was demonstrated that iTregs could be generated using antigen or polyclonal activators and immunosuppressive cytokines, like IL10 (18, 179). It has also been shown that the frequency of Foxp3$^+$ Tregs is higher at mucosal sites compared to other tissues (210, 287), which is probably due to peripheral induction of Tregs caused by the microbial environment (228, 281). For example bacteria of the genus of *Clostridium* or *Bacillus fragilis* were able to cause Foxp3 expression in Tcon (14).

Interestingly, iTregs can be induced by different routes of antigen administration, like intra-nasal or oral (59). Chen *et al.* showed that that oral tolerance was associated with the generation of transforming growth factor β (TGFβ) producing T cells in the gut. These were different from Th2 cells and were named Th3 cells (Figure 1. 4) (59). Groux *et al.* were able to show that repeated stimulation of T cells with their cognate antigen *in vitro* with high concentrations of IL10 present in the culture lead to the expansion of an iTreg population producing IL10. These Tr1 termed iTregs were able to suppress Th1 responses *in vitro* and *in vivo* (Figure 1. 4) (125, 197).

The induction of virus-specific iTregs has been observed in multiple viral infections of humans, with many of these being chronic infections. In hepatitis C virus (HCV) infection Tr1 cells and Th1 cells were induced against the same core protein epitope (189). Additionally, virus-specific Foxp3$^+$ Tregs were found in hepatitis C virus (HCV) infection (86) and similar findings were made for human immunodeficiency virus-1 (HIV-1) infection where Foxp3$^-$IL10$^+$ suppressive virus-specific Tregs were found (304). However, virus-specific iTregs can also be induced in acute viral infections that are cleared. An example for this is the induction of IL10 producing Tregs (Foxp3$^+$ and Foxp3$^-$) specific for matrix-1 of influenza A virus in individuals displaying influenza-specific immunity (233).

In general, iTregs vary in their expression of CD25 and Foxp3 (Figure 1. 4) (114, 332). Interestingly, unlike nTregs, iTregs seem to mainly use immunosuppressive cytokines, such as IL10 and TGFβ, for their suppressive mechanisms (15, 158, 216).

1.2.2.2 Mechanisms of Treg mediated suppression

Many different mechanisms of Treg mediated suppression have been observed in various *in vivo* and *in vitro* models, showing overlapping mechanisms for nTregs and iTregs (310). Many different targets of Treg mediated suppression, including T cells, B cells, NK cells, DC, macrophages and osteoclasts have been described. The suppression can result in loss of proliferation, diminished cytotoxic potential, decreased cytokine production or even cell death (270). In general, the suppressive mechanisms of Tregs can be classed into four different categories: action via inhibitory cytokines, cytolysis of adjacent cells, suppression via metabolic disruption and inhibition of DCs, which ultimately results in the suppression of T cells. These mechanisms can be either contact-dependent or -independent and directly or indirectly suppress the effector cells (Figure 1. 5).

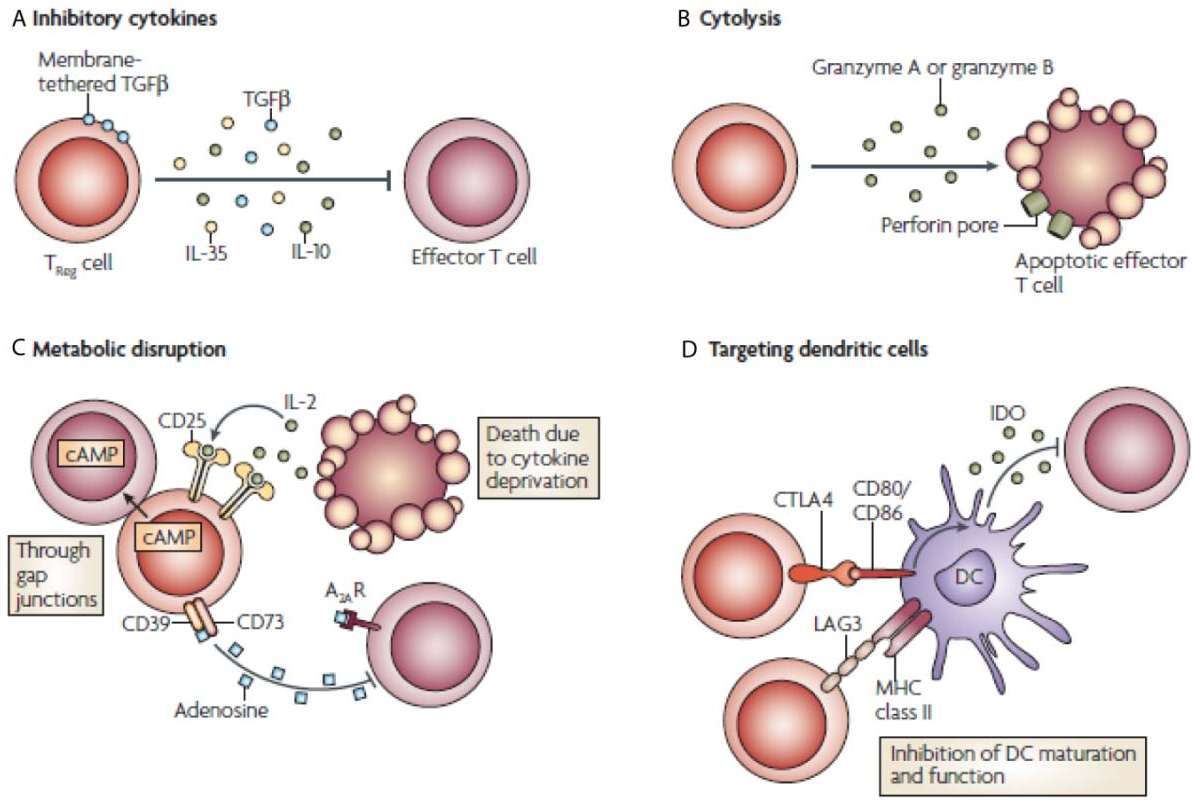

Figure 1. 5 **Supression mechanisms utilised by Tregs. (A)** With the secretion of inhibitory cytokines (TGFβ, IL35 or IL10) Tregs can inhibit effector T cell function. **(B)** The secretion of cytotoxic molecules (GzmA, GzmB and perforin) by Tregs can mediate the apoptosis of surrounding effector T cells. **(C)** Metabolic disruption of effector T cells resulting in inhibition or cell death can be achieved by multiple mechanisms carried out by Tregs, like IL2 consumption, production of adenosine with the help of CD39 and CD73 and cAMP transfer through gap junctions. **(D)** Tregs can also directly target DCs via different molecules (CTLA-4 or Lag3), which results in impaired DC maturation and function and therefore in suppression of effector T cell functions, for example via indolamine 2,3-dioxygenase (IDO). (310)

The search for Treg mechanisms has shown that Tregs are able to suppress via different immunosuppressive molecules (Figure 1. 5 A). In allergy and asthma models it was demonstrated that Tregs can mediate suppression, at least in part, via IL10 and TGFβ (11, 133). The role of soluble TGFβ is still critically discussed, however there have been reports showing that membrane-tethered TGFβ plays a crucial role and is important for cell contact dependent mechanisms of Treg mediated suppression (216, 310). Another inhibitory cytokine produced by Tregs is IL35, which has been described to be required for their suppressive activity (71). So far it remains to be determined in what way IL35 acts and which cells are generally affected.

It was long thought that cytolysis is only mediated by $CD8^+$ effector T cells and NK cells, but recently it has been shown that $CD4^+$ effector T cells and Tregs can also express Gzms (123, 182). A reduced suppressive activity was described for mouse Tregs in GzmB-deficient mice. This GzmB-mediated suppression appeared to be perforin-independent and resulted in the apoptosis of effector T cells (Figure 1. 5 B) (113). Strong evidence exists in tumour models for GzmB-mediated killing as an effector mechanism of Tregs towards NK and $CD8^+$ T cells (6, 47). Additional mechanisms of cell cytolysis by Tregs have been investigated and it has been suggested that Tregs can induce apoptosis in a TRAIL-DR5 (TRAIL – death receptor 5) dependent manner (242) or via galectin-1 (106).

The next mechanism by which Tregs are able to suppress effector cell responses is by metabolic disruption (Figure 1. 5 C). It has always been a matter of debate if the consumption of IL2 by Tregs, through high expression of CD25 on Tregs, and therefore deprivation of effector T cells of this important cytokine is a mechanism of Treg mediated suppression (310).

An interesting and newly described mechanism involving the two ecto-enzymes CD39 (ecto-nucleoside triphosphate diphosphohydrolase 1 or ATPase/ADPase) and CD73 (ecto-5'-nucleotidase) has been discovered for Tregs, which removes the pro-inflammatory signal ATP from extracellular spaces and generates anti-inflammatory adenosine (Figure 1. 5 C and Figure 1. 6) (241). Mouse Tregs show co-expression of both enzymes and CD39 is the rate-limiting enzyme in the cascade. It converts immune activating extracellular ATP or ADP into AMP, which can then be used by CD73 to generate adenosine. Adenosine is an immune suppressive molecule and

binds to the A2A receptor on effector T cells, which then become suppressed because of elevated intracellular production of cyclic AMP (cAMP) (34, 78, 162). Adenosine has also been shown to modulate DC maturation and thereby favour a tolerogenic phenotype (243). Adenosine has a very short half-life, which makes close proximity necessary for effective suppression through this pathway. Interestingly, it has also been shown that the transfer of cAMP from Tregs through gap junctions into effector cells or DCs can directly inhibit these cells (Figure 1. 5 C) (33).

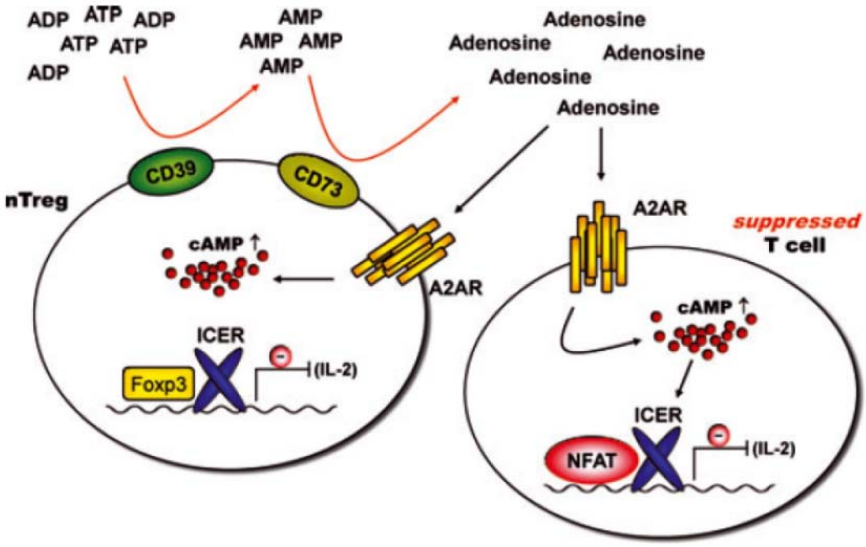

Figure 1. 6 **The CD39-CD73 cascade of adenosine generation and subsequent Tcon suppression.** Tregs are able to express both ectoenzymes, CD39 and CD73. CD39 first metabolises ATP or ADP to AMP and in a second process CD73 generates adenosine from AMP. This adenosine is then able to bind to the A2A receptor (A2AR) on effector cells, which leads to increased intracellular cAMP levels. This activates ICER (Inducible cAMP early repressor) and NFAT (nuclear factor of activated T cells) driven IL2-transcription is abolished, thereby suppressing T cells (31).

The last mechanism of Treg mediated suppression concerns the suppression by targeting DCs (Figure 1. 5 D). There have been reports showing that the expression of CTLA-4 on Tregs is important to inhibit DCs by interaction with CD80/CD86 on the DCs (226, 267). Tregs were also shown to induce the production of IDO by DCs resulting in suppression of effector T cells (91). Other studies have also shown that Tregs down-regulate the expression of co-stimulatory molecules on DCs rendering them less potent for the induction of effector T cell responses (51, 267). The CD4 homolog Lag3, expressed on Tregs, strongly binds to MHC class II molecules and has also been shown to block DC maturation (139).

In summary, there are many possible mechanisms of Treg mediated suppression, which have been observed in different settings for nTregs and iTregs. It appears that Treg-mediated suppression depends on the disease (autoimmunity, cancer, pathogen encounter) and the organ affected (or experimental system). The cytokine milieu and other environmental factors might play a role in shaping the suppressive repertoire of Tregs. It is possible that Tregs act via multiple mechanisms (153).

1.2.2.3 Regulatory T cells in viral infections

Tregs have two potential roles during infections. Beneficially, they can limit immune mediated tissue damage during infection, or detrimentally, they can lead to the suppression of beneficial immune responses and impair pathogen clearance, aiding in the establishment of a chronic infection. These effects critically depend on the ratio of effector to regulatory T cells and pathogen abundance (Figure 1. 7) (202). In the following section a few examples of how Tregs influence the immune response during infection will be given.

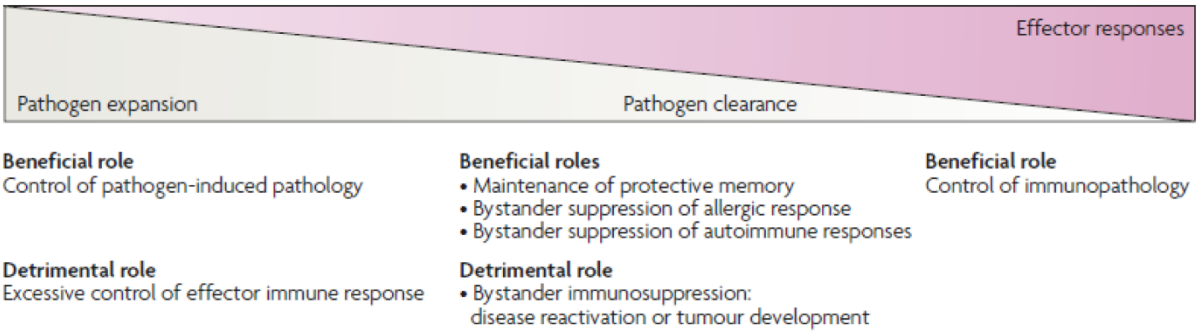

Figure 1. 7 **Positive and negative effects of Treg-mediated suppression during infection.** (23)

In HCV infection virus-specific Tr1 cells were induced (189) and also nTregs were expanded during chronic HCV-infection (45, 285). $CD4^+CD25^+$ Tregs isolated from HCV-infected patients showed suppression of HCV-specific $CD4^+$ and $CD8^+$ T cell responses *in vitro* (32, 45, 285). The induction of iTregs and activation of nTregs during HCV-infection is associated with viral persistence and chronic HCV infection

(285). However, it has been shown that HCV-infected patients with low amounts of $CD4^+CD25^+$ Tregs develop an autoimmune syndrome characterised by B cell proliferation and autoantibody production with higher incidence (35).

Decreased immunopathology due to Treg action could have important implications for protecting immune-privileged environments like the liver or the eyes. It has been shown that Tregs can suppress the $CD8^+$ T cell response directed against herpes simplex virus-1 (HSV-1) and the removal of $CD4^+CD25^+$ Tregs improves viral clearance after footpad infection of mice (291). If mice were depleted for Tregs before infection, the subsequent infection resulted in a strong Th1 response and severe eye lesions (290). For this reason Tregs are likely beneficial in limiting the migration of pathogenic $CD4^+$ T cells to sites of inflammation.

Lund *et al.* showed that Tregs increased in vaginally HSV-2-infected mice. However, when the Tregs were depleted, increased viral replication was observed at epithelial sites and the infection was able to rapidly spread to the central nervous system causing paralysis and death. This was contradictious at first, but they could show that Treg depletion resulted in increased effector T cells, cytokines and chemokines in the lymph nodes of these mice. However, because of the lack of Tregs, there was a reduction of DC, NK and T cell recruitment to the site of infection in the mucosa, and the virus could replicate more efficiently, causing the fatal disease (188). In conclusion, by suppressing the immune response in the initial infection, Tregs redirect immune cells to the site of infection and help promote an antiviral immune response where needed.

Similar results were obtained for the infection with respiratory syncytial virus (RSV). Fulton *et al.* demonstrated that $CD4^+Foxp3^+$ accumulate in the lung-draining mediastinal lymph nodes and the lung during acute RSV-infection. These Tregs showed an activated phenotype and Treg depletion resulted in delayed viral clearance, exacerbated disease severity and an early lack of $CD8^+$ T cell recruitment to the lung. However, an increase in virus-specific IFNγ and TNFα producing $CD8^+$ T cells was detected. This shows that Tregs play a critical role during acute pulmonary infections in limiting immunopathology (101).

1.3 Retroviruses

Members of the retrovirus family (**RE**verse **TR**anscripase **O**ncovirus) can be found in all vertebrates and are a large and diverse group of viruses. Retroviruses have a unique life cycle which accounts for their diverse biological activities. The discovery, structure and life cycle of retroviruses will be described here.

1.3.1 Discovery of Retroviruses

The first isolates of retroviruses, now collectively known as avian leucosis virus, were discovered by two investigators in 1909. Ellermann and Bang showed that chicken leucosis could be transmitted by a cell-free filterable agent. In 1911, Rous also discovered a filterable agent which was able to induce sarcoma in chickens (Rous sarcoma virus). Over the following decades, when cell culture techniques improved, further tumour-inducing viruses were discovered in mammalian species. In 1936, Bittner discovered the transmission of mammary carcinoma in mice through a filterable agent detected in milk (mouse mammary tumour virus (MMTV)). 1957. Gross found a leukaemia virus transmitted vertically in mice (murine leukaemia virus (MLV)). In the following years, more and more such tumour inducing agents were discovered and became important model systems for studying retroviruses. The hallmark of retroviruses, the reverse transcriptase (RT), an RNA-dependent DNA polymerase, was discovered by Baltimore in 1970.

The first human retrovirus to be discovered was human T-cell leukaemia virus in 1981. At the same time a mysterious epidemic disease of immunodeficiency (acquired immunodeficiency syndrome (AIDS)) arose in developed countries and soon after the discovery of HIV-1 was made. HIV-1 was later shown to be the causative agent of AIDS. (70)

1.3.2 Taxonomy of retroviruses

Viruses of the *Retroviridae* family can be subdivided into several genera. Alpha-, beta- and gamma- retroviruses are considered simple retroviruses, because they only encode the three core genes: *gag* (group-specific antigen), *pol* (polymerase) and *env* (envelope) (Figure 1. 8 A). In contrast to this delta- and epsilon-retroviruses as well as lenti- and spuma-viruses are considered complex retroviruses (Figure 1. 8 A).

Complex retroviruses encode additional gene products over the top of *gag*, *pol* and *env*. (161)

1.3.3 Genomic organisation and virion structure of retroviruses

The genome of retroviruses is a homodimer of linear, positive sense single-stranded RNA sequences (+ssRNA) with a size of 7 to 13 kilobases per molecule. The genome exhibits many features in common with mRNAs, like a 5' cap and a 3' polyA tail. All replication competent retroviruses contain three core genes which are arranged in the genome from 5' to 3': *gag*, *pol* and *env*. *Gag* encodes for the structural proteins: matrix (MA), capsid (CA) and nucleocapsid (NC). *Pol* encodes for the enzymes: protease (PR), reverse transcriptase (RT) and integrase (IN). The *env* gene encodes for the components of the envelope glycoprotein complex: surface glycoprotein (SU) and transmembrane (TM).

In addition to the coding sequences, the retroviral genome contains a number of sequence blocks with different functions clustered at the terminal ends of the RNA. At the 5' end these sequences are R (repeated region), U5 (unique 5') and pbs (primer binding site). The U5 contains an *att* site required for proviral integration. The pbs is important for hybridisation of the tRNA for initiation of minus-strand DNA synthesis. This is followed by the Psi (Ψ) element, containing signals for encapsidation. Closer to the 5' end of the genome, the ppt (polypurine tract, initiation of plus-strand DNA synthesis), U3 (unique 3', containing cis-acting elements for viral gene expression and an *att* site) and R sequences are located.

When the retroviral RNA genome is reverse transcribed the U3 and U5 regions are duplicated, resulting in a longer pre-integrative dsDNA compared to the RNA template. These extended sequence blocks consist of U3, R and U5 are called long terminal repeats (LTRs). The sequences for accessory and regulatory proteins, encoded by complex retroviruses, are situated in the *pol-env-U3* region (Figure 1. 8 A).

Mature virions (Figure 1. 8 B) are spherical with a rough diameter of 100-120 nm. All retroviruses are enveloped and contain a lipid bilayer membrane derived from the membrane of the producer cell, which contains the Env glycoprotein complex. The

MA protein is thought to be associated with the two envelope proteins. The viral capsid core is formed by CA and NC coating the viral RNA (Figure 1. 8 B). (50, 161)

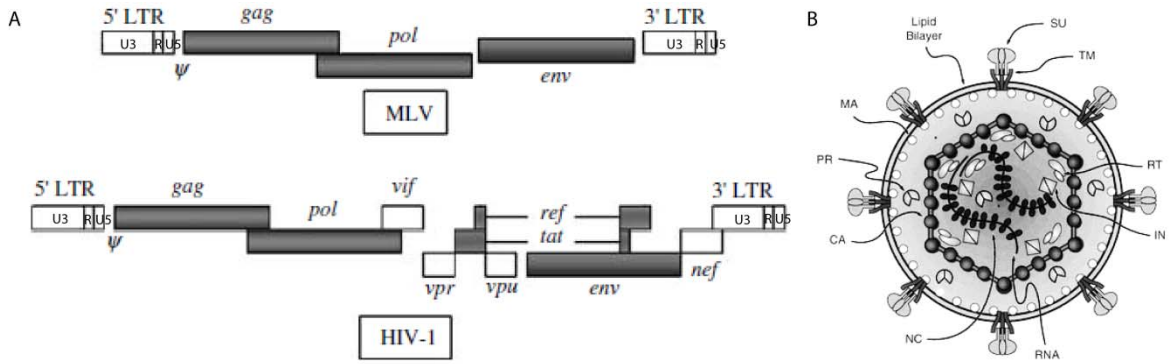

Figure 1. 8 **Genome organisation and structure of the retroviral particle. (A)** The proviral genome of a simple (MLV) and a complex (HIV-1) retrovirus is shown. *Vif, vpr, vpu, ref, tat* and *nef* indicate the regulatory and accessory proteins of HIV-1. Adapted from (36). **(B)** This schematic shows the principle organisation of a retroviral particle. A lipid bilayer in which the *env* products SU and TM are anchored surrounds the capsid core. The core is formed by CA and encloses the viral RNA dimer to which NC is bound (70).

1.3.4 The retroviral life cycle

The retroviral life cycle (Figure 1. 9) begins with the attachment of the mature virion to the target cell. Interaction between the Env glycoprotein complex and its specific receptor on the cell surface causes conformational changes in the TM protein, resulting in fusion of the viral membrane with the cellular membrane, releasing the viral capsid core into the cytoplasm. After its entry into the cytoplasm, the viral RNA is reversed transcribed within the reverse transcription complex (RTC). In the RTC, the viral enzyme RT converts the viral RNA into the dsDNA viral genome, flanked by the LTRs. After synthesis of the viral DNA the complex is often referred to as a pre-integration complex (PIC). Once the PIC has reached the nuclear periphery it must gain access to the host chromatin for integration to occur. Simple retroviruses require breakdown of the nuclear membranes to access the chromosomes, whereas complex retroviruses, like the lentiviruses, are able to access the nuclear compartment through an active mechanism. Once in the nucleus the viral dsDNA can be integrated into the host DNA with the help of the virally encoded IN enzyme. Integration into the genome is a significant feature of retrovirus biology as it leads to persistent viral infection despite host immune responses.

Once integrated, the viral genome is transcribed by the RNA polymerase II, where the LTRs serve as transcription initiation and termination sites. The full length transcribed viral RNA is exported into the cytoplasm using different transport mechanisms depending on the retrovirus in question. The viral RNA either serves as a template for translation of the Gag or Gag-Pol poly-proteins or as the genome for progeny virions. The Env proteins TM and SU are generated from a spliced mRNA by translation into the rER, glycosylation and transport through the Golgi where host proteases cleave Env into TM and SU, which remain in close proximity. They are then transported to the cell membrane.

After synthesis of the viral genome and proteins the viral particles assemble at the plasma membrane. It should be noted that not all retroviruses assemble at the plasma membrane and some assemble at cytoplasmic membranes. Gag and Gag-Pol proteins become anchored to the plasma membrane, which is stabilised by the interaction of the MA domain in Gag with the plasma membrane. The viral RNA is bound by the NC domain and becomes coated with many copies of Gag and a few Gag-Pol copies. The immature virion then buds from the cell membrane acquiring its virion membrane. The final stage of retrovirus generation is maturation. Maturation occurs when PR cleaves the Gag and Gag-Pol poly-proteins, resulting in a mass rearrangement within the core, which produces the infectious mature virus. (50)

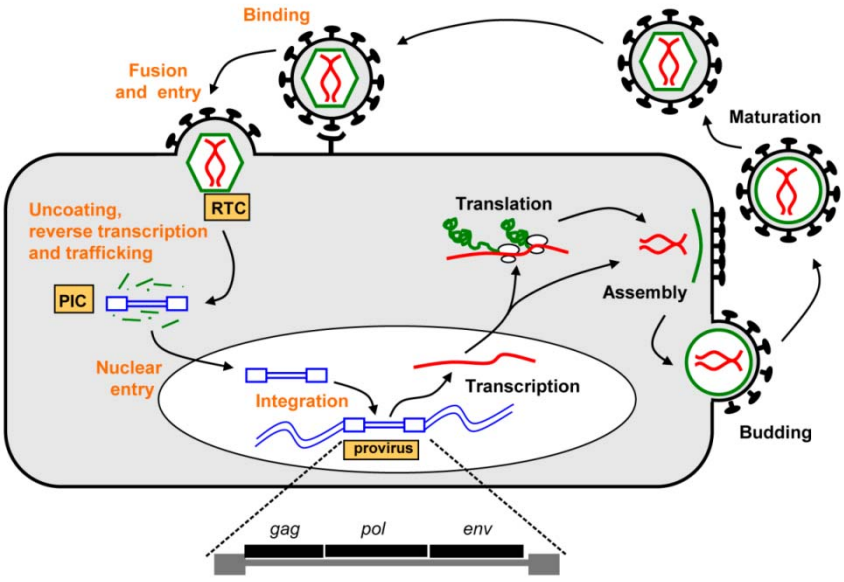

Figure 1. 9 **Retroviral life cycle.** Schematic showing the main steps in retroviral replication. The early stages of the retroviral life cycle are depicted in orange and the later stages in black. Picture kindly provided by D. J. Wight.

1.3.5 Endogenous Retroviruses

Endogenous retroviruses (ERV) are derived from retroviral infections of germ line cells. Typically, retroviral infection is not cytolytic and therefore a daughter cell can inherit the integrated provirus. ERVs are usually transmitted in a stabile Mendelian fashion and are replicated and transcribed as cellular genes. It is estimated that up to 30% of the sequence in mammalian genomes is of retroviral or transposable element origin (25). Endogenous retroviruses have colonised vertebrates at different times throughout history. The discovery that MLVs and endogenous MMTVs (*mtv*) are only present in some subspecies of mice indicates their origin from a recent integration event (167). In contrast, human endogenous retroviruses (HERVs) can be found at the same chromosomal location in baboons and humans, dating the origin at least 30 million years ago, when the divergence of these species occurred (115).

Even though ERVs have the same general structure as exogenous retroviruses they are often transcriptionally silenced, caused by heavy methylation and many alterations in their sequence, making them replication incompetent (25). Regardless of these silencing mechanisms, viral RNAs are often produced from the ERVs which can be packed efficiently by exogenous retroviruses. These ERV sequences can then alter the genome of exogenous viruses by the virtue of homologous recombination (161).

Interestingly, some ERVs may actually provide a selective advantage to the host, for example by inhibiting infection with pathogenic exogenous retroviruses (25). Examples for this are the mouse genes *Fv1* (derived from the Gag region of an ancient retrovirus) and *Fv4* (a gp70 molecule related to SU of ecotropic viruses), which protect the host from infection by exogenous Friend virus (FV). Another example is the superantigen (Sag) gene of *mtv*, which results in thymic deletion of T cells when present in the genome, and thereby protects from MMTV-induced disease (25, 161).

1.3.5.1 Endogenous retroviral superantigens

Sags are viral or bacterial proteins that can activate T cells by crosslinking a specific Vβ chain of the TCR with an MHC class II molecule. This causes “clonal” stimulation of T cells and thus T cell activation and proliferation. Sags of bacteria are secreted

upon infection as soluble proteins like the staphylococcal enterotoxins or toxic-shock-syndrome toxins (327). Some viruses also encode Sags in their genome and the most prominent example is the retrovirus MMTV. MMTV initially infects B and T cells and uses the Sag to stimulate proliferation, which increases the pool of cellular targets for MMTV. However, due to its nature as a retrovirus, MMTVs have become incorporated into the mouse genome as defective ERVs. The Sag is encoded in the 3' LTR region of the virus and is still present in the integrated endogenous virus. If expressed in the thymus, the Sag functions as a self-antigen and causes deletion of reactive T cells, resulting in the depletion of certain Vβ-bearing T cells dependent on the *mtv* incorporated into the mouse genome. Different mouse strains usually contain a limited number of *mtv* Sags, which possess different specificities for Vβ chains (2, 302, 325).

1.4 Human Immunodeficiency Virus-1

HIV-1 the causative agent of AIDS (acquired immunodeficiency syndrome) was discovered in 1983 (19, 105). It is a complex retrovirus (lentivirus) and possesses all components of a simple retrovirus with the addition of regulatory (Tat and Rev) and accessory (Nef, Vif, Vpr and Vpu) proteins. HIV-1 infects cells by binding of gp120 to CD4, present on $CD4^+$ T cells, macrophages and DCs as well as by interaction with a co-receptor. There are two co-receptors which can potentiate infection, CXCR4 and CCR5. Different strains of HIV-1 can utilise these two co-receptors to varying degrees which is a major determinant of viral tropism. HIV-1 infection causes a long lasting disease characterised by a long incubation period, which is usually asymptomatic, and eventual progression to AIDS, if untreated (69). The routes of transmission are either horizontally; by sexual contacts or contact to contaminated blood (blood transfusion, intravenous drug use); or vertically (mother to child) (146). (199).

The first antiretroviral drugs were developed in the nineties and given in single or dual combination. However, this could only control viral loads temporarily due to drug resistance by viral escape mutants. In the following years, the highly active antiretroviral therapy (HAART) a combination of three different antiretroviral drugs was developed. There are different antiretroviral drugs available targeting different

stages of the retroviral life cycle: reverse transcriptase inhibitors (nucleoside or non-nucleoside), protease inhibitors, entry blockers and integrase inhibitors. This combination therapy has been shown to be more efficient in suppressing viral loads and reducing the levels of drug resistant HIV-1 strains in infected individuals. Some retroviral drugs have severe side effects, but due to the development of new drugs and better treatment regimes, these side effects have been greatly reduced. This makes HIV-1 infection a chronic but treatable disease in the western world where the access to HAART is available. However, due to the high costs of HAART and insufficient education about HIV-1 infection routes, there is still a high incidence of HIV-1 infection and AIDS-induced death in developing countries, with millions of new infections every year. (70, 199)

1.4.1 Pathogenesis and role of the immune system

The HIV-1 infection can be classed into three phases: the acute infection (asymptomatic or flu-like symptoms), the chronic stage (first asymptomatic, then non-AIDS defining symptoms) and AIDS. The acute phase is characterised by the spread of the virus from the site of infection throughout the whole body, especially into the lymph nodes and other lymphoid organs. Massive virus production by gastro-intestinal associated lymphoid tissue (GALT) is often observed. In the first few weeks a rapid decline of $CD4^+$ T cells is observed, most pronounced in the GALT. When the adaptive cellular and antibody immune response starts the viral load drops immediately and reaches an equilibrium between viral replication and the suppressive immune response. However, due to limited capacity of $CD4^+$ T cell renewal, the $CD4^+$ T cell count declines gradually. This phase can last up to ten years, with no obvious symptoms. Eventually, the immune system becomes exhausted due to chronic immune activation, T cell depletion and degeneration of lymphoid organs. This results in opportunistic infections which cannot be controlled as they would in an immune-competent patient, resulting in severe diseases. Typical AIDS-related diseases are also various neoplasms (like Kaposi's sarcoma). (70, 199)

1.4.2 Regulatory T cells in HIV-1 infection

It has been described that Tregs expand during chronic HIV-1 infection in the lymph nodes, GALT and the blood (206). Two hypothesises have been postulated based on several findings: (i) Tregs have a detrimental role in HIV-1 infection by suppressing

anti-viral immune responses (1, 87, 222, 321) or (ii) Tregs have a beneficial role during infection by limiting the generalised immune activation thereby controlling the repertoire of HIV-1 target cells and limiting immunopathological effects (48, 177, 184, 207).

HIV-1 can infect DCs at low levels and alter their function and maturation, which could lead to the induction of Tregs by immature HIV-1-infected DCs (181). It has been shown that iTregs from HIV-1 infected patients were able to suppress $CD4^+$ and $CD8^+$ T cell responses. Additionally, nTregs have also been shown to be involved in HIV-1 infection, where it has been postulated that they have a beneficial role for the host, as infection-induced depletion of nTregs contributed to immune activation and higher viral loads resulting in disease progression (251). Despite some evidence for Treg involvement in HIV-1 infection, the actual role of Tregs in this infection remains controversial.

1.4.3 Approaches to study HIV-1

Humans and chimpanzees are hosts for HIV-1, and for this reason either *in vitro* studies with human blood or *in vivo* studies with chimpanzees can be done. Although chimpanzees are susceptible to HIV-1 infection, the replication is greatly inhibited and usually there is no progression to AIDS (223, 225). Simian immunodeficiency virus (SIV) is very similar to HIV-1 and has been used in its natural host (sooty mangabeys), although the infection does not induce immune activation and progression to an AIDS-like syndrome is rare. However, the infection of rhesus macaques with SIV results in a decline of $CD4^+$ T cells and the progression to AIDS (274). The downside of these *in vivo* models for HIV-1 infection is that they are very expensive with very low numbers of animals available due to ethical issues. Furthermore these animals are not inbred and thus there is a great level of genetic heterogeneity often making the results of such studies difficult to interpret.

1.4.3.1 *In vitro* mucosal infection with HIV-1

Certain steps of HIV-1 infection can be investigated *in vitro*. *In vivo* DCs can be infected with HIV-1 or unspecifically take up virus at the mucosal sites after initial encounter with the virus. The infected DCs are able to transmit HIV-1 to $CD4^+$ T cells via the immunological synapse formed between DCs and $CD4^+$ T cells. This mechanism is thought to have important implications for HIV pathogenesis (330).

With the help of *in vitro* co-culture between infected DCs and $CD4^+$ T cells, these mechanisms can be investigated.

1.4.3.2 Small animal models for retroviral infections

Studies in mice are easier to realise as large numbers of these animals with a highly controlled and homogenous genomic background are available. Additionally, the immune system of mice is very well known and different congenic, transgenic and knockout strains are breed. Compared to bigger animal models, mice are also cheaper. However, mice are not susceptible to HIV-1 infection but can be infected with mouse retroviruses such as the Friend retrovirus (FV).

An interesting prospect is the study of humanised mice that can be infected with HIV-1 due to their humanised immune system. The most successful approach in this regard is the BLT (bone marrow-liver-thymus) model. Immunodeficient mice receive a transplant of foetal human liver and thymus under the kidney capsule. This transplant forms an organoid, able to mature human T cells, provided by the additional transfer of human hematopoietic stem cells from the same donor. In these mice, a normal human T and B cell system develops, which can be used to study HIV-1 infections (80). Unfortunately the immune system of these mice does not function normally and is constitutively activated. In the worst form, these mice suffer from graft-versus-host disease (GVHD) which eventually leads to the rejection of the transplant. Recently, an interesting approach was carried out where an additional knockout of CD47 was included for the generation of BLT humanised mice. These C57BL/6 *Rag2*$^{-/-}$ $\gamma_c^{-/-}$ *CD47*$^{-/-}$ mice do not show any signs of GVHD and were shown to be efficiently infected with HIV-1 with the development of virus-specific T and B cell responses (174). The down-side of this model, however, is that it is relatively expensive and time consuming to generate and care for these mice.

FV induces an acute infection followed by a chronic phase in resistant C57BL/6 (B6) mice. This mouse system is not applicable to pathological studies of HIV-1 infection, although there is a high level of similarity in the T and B cell responses during HIV-1 and FV infection. This makes it possible to use FV as a tool to study the immunological effects of retroviral infections.

1.5 The Friend Virus model for retroviral infections

FV was originally discovered by Charlotte Friend in 1957 (100) and is an ecotropic gammaretrovirus complex composed of the pathogenic spleen focus forming virus (SFFU) and the apathogenic helper virus, the Friend murine leukaemia virus (F-MuLV). Both retroviruses have high sequence homology. Due to major deletions in the *env* gene of SFFV it is not able to produce its own particles, therefore F-MuLV is necessary for the replication and packaging of the SFFV genome into viral particles (67). FV infects cells presenting the cationic amino acid transporter mCAT-1 (ecotropic receptor), which is expressed on all mouse cells but hepatocytes (8, 190, 333). During the acute infection predominantly erythroid precursors are infected, however other dividing cells, including lymphocytes, can also be infected (85).

1.5.1 Pathogenesis of FV infection in mice

F-MuLV is apathogenic in adult mice but can cause splenomegaly, anaemia and erythroleukaemia in new born mice that have not yet developed an effective adaptive immune system (100). The FV complex is able to induce a severe splenomegaly and lethal erythroleukaemia associated with generalised immunosuppression in immunocompetent susceptible adult mice (67). The initial step of FV-induced disease is caused by a false proliferation signal transmitted to erythroid precursors by binding between the SFFV gp55 envelope glycoprotein and the erythropoietin receptor. This causes uncontrolled expansion of erythroid precursors leading to grossly enlarged spleens and provides a perfect target population for further infection.

The second step is the transformation phase where SFFV integrates eventually into specific target sites, usually the *spi-1* locus (SFFV proviral integration site-1; 95% of FV tumour cells), which is transformation-associated. This results in enhanced transcription factor PU.1 levels in erythroid cells and inhibits their commitment to differentiation (205). At a later time point, loss of p53 (tumour suppressor gene) function often occurs resulting in full cell transformation (67). The disease severity in resistant mice is minimal, as these mice are able to mount efficient immune responses and eliminate transformed cells. However, they are unable to completely clear the infection and remain chronically infected for life (205).

1.5.2 Immunity to FV infection

The development of the FV-induced disease is dependent on the initial dose of virus and the mouse strains' genetic background. Mice contain several host genes that are responsible for susceptibility to FV infection. These host genes comprise the Friend virus susceptibility factors *Fv* (1-6) (non-immunological) and at least four genes in the MHC (immunological), which influence cellular and antibody mediated immune responses to FV infection (62). There are several genes that interfere with the infection (*Fv1* and *Fv4*) and others that interfere with the immune response (*Rfv1-3*) or regulate erythroid cell proliferation and differentiation (*Fv2, Fv5*) (219). $Fv2^r$ prevents the polyclonal cell activation of erythroid progenitor cells thereby limiting splenomegaly, whereas $Fv2^s$ makes mice susceptible to FV-induced splenomegaly. The *Fv2* gene encodes for the tyrosine kinase Stk/RON, which in its short form (sf-Stk) accounts for the susceptible phenotype, whereas in resistant mice a longer form of Stk is present that cannot mediate the signalling from gp55 (205). The *H-2D* genes are important for effective presentation of viral T cell epitopes. For example mice bearing $H\text{-}2D^{b/b}$ have a high incidence of recovery from FV leukaemia due to efficient presentation of FV-epitopes. (62, 132).

1.5.3 Immune responses during FV infection

B6 mice (*H-2D*$^{b/b}$*, Fv-1*$^{b/b}$*, Fv-2*$^{r/r}$*, Rfv3*$^{r/r}$) are resistant to FV induced erythroleukaemia but develop a chronic infection, like other resistant mouse strains (61). All these mice carry different resistance genes which enable them to mount an efficient B and T cell response against the pathogen. However, when either $CD4^+$ or $CD8^+$ T cell populations are deleted during the acute infection, B6 mice are no longer able to control the virus and develop FV-induced disease (129, 245). It was also shown that B cells and virus-specific antibodies were important for recovery from FV-disease (130). FV titres peak rapidly in the acute infection (at day 7 in B6 mice) but drop soon after the initial peak when the adaptive immune response, including an effective CTL response and development of Th1 $CD4^+$ T cells, develops. This shows that an effective T cell response is important during acute FV infection.

The depletion of $CD4^+$ T during acute infection shows the importance of this T cell subset. $CD4^+$ T cells provide important help for B cells and the development of neutralising antibody responses is vitally important for the recovery from acute FV

infection (63, 130). Furthermore, $CD4^+$ T cells are important for efficient $CD8^+$ T cell responses during acute infection (215). It has been shown that $CD4^+$ T cells also mediate virus control during chronic FV infection., as when $CD4^+$ T cells were depleted in this phase viral replication increased dramatically and leukaemia was induced (131, 145). It has been shown that $CD4^+$ T cells can provide direct anti-viral immunity during chronic infection by secretion of IFNγ rather than offering help to effector B cells or $CD8^+$ T cell (145). In contrast, the depletion of $CD8^+$ T cells during this phase did not have an effect on virus infection or disease development, as $CD8^+$ T cells appeared to be dysfunctional during the chronic phase of infection (131).

Even though CTLs do not to play a major role in chronic infection, they are very important during acute FV infection, critical for recovery and at least partially dependent on $CD4^+$ T cells (83, 245). CTLs kill FV-infected cells with the help of GzmA and B and perforin (338). Furthermore, they secrete high amounts of IFNγ, which has direct anti-viral activities and further boosts the cellular immune response.

1.5.4 Regulatory T cells in FV infection

The initial clue showing that $CD8^+$ T cells were dysfunctional during chronic FV infection came from experiments in which a FV-induced tumour was transplanted into naïve and chronically infected mice. Naïve mice were able to mount an efficient immune response and reject the tumour, but chronically infected mice were not, despite the tumour expressing FV antigens (144). By transferring naïve $CD8^+$ T cells specific to the immunodominant CTL epitope into acute or chronically infected mice, it was found that $CD8^+$ T cells became dysfunctional during chronic infection, resulting in impaired production of GzmA and B, perforin, and IFNγ. This was not observed after $CD8^+$ T cell transfer into acutely infected mice (84, 342).

Studies on this dysfunction concentrated on *in vitro* mixed lymphocyte cultures. It was shown that whenever the $CD8^+$ T cells were mixed with $CD4^+$ T cells from chronically infected mice they were functionally suppressed, whereas this was not the case when $CD4^+$ T cells from naïve mice were added to the culture (144). These findings implicated a role for a suppressive $CD4^+$ T cell subset in chronic FV infection. The final proof came from an experiment were naïve mice were supplemented with $CD4^+$ or $CD8^+$ T cells from chronically FV-infected mice and then

challenged with FV induced tumours or unrelated tumours. Mice that had received $CD4^+$ T cells were not able to reject the tumour, in contrast to mice receiving $CD8^+$ T cells. These results provided evidence that Tregs could be induced during chronic viral infections and were involved in establishment of the chronic infection. Furthermore, this data also showed that the suppressive effect was not restricted to virus-specific cells, as the rejection of unrelated tumours was also suppressed (144).

Further research showed that Tregs suppressed the production of IFNγ by $CD8^+$ T cells during chronic infection, and this suppression was not restricted to the $CD25^+$ Treg population, as $CD25^-$ Tregs were also suppressive (84). Interestingly, it has been shown that FV-induced Tregs suppress the effector functions of $CD8^+$ T cells but not their proliferation and activation, and these Tregs were readily suppressive *ex vivo* without further stimulation (84). *In vitro* studies have shown that FV-induced Tregs suppress $CD8^+$ T cells in a contact-dependent manner, independent of APCs and not dependent on the TCR specificity of the $CD8^+$ T cells (248).

Recently, it has been shown that Tregs expand during acute FV infection with elevated levels remaining present in the spleen during chronic infection (340, 341). Tregs gain the ability to suppress $CD8^+$ T cell responses at two weeks post infection, where viral loads are still high (341). A new mouse model was engineered (DEpletion of REGulatory T cells /DEREG mice (172)), expressing the diphtheria-toxin receptor under the control of an additional Foxp3 promoter. This mouse has made it possible to selectively deplete $Foxp3^+$ Tregs in the immune system. Depletion studies in acutely infected DEREG mice have shown that the $CD8^+$ T cell response could be augmented (GzmA, GzmB, CD107a) and viral loads were reduced when Tregs were deleted (339, 340). Similar results of functional $CD8^+$ T cell recovery (production of GzmB, IFNγ, TNFα and IL2) and decrease of viral loads due to Treg depletion were shown for the chronic phase of infection with FV (81). Furthermore, it has also been shown that Tregs were able to suppress $CD4^+$ T cell responses, especially IFNγ production, in the chronic phase of FV infection (215). Although Tregs expanding during FV infection suppress virus-specific immune responses, the developmental origin and specificity of this action has not yet been determined. Furthermore, the mechanism(s) behind the suppressive activity of Tregs during FV infection are not clearly defined.

1.6 Aims and scope of the work

$CD4^+Foxp3^+$ Tregs constitute a major subset of suppresser T cells. The function of Tregs is essential in both the prevention of autoimmune diseases in healthy individuals and protection from immune response-mediated tissue damage during viral infections. While generally beneficial, these suppressive effects can be limiting for anti-viral immune responses, resulting in a delayed or incomplete clearance of the pathogen (23). The immunosuppressive role of Tregs in virus-specific immunity was first described using the FV model, but has also been reported for viruses causing human infections such as HBV, HCV and HIV (181).

The aim of this PhD project was to better define the molecular characteristics of FV-induced Tregs. For this purpose it was of importance to determine the phenotype acquired by Tregs during acute and chronic FV infection by analysing the expression of various activation, differentiation, and proliferation markers. Furthermore, it was of great interest to determine the specificity and origin of the Treg population and the molecular mechanism of expansion during viral infection. This was especially important as knowledge on this topic will provide new concepts to therapeutically interfere with Treg cell expansion. It was also of interest to determine the mechanism of effector T cell suppression mediated by Tregs during acute FV infection. For this purpose a recently discovered Treg suppression pathway involving the enzymes CD73 and CD39 was investigated by performing experiments in mice deficient for these molecules. As a last step, the acquired knowledge about the phenotype and function of Tregs in a mouse retrovirus model was translated to the human infection with HIV-1, where Treg responses also play an important role in pathogenesis.

2. Material

2.1 Microarray data

The samples for the microarray data were prepared by Gennadiy Zelinskyy (Institute for Virology, University Hospital Essen, Essen, Germany) and the Microarray was done on an Affymetric Mouse430_2 chip by Robert Geffers (Immune Regulation group, Helmholtz Centre for Infection Research, Braunschweig, Germany). The samples for the microarray were $CD4^+CD25^+GFP^+$ Tregs of $DEREG^{tg}$ mice (172). $DEREG^{tg}$ mice express a diphtheria toxin-green fluorescent protein (DT-GFP) fusion protein under the control of an additional Foxp3 promoter, which makes it possible to sort for live $Foxp3^+$ Tregs (GFP^+). In a first step, spleen or bone marrow cells of naïve or FV-infected $DEREG^{tg}$ mice, respectively, were enriched for $CD4^+CD25^+$ T cells using magnetic beads (see 3.12 for MACS isolation). The enriched $CD4^+CD25^+$ T cells were subsequently subject to cell sorting for GFP^+ Tregs (see 3.11.1 for the principle of cell sorting). The RNA of these $CD4^+CD25^+GFP^+$ Tregs was then isolated and sent to Braunschweig for microarray analysis. The Treg samples used were splenic Tregs from naïve mice and bone marrow Tregs from FV-infected mice (7 or 15 days post infection (dpi)).

2.2 Equipment and materials

Table 2. 1 **Equipment**

Equipment	Manufacturer
Accu-Jet Pro	Brand, Wertheim, Germany
Air Clean 600 PCR Workstation	STARLAB, Ahrensburg, Germany
ImmageStream	Amnis
AutoMACS Pro	Miltenyi Biotec, Bergisch Gladbach, Germany
Biofuge fresco	Heraeus, München, Germany
Cellometer™ Auto T4 Cell Counter	Nexcelcom Bioscience, Lawrence, MA, USA
Centrifuge Forma 3L GP4500	Thermo Scientific, Waltham, MA, USA
Centrifuge 5415R	Eppendorf, Hamburg, Germany
Centrifuge Avanti J-26XPi	Beckman Coulter, Krefeld, Germany
Centrifuge Megafuge 1.0R	Heraeus, München, Germany
Centrifuge Rotina, 420	Hettich, Mülheim a.d.Ruhr, Germany
Centrifuge Alegra X-1512	BD, San Jose, California, USA

Forma Series II water jacketed CO_2 incubator	Thermo Scientific, Waltham, MA, USA
Freezer Liebherr premium	LIEBHERR, Ochsenhausen, Germany
Freezer -80 °C	Fisher Scientific, USA
Freezer -80 °C	SANYO, Germany
Handysteps Stepper	Eppendorf, Hamburg, Germany
Heating block	Grant, QBC, Germany
Heracell 240i CO_2 Incubator	Thermo, Dreieich, Germany
Ice machine	ICE-O-Matic, Denver, CO, USA
Ice machine MF30	Scotsman, Milan, Italy
Infrared lamp	Phillips, Amsterdam, Neatherlands
Invertoskop	Zeiss, USA
Laminar flow	Labgard ClassII Type2A, Plymouth, MN, USA
Laminar flow	KOJAIR®, Meckenheim, Germany
Laminar flow Herasafe	Heraeus, München, Germany
Liquid Nitrogen Vessel Locator4	Thermo Scientific, Waltham, MA, USA
LSRII flow cytometer, 4 Lasers	Becton Dickinson, Heidelberg, Germany
Minispin	Roth, Karlsruhe, Germany
MoFlo cell sorter	Beckman Coulter, USA
Multi-channel pipettes (50, 200, 300 µL)	Eppendorf, Hamburg, Germany
MultiStend magnet holder and magnets	Miltenyi, Auburn, California, USA
Neubauer cell counting chamber	Becton Dickinson, Heidelberg, Germany
QuadroMACS	Miltenyi, Auburn, California, USA
Reflected-light microscope CK 2	Hund, Wetzlar, Germany
Refrigerator	LIEBHERR, Ochsenhausen, Germany
Scales Scout Pro	Ohaus, Kirchheim, Germany
Single channel pipettes (10, 20, 100, 200, 1000 µL)	Eppendorf, Hamburg, Germany
Sorvall centrifuge fresco	Thermo, Dreieich, Germany
Thermomixer comfort	Eppendorf, Hamburg, Germany
VortexGenie2	Scientific Industries, Bohemia, NY, USA
Waterbath Isotemp210	Fisher Scientific, USA
Waterbath	GFL, Burgwedel, Germany

Table 2. 2 **Materials**

Item	Manufacturer
500 mL filter system	Corning, NY, USA
Amicon Ultra 100 MW filter tube (100	Merck Millipore, Darmstadt, Germany

kDa)	
Cannulae (20G; 23G; 27G)	Becton Dickinson, Heidelberg, Germany
Cell culture flasks (T25; T75; T175)	Greiner bio-one, Frickenhausen, Germany
Cell culture multi flask 75 m^2	BD Bioscience, San Jose, California, USA
Cell culture plates, sterile (6; 24; 96 well)	Greiner bio-one, Frickenhausen, Germany
Cell culture plates, sterile (6; 24; 96 well)	BD Bioscience, San Jose, California, USA
Cellometer™ Auto T4 counting chamber	Peqlab Biotechnologie GmbH, Erlangen, Germany
Cell strainer (70 µm; 30 µm)	Falcon BD, Heidelberg, Germany
Cryo.S™, PP with screw cap, sterile	Greiner bio-one, Frickenhausen, Germany
Cryosystems 4000 series	Marathon Products, San Leandro, California, USA
Cryotubes	Wheaton, USA
Disposable haemocytometers	Fisher Scientific, USA
Disposable syringes (1 mL; 2 mL)	Thermo, Dreieich, Germany
Erlenmeyer flasks	Schott, Mainz, Germany
FACS tubes	Becton Dickinson, Heidelberg, Germany
Forceps, pointed and curved	Oehmen, Essen, Germany
Glassware	Schott, Mainz, Germany
Leucosept™	Greiner bio-one, Frickenhausen, Germany
LS separation columns	Miltenyi, Auburn, California, USA
Microtest™ cell culture plates, 96-well	BD, Heidelberg, Germany
Nunc MaxiSorp 96-well plate	Sigma-Aldrich, Steinheim, Germany
Parafilm Laboratory film	American National Can, Chicago, IL, USA
Pipet tips (10; 20; 100; 200; 1000; 5000 µL)	Eppendorf, Hamburg, Germany
Pipet tips, sterile (10; 20; 100; 200; 1000 µL)	STARLAB, Ahrensberg, Germany
Plastic pipettes (sterile; 1 mL; 5 mL; 10 mL; 25 mL)	Greiner bio-one, Frickenhausen, Germany
Plastic pipettes (sterile; 1 mL; 5 mL; 10 mL; 25 mL)	BD Bioscience, San Jose, California, USA
PP screw-cap tubes (15 mL; 50 mL)	Greiner bio-one, Frickenhausen, Germany
PP screw-cap tubes (15 mL; 50 mL)	BD Bioscience, San Jose, California, USA
Reaction tubes (1,5 mL; 2 mL)	Eppendorf, Hamburg, Germany
Scissors, large and small	Oehmen, Essen, Germany
U-shaped 96-well microplates	Greiner bio-one, Frickenhausen, Germany

2.3 Laboratory animals

All animal experiments were performed in strict accordance with the German regulations of the Society for Laboratory Animal Science (GV-SOLAS) and the European Health Law of the Federation of Laboratory Animal Science Associations (FELASA). Protocols were approved by the North Rhine-Westphalia State Agency for Nature, Environment and Consumer Protection (LANUV). All experiments were performed with mice older than six weeks. The mice were kept in a pathogen-free environment with free access to water and standard mouse food. All mice were under controlled and regular examination by veterinarians of the University Hospital Essen. The mice used in this PhD thesis had the resistance genotype of *H-2D*$^{b/b}$*, Fv-1*$^{b/b}$*, Fv-2*$^{r/r}$*, Rfv3*$^{r/r}$ and were bred on C57BL/6 (B6) background. The exceptions are BALB/c mice, which are susceptible to FV-induced leukaemia and splenomegaly and were used to produce virus stocks *in vivo,* and Y10A (F1: A.BY x C57BL/10A) mice, which are also susceptible to FV and were used to titrate the virus stocks.

2.3.1 Wild type mice

BALB/c	Harlan Winkelmann GmbH, Borchen, Germany, Resistance genotype: *H-2D*$^{d/d}$*, FV-2*$^{s/s}$
C57BL/6 (B6)	Harlan Winkelmann GmbH, Borchen, Germany Resistance genotype: *H-2D*$^{b/b}$*, FV-2*$^{r/r}$
F1: A.BY x C57BL/10A (Y10A)	Bred at the Animal Facility, University Hospital Essen, Germany, Resistance genotype: *H-2D*$^{a/b}$*, FV-2*$^{r/s}$

2.3.2 Congenic mice

CD45.1-congenic B6	Genotype: B6.SJL-Ptprc^{a}Pep3^{b}/BoyJ; Inbred at Central Animal Facility, University Hospital Essen, Germany

2.3.3 Knockout and transgenic mice

CD8$^{-/-}$ (CD8 deficient)	Mice deficient for CD8^{+} T cells because of a targeted disruption in exon 1 of the *lyt-2* gene (102). Inbred at the

	Central Animal Facility, University Hospital Essen, Germany.
CD39$^{-/-}$ (CD39-KO)	Mice with a targeted disruption of exon 1 in the ectonucleotide triphosphate diphosphohydrolase (*entpd1*) gene, which leads to a shorter transcript of the gene and no detectable function of the enzymatic protein product CD39. Mice were kindly provided by Verena Jendrossek (Institute for Cell Biology, University Hospital Essen, Germany). MTA: Simon C. Robson (Department of Medicine, Beth Israel Deaconess Medical Center, Harvard Medical School, Boston, MA, USA) (88). Inbred at the Central Animal Facility, University Hospital Essen, Germany.
CD73$^{-/-}$ (CD73-KO)	Mice with a targeted disruption of exon 3 in the ecto-5' nucleotidase (*nt5e*) gene, which leads to a shorter transcript of the gene and no detectable function of the enzymatic protein product CD73. Mice were kindly provided by Verena Jendrossek (Institute for Cell Biology, University Hospital Essen, Germany). MTA: Linda Thompson (Oklahoma Medical Research Foundation, Oklahoma City, OK, USA) (300). Inbred at the Central Animal Facility, University Hospital Essen, Germany.
Evα3	Mice are doubly transgenic for the TCRα and the TCRβ chains of the Env122-141-specific CD4^{+} T cell clone H18 (336). Mice were kindly provided by George Kassiotis (National Institute for Medical Research, London, UK). Inbred at the Central Animal Facility, University Hospital Essen, Germany.
GzmB$^{-/-}$ (GzmB-KO)	Mice deficient for GzmB due to a targeted disruption of the g*zmB* gene (135). Inbred at the Central Animal Facility, University Hospital Essen, Germany.

iRhom2$^{-/-}$ (iRhom2-KO)	Mice with a deletion of the exons 4-to-15 in the *Rhbdf2* gene encoding iRhom2, a member of the rhomboid protein family. iRhom2 regulates the maturation of TACE, which in turn controls the shedding of TNFα. Mice were kindly provided by Phillip Lang (Department of Gastroenterology, Hepatology and Infectious Diseases, Heinrich-Heine-University Düsseldorf, Germany) (198). Inbred at the Central Animal Facility, University Hospital Essen, Germany.
JH-mice	Mice lacking mature B cells because of a deficiency in the antibody heavy chain J_h gene. Mice were kindly provided by Karl Lang (Institute for Immunology, University Hospital Essen, Germany) (53).
muMT-mice (μMT)	Mice lacking mature B cells due to a targeted disruption of the *μM* gene (exon 1 and 2) and the *δ* gene (constant region, exon 1 to 3). Mice were kindly provided by George Kassiotis (National Institute for Medical Research, London, UK) (Kitamura et al., 1991).
Nur77-GFP	Mice expressing GFP from the *nr4a1* (Nur77) gene. GFP signal indicates the strength of TCR stimulation (204). Mice were kindly provided by Hans Christian Probst (University Medical Center, Institute for Immunology, Johannes Gutenberg University Mainz, Germany).
TCR^{tg}	CD8 TCR transgenic mice specific for the DbGagL FV epitope (55). Inbred at Central Animal Facility, University Hospital Essen, Germany.
TNFRI$^{-/-}$	Mice were generated by disrupting the coding sequence at base pair 535 of the *tnfrsf1a* gene (231). Mice were kindly provided by Karl Lang (Institute for Immunology, University Hospital Essen, Germany).

TNFRII$^{-/-}$	Mice were generated by targeted disruption of the second exon in the *tnfrsf1b* gene (90). Mice were kindly provided by Daniela Männel (Institute for Immunology, University of Regensburg, Germany).
TNFRI+II$^{-/-}$	Mice deficient for both TNFRI and TNFRII, generated by homozygote breeding of TNFRI$^{-/-}$ and TNFRII$^{-/-}$ mice. Mice were kindly provided by Percy Knolle (Institutes for Molecular Medicine and Experimental Immunology, University of Bonn, Germany). Inbred at Central Animal Facility, University Hospital Essen, Germany.

2.4 Chemicals and media

Chemicals, buffers and media were purchased from Applichem, Invitrogen, Merck, Roth and Sigma-Aldrich unless otherwise stated.

3-amino-9-ethylcarbazole (AEC), 4-(2-hydroxyethyl)-1-piperazineethanesulfonic acid (HEPES), 5-bromo-4-chloro-3-indolyl-β-D-galactopyranoside (X-gal), adenosine 5'-(α,β-methylene)diphosphate (AMPCP), acetic acid, autoMACS run and wash buffer (Miltenyi Biotec), β-mercaptoethanol (β-ME), bovine serum albumin (BSA), brefeldin A (BFA), calcium chloride, dextran, dimethyl sulfoxid (DMSO), disodium hydrogen phosphate, Dulbecco´s modified Eagle medium (DMEM) (Gibco) and DMEM high glucose (Gibco), ethanol, ethylendiaminetetraacetic acid (EDTA), FACS Clean (BD Bioscience), FACS Flow (BD Bioscience), FACS Rinse (BD Bioscience), foetal calve serum (FCS) (Biochrom), Ficoll (GE Healthcare), 37 % formaldehyde, formalin, FuGENE® transfection reagent (Promega), glucose, hydrogen peroxide (H_2O_2), incidine 8%, isopropanol, L-Glutamine, magnesium chloride ($MgCl_2$), N-N-dimethylformamid, penicillin-streptomycin (PenStrep), phosphate buffered saline (PBS) (Gibco), picric acid, polybrene A, potassium ferricyanide, potassium ferrocyanide, RPMI-1640-Media (Gibco), saponin, sodium carbonate, sodium acetate, sodium azide (NaN_3), sodium pyruvate, trypan blue, trypsin-EDTA.

2.5 Buffer and supplemented cell culture media

If not stated otherwise all buffer and media were prepared using bi-distilled H_2O.

Table 2. 3 **Buffers and Media**

Name	Ingredients
AEC working solution	AEC stock solution was prepared 1:20 in 0.05 M sodium acetate and the reaction was started by addition of 0.5 µL of 30 % H_2O_2 per 1 mL of solution.
AEC stock solution (4 mg/mL)	20 AEC tablets were solubilised in 100 mL N-N-dimethylformamid
Boulin´s solution	75 mL picric acid, 25 mL 40% formalin, 5 mL acetic acid
Coating buffer for *in vitro* cell stimulation	0.05 M sodium carbonate pH 9.6
Complete DMEM for cell lines	DMEM supplemented with 10 % FCS and 1 % PenStrep, sterile filtered if needed
Complete DMEM for HIV-1 and SIV_{mac}-VLP stock production	DMEM supplemented with 10 % FCS, 1 % PenStrep and 50 mM HEPES, sterile filtered
Complete RPMI for primary cells	RPMI supplemented with 10 % FCS and 1 % PenStrep, sterile filtered if needed
DC media for human cells	Complete RPMI supplemented with 500 U/mL hrIL4 and 1000 U/mL hrGM-CSF, sterile filtered
DC media for mouse cells	100 mL RPMI with 10 % FCS, 50 µM β-ME, 4 mM L-Glutamine, 1 mM sodium pyruvate, 1 % PenStrep, supplemented with 1 ng/mL mrIL4 and 5 ng/mL mrGM-CSF (both cytokines from cell culture supernatant)
FACS buffer	PBS supplemented with 0.1 % BSA and 0.02 % NaN_3
Freezing media	FCS supplemented with 10 % DMSO
HIV-1 titration staining solution	0.5 mg/mL X-Gal, 4 mM potassium ferrocyanide, 4 mM potassium ferricyanide, 2 mM $MgCl_2$ in PBS
MACS buffer	PBS supplemented with 0.5 % BSA and 2 mM EDTA
PBBS	1 L PBS with 1 g glucose
Sorting buffer	PBS with 10 % FCS and 5 mM HEPES

2.6 Antibodies and staining reagents

2.6.1 Characteristics of fluorophores

Table 2. 4 **Characteristics of fluorophores**

Dye	Full name	Laser used for excitation	Emission in nm
FITC	Fluorescein isothiocyanate		525
AF488	Alexa flour 488		519
GFP	Green fluorescent protein	Blue	395/475
PE	Phycoerythrin	Laser	575
PerCP	Peridinin-chlorophyll	488nm	675
PE-Cy5	PE-cyanine5		670
PE-Cy5.5	PE-cyanine5.5		690
PerCP-Cy5.5	PerCP-cyanine5.5		690
PE-Cy7	PE-cyanine7		775
APC	Allophycocyanin		660
AF647	Alexa flour 647	Red	647
AF680	Alexa flour 680	Laser	680
AF700	Alexa flour 700	633nm	723
APC-Cy7	APC-cyanine7		774
eF780	eflour780		780
LD Blue	Live/Dead Blue	UV Laser 355nm	450
eF450	eFlour450		450
Pacblue	Pacific Blue	Violet	455
BV421	Brilliant violet 421	Laser	421
BV605	Brilliant violet 605	405nm	605
eF650	eFlour650		650
BV650	Brilliant violet 650		650

2.6.2 Antibodies

Anti-mouse and anti-human antibodies were purchased from eBioscience (Affymetrix), BD Bioscience or BioLegend unless otherwise stated.

2.6.2.1 Mouse reactive antibodies

Table 2. 5 **List of antibodies utilised for staining of mouse cells**

Antibody	Conjugate	Clone
AB720 (α-MuLV Env, Isotype IgG_{2b})*	Cell culture supernatant	-
BrdU	FITC	B44
CD3	purified	145-2C11
CD4	AF700	RM4-5
CD8	eF450	53-6.7
CD11a	PE	M17/4
CD11b (Mac1)	FITC,	M1/70
CD25	PerCP, PE-Cy7, APC	PC61.5
CD28	purified	37.51
CD39	PE Cy5	24DMSI
CD43	PerCP	1B11
CD44	FITC, APC	IM7
CD45.1	PE, PE-Cy7, APC	A20
CD62L	PE-Cy7	MEL-14
CD69	FITC, PE	H1.2F3
CD73	PE Cy7	Ty/11.8
CD103	PE	2E7
CD107a	FITC	ID4B
CD127	eF450	AFR34
CD152 (CTLA-4)	PE	UC10-4F10-11
CD223 (Lag3)	PE	eBioC9B7W
Foxp3	FITC, eF450	FJK-16S
GITR	PE	DTA-1
goat-α-mouse Ig HRP**	HRP	-
GzmB	APC	GB11
Helios	PacificBlue	22F6
ICOS (CD278)	PerCP	7E.17G9
IFN-gamma	FITC, APC	XMG1.2
IL2	PE	JES6-5H4

Ki67	PE-Cy7	B56
KLRGI	APC	2F1
Nrp-1***	APC	761705
PD-1 (CD279)	PE	J43
PD-L1 (CD274)	PerCP	MIH5
TCR-Vβ5	PE, PerCP Cy5.5, biotin	MR9-4
Tetramer I	PE	-
Tetramer II	APC	-
TIM3	APC	8B.2C12
TNFRI (CD120a)	PE	55R-286
TNFRII (CD120b)***	APC	FAB
TNFα	PE-Cy7, APC	MP6-XT22

* own production, ** Dako, *** R&D Systems

2.6.2.2 Human reactive antibodies

Table 2. 6 **List of antibodies utilised for staining of human cells**

Antibody	Conjugate	Clone	Application	Concentration per $1x10^6$ cells
CD3	PerCP-Cy5.5	SK7	FACS	5 µL
CD3	Unconjugated	HIT3a	Stimulation	5 µL per 0.5 mL
CD4	AF700	RPA-T4	FACS	0.5-1 µL
CD8	AF488	RPA-T8	Sort	5 µL per 0.5 mL
CD19	AF700	HIB19	FACS	0.5-5 µL
CD25	BV785	BC96	Amnis	5 µL
CD25	APC	M-A251	Sort	5 µL per 0.5 mL
CD25	APC-H7	M-A251	FACS	4 µL
CD127*	PE	R34.34	Sort	5 µL per 0.5 mL
CD127	eF450	RDR5	FACS	10 µL
CTLA-4*	Unconjugated	BNI3	Block	10 µg/ml
Foxp3	PE	PCH101	FACS	5 µL
HLA-DR	BV570	L243	Amnis	10 µL
KLRGI**	FITC	-	FACS	1 µL
TGF-β	Unconjugated	TW4-2F8	Block	10 µg/mL
TNFRII***	APC	FAB226A	FACS	5 µL
hIgG	-	-	Block	1:50 in 25 µL
Normal rat serum	-	-	Block	1:25 in 50 µL

* Beckman Coulter; ** Kindly provided by Hanspeter Pircher (Institute for Immunology, University Hospital Freiburg, Germany); *** R&D Systems

2.6.2.3 MHC tetramers and F-MuLV specific peptide

MHC I tetramer

PE labelled MHC class-I H-2D^b tetramer loaded with the peptide AbuAbuLAbuLTVFL (D^{b}GagL tetramer, FV gagCD8$^+$ epitope gPr80gag85-93) recognised by D^{b}GagL-specific CD8$^+$ T cells (9, 55, 262, 283). The MHC class-I tetramer was purchased from Beckman and Coulter (Krefeld, Germany) or MBL International Corporation (Woburn, MA, USA).

MHC II tetramer

APC labelled MHC class-II I-A^b tetramer loaded with F-MuLV Env f_{n20} peptide DEPLTSLTPRCNTAWNRLKL (F-MuLV Env CD4$^+$ T cell epitope Env122-141) (272). The MHC class-II tetramer was provided by the NIH Tetramer Facility (Emory University, Atlanta, USA).

CD8 peptide

The F-MuLV CD8$^+$ T cell peptide was synthesised by PAN Tecs (Tübingen, Germany) and reconstituted in 100 % sterile DMSO. Peptide name: FMR-H-2D^b GagL CD8 epitope. Sequence: AbuAbuLAbuLTVFL (262).

2.6.3 Discrimination of dead cells

To discriminate dead from live cells, either Live/Dead aqua or fixable viability dye (FVD) eF780 were used.

2.6.4 Staining reagents

Table 2. 7 **Staining reagents**

Staining Reagent	Manufacturer	Application	Concentration per 1x10^6 cells
FVD eF780	eBioscience	FACS	1 µL
Live/death aqua	Invitrogen	FACS	2.5 µL of a 1:10 dilution
Phalloidin-APC	Invitrogen	Amnis	1 µL
Violet tracer	Invitrogen	Amnis	0.5 µg

2.7 Biological reagents and cytokines

Biological reagents and cytokines were purchased at Peprotech, unless otherwise stated (hr: human recombinant): hrGM-CSF (granulocyte macrophage colony-stimulating factor), hrIL4 (interleukin 4), 2',5'-DiDeoxyadenosine (ddADA).

Human soluble wild type trimetric single chain (sc) TNFα (solTNFα) (169) was kindly provided by Peter Scheurich (Institute for Cell Biology and Immunology, University Stuttgart, Germany). The trimetric single chain TNFα was engineered by using a single chain cassette in which three TNFα domains were genetically liked by short peptide linkers (structure: TNFα-linker-TNFα-linker-TNFα). The solTNFα was produced by transfecting 293T cells with the TNFα-linker-construct and harvesting the cell culture supernatant. The supernatant was then tested for biological activity using an NF-κB activation reporter assay using hrTNFα as a control. The material was kindly provided by Khanh Le (Institute for Virology, University Hospital Essen, Germany)). In the stock used for this study, 15 µL of cell culture supernatant (containing solTNFα) was equal to 10 ng/mL hrTNFα. 100 µL cell culture supernatant was used to treat mice i.p..

Complexed TNF (compTNFα, construct: scTNF80(mu)-Flag-TNC), simulating the membrane-bound form of TNFα, was kindly provided by Harald Wajant (Division of Molecular Internal Medicine, Department of Internal Medicine II, University Hospital Würzburg, Germany). To permit self-assembly of three scTNFα, the trimeric scTNFα-construct was further engineered by linking the cassette N-terminally with the FLAG-tagged trimerisation domain of chicken tenascin-C (TNC) (scTNFα-Flag-TNC), which creates a TNFα nonamer. Furthermore, to make the scTNFα-Flag-TNC more specific, mutations which render TNFα specific to TNFRII and not TNFRI were introduced, creating the scTNF80-Flag-TNC. This has been described for human compTNFα (scTNF80(hu)-Flag-TNC) (240) and for mouse compTNFα (scTNF80(mu)-Flag-TNC) (Harald Wajant, unpublished data). The mouse compTNFα was utilised in this study.

2.8 Standard kits

Table 2. 8 **Standard kits**

Kit	Manufacturer
α-CD3/α-CD28 human or mouse T cell stimulation dynabeads	Invitrogen, Grand Island, NY, USA
Cytofix/cytoperm intracellular staining kit	BD Pharmingen, Heidelberg, Germany
FITC BrdU Flow kit	BD Pharmingen, Heidelberg, Germany
Foxp3 staining set	eBioscience, San Diego, USA
Human CD14 MicroBeads	Miltenyi, Auburn, California, USA
Human $CD4^+CD25^+$ Treg isolation kit	Miltenyi, Auburn, California, USA
Mouse $CD4^+$ T cell isolation kit II	Miltenyi Biotec, Bergisch Gladbach, Germany
Mouse CD8α (Ly-2) MicroBeads	Miltenyi Biotec, Bergisch Gladbach, Germany
Reverse Transcriptase Assay, colorimetric	Roche, Basel, Switzerland

2.9 Cell lines and viruses

2.9.1 Friend retrovirus complex

Preparations of FV were obtained from mice infected with the replication competent FV complex (see 3.6.1). The FV complex stock contains B-tropic F-MuLV and polycythemia-inducing SFFV (62). Two different virus stocks were used: one containing only the FV complex (246), for acute infections; and the other containing additionally lactate dehydrogenase-elevating virus (LDV), for chronic infections. The addition of LDV enables a more stable chronic infection with the FV to be established (246). Unless otherwise stated the FV stock without LDV was used.

2.9.2 HIV-1 JRFL-iGFP

CCR5-tropic HIV-1 JRFL-iGFP was kindly provided by Benjamin Chen (Mount Sinai Medical School, NY, USA (54)). This construct contains a GFP inserted internally into Gag between MA and CA and is a variant of an NL4-3-based molecular HIV-1 clone (140). For the construct used here the *env* gene from NL4-3 was replaced with the corresponding sequence of JRFL.

2.9.3 SIV_{mac}-VLPs

SIV_{mac}-VLPs were kindly provided by Andrea Cimareli (Ecole Normale Supérieure, Lyon, France (118)). These SIV_{mac}-VLPs were synthesised by transfection of the two constructs pSIV3 and pVSVg into 293T cells.

2.9.4 pAdVAntage™

pAdVAntage™ vector was used in co-transfections of mammalian cells to enhance transient protein expression in 293T cells (Promega).

2.9.5 Cell lines

Table 2. 9 **Cell lines**

Cell line	Source
AB720-hybridoma	Hybridoma cell line produces the monoclonal IgG_{2b} α-MuLV Env antibody (244).
293T	Human embryonic kidney cell line (268).
Mus dunni	Murine fibroblast cell line susceptible to infection with FV (173).
NIH 3T3-GM-CSF	Cell line producing mouse GM-CSF (Thomas Blankenstein, Institute for Immunology, FU Berlin, Germany).
NIH 3T3-IL4	Cell line producing mouse IL4 (kindly provided by Dr. Schmitt, Vienna, Austria)
PK136	Hybridoma cell line PK136 produces the monoclonal mouse-IgG_{2a} α-mouse-α-NK1.1 antibody (165). Supernatant was used to deplete NK and NKT cells via i.p. injection.
TZM-bl (JC.53bl-13)	HeLa cell line engineered to express CD4, CXCR4 and CCR5 and a Tat-inducible Luc and *Escherichia coli* β-galactosidase reporter gene (235).
YTS 169.4.2.1	Hybridoma cell line YTS 169.4.2.1 produces the monoclonal rat-IgG_{2b} α-mouse-α-CD8 (Lyt-2) antibody (68). Supernatant was used to deplete $CD8^+$ T cells in mice by i.p. injection.

2.9.6 Depletion antibodies

$CD8^+$ T cell depletion antibody	Clone 169.4.2.1, produced by YTS 169.4.2.1 hybridoma cell line.
NK1.1 depletion antibody	Clone PK136, produced by PK136 hybridoma cell line.
TCR-Vβ5 depletion antibody	Clone MR9-4, custom LEAF purified, (BioLegend, London, UK).

2.10 Human samples

2.10.1 Healthy volunteers

Blood samples came from healthy HIV-negative individuals recruited by the Hoxworth Blood Center (Cincinnati, OH). The samples were not collected for research purposes and no identifier was provided, thus the University of Cincinnati Institutional Review Board (IRB) has determined this activity to be exempted from IRB review and surveillance. These samples were used for *in vitro* cell culture studies described later. Additionally, age- and sex-matched healthy controls were enrolled to provide a control group for the comparison to HIV-1 infected study subjects.

2.10.2 HIV-1 infected volunteers

Eight untreated HIV-1 infected individuals were enrolled in this study. All patients were part of a clinical trial for treatment with tenofovir/emitricitabine (RT-inhibitor) 300/200 mg tablets and lopinavir/ritonavir (protease inhibitor) 400/100 mg tablets, twice daily. None of the patients had opportunistic infections or cancer at enrolment. All patients were either untreated or had not received treatment for six months prior to the initial blood collection. Blood samples were drawn at various times after the initiation of treatment and an initial sample was drawn before treatment.

3. Methods

3.1 Evaluation of the microarray data

The initial evaluation of the microarray data was performed by Robert Geffers (Immune Regulation group, Helmholtz Centre for Infection Research, Braunschweig, Germany) and subsequent analysis was performed on the excel files produced. For certain markers of interest the absolute values of detection were used to calculate the fold changes from naïve to 7 dpi, naïve to 15 dpi and 7 dpi to 15 dpi Treg samples. Furthermore, only absolute values that showed a significant signal-to-noise ratio were chosen for analysis. When markers were used where more than one primer set was available, the mean fold change was calculated.

3.2 Cell counting

To count cells, an aliquot of the cell suspension was mixed with 0.4 % trypan blue. Dead cells are more permeable than live cells to trypan blue and these cells stain blue. An appropriate dilution was chosen to count the cells and only live cells were counted for the determination of cell numbers. The cells were counted using either: a disposable haemocytometer, a Cellometer^{TM} Auto T4 counting chamber or a Neubauer counting chamber. The counting was done using a light microscope (haemocytometer and Neubauer chamber) or the Cellometer^{TM} Auto T4 cell counter with the appropriate settings. The Cellometer automatically displayed the absolute cell count and dead cells were excluded. For manual cell counting the cell number was determined by counting four squares of a big 16-square field in the chamber. The absolute cell number was then calculated by multiplying the average cell count with the chamber factor ($1x10^4$), the dilution applied to the sample and the volume of the cell suspension.

3.3 Preparation of cells for storage

Cells were spun at 520 xg for 7 min at 4 °C and the supernatant was discarded and replaced with the appropriate amount of ice-cold cell freezing media (FCS supplemented with 10% DMSO). Cells were then transferred into pre-cooled liquid

nitrogen screw-cap tubes and stored for a minimum of 24 hours (to a maximum of one week) in an IPA bath at -80 °C. The frozen cells were then transferred into a liquid nitrogen tank and stored until use.

3.4 Re-constitution of cells from storage

To thaw cells an aliquot was taken out of the liquid nitrogen and quickly thawed in a 37 °C water bath until almost fully thawed. To prevent damage to the cells by DMSO, the cells were diluted in four times the volume of FCS and spun at 520 xg for 7 min at 4 °C. The cells were re-suspended in media or PBS according to the down-stream procedure used, counted and/or directly put into culture dishes.

3.5 Cell culture of cell lines

Adherent cells were grown in a monolayer using the appropriate culture medium, usually complete DMEM, which at minimum contains 10 % FCS and 1 % PenStrep. All cells lines were maintained at 37 °C and 5 % CO_2 and checked regularly. Depending on the cell line, the cells were passaged as soon as they grew to ~95% confluence. To passage cells, the medium was discarded and cells were washed once with PBS. Trypsin-EDTA (3 mL) was then added and the cells checked frequently for their morphology under a light microscope. When the cells appeared round they were carefully re-suspended in 7 mL of complete cell culture media to inhibit the trypsin. To wash the cells, they were transferred into a 50 mL tube and centrifuged at 520 xg for 7 min. Cells were then counted (if required) and seeded into a fresh tissue culture flask followed by incubation at 37 °C and 5 % CO_2 until ready for use.

3.6 Virus preparation and titre determination

3.6.1 FV stock

3.6.1.1 *In vivo* production of a FV stock

To obtain a FV stock, susceptible BALB/c mice were infected intra venous (i.v.) with 3,000 spleen focus forming units (SFFU) of FV. Nine dpi the mice were sacrificed

and the spleens removed. A 15 % spleen homogenate was prepared in PBBS with 1 mM EDTA. The homogenate was then aliquoted and stored at -80°C until use.

3.6.1.2 Titre determination of a FV stock

Titration of a FV stock was done by infecting Y10A mice i.v. with different amounts of virus stock. The spleens were removed 14 dpi. During the course of FV infection, malignant cell populations develop on the surface of the spleen. These foci can be visualised by incubation of the whole spleens in Boulin´s solution which enhances the visual contrast of foci on the spleen surface. SFFUs can be determined by counting these foci.

3.6.2 HIV-1 stock

3.6.2.1 Preparation of an HIV-1 JRFL-iGFP virus stock

293T cells were harvested and seeded at a concentration of $1x10^5$ cells per well of a 24-well plate. At 50 % confluence, the cells were transfected with the HIV-1 JRFL-iGFP plasmid. For transfection the following mixture was prepared with the reagents added in the order they appear in the list.

Table 3. 1 **Transfection mix for HIV-1 JRFL-iGFP virus synthesis**

Reagent	Volume
DMEM serum-free	45.205 µL
FuGENE®	3.375 µL
1 µg HIV-1 JRFL-iGFP [700 ng/µL]	1.4 µL
0.125 µg pAdVAntage™ vector [5836 ng/µL]	0.02 µL
Final volume	*50 µL*

The mixture was incubated for 15 min at room temperature and 50 µL were then added drop by drop to each well of the 24-well plate. The cells were then incubated for the next three days at 37 °C and 5 % CO_2. To harvest the virus, the supernatant was collected three days later and centrifuged at 600 xg for 7 min at 4 °C to clear any cell debris. The virus containing supernatant was concentrated using Amicon Ultra

100 MW filter tubes. For this the supernatant was added to the upper chamber of the tube and centrifuged at 4000 xg for 10 to 20 min at 4 °C. This step was repeated until the whole supernatant containing the virus was concentrated. The virus preparation was then aliquoted into 20 to 50 µL aliquots and stored at -20 °C until use.

3.6.2.2 Titration of an HIV-1 JRFL-iGFP virus stock

To titrate the virus, TZM-bl cells were harvested and seeded into 12 wells of a 96-well plate at a concentration of $1x10^4$ cells per 200 µL complete DMEM. The cells were left to incubate at 37 °C and 5% CO_2 until they were 50-60 % confluent. An aliquot of the frozen HIV-1 JRFL-iGFP virus stock was thawed and a 5-fold dilution series (1:5-to-1:3125) was prepared in complete DMEM with additional 2 µg/mL dextran in each tube. The media was removed from the cells and replaced by 50 µL of the virus dilutions. All infections were performed in duplicates. As a negative control, two wells were challenged with complete DMEM and dextran. The cells were incubated with the virus for 1 hour in the incubator and an additional 50 µL of complete DMEM was added to each well followed by incubation for another two days under the same conditions. After two days the supernatant was removed and the cells were rinsed with PBS. The fixation was carried out with 2 % formaldehyde for 20 min at 4 °C followed by two washes with PBS. To stain the cells 100 µL of HIV-1 titration staining solution (0.5 mg/mL X-gal, 4 mM potassium ferrocyanide, 4 mM potassium ferricyanide, 2 mM $MgCl_2$ in PBS) was added to each well and left to incubate for 2 hours at 37 °C and 5% CO_2. To determine the virus concentration the number of blue cells were counted in each well using a light microscope. The mean number of blue cells for each virus dilution was calculated and multiplied by the dilution factor. The calculated values indicate the number of infectious viral particles per 1 µL.

3.6.3 SIV_{mac}-VLP stock

3.6.3.1 Preparation of an SIV_{mac}-VLP stock

To prepare SIV_{mac}-VLPs, $1x10^5$ 293T cells were seeded per well of a 24-well plate in complete DMEM. The cells were left to grow until the wells were 70 to 80 % confluent. Cells were transfected with pSIV3 and pVSVg plasmids for SIV_{mac}-VLP

production. For transfection the following mixture was prepared and the reagents were added in the order they appear in the list.

Table 3. 2 **Transfection mix for SIV_{mac}-VLP synthesis**

Reagent	Volume
DMEM serum-free	46.117 µL
FuGENE®	3.375 µL
0.67 µg pSIV3 [1635 ng/µL]	0.4 µL
0.33 µg pVSVg [4336 ng/µL]	0.08 µL
0.125 µg pAdVAntage™ vector [5836 ng/µL]	0.028 µL
Final volume	*50 µL*

The mixture was then incubated for 15 min at room temperature and 50 µL were added drop by drop to each well of the 293T cells. The cells were then incubated for the next three days at 37 °C and 5 % CO2. To harvest the SIV_{mac}-VLPs, the supernatant was collected and centrifuged at 600 xg for 7 min at 4 °C to clear any cell debris. The virus containing supernatant was concentrated using Amicon Ultra 100 MW filter tubes. For this the supernatant was added to the upper chamber of the tube and centrifuged at 4000 xg for 10 to 20 min at 4 °C. This step was repeated until the whole supernatant containing virus was concentrated. The SIV_{mac}-VLP solution was then aliquoted into 20 to 50 µL aliquots and stored at -20 °C.

3.6.3.2 Determination of the RT activity of an SIV_{mac}-VLP stock

The titration of the SIV_{mac}-VLPs was done using the colorimetric reverse transcriptase assay (Roche Applied Science) and carried out according to the manufacturer's protocol. In principle, this assay uses the ability of the RT (of the SIV_{mac}-VLPs) to synthesise DNA from a hybrid poly (A) x oligo $(dT)_{15}$ as primer and template. The nucleotides used for this reaction are digoxigenin- and biotin-labelled and are incorporated in an optimal ratio into the same DNA molecule synthesised by the RT. The synthesised DNA is then detected following the principle of a sandwich ELISA, where the biotin-labelled DNA binds to a streptavidin-coated plate and an α-

digoxigenin-peroxidase antibody is added, which also binds to the DNA molecule. To finally quantify the RT activity, the peroxidase substrate 2,2'-azino-bis(3-ethylbenzthiazoline-6-sulphonic acid) is added. The peroxidase catalyses the reaction and thereby a coloured product is formed, which can be detected using an ELISA reader. The absorbance of the sample is directly correlated to the RT activity in the sample.

3.7 Animals

3.7.1 Infection with FV

Mice were i.v. infected into the lateral tail vein using a 27G-hollow needle. For this the virus stock was thawed, centrifuged at 17,000 xg for 5 min and the supernatant diluted with PBS to reach the required concentration. Usually $2x10^4$ SFFU of FV were used for acute infection experiments. For chronic infection experiments $1.5x10^4$ SFFU of FV containing LDV were used.

3.7.2 Adoptive cell transfer

To transfer cell populations, the desired cell population was isolated from the spleen and the lymph nodes of naïve mice utilising the MACS technology (see 3.12) and diluted to the needed cell concentration in PBS. The cells were then injected i.v into the mouse through the lateral tail vein using a 27G-hollow needle.

3.7.3 Intraperitoneal injection (i.p.)

The *in vivo* depletion antibodies were administered via i.p. injection. To do this, mice were gently grasped by the skin at the back of the neck and the tail was held back. The mice were then brought into a tilted position with their ventral side exposed. In this position internal organs are not harmed by the injection. The injection was done with a 27G-hollow needle in a 45° angle into the lower abdomen and slowly administered.

3.7.4 *In vivo* depletion of cell populations

To deplete cell populations *in vivo*, the supernatant of different hybridoma cell lines producing the desired antibody (or purchased depletion antibodies) were injected i.p.. For depletion of $CD8^+$ cells, the supernatant of the cell line YTS 169.4 was used and 500 µL were administered every two days starting at different time points post FV infection. For the depletion of NK and NKT cells, the supernatant of the cell line PK136 was used and 300 µL were administered every four days starting at the day of FV infection. TCR-$V\beta5^+$ T cells were depleted using a purchased TCR-Vβ5 depletion antibody at a concentration of 300 µg per i.p. injection. This i.p. injection was only done once four days after FV infection. The depletion efficiency was assessed via cell specific markers using flow cytometry.

3.7.5 Blocking of CD73 with AMPCP

To block CD73 *in vivo*, 200 µg of AMPCP dissolved in PBS was administered i.p. every three days starting at six dpi.

3.7.6 Treatment with TNFα

To treat mice with different kinds of TNFα (mbTNFα and solTNFα), they were injected twice with either mbTNFα or solTNFα every other day via i.p. injection. For mbTNFα, 25 µg per injection dissolved in sterile H_20 and for solTNFα 100 µL cell culture supernatant were used.

3.7.7 Dissection of mice

To prepare mice for dissection they were sacrificed using cervical dislocation after anaesthesia with isofloran. The mice were then fixed with 23G-hollow needles and cut open carefully not to destroy any internal organs. First the cervical, axillary and inguinal lymph node were removed. Next the peritoneal cavity was opened and the spleen removed by excising both blood vessels. To obtain the bone marrow, both hind legs were cut loose and the flesh removed. All organs and tissues were stored in PBBS on ice until required.

3.7.8 Preparation of spleen or lymph node cell suspensions

Spleen and lymph nodes were homogenised through a 70 µm cell strainer using the plunger of a syringe. All remaining cells were washed from the strainer using PBBS. Of these cell suspensions an aliquot was removed to count the cells. Cells were centrifuged at 520 xg for 10 min and the supernatant was discarded. Based on the cell number, cells were re-suspended in an appropriate volume of buffer suitable for the down-stream application.

3.7.9 Preparation of bone marrow cell suspensions

A bone marrow cell suspension was achieved by flushing the femur and tibia of each hind leg with a 23G-hollow needle with PBBS. An aliquot for counting the cells was taken. The cells were subsequently centrifuged at 520 xg for 10 min and the supernatant discarded. Based on the cell number the cells were re-suspended in an appropriate volume of buffer suitable for down-stream applications.

3.7.10 Preparation of DCs from a bone marrow cell suspension

For generating mouse DCs, the bone marrow from a naïve mouse was prepared as described above and re-suspended in 50 mL mouse DC media supplemented with 1 ng/mL mrIL4 and 5 ng/mL mrGM-CSF. 10 mL were then seeded into a 10 cm cell culture dish and incubated at 37 °C and 5 % CO_2 for seven days. After 24 hours an additional 10 mL of supplemented mouse DC media was added to the culture. Five days after seeding, the cells were washed once by centrifuging the cell culture media at 400 xg for 6 min (these cells are non-adherent). The cells were then re-suspended in 20 mL supplemented mouse DC media and cultured for another two days. Seven days after initially seeding the bone marrow cells, the differentiated DCs could be used for other applications.

3.8 Infectious centre assay (IC assay)

To detect the number of infectious centres of FV-infected cells, $2x10^4$ *Mus dunni* cells in 3 mL complete RPMI were seeded into each well of a 6-well plate. The cells were then incubated over night at 37 °C with 5 % CO_2. The following day mouse cell suspensions (derived from spleen or bone marrow of FV-infected mice) were prepared, a 10-fold dilution series formed (starting with $1x10^7$ cells) and 1 mL of each

dilution was added to a single well of the 6-well plate. The plate was then incubated for three days under the same conditions. During this incubation period, infected cells spread the infection to the *Mus dunni* cells via cell-cell contacts. Cell division of the *Mus dunni* transfers the provirus to their daughter cells and an infected cell colony forms. To visualise the infected cell clones, the media on the *Mus dunni* cells was discarded and the cells were fixed by overlaying them with 95 % ethanol for 10 min. The ethanol was discarded and the plates washed twice with PBS plus 0.1 % BSA. The cells were then incubated for 2 hours at room temperature with 600 µL of culture supernatant of an AB720 producing hybridoma cell line. This hybridoma cell line produces an antibody (AB720) which specifically binds to the Env-protein of F-MuLV recognising FV-infected cells.

After two hours the plates were washed twice with PBS plus 0.1 % BSA. 600 µL of a 1:500 dilution (into PBS) of secondary antibody conjugated to HRP (goat-α-mouse-IgG2b-HRP (0.05 mol/L)) was added to the cells for 90 min. After the incubation, the antibody was discarded and the plates were washed twice with PBS. The cells were then incubated for 20 min in the dark with 2 mL of fresh AEC substrate solution. A red precipitate is formed by conversion of the soluble substrate AEC in the substrate solution into an in-soluble precipitate catalysed by the HRP coupled to the secondary antibody. The substrate solution was discarded and the plates were washed twice with H_2O. After the plates had dried over night the red spots in each well were counted and calculated for $1x10^6$ added cells. To determine the IC count per $1x10^6$ spleen or bone marrow cells the mean off all dilutions was formed.

As a control an additional plate of *Mus dunni* cells was prepared a day before the experiment. Three wells of this plate were left uninfected and the other three wells were infected with free F-MuLV (with 8 µg/ml polybrene A to facilitate virus uptake). The appearance of red dots after developing the assay indicated functionality.

3.9 Human samples

3.9.1 Human peripheral blood mononuclear cell (PBMC) isolation

Blood samples were obtained from Hoxworth Blood Bank Center (Cincinnati, OH, USA). 30 mL of total blood of healthy donors was poured into 50 mL falcon tubes containing 10 mL PBS. Ficoll was added after mixing the blood with the PBS by

slowly pipetting 10 mL Ficoll underneath the blood-PBS mixture, to prevent mixing with the blood-PBS solution. The tubes were then spun at 800 xg for 25 min at room temperature and slowed down without brakes to not destroy the layers that had formed. After centrifugation, three layers formed with the PBMCs on top of the intermediate Ficoll layer. The PBMCs were harvested with a pipette and transferred into a fresh 50 mL tube. To wash the PBMCs, cells harvested from 2 Ficoll tubes were combined and topped up with PBS to a volume of 50 mL followed by centrifugation at 600 xg for 7 min at 4 °C. PBMCs were then re-suspended in 5 mL PBS and counted.

Blood samples of HIV-1 infected subjects enrolled in the clinical trial for treatment with tenofovir/emitricitabine (RT-inhibitor) 300/200 mg tablets and lopinavir/ritonavir (protease inhibitor) 400/100 mg tablets (twice daily), were prepared in the same way.

3.10 Stimulation of cells

3.10.1 Re-stimulation of freshly isolated mouse cells for cytokine production

For the intracellular staining of cytokines (like TNFα, IFNγ and IL2), freshly isolated mouse cells were re-stimulated *in vitro* to provide an enhanced signal. The wells of a Nunc MaxiSorp 96-well plate were coated with 50 µL purified α-CD3 antibody (10 µg/mL) in sodium carbonate coating buffer. The coating of the plate was done for 2 hours at 37°C or overnight at 4°C. After α-CD3 coating, the plate was washed three times with PBS. For re-stimulation of freshly isolated mouse cells, $3x10^3$ cells were added to each well in duplicates. The cells were re-suspended in complete RPMI supplemented with 50 µM β-ME, 2 µg/mL purified α-CD28 and 2 µg/mL BFA and incubated for 5 hours at 37°C. After re-stimulation, the cells were transferred into new wells and processed for antibody staining. For controls, a sample was left un-stimulated but stained with intracellular antibodies and a re-stimulated sample did not get stained with the intracellular antibodies.

3.10.2 Peptide-stimulation of mouse $CD8^+$ T cells with peptide-loaded mouse DCs for detection of mbTNFα

Bead-isolated $CD8^+$ T cells from naïve TCR^{tg} mice were incubated for different lengths of time with F-MuLV $CD8^+$ T cell peptide loaded onto mouse DCs in complete

RPMI. DCs were loaded with 5 µg peptide (AbuAbuLAbuLTVFL) for 1 hour at 37 °C. After loading, the DCs were washed, counted and seeded at a ratio of 1 DC to 5 $CD8^+$ T cells. After incubation the cells were stained for mbTNFα as described (3.11.2 Staining of mouse cells for flow cytometry).

3.10.3 Unspecific stimulation of mouse $CD8^+$ T cells α CD3/α CD28 beads for detection of mbTNFα

Bead-isolated $CD8^+$ T cells from naïve iRhom2-WT or iRhom2-KO mice were incubated for different lengths of time with α-CD3/α-CD28 mouse T cell stimulation dynabeads in complete RPMI. Before incubation with the cells the beads were washed once on a magnetic holder and re-suspended in the desired volume of complete RPMI. The beads were then added to the cells. After incubation, the cells were stained for mbTNFα as described (3.11.2 Staining of mouse cells for flow cytometry).

3.10.4 *In vitro* stimulation of human PBMCs

For *in vitro* stimulation of human PBMCs, the cells were thawed and re-suspended in complete RPMI. While half of the cells were left un-stimulated, the rest were stimulated with α-CD3/α-CD28 human T cell stimulation dynabeads at a 1:1 ratio. The beads were washed once on a magnetic holder and re-suspended in the desired volume of complete RPMI. The beads were then added to the cells and all cells (stimulated und un-stimulated) were seeded in 24-well-plates at a concentration of $1x10^6$ cells per well and cultured for 24 hours at 37 °C and 5% CO_2.

3.11 Multicolour flow cytometry

3.11.1 Principle of flow cytometry

Flow cytometry can be used for the characterisation and quantification of heterogeneous cell populations in solution. With this technique it is possible to detect surface and intracellular molecules using fluorescence labelled antibodies or fluorescently tagged proteins. The cells are labelled and prepared and are then measured on a fluorescence-activated cell sorting (FACS) machine. The main components of a FACS analyser can be divided in the fluidic system, the optical system and the detection system.

In a cell solution the cells are randomly distributed in a three dimensional space. To detect the fluorescence signal of labelled molecules they need to be focused in a stream of single cells. The fluidic system is responsible for this process, whereby the cell suspension is taken up by the sample injection port and then usually hydrodynamically focused (other methods exist, but are less common) (Figure 3. 1).

After focusing, the cells pass through the optical system and can be analysed. FACS machines are equipped with different lasers, mirrors and filters. Two initial parameters are acquired by all FACS analysers: forward scatter (FSC) and side scatter (SSC). To measure the size of cells, light that is scattered in a forward direction (FSC) is used. The granularity of cells is measured by the SSC channel, which is the light measured at a 90° angle. Combining the information of the FSC and the SSC is used for a pre-selection of cell types in a heterogeneous sample (Figure 3. 1).

If a FACS antibody labelled cell passes through a light beam emitted by a single laser, the different fluorophores sensitive to that specific wavelength of light are specifically excited. When the electrons in the fluorophores become excited by the laser light they are lifted to a higher energy level and shortly after this they fall back to the original energy state emitting energy in the form of photons. The wavelength of these released photons is longer than that of the excitation light source, which is part of the phenomenon known as Stoke´s shift. The emitted light is reflected, filtered and detected with specific sets of optical mirrors, filters and detectors. The mirrors reflect the light onto filters, which filter light of specific wavelength. Short pass or long pass filters only allow light under or above a certain wavelength (respectively) to pass and band pass filters are used to filter a certain range of wavelengths (Figure 3. 1).

The emitted and filtered light is then detected by the detectors (usually photomultiplier tubes (PMTs)). These detectors measure the amount of photons and their output signal is proportional to the amount of antibody bound to the cell. This type of measurement provides the necessary information to quantify and characterise the cells within a sample. The optical signal is then amplified and converted into an electric signal which can be visualised in the analysis software (Figure 3. 1).

Multicolour flow cytometry is made possible by using different fluorophores which emit at wavelengths that can be discerned from each another. In this thesis an LSR II with four lasers (488 nm, 633 nm, 355 nm and 405 nm) and the software FACS DiVa (BD bioscience) and FlowJo7.6.5 (Treestar) were used for acquiring and analysing, respectively. The principle of a FACS machine is shown in Figure 3. 1.

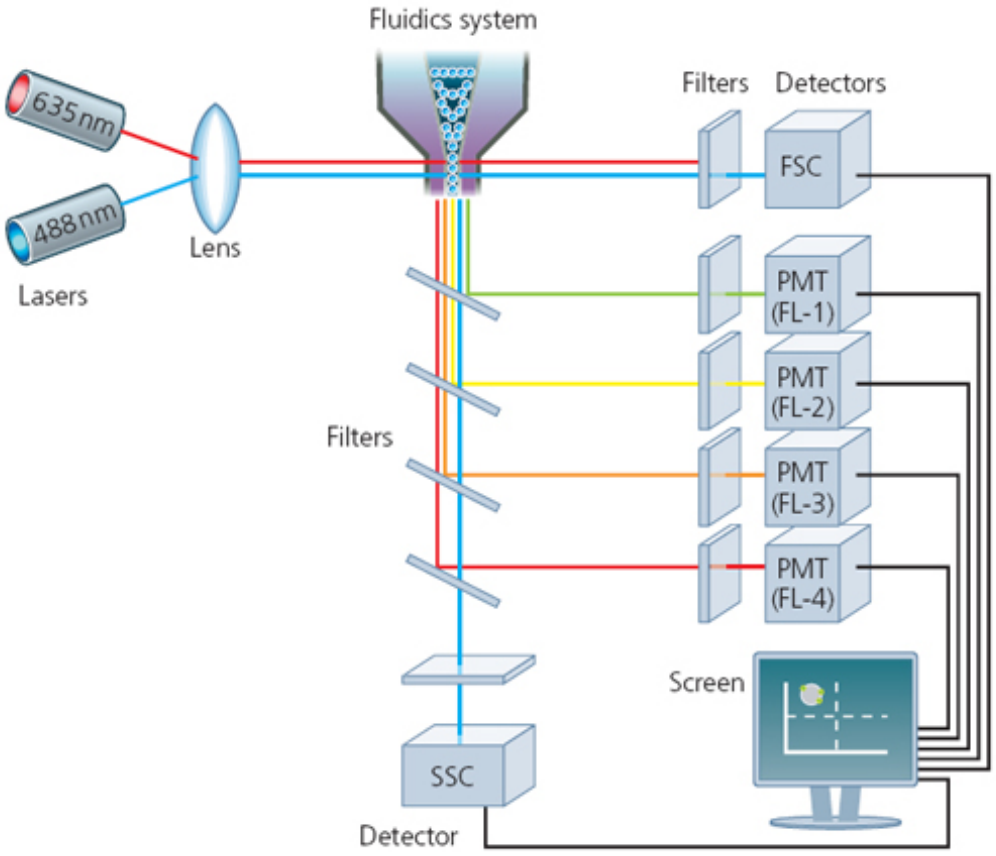

Figure 3. 1 **Schematic showing the principles of the optical and detection systems of a flow cytometer.** Two lasers (635 and 488 nm) send light trough the sample. The light emitted by the sample is then isolated by different filters and sent to the different PMT detectors. The PMT detectors transform and enhance the optical signal into an electric signal, which can then be visualised in the analysis software on a computer. (http://www.abdserotec.com/flow-cytometry-signal-processing.html; 10.02.2014)

It is also possible to sort cells, for this method cells pass through the above described system and are immediately characterised by previously established parameters. For sorting, the fluidic stream is broken into droplets, containing a cell each. These droplets then become charged by passing through an electric field and can be diverted into collection tubes by plates of opposite polarity. The principle of cell sorting is shown in Figure 3. 2.

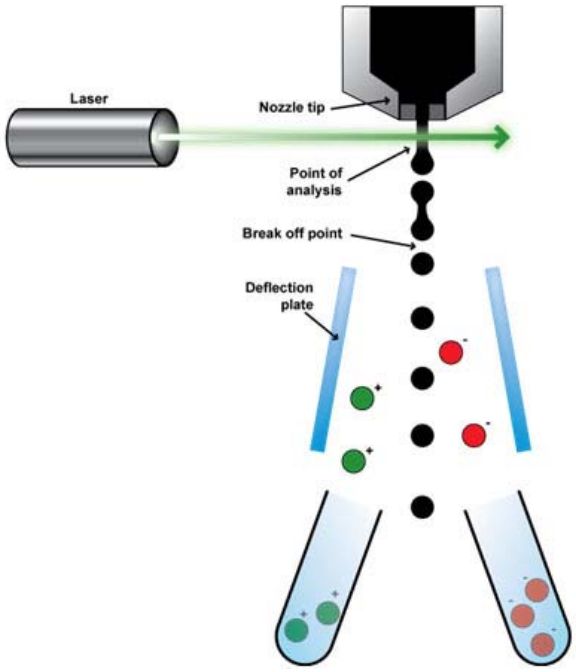

Figure 3. 2 **Schematic showing the principles of cell sorting.** After passing through the laser system, the flow stream breaks up into droplets containing one cell (under optimal conditions). The droplets become charged and are diverted into different collection tubes by the deflection plates. (http://www.abcam.com/index.html?pageconfig=resource&rid=12803, 10.02.2014)

3.11.2 Staining of mouse cells for flow cytometry

For flow cytometry cell staining of mouse cells usually 3-7x10^6 cells per sample of freshly isolated mouse cells were transferred into a well of a 96-well U-bottom plate and washed with the addition of 100 µL FACS buffer at 520 xg for 3 min at 4 °C. The supernatant was discarded by flicking the plate. All following steps were carried out in the dark whenever possible.

3.11.2.1 Extracellular stain of mouse cells

An antibody mix was prepared in 50-100 µL FACS buffer and added to the cells. The cells were re-suspended in the antibody mix and incubated for 15 min at room temperature or 30 min at 4 °C. After incubation, the cells were washed by addition of 100 µL FACS buffer per well and spun at 520 xg for 3 min. The cells were then either re-suspended in FACS buffer for further processing or directly transferred into FACS tubes for measurement on the LSRII or fixed as described below. For the analysis of acquired mouse FACS samples first live single cells were gated to out-gate any debri and get a clean population for the performance of subsequent analysis. This procedure was the same for all FACS samples.

3.11.2.2 Fixation of mouse cells

Depending on the down-stream intracellular stain performed, the cells were either fixed with Cytofix/Cytoperm from BD or with the Foxp3 staining set from eBioscience. If only cytoplasmic molecules were to be stained, the Cytofix/Cytoperm kit was used. For this the cells were re-suspended in 100 µL fixing buffer and incubated for 5 to 15 min at room temperature. Next the cells were washed with addition of 100 µL Cytofix/Cytoperm wash buffer and centrifuged at 700 xg for 4 min and processed for down-stream applications

If nuclear molecules were to be stained, the Foxp3 staining set was used. The cells were re-suspended in 100 µL Foxp3 Fix/Perm fixing solution which was prepared according to the manufacturer's instructions (1:4 of Foxp3 Fix/Perm concentrate into diluent). The cells were left to fix for 2 to 4 hours at 4 °C. To stop the reaction 100 µL Foxp3 Fix/Perm wash buffer was added to each well and the cells were centrifuged at 700 xg for 4 min at 4°C and processed for down-stream applications.

For the staining of mbTNFα only fixation with 4 % formaldehyde for 10 min at 4 °C was necessary. The cells were then subsequently washed with the addition of FACS buffer and centrifuged at 700 xg for 4 min. Subsequently the cells were re-suspended in FACS buffer for this application and measured immediately on the LSRII.

3.11.2.3 Intracellular stain of mouse cells

For intracellular staining, an antibody mix was prepared in 50-100 µL of either Cytofix/Cytoperm wash buffer, for cytoplasmic molecule staining, or Fix/Perm wash buffer (Foxp3 staining set), for nuclear molecule staining. The cells were re-suspended in the antibody mix and stained for 30 min at 4 °C and, after addition of 100 µL of the appropriate buffer, centrifuged at 700 xg for 4 min. Subsequently, the cells were re-suspended in FACS buffer and transferred into FACS tubes for measurement on the LSRII. Typically GzmB, TNFα, IFNγ and IL2 were stained using the Cytofix/Cytoperm kit, whereas the stain of Foxp3, Helios and Ki67 was typically performed with the eBioscience Fix/Perm kit.

3.11.2.4 Tetramer class I and class II stain

A method to detect small populations of virus-specific $CD8^+$ or $CD4^+$ T cells is by the use of specific tetramers. MHC class I and class II-tetramers consist of four peptide-MHC class I or II-complexes, respectively, which are linked by biotin-streptavidin. The complex can be detected via conjugated fluorophores in a flow cytometer. The peptide used to build the tetramer complex is only bound by the TCR of specific $CD8^+$ or $CD4^+$ T cells in combination with the MHC class I or class II, respectively. A schematic of the MHC class I and class II tetramers are shown in Figure 3. 3.

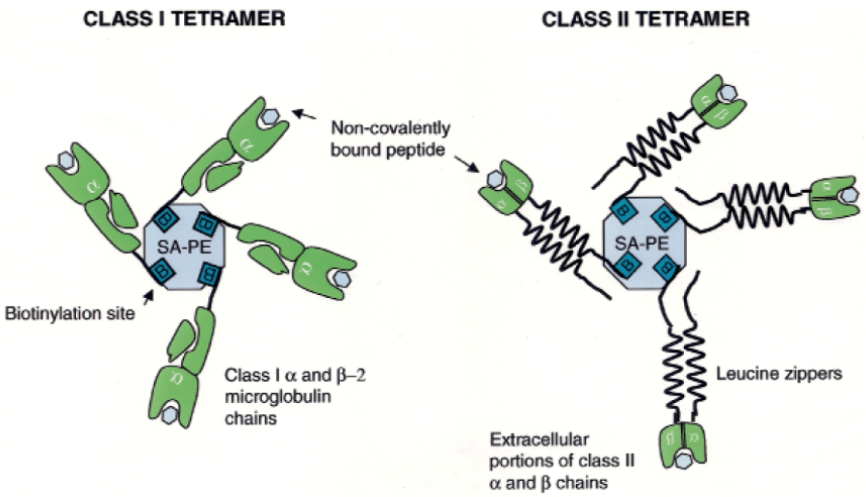

Figure 3. 3 **Schematic showing the organisation of MHC class I or class II tetramers.** MHC class I tetramers (left) and MHC class II tetramers (right) consist of four MHC class I or class II molecules, respectively, linked via biotin (B) to a streptavidin (SA) on the fluorophore (PE in this case). The MHC complexes are loaded with a specifically chosen peptide. (41)

The tetramer class I stain was done as described for the extracellular flow stain with a dilution of 1:200. The tetramer class I stain was also robust to fixation with Cytofix/Cytoperm for 8 min.

The tetramer class II stain was carried out by first blocking the cells with 10 µL FC block (1:20 in RPMI) for 5 min at room temperature. Subsequently the cells were incubated with a 1:100 tetramer class II solution in complete RPMI for 3 hours at 37 °C and 5% CO_2. After incubation the cells were washed and stained for other extracellular markers (as described above) and analysed without fixation. Tetramer II specific $CD4^+$ T cells were detected by gating on $CD4^+CD11b^-$ T cells.

3.11.2.5 Sample preparation and stain for detection of incorporated bromodeoxyuridine (BrdU)

To determine the proliferation of cells *in vivo*, mice were fed with BrdU in their drinking water. BrdU is a thymidine analogue which becomes integrated into the DNA while the cells are in the S-phase of the cell cycle. Mice were fed with a freshly prepared 0.8 mg/mL BrdU-drinking water solution every day for three days before sacrifice. To determine cell proliferation the mouse organs of interest were prepared as described above and an extracellular stain was carried out if needed. The staining for BrdU was done according to the manufacturer's instructions. In short: the cells were washed with FACS buffer at 520 xg for 3 min and fixed with the supplied fixation reagents in two steps. Then, the DNA was digested with DNase provided in the kit for an hour at 37 °C. The intracellular staining was done with 0.5 µL α-BrdU-FITC antibody for 30 min at 4 °C using the supplied buffer. The cells were then washed with the supplied buffer and prepared for FACS measurement in FACS buffer.

3.11.3 Stain of human PBMCs for flow cytometry

For FACS staining the cells were either harvested from a culture or used freshly thawed and were transferred into the wells of a 96-well U-bottom plate (usually $1x10^6$ cells were used). To wash the cells, the plate was centrifuged at 700 xg for 4 min, the supernatant removed with a pipette and washed with 200 µL PBS. For surface staining the cells were carefully re-suspended in 25 µL FACS buffer with the addition of 20 µg/mL hIgG and incubated for 10 min at 4°C in the dark. All following steps were carried out in the dark as much as possible. The appropriate concentration of surface-stain antibody-cocktail was added and the cells were left to stain for 30 min at 4 °C. Next, the cells were washed with 200 µL FACS buffer and centrifuged at 700 xg for 4 min at 4 °C. Again, the supernatant was carefully removed using a pipette. To prepare the cells for intracellular staining the Foxp3 staining kit was used. 200 µL of Foxp3 Fix/Perm fixing solution was used to fix the cells for 30 min at 4 °C. The cells were then washed as before and re-suspended in 10 µL Foxp3 Fix/Perm wash buffer supplemented with normal rat-serum for intracellular Foxp3 staining for 15 min

at 4 °C. After this the antibodies for intracellular staining were added and the cells were stained for 30 min at 4 °C. Cells were then washed with the addition of 100 µL Foxp3 Fix/Perm wash buffer as before and re-suspended FACS buffer to measure on the LSRII.

3.11.4 Gating strategy of human Tregs for flow cytometric analysis

To gate on human Tregs a special strategy was utilised. The reason for this is that Foxp3 is not only a Treg marker in humans but also a marker for activation. To guarantee that only Tregs were considered, the following gating strategy for flow cytometric analysis was used (see Figure 3. 4):

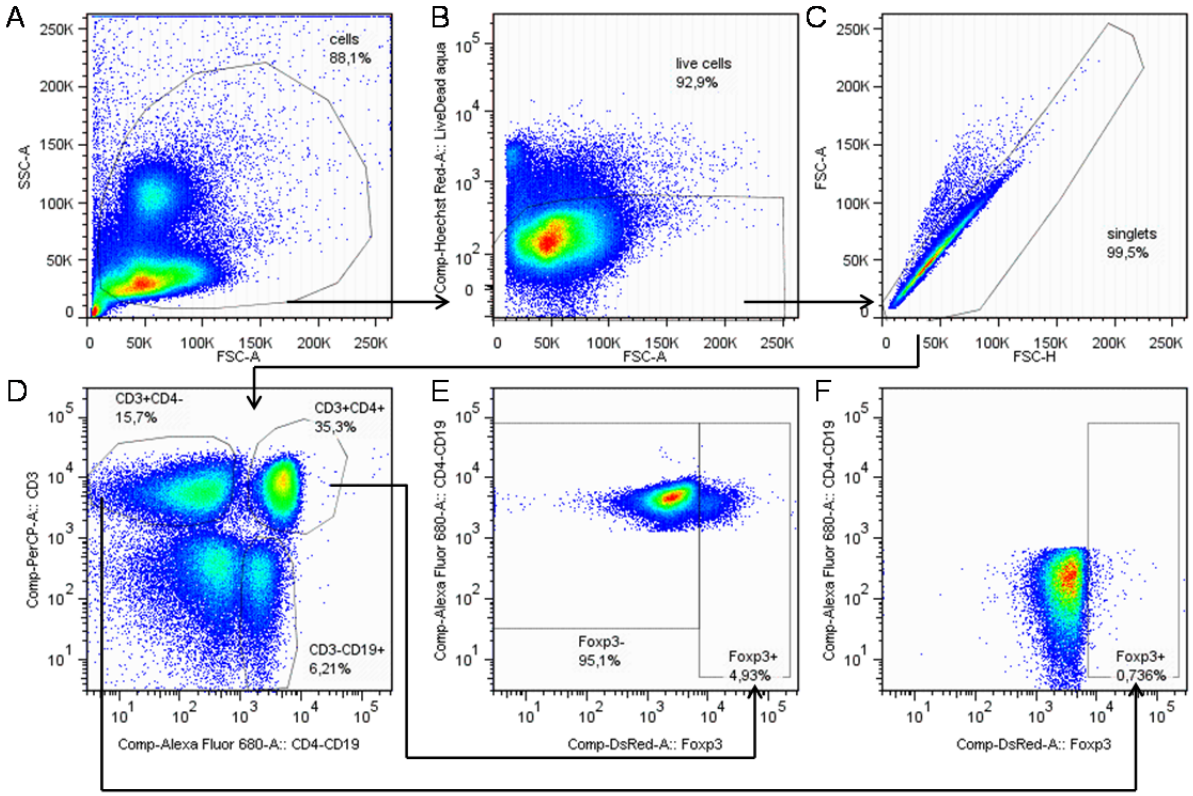

Figure 3. 4 **Gating strategy for human Tregs.** To gate human Tregs firstly **(A)** lymphocytes, **(B)** live cells and **(C)** singlets were identified. **(D)** To separate the different lymphocyte groups CD3, CD4 and CD19 were used for $CD4^+$ T cells ($CD3^+CD4^+CD19^-$), B cells ($CD3^-CD4^-CD19^+$) and $CD8^+$ T cells and NKT cells ($CD3^+CD4^-CD19^-$). **(F)** The $CD8^+$ T cell and NKT cell compartment was used to set the gate for $Foxp3^+$ T cells. **(E)** The same gate was then applied to the $CD4^+$ T cell subset to define $CD3^+CD4^+CD19^-Foxp3^+$ Tregs and $CD3^+CD4^+CD19^-Foxp3^-$ Tcon.

3.12 Cell isolation with the MACS technology

3.12.1 MACS isolation of mouse cells

To isolate mouse $CD4^+$ T cells the mouse $CD4^+$ T cell isolation kit II was used. The antibody mix provided only labels non-$CD4^+$ T cells and therefor the pre-activation of $CD4^+$ T cells is prevented. In summary, the cells were counted and re-suspended in MACS buffer (40 µL buffer per $1x10^7$ cells). To stain all non-$CD4^+$ T cells, a biotinylated antibody cocktail was added (10 µL cocktail per $1x10^7$ cells). The cell suspension was then incubated for 20 min at 4 °C in the dark. An additional volume of 30 µL MACS buffer per $1x10^7$ cells was added. To label the non-$CD4^+$ T cells for magnetic separation they were additionally stained with α-biotin magnetic MicroBeads (20 µL beads per $1x10^7$ cells). The solution was incubated for 20 min at 4 °C in the dark. After the incubation period 10-20 times the labelling volume of MACS buffer was added and the cells were centrifuged for 10 min at 520 xg. After the centrifugation the supernatant was discarded and the cells were re-suspended in up to 500 µL MACS buffer per $1x10^7$ cells. To protect the AutoMACS from clogging the cells were passed through a 30 µm cell strainer before applying to the MACS columns. To enrich $CD4^+$ T cells the Deplete05 programme was used. After enrichment the cells were centrifuged, counted and processed for the necessary down-stream application. A sample for determining the CD4 T cell purity by FACS analysis was always taken.

For the isolation of mouse $CD8^+$ T cells mouse CD8α (Ly-2) MicroBeads were used. Using these beads $CD8^+$ T cells are directly labelled. In general, the cells were counted and re-suspended in MACS buffer (90 µL buffer per $1x10^7$ cells) and the CD8α MicroBeads were added (10 µl beads per $1x10^7$ cells). The mix was incubated for 20 min at 4 °C in the dark and subsequently re-suspended in 10-20 times the labelling volume of MACS buffer and centrifuged for 10 min at 520 xg. Finally, the supernatant was carefully discarded and the cells were processed as described above. For magnetic separation of $CD8^+$ T cells the Possel05 programme was used.

3.12.2 CD14$^+$ cell enrichment from human PBMCs

For the isolation of CD14$^+$ cells from human PBMCs the cells were either used after thawing or directly after PBMC isolation. The cell number was determined and the cell pellet was re-suspended in 12 µL MACS buffer per 1x10^7 cells. 3 µL of human CD14 MicroBeads were added per 1x10^7 cells and incubated for 15 min at 4 °C in the dark. The cells were washed with MACS buffer and spun at 520 xg for 7 min at 4 °C. In the following the supernatant was discarded and the cells were re-suspended in 1 mL MACS buffer. For separation, LS columns were prepared on a magnet by adding 3 mL of MACS buffer. The cells were then added to the column with 500 µL per column and additional 9 mL of MACS buffer were used to wash off unbound cells. The negative fraction (CD14$^-$ cells) was obtained by collecting the flow through. This fraction was used for further CD4$^+$ T cell separation as described below. To collect the CD14$^+$ fraction the columns were removed from the magnet and placed onto 15 mL tubes. The cells were washed from the columns using 5 mL MACS buffer and a plunger to flush the liquid into the 15 mL tube. The CD14$^+$ cells were then washed and spun at 520 xg for 7 min at 4 °C followed by re-suspension in 1 mL PBS plus 2 % FCS. Depending on the down-stream application the cells were either frozen or used immediately.

3.12.3 CD4$^+$ T cell enrichment from human PBMCs

To obtain CD4$^+$ T cells, the human CD4$^+$CD25$^+$ T cell isolation kit was used. The CD14$^-$ fraction of cells was washed at 520 xg for 7 min at 4 °C, re-suspended in PBS plus 2 % FCS and counted. The cells were then washed again and re-suspended in 40 µL MACS buffer per 1x10^7 cells. 10 µL of CD4$^+$ T cell biotin-antibody cocktail was added to 1x10^7 cells and the mixture was incubated for 10 min at 4 °C in the dark. Following this, additional 30 µL of MACS buffer and 20 µL α-biotin MicroBeads per 1x10^7 cells were added. The cells were further incubated for 10 min at 4 °C and washed and spun at 520 xg for 7 min at 4 °C. After the wash, the supernatant was discarded and the cells were re-suspended in 1 mL MACS buffer. For separation, LS columns were re-constituted on a magnet by adding 3 mL of MACS buffer. The cells were added to the column with 500 µL per column and additional 9 mL of MACS

buffer were used to wash off all unbound cells. The negative fraction ($CD4^+$ cells) was then obtained by collecting the flow through and was centrifuged at 520 xg for 7 min at 4 °C and re-suspended in 1 mL PBS plus 2 % FCS. Depending on the down-stream application the cells were either frozen or used immediately.

3.12.4 $CD4^+CD25^+$ T cell enrichment from human PBMCs

For some applications Tregs ($CD127^{lo}CD25^{hi}$) and Tcon ($CD127^{hi}CD25^{lo}$) cells were sorted. For this, previously collected un-labelled $CD4^+$ T cells were pre-enriched for $CD25^+$ cells using the human $CD4^+CD25^+$ Treg isolation kit. The cell number of $CD4^+$ T cells was determined and the cells were re-suspended in 90 µL MACS buffer and 10 µL CD25 MicroBeads per $1x10^6$ cells followed by incubation for 15 min at 4 °C in the dark. The labelled cells were then washed with MACS buffer and centrifuged at 520 xg for 7 min at 4 °C. The supernatant was discarded and the cells were re-suspended in 1 mL MACS buffer. For separation, LS columns were re-constituted on a magnet by adding 3 mL of MACS buffer. The cells were then added to the column in 500 µL per column and allowed to flow through. The column was washed with 1 mL of MACS buffer and the flow-through was transferred to another re-constituted LS column. The second column was then washed with 1 mL of MACS buffer. The flow-through, the negative fraction ($CD4^+CD25^-$ cells), was collected and centrifuged at 520 xg for 7 min at 4 °C. Next, the sample was re-suspended in 1 mL PBS plus 2 % FCS and kept at 4 °C until the $CD4^+CD25^+$ T cells were sorted.

To collect the $CD4^+CD25^+$ (enriched) fraction both LS columns were removed from the magnet and placed onto a 15 mL tube. The cells were washed from the columns using 5 mL MACS buffer and a plunger to flush the liquid through into the tubes. The $CD4^+CD25^+$ cells were then washed and spun at 520 xg for 7 min at 4 °C and re-suspended in 2 mL PBS plus 2 % FCS.

3.13 Sorting of Tregs and Tcon from human PBMCs

The cells of the $CD4^+CD25^+$ enriched fraction were stained with α-CD8, α-CD25 and α-CD127 (see Table 2. 6 on page 45 for concentrations) for 30 min at 4 °C. After

incubation, the cells were washed with the addition of 8 mL cold PBS plus 2 % FCS and spun at 520 xg for 7 min at 4 °C. The supernatant was discarded and $1x10^6$ cells were re-suspended in 1 mL cold sorting buffer. Subsequently, the pre-enriched $CD4^+CD25^+$ T cells were sorted on a MoFlo cell sorter (Flow core facility at Children's Hospital Cincinnati, Ohio, USA) for $CD25^{hi}CD127^{lo}$ (Tregs) and $CD25^{lo}CD127^{hi}$ (Tcon). After the sort, both fractions were washed and spun at 520 xg for 7 min at 4 °C and re-suspended in 0.5 mL PBS plus 2 % FCS.

3.14 Differentiation of MoDCs from $CD14^+$ cells

$CD14^+$ cells were thawed and counted as described earlier and re-suspended in DC media for human cells (complete RPMI media supplemented with 500 U/mL hrIL4 and 1000 U/mL hrGM-CSF). $5x10^5$ cells per 1 mL were cultured at 37 °C and 5% CO_2 in a well of a 24-well plate. After 3 days, 330 µL of media were replaced with 330 µL of fresh DC media. The cells were cultured for an additional day at 37 °C and 5% CO_2. To guarantee the success of differentiation the cells were frequently checked for a DC-like morphology under a light microscope.

3.15 Infection of MoDCs

On day four of MoDC culture the differentiated DCs in suspension were carefully harvested, washed and centrifuged at 520 xg for 7 min at 22 °C. The cells were re-suspended in 1 mL and counted. According to the cell count, and the number of cells to be infected, the amount of virus required was calculated. In general an MOI of 2-3 was used for HIV-1 JRFL-iGFP and SIV_{mac}-VLPs. To infect the cells, both viruses were added to a small volume of cell suspension in complete RPMI and left to incubate for 1.5 to 3 hours at 37 °C and 5 % CO_2. After incubation, DC media was added and $5x10^5$ cells per 1 mL were plated into a well of a 24-well-plate. The cells were further incubated at 37 °C and 5 % CO_2 for 3 days. The uninfected control cells were treated the same way as the infected cells but minus virus.

3.16 Sorting of infected MoDCs

The infection of MoDCs with HIV-1 is poorly efficient thus the infected MoDCs were enriched using sorting. DCs were carefully harvested four days after infection with HIV-1 JRFL-iGFP and after centrifugation at 520 xg for 7 min (4 °C) were re-suspended in an appropriate volume of sorting buffer. The cells were sorted on a MoFlo cell sorter (Flow core facility at Children's Hospital Cincinnati, Ohio, USA). The gate was set on the GFP^+ population including a bit of the GFP^- population to enrich the sample for HIV-1 JRFL-iGFP infected cells. The uninfected cells were treated in the same way to keep experimental conditions the same and GFP^- cells were sorted. After sorting, the cells were washed with complete RPMI and spun at 520 xg for 7 min at 4 °C, re-suspended in complete RPMI and counted to determine the cell number for subsequent co-cultures.

3.17 Labelling of human Tcon cells with violet tracker

For co-cultures $CD4^+CD14^-$ T cells or $CD4^+CD14^-CD8^-CD127^{hi}CD25^{lo}$ Tcon cells were stained with violet tracker. The cells were washed as described before and re-suspended in 900 µL sterile H_2O. 100 µL of a 1:1000 dilution of violet tracker in H_2O was added and the cells were incubated for 20 min at 37 °C and 5 % CO_2 in the dark. The reaction was stopped by adding 700 µL FCS and 4 mL PBS. The stained cells were then washed, counted and re-suspended in the desired amount of complete RPMI for further culture.

3.18 Co-culture of human cells

The co-culture of human donor cells was done with autologous cells. In general, violet tracker labelled Tcon were co-cultured with sorted infected or un-infected MoDCs and Tregs at a ratio of 10:1:10 ($5x10^5$ Tcon and $5x10^4$ MoDCs and $5x10^4$ Tregs) in 500 µL of complete RPMI (supplemented with 10 µg/mL α-CD3 for stimulation) in 24-well-plates for 36 hours at 37 °C and 5% CO_2. In some cultures the Treg inhibitors α-CTLA4 (10 µg/mL), α-TGFβ (10 µg/mL) and ddADA (200 µM) were used. For this Tregs were incubated 24 hours prior co-culture with 200 µM ddADA, washed subsequently and then co-cultured as described. The other two inhibitors, α-CTLA4 and α-TGFβ, were directly added to the co-culture.

3.19 Acquisition with the Amnis ImageStream

3.19.1 Principle of the Amnis ImageStream

The Amnis ImageStream is a combination of a FACS machine and a fluorescence microscope. In general it works like a FACS machine, but is also combined with the properties of a microscope. Two cameras take pictures of every measured event and these events can then be visualised in the acquiring software INSPIRE and analysed with the statistical software IDEAS. The ImageStream is a useful machine for investigating marker co-localisation, cell morphology, cell-cell interactions and many other applications where the visualisation of cells is necessary. Due to its characteristics as a FACS machine it can measure more events in a faster manner than can be acquired by microscopy alone. These acquired events can be analysed using statistical software with a multitude of different applications. For example the correlation of two markers can be measured as an indicator of co-localisation.

3.19.2 Staining for Amnis ImageStream measurements

After 36 hours the co-cultures were carefully harvested to keep the $CD4^+$:DC clusters intact and transferred into a 96-well U-bottom plate for staining. The plate was centrifuged at 700 xg for 4 min at 4 °C. The supernatant was carefully taken up and the cells were washed again with PBS. For surface staining the cells were carefully re-suspended in 25 µL FACS buffer with the addition of 20 µg/mL hIgG and incubated for 10 min at 4 °C. The appropriate concentration of surface-stain antibodies (α-CD25-BV785 and α-HLA-DR-BV570) was added and the cells were incubated for 30 min at 4 °C in the dark. The cells were washed with 200 µL FACS buffer and centrifuged at 700 xg for 4 min at 4 °C. To prepare the cells for intracellular staining 200 µL of 4 % formaldehyde (methanol free) in H_2O was used to fix the cells for 20 min at 4 °C in the dark. The cells were then washed as before and re-suspended in 50 µL 0.3 % saponin-buffer supplemented with the reagents for intracellular staining (phalloidin-APC). Staining was then done for 30 min at 4 °C. After the staining the cells were washed as before and re-suspended in 100 to 150 µL FACS buffer without bubbles, transferred into 1.5 mL tubes and analysed on the Amnis ImageStream.

4. Results

4.1 Tregs expand during FV infection in the spleen and bone marrow

Previous work has shown that Tregs play an important role in suppressing the effector $CD4^+$ and $CD8^+$ T cell response in FV-infected mice during the acute and chronic phase of infection (84, 144, 339, 340). It has also been shown that Tregs expand in highly infected organs, like the spleen and bone marrow during the acute phase of FV infection (340). Elevated levels of Tregs are still detectable in the spleen during the chronic phase of infection (213). During acute FV infection cytotoxic $CD8^+$ T cells eliminate the majority of infected cells; however the expanded population of Tregs suppresses the cytotoxicity of virus-specific $CD8^+$ T cells. Consequently, incomplete immune clearance results in the establishment of a chronic FV infection. (213, 339-341).

To confirm the results described above the kinetics of Treg expansion after FV infection in B6 mice (20,000 SFFU) was determined in the organs of interest, the spleen and bone marrow. Foxp3 is the master transcription factor for Tregs and in mice exclusively expressed in these (345). The numbers of $CD4^+Foxp3^+$ Tregs per $1x10^6$ live cells in the spleen and bone marrow for different times post FV infection was enumerated (Figure 4. 1 A). The expansion of Tregs peaked at 12 to 14 dpi. Furthermore, the frequency of Tregs in the spleen was much higher than the frequency of Tregs in the bone marrow. In both organs only slightly elevated levels of Tregs were detected at 40 dpi compared to uninfected controls (Figure 4. 1 A).

To investigate the expansion of activated Tregs, Helios, a marker first described for nTregs and now rather classed as a marker of Treg activation, was used. When the percentage of $Foxp3^+Helios^+$ Tregs (activated Tregs) and the percentage of $Foxp3^+Helios^-$ Tregs (non-activated Tregs) was assessed at different time points post FV infection, an expansion of activated Tregs was seen after infection in both the spleen and bone marrow. In the spleen the frequency of activated Tregs peaked at 12 to 14 dpi and in the bone marrow around 12 dpi. In contrast, the frequency of non-activated Tregs did not increase but rather decreased after infection in both organs

(Figure 4. 1 B and C). In conclusion, previous data on Treg expansion during FV infection was confirmed and an expansion of activated, but not non-activated, Tregs that peaked at 12-14 dpi was observed.

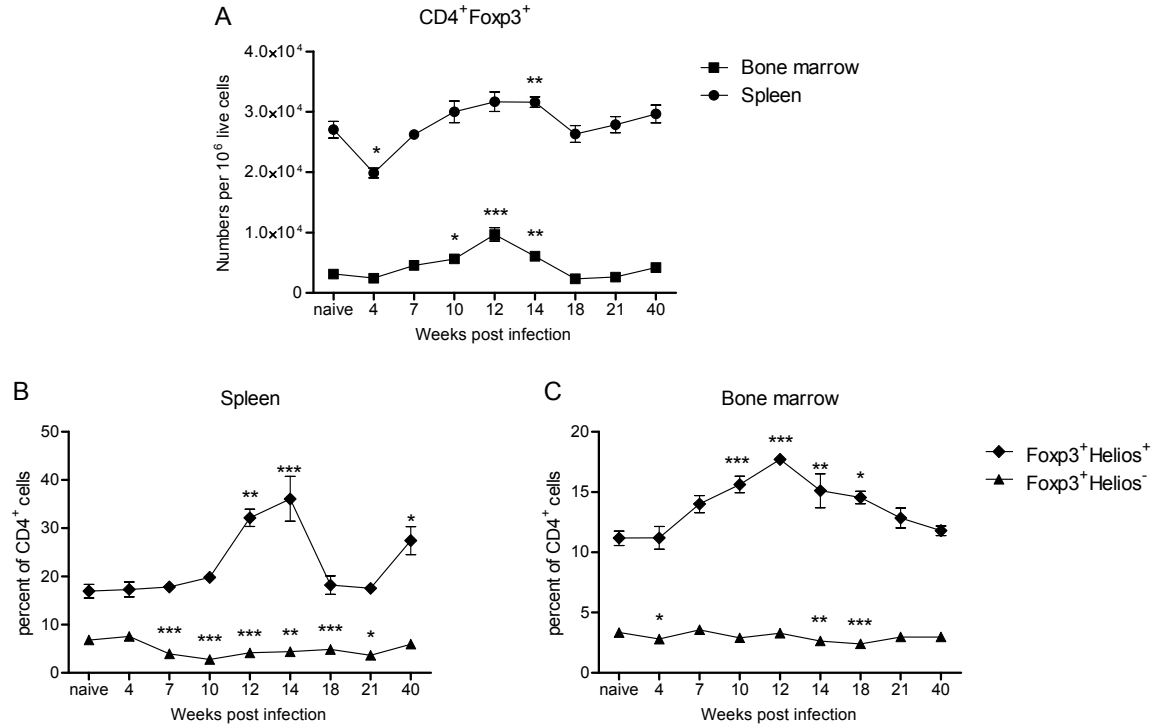

Figure 4. 1 **Time course of Treg expansion in the spleen and bone marrow of FV-infected mice.** B6 mice were infected i.v. with 20,000 SFFU of FV or left un-infected and Treg abundance was measured using flow cytometry for spleen or bone marrow cells at various times post infection. **(A)** The numbers of $CD4^+Foxp3^+$ Tregs per $1x10^6$ live cells in both organs are displayed. The frequencies of activated ($Foxp3^+Helios^+$) and not-activated ($Foxp3^+Helios^-$) Tregs of total $CD4^+$ T cells in **(B)** the spleen and **(C)** bone marrow are shown. At least four mice per group from two independent experiments were analysed. The bars represent the mean and SEM. For statistical analysis a Dunnett's multiple comparison test was carried out with the naïve group as a reference (* < 0.05, ** < 0.005, *** < 0.0005).

4.2 mRNA expression of Treg-associated genes during acute FV infection

As the time course of Treg expansion during FV infection had been delineated, it was important to assess the regulation of various genes associated with Treg activation and function during FV infection and for this purpose microarray data was analysed (data courtesy of Gennadiy Zelinskyy). The samples used for the microarray were $CD4^+CD25^+Foxp3^+$ Tregs isolated from the spleens of naïve mice or the bone marrow of 7 dpi or 15 dpi FV-infected mice (20,000 SFFU). To analyse the data, fold

changes of selected genes were calculated. For this calculation the absolute mRNA chip signals were used and the fold change of naïve to 7 dpi, naïve to 15 dpi and 7 dpi to 15 dpi were calculated. Treg markers of interest with detectable signals were chosen and divided into four different groups: Treg-associated, T cell activation and homing, T cell co-stimulation and inhibition, and T cell proliferation and differentiation. For more details on how the samples were analysed please refer to page 51 (3.1 Evaluation of the microarray data)

Foxp3 and CD25 are classical markers of naïve Tregs and their mRNA levels were only slightly up-regulated after 15 dpi compared to naïve Tregs. Nrp1, a marker for nTregs, remained largely unaltered at 7 dpi and 15 dpi, but Helios showed an increase at 15 dpi. Interestingly, three Treg-associated molecules which are expressed on suppressive Tregs, CD73, CD39 and TNFRII, also showed an increase at 15 dpi compared to naïve Tregs or Tregs at 7 dpi (Table 4.1, page 78,Treg-associated).

Within the different T cell activation and homing markers only the mRNAs of CD103 and CD44 showed an increase 15 dpi after infection, and for CD44 this effect was already detectable at 7 dpi (Table 4.1, page 78, Activation and Homing). In contrast, all but one (PD-L2, only minimal change) mRNAs for co-stimulatory and inhibitory markers showed an increase 15 dpi after infection compared to 0 or 7 dpi (Table 4.1, page 78, Co-stimulatory and Inhibitory).

The mRNA expression of the proliferation marker Ki67 and differentiation marker KLRG1, both showed high fold changes after infection, and this effect was already detected 7 dpi with an even further increase at 15 dpi (Table 4.1, page 78, Proliferation and Differentiation).

In conclusion, mRNA expression was altered for most of the Treg markers studied, the majority of which were up-regulated at 15 dpi but not at the earlier time point 7 dpi. This suggested Treg activation during the late phase of acute FV infection and a differential protein expression in Tregs of infected compared to naïve mice.

Table 4. 1 **Microarray analysis of different genes for Tregs.** Microarray data (data courtesy of Gennadiy Zelinskyy) was used to analyse various mRNA expression profiles in Tregs of naïve and infected mice. RNA of splenic $CD4^+CD25^+GFP^+$ Tregs from naïve $DEREG^{tg}$ mice or bone marrow $CD4^+CD25^+GFP^+$ Tregs of 7 and 15 day infected $DEREG^{tg}$ mice were harvested, and an Affymetric Mouse430_2 chip was used. The fold changes from naïve to 7 dpi, naïve to 15 dpi and 7 dpi to 15 dpi were calculated and are displayed in the table.

Marker	Fold change naïve to 7 dpi	Fold change naïve to 15 dpi	Fold change 7 dpi to 15 dpi
Treg-associated			
CD25	0.81	1.13	1.39
Foxp3	0.80	0.96	1.20
Nrp1	0.98	1.04	1.06
Helios	0.97	2.12	2.20
TNFRII	1.03	2.55	2.48
CD39	1.16	1.76	1.51
CD73	0.60	1.17	1.94
Activation and Homing			
CD127	1.10	1.20	1.09
CD62L	0.53	0.52	0.98
CD103	0.97	2.14	2.20
CD44	2.03	2.36	1.16
CD69	1.03	0.91	0.88
Co-stimulatory and Inhibitory			
ICOS	0.75	1.15	1.53
GITR	0.97	1.62	1.68
CTLA4	0.90	2.10	2.33
PD-1	0.92	1.41	1.53
PD-L1	1.18	1.76	1.49
PD-L2	1.17	1.27	1.08
Proliferation and Differentiation			
Ki67	1.47	3.66	2.49
KLRG1	1.88	3.31	1.76

4.3 Marker profiles of Tregs and Tcon during acute FV infection

To validate the marker profiles suggested by the mRNA expression analysis, the expression of the proteins were investigated using flow cytometry. The aim was to find adequate markers to characterise Treg activation, differentiation and proliferation based on findings known for Tcon. For all the following analyses $CD4^+Foxp3^+$ Tregs and $CD4^+Foxp3^-$ Tcon from naïve mice and mice infected with FV for 12 days, the peak of Treg expansion in the spleen and bone marrow, were compared. B6 mice were infected with 20,000 SFFU of FV and the expression of CD25, as the first identified Treg marker (254), was analysed. As expected, CD25 expression was much higher on Tregs compared to Tcon (Figure 4. 2 A and B). However, no increase was seen in the expression levels of CD25 on Tregs or Tcon after FV infection (Figure 4. 2 A and B). In contrary, in the bone marrow a lower frequency of Tregs expressing CD25 was detectable for infected mice when compared to naïve mice (Figure 4. 2 B). The results confirm that high expression of CD25 is a hallmark of Tregs but not a useful marker to distinguish activated from non-activated Tregs.

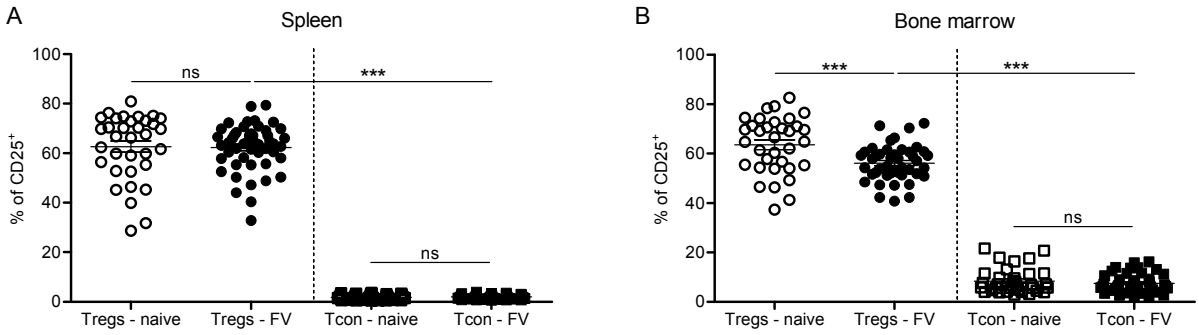

Figure 4. 2 **Expression of CD25 on Tregs and Tcon in naïve and FV-infected mice.** B6 mice were infected i.v. with 20,000 SFFU of FV or left un-infected and the expression of CD25 was measured on Tregs ($CD4^+Foxp3^+$) and Tcon ($CD4^+Foxp3^-$) using flow cytometry for **(A)** spleen or **(B)** bone marrow cells at 12 dpi. Multiple independent experiments were carried out, with each dot representing a single mouse. The bars represent the mean and SEM. For statistical analysis a Student's t-test was used (ns not significant and *** < 0.0005).

To analyse the activation profile of Tregs in comparison to Tcon, selected T cell activation (CD69, CD43, CD11a and CD44) and homing markers (CD62L and CD103) were investigated in naïve or mice infected with FV for 12 days by flow cytometry. The most common T cell activation (CD69, CD43, CD11a and CD44) and homing (CD62L and CD103) markers were chosen.

A higher frequency of $CD43^+$ and $CD11a^+$ Tregs was observed in the spleen of acutely infected mice compared to naïve mice (Figure 4. 3 B and C, left side). Moreover, in the bone marrow higher frequencies of $CD69^+$, $CD43^+$, $CD11a^+$, $CD44^+$ and $CD62L^-$ Tregs in acutely infected mice compared to naïve mice were detected (Figure 4. 3 A – E, right side). However, no difference in the percentage of Tregs expressing CD103 was found between naïve and infected mice in either organ (Figure 4. 3 F). A similar activation profile after infection was observed for Tcon from the spleen or bone marrow (Figure 4. 3 B – E). This confirms an activated phenotype for both: $CD4^+Foxp3^+$ Tregs and $CD4^+Foxp3^-$ Tcon, in the spleen and bone marrow of FV-infected mice.

Interestingly, in the spleen from FV-infected mice, even higher frequencies of activated Tregs compared to Tcon were found. This observation was not entirely true for the bone marrow, where Tregs showed lower ($CD43^+$, $CD11a^+$, $CD44^+$ and $CD62L^-$) as well as higher ($CD69^+$ and $CD103^+$) frequencies of activated cells compared to Tcon. This hinted towards a stronger activation of Tcon in the bone marrow (Figure 4. 3 A – F, left and right).

In conclusion, the well described activation and homing markers of Tcon were also expressed on Tregs and up-regulated upon FV infection. The use of CD11a and CD43 showed to be the most reliable indication of Treg activation, however, CD69, CD44 and CD62L can be used but with restriction to bone marrow cells.

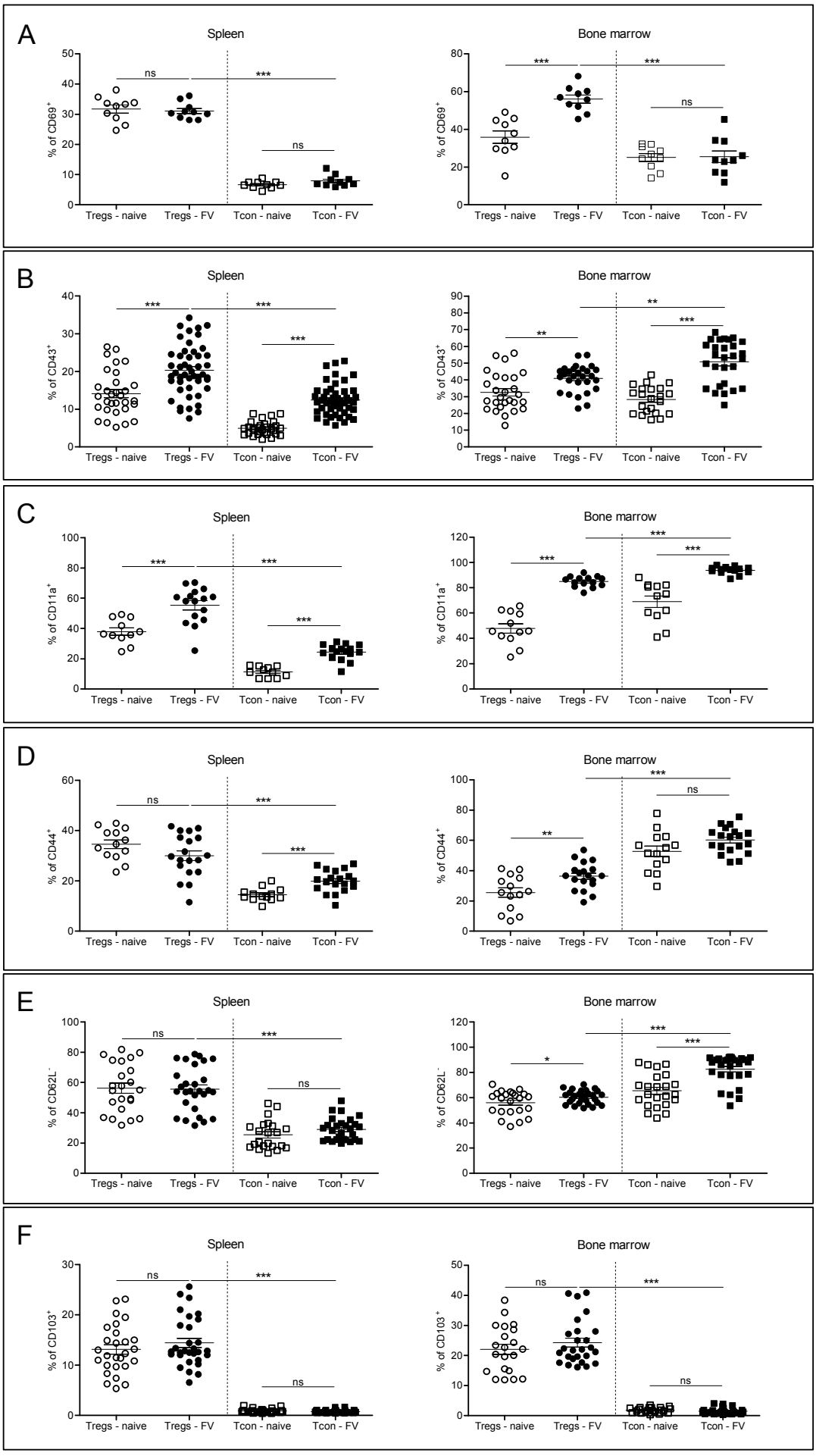
A
Spleen
Bone marrow
% of CD69+
B
% of CD43+
C
% of CD11a+
D
% of CD44+
E
% of CD62L-
F
% of CD103+
Tregs - naive
Tregs - FV
Tcon - naive
Tcon - FV
ns
*
**
***

Figure 4. 3 **Expression of activation and homing markers on Tregs and Tcon from naïve or FV-infected mice.** B6 mice were infected i.v. with 20,000 SFFU FV or left un-infected and the expression of various activation markers on Tregs ($CD4^+Foxp3^+$) and Tcon ($CD4^+Foxp3^-$) were measured by flow cytometry for spleen and bone marrow cells at 12 dpi. The markers investigated were: **(A)** CD69, early activation; **(B)** CD43 and **(C)** CD11a, both activation; **(D)** CD44, antigen contact; **(E)** CD62L and **(F)** CD103, activation and homing. Multiple independent experiments were carried out, with each dot representing a single mouse. The bars represent the mean and SEM. For statistical analysis a Student's t-test was used (ns not significant, * < 0.05, ** < 0.005 and *** < 0.0005).

T cells express various co-stimulatory and inhibitory receptors when activated, which were also stained. Tregs showed to have a higher frequency of cells positive for TIM3, ICOS, Lag3, PD-1 and PD-L1 in infected compared to cells from naïve mice in both the spleen and bone marrow (Figure 4. 4 A, B, C, E and F). A similar profile was observed for Tcon, which shows that these markers can be used for characterising Tregs. No changes during infection were found for the expression of CTLA-4 and GITR on Tregs (Figure 4. 4 D and G). These two markers are described to be important for Treg suppressive function, and showed higher levels for Tregs compared to Tcon (Figure 4. 4 D and G). When Tregs and Tcon from infected mice were compared to each other, Tregs showed higher expression of all markers in the spleen compared to the bone marrow with only two exceptions (Tim3 and PD-L1).

In summary, the co-stimulatory molecule ICOS and inhibitory receptors TIM3, Lag3, PD-1 and PD-L1 described for Tcon can also be used to characterise Tregs during acute FV infection. Furthermore, CTLA-4 and GITR were mainly expressed on Tregs and not Tcon in both organs, which is in line with the literature.

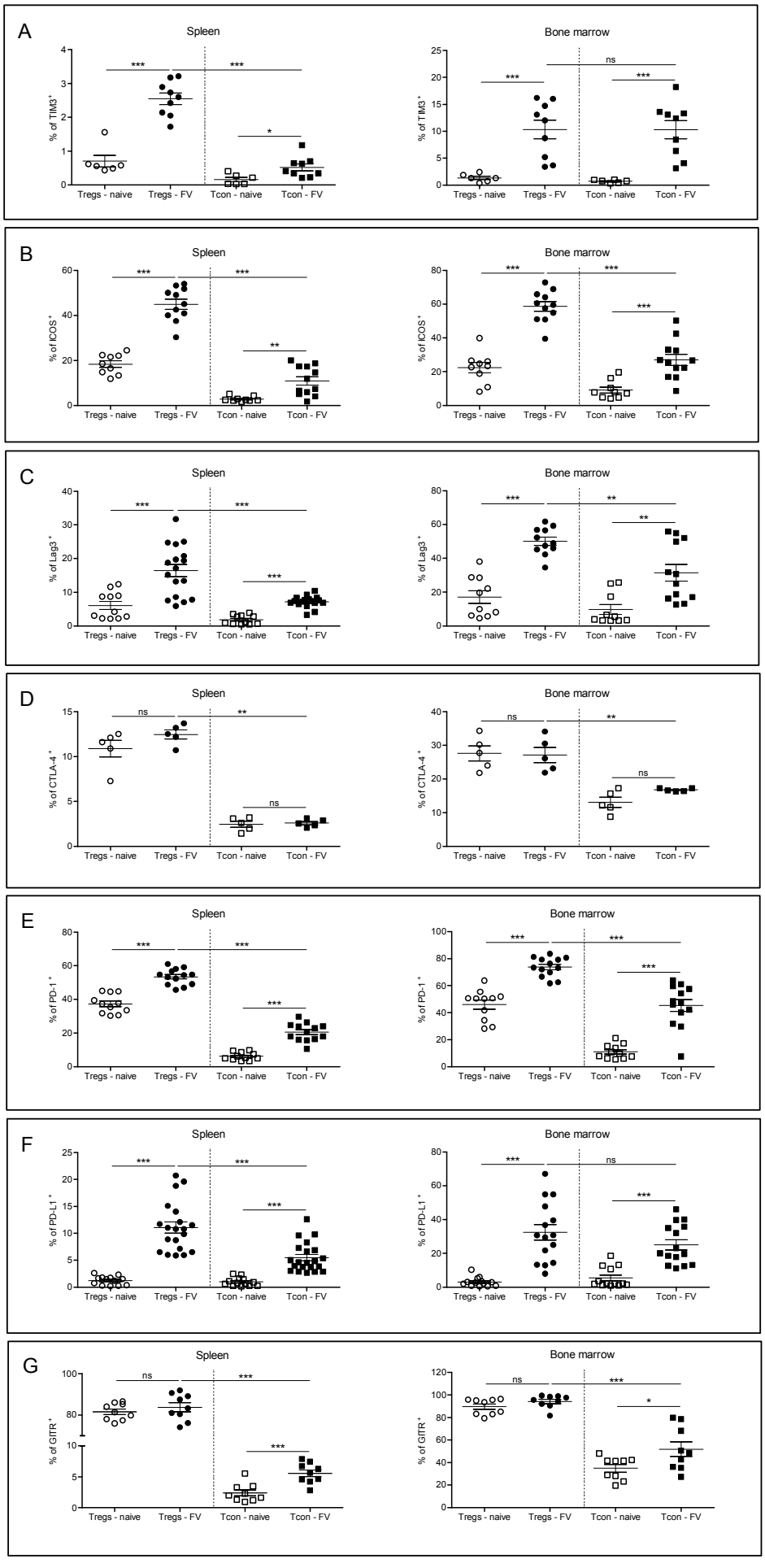
A
Spleen
Bone marrow
% of TIM3+
B
% of ICOS+
C
% of Lag3+
D
% of CTLA-4+
E
% of PD-1+
F
% of PD-L1+
G
% of GITR+
Tregs - naive
Tregs - FV
Tcon - naive
Tcon - FV
ns
*
**
***

Figure 4. 4 **Expression of co-stimulatory markers and inhibitory receptors on Tregs and Tcon from naïve and FV-infected mice.** B6 mice were infected i.v. with 20,000 SFFU FV or left un-infected and the expression of various co-stimulatory and inhibitory markers on Tregs ($CD4^+Foxp3^+$) and Tcon ($CD4^+Foxp3^-$) were measured by flow cytometry for spleen and bone marrow cells at 12 dpi. The markers investigated were **(A)** TIM3, **(B)** ICOS, **(C)** Lag3, **(D)** CTLA4, **(E)** PD-1, **(F)** PD-L1, and **(G)** GITR. Multiple independent experiments were carried out, with each dot representing a single mouse. The bars represent the mean and SEM. For statistical analysis a Student's t-test was used (ns not significant, * < 0.05, ** < 0.005 and *** < 0.0005).

Finally, to characterise the differentiation and proliferative capacity of Tregs during FV infection, a number of makers indicating differentiation (CD127 and KLRG1) and proliferation (Ki67 and BrdU) were analysed. For BrdU staining mice were fed with BrdU in their drinking water for three days before the experiment.

CD127 expressing Tregs were reduced in the bone marrow of infected mice compared to Tregs from naïve mice, indicating the differentiation to effector T cells, but no changes were seen in the spleen (Figure 4. 5 A). Tregs of FV-infected mice showed higher frequencies of $KLRG1^+$, $Ki67^+$ and $BrdU^+$ cells compared to cells from naïve mice in both organs (Figure 4. 5 B – D). In addition, Tregs from the spleen of FV-infected mice showed to be more differentiated ($CD127^{lo}$ and $KLRG1^+$) and proliferated stronger in comparison to Tcon from these mice. However in the bone marrow, the frequency of $Ki67^+$ Tcon and Tregs showed no significant differences in infected mice and Tregs were more positive for CD127 than Tcon, indicating less Treg differentiation compared to Tcon (Figure 4. 5 A and C).

In summary, markers used to show proliferation and differentiation of Tcon can also be used for Tregs in infected mice. KLRG1 was a more reliable marker to characterise Treg differentiation than CD127 and both Ki67 and BrdU can be used to study the proliferation of Tregs during infection. This proved that Tregs proliferate during FV infection and show signs of effector T cell differentiation.

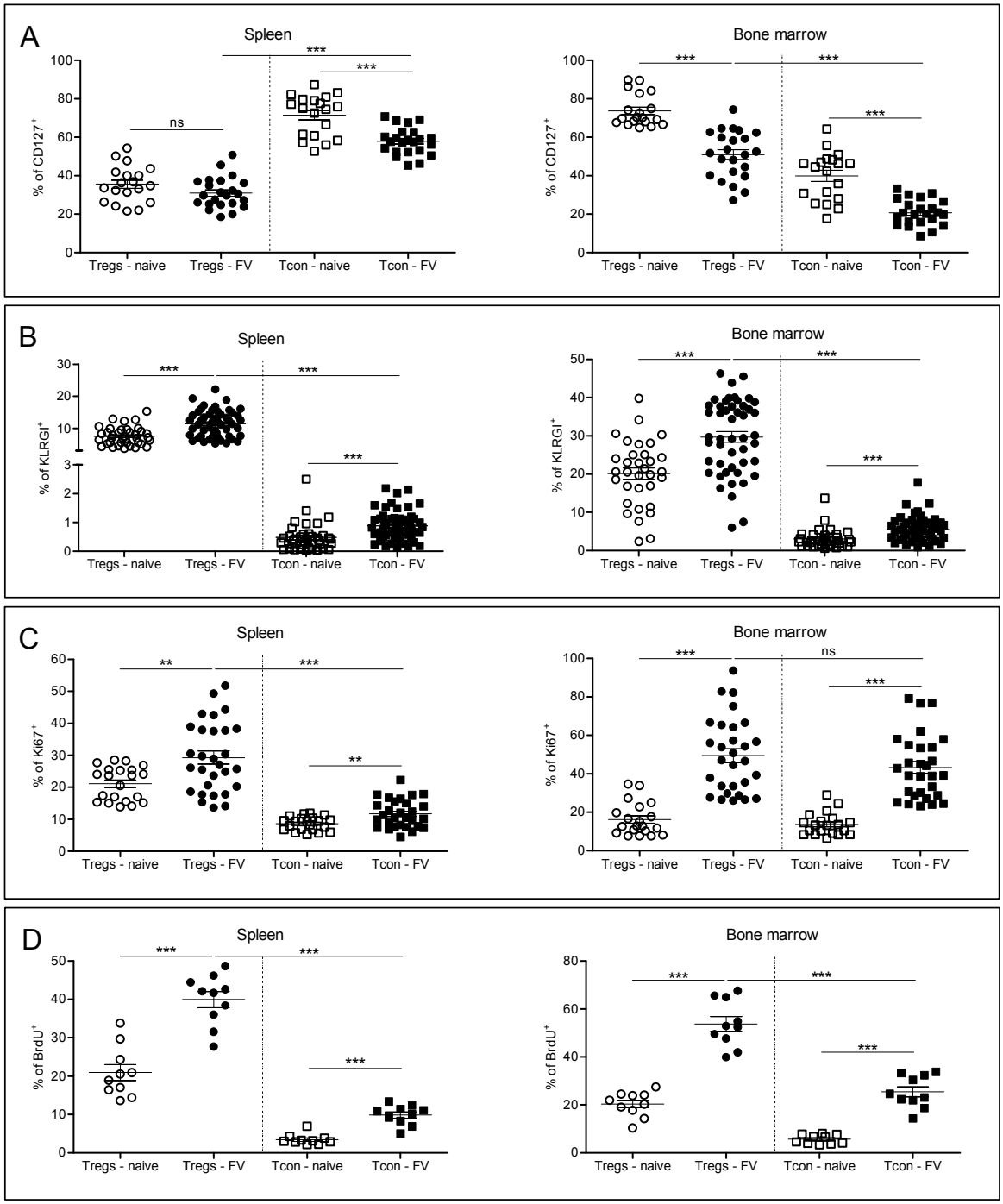

Figure 4. 5 **Expression of differentiation and proliferation markers on Tregs and Tcon from naïve and FV-infected mice.** B6 mice were infected i.v. with 20,000 SFFU of FV or left un-infected. For BrdU staining the mice were fed with BrdU in their drinking water three days before they were sacrificed. The expression of differentiation markers: **(A)** CD127 and **(B)** KLRG1; and proliferation markers: **(C)** Ki67 and **(D)** BrdU, of Tregs ($CD4^+Foxp3^+$) and Tcon ($CD4^+Foxp3^-$) were measured using flow cytometry for spleen and bone marrow cells at 12 dpi. Multiple independent experiments were carried out, with each dot representing a single mouse. The bars represent the mean and SEM. For statistical analysis a Student's t-test was used (ns not significant, * < 0.05, ** < 0.005 and *** < 0.0005).

4.4 Tregs remain activated and expanded during chronic FV infection

In FV infection, Tregs supress effector T cells, especially $CD8^+$ T cells, and render them dysfunctional during the chronic phase of infection (84, 144, 339, 340). When Tregs were depleted in the chronic phase of FV infection, $CD8^+$ T cells were reactivated and able to significantly lower viral loads (81, 339, 340). This shows that Tregs are required to supress $CD8^+$ T cells, suggesting that Tregs remain activated during chronic FV infection. The kinetics of virus replication in the different organs during FV infection have been investigated by Zelinskyy *et al.* (340). The virus was mostly present in the spleen and bone marrow and to a lesser extent in the lymph nodes during the acute phase of infection. However, during chronic FV infection higher titres of virus were found in the lymph nodes and spleen and only very low titres were detected in the bone marrow (340). Based on these findings, it was important to investigate Treg responses in all three organs of chronically infected mice.

Investigating the frequencies of Tregs in the spleen, bone marrow and lymph nodes of chronically FV-infected mice revealed that they all had significantly increased levels of Tregs compared to naïve mice (Figure 4. 6 A to C). Treg activation and proliferation during chronic FV infection was investigated. For this analysis three markers were chosen: Helios, for activation (Figure 4. 7 A); CD43, for activation (Figure 4. 7 B) and Ki67, for proliferation (Figure 4. 7 C). In all three investigated organs significantly higher frequencies of $Foxp3^+Helios^+$ and $CD43^+$ Tregs were observed, indicating activation of Tregs in chronically infected mice. However, for $Ki67^+$ Tregs, a lower frequency was measured in the lymph nodes of chronically infected compared to naïve mice and no significant changes were seen for the bone marrow or spleen. In conclusion higher frequencies of Tregs were present during chronic FV infection and these cells were still activated but did not show signs for increased proliferation.

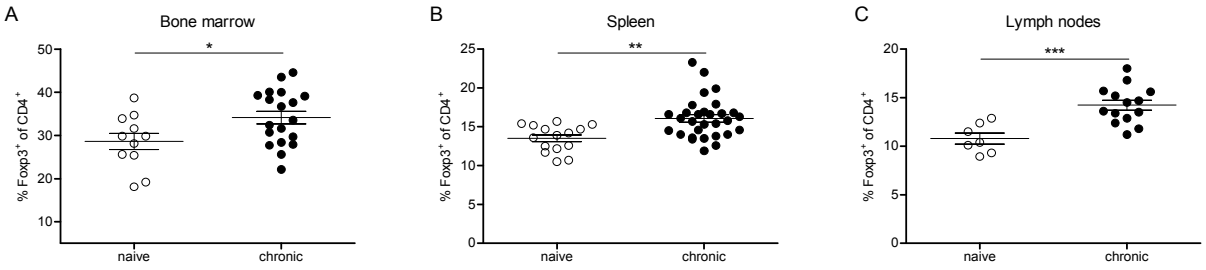

Figure 4. 6 **Treg expansion in mice chronically infected with FV.** B6 mice were infected i.v. with 15,000 SFFU FV+LDV for four to ten weeks or left un-infected and the frequency of $CD4^+Foxp3^+$ T cells were evaluated using flow cytometry for: **(A)** bone marrow, **(B)** spleen and **(C)** lymph node cells. For statistical analysis a Student's t-test was used (ns not significant, * < 0.05, ** < 0.005 and *** < 0.0005). The bars indicate the mean and SEM.

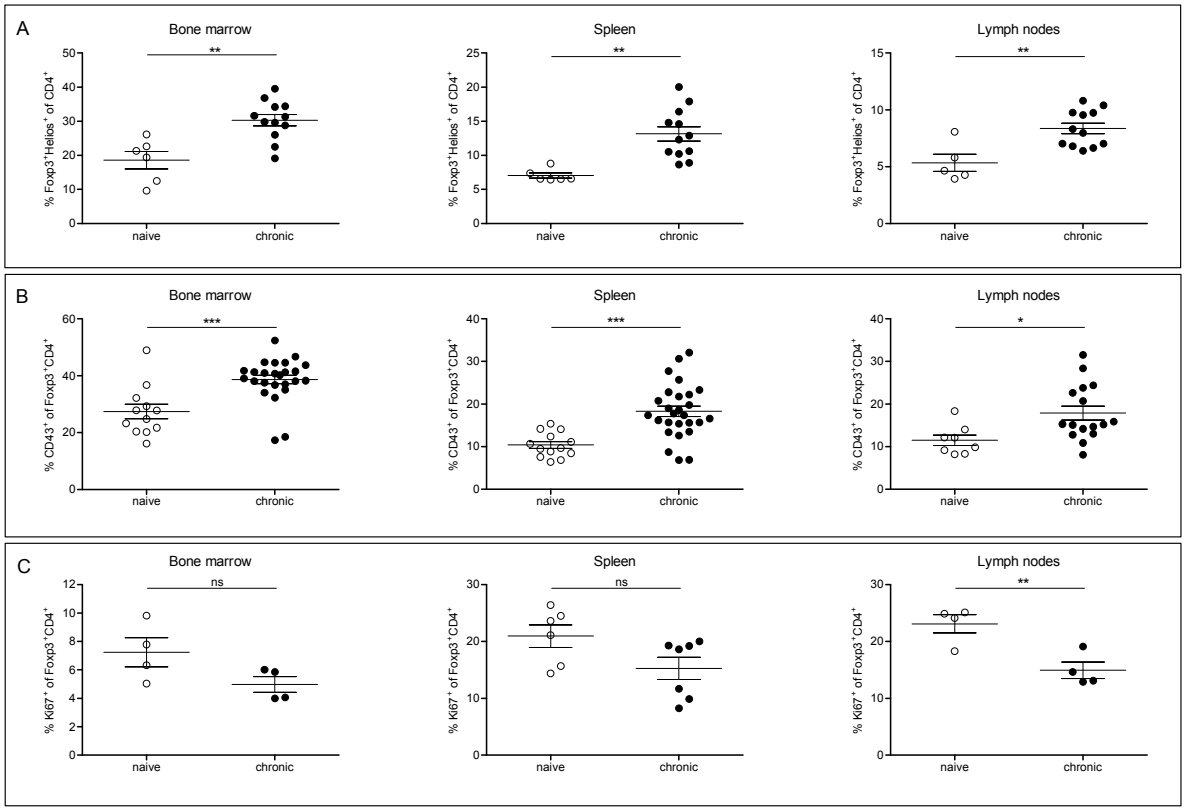

Figure 4. 7 **Expression of activation and proliferation markers by Tregs in mice chronically infected with FV.** B6 mice were infected i.v. with 15,000 SFFU FV+LDV for four to ten weeks or left un-infected and the expression of different markers on $CD4^+Foxp3^+$ Tregs was evaluated using flow cytometry for bone marrow, spleen and lymph node cells. Two activation markers; **(A)** Helios and **(B)** CD43 and one proliferation marker; **(C)** Ki67 were used to characterise the Tregs. For statistical analysis a Student's t-test was used (ns not significant, * < 0.05, ** < 0.005 and *** < 0.0005). The bars indicate the mean and SEM.

4.5 Natural Tregs expand in acute FV infection

After characterising the phenotype of Tregs during acute and chronic FV infection, it was of interest to determine their origin. Tregs can be either thymically derived nTregs or peripherally induced iTregs. Initially, Helios was recognised as a marker of nTregs (286, 301), but recently it was mainly used as marker for Treg activation (7). Nrp1, a newly identified marker for nTregs, shows a very similar expression pattern on Tregs as Helios, arguing in favour of Helios as an nTreg marker that can be induced by certain stimuli (320, 331).

The absolute numbers of $Nrp1^+$ nTregs and $Nrp1^-$ iTregs from the spleen (Figure 4. 8 A) and bone marrow (Figure 4. 9 A) of naïve and 12 to 14 dpi FV-infected mice were compared. $Nrp1^+$ nTregs showed a significant increase in numbers from FV-infected mice compared to $Nrp1^+$ nTregs from naïve mice for both organs. Moreover, a significant expansion of $Nrp1^-$ iTregs from naïve to FV-infected mice was found for both organs. However, these numbers were significantly lower than the numbers of $Nrp1^+$ nTregs in FV-infected mice. The same expansion of Tregs after infection was observed for $Helios^+$ and $Helios^-$ Tregs in the spleen and bone marrow (data not shown).

Interestingly, when the numbers of $Helios^-Nrp1^+$ (non-activated nTregs), $Helios^+Nrp1^+$ (activated nTregs) and $Helios^+Nrp1^-$ (activated iTregs) were analysed, the highest increase in numbers was found for $Helios^+Nrp1^+$ Tregs in the spleen and bone marrow of 12 dpi FV-infected mice compared to naïve mice and the other sub-populations in infected mice (Figure 4. 8 B and Figure 4. 9 B). Infected mice did not show any increase in numbers of $Helios^-Nrp1^+$ Tregs compared to naïve mice. However, a significant increase of $Helios^+Nrp1^-$ iTregs was observed after infection, although only very low cell numbers of this subset were detected (Figure 4. 8 B and Figure 4. 9 B). In summary, the most prominent subset of Tregs that accounts for most of the Treg expansion during FV infection are $Helios^+Nrp1^+$ Tregs, which suggests that nTregs get activated and expand in response to infection.

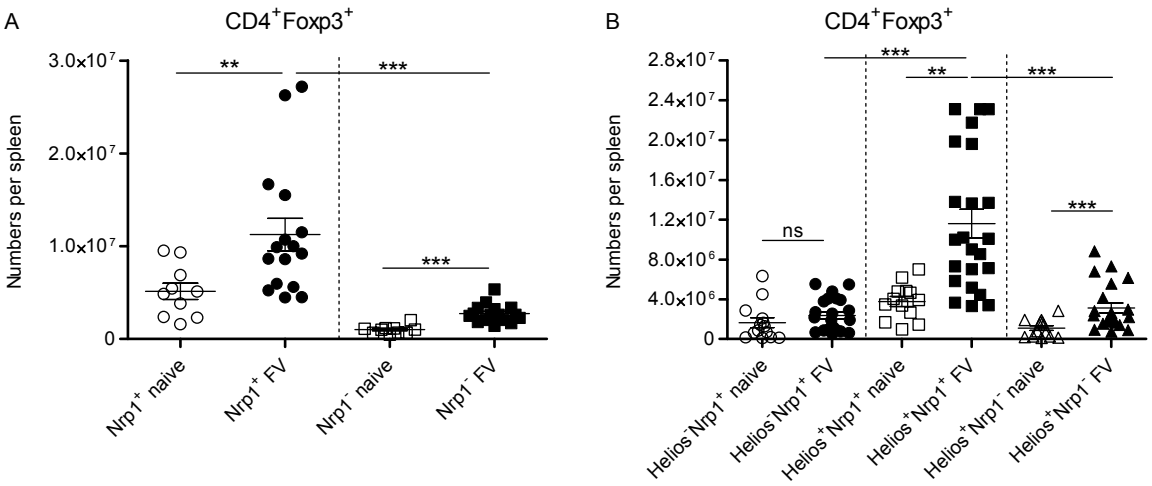

Figure 4. 8 **Numbers of Tregs expressing Nrp1 and Helios in the spleen during acute FV infection.** B6 mice were infected i.v. with 20,000 SFFU FV for 12 to 14 days or left uninfected. The numbers of Tregs ($CD4^+Foxp3$) positive or negative for Nrp1 or Helios were assessed in the spleen using flow cytometry. **(A)** Numbers of Tregs positive or negative for Nrp1 and **(B)** the Tregs categorised into $Helios^-Nrp1^+$, $Helios^+Nrp1^+$ or $Helios^+Nrp1^-$ subsets. For statistical analysis a Student's t-test was used (ns not significant, ** < 0.005, *** < 0.0005). The bars indicate the mean and SEM.

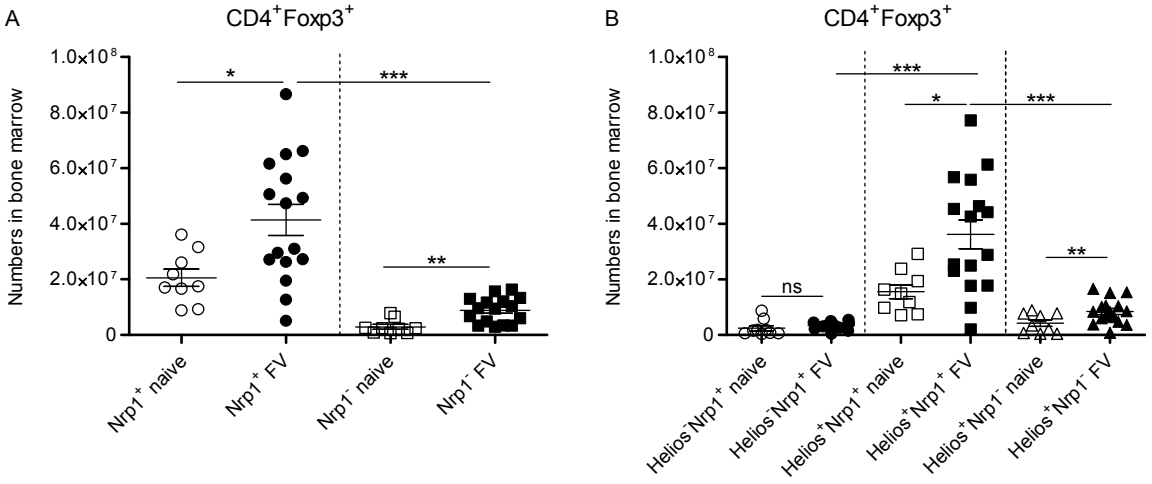

Figure 4. 9 **Numbers of Tregs expressing Nrp1 and Helios in the bone marrow during FV infection.** B6 mice were infected i.v. with 20,000 SFFU FV for 12 to 14 days or left uninfected. The numbers of Tregs ($CD4^+Foxp3$) positive or negative for Nrp1 or Helios were assessed in the spleen using flow cytometry. **(A)** Numbers of Tregs positive or negative for Nrp1 and **(B)** Treg subsets categorised into: $Helios^-Nrp1^+$, $Helios^+Nrp1^+$ or $Helios^+Nrp1^-$. For statistical analysis a Student's t-test was used (ns not significant, ** < 0.005, *** < 0.0005). The bars indicate the mean and SEM.

4.6 Vβ5$^+$ Tregs disproportionally expand during acute FV infection

The discovery that mostly activated nTregs expand during acute FV infection was a hint for self-specificity of these Tregs as thymus derived nTregs usually recognise self-antigens (269). Identification of self-antigens is not an easy task as virtually any expressed self-protein could be a candidate. Therefore the breadth of the TCR Vβ usage by Tregs expanding during FV infection was analysed. This analysis was done by our collaborators Kim Hasenkrug and Lara Myers (Laboratory of Persistent Viral Diseases, Rocky Mountain Laboratories, NIAID, NIH, Hamilton, MT, US).

Fourteen different TCR Vβ chains were examined at the peak expansion of Tregs during acute FV infection. These 14 different TCR Vβ chains represent about 70 % of all TCR Vβ chains utilised by Tregs in naïve and infected mice. When Tregs from naïve and acutely FV-infected mice were investigated for their numbers, all TCR Vβ subset showed equal expansion after infection with only one exception (212). The Vβ5$^+$ Treg subset showed a disproportional expansion from naïve to acutely FV-infected mice (Figure 4. 10 A), with the largest fold increase in absolute cell numbers compared to all other Vβ Treg subsets (212).

The disproportional expansion of T cell subsets suggests the involvement of superantigen stimulation; however no Sag has been described for FV. It is known that the Sag encoded by mouse endogenous *mtv-9* is able to crosslink the Vβ5 chain of T cells with the MHC class II on APCs (Figure 4. 10 B) (3, 324, 326). This leads to deletion or anergy of T cells in the thymus, a phenomenon that Tregs are relatively resistant to (27, 151, 152, 230, 277).

To investigate the kinetics of Vβ5$^+$ Treg expansion during FV infection, the percentage of Vβ5$^+$ Tregs was investigated at various times post infection in the spleen (Figure 4. 11 A) and bone marrow (Figure 4. 11 B). In the spleen, Vβ5$^+$ Treg expansion peaked at 10 dpi, whereas the peak was seen at 12 dpi in the bone marrow. Interestingly, no significant expansion of Vβ5$^+$ Tregs was seen in the chronic phase of FV infection (40 dpi) for either organ. In summary, a disproportional expansion of Vβ5$^+$ Tregs was detectable in the acute phase of FV infection, which was lost during chronic infection. The expansion suggested a role for *mtv-9* Sag stimulation in Treg expansion.

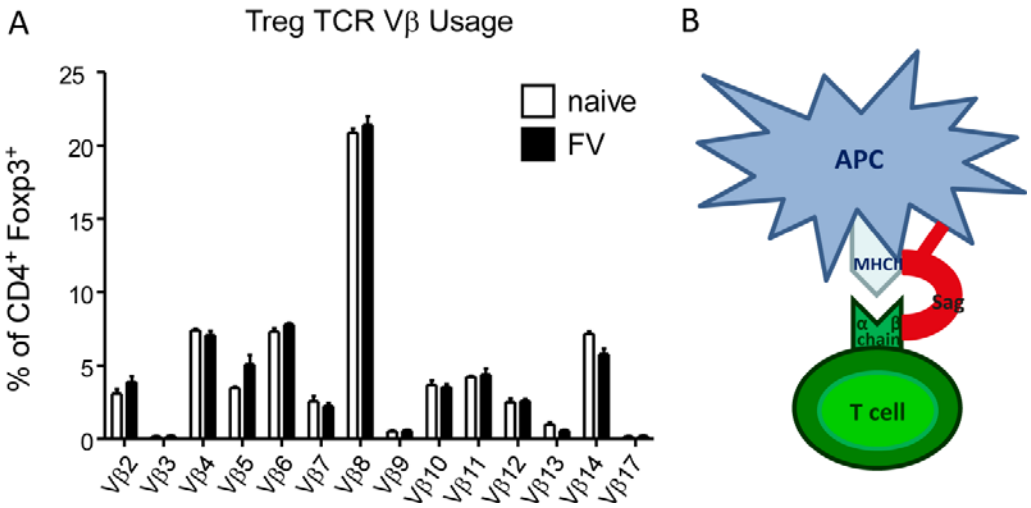

Figure 4. 10 **Vβ usage of Tregs during FV infection and the principle of superantigenic stimulation. (A)** The proportions of TCR Vβ subsets expressed by $CD4^+Foxp3^+$ Tregs from the spleens of naïve Y10 mice (white bars) and 14 dpi FV-infected mice (black bars) are shown. Bars represent the mean and standard deviation from five mice. Only the increase in $Vβ5^+$ Tregs was significant ($P < 0.05$ by t-test). Data courtesy of Kim Hasenkrug and Lara Myers. **(B)** Schematic showing the binding of an *mtv* Sag to the MHC class II molecule of an APC and the Vβ chain of the TCR on a T cell, independent of antigen specificity. The *mtv* Sag is a transmembrane protein. In general, this interaction leads to strong stimulation and proliferation of the T cell.

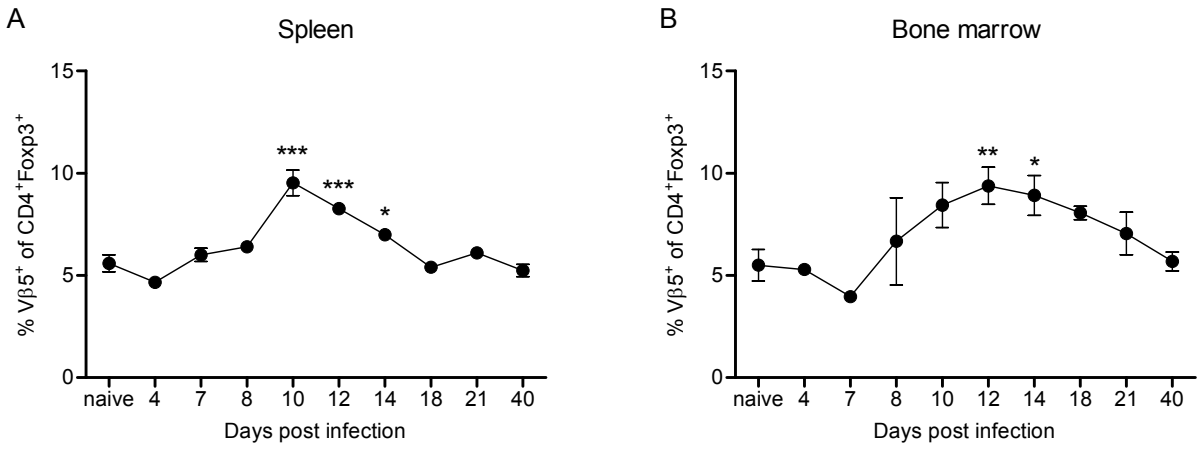

Figure 4. 11 **Kinetic of $Vβ5^+$ Treg expansion during FV infection.** B6 mice were infected i.v. with 20,000 SFFU FV or left un-infected. The percentage of $Vβ5^+$ Tregs ($CD4^+Foxp3^+$) was assessed using flow cytometry for **(A)** spleen and **(B)** bone marrow cells at various times post infection. At least four mice per group were analysed from two independent experiments. The bars indicate the mean and SEM. For statistical analysis a Dunnett's multiple comparison test was carried out with the naïve group as a reference (* < 0.05, ** < 0.005, *** < 0.0005).

The marker sets investigated in the previous sections were utilised to detect any phenotypical discrepancies between the Vβ5$^+$ and Vβ5$^-$ Treg populations during FV infection. To test this, the frequency of markers expressed on all Tregs from naïve mice were compared to the frequencies of the same markers on Vβ5$^+$ and Vβ5$^-$ Tregs from FV-infected mice (12 dpi). First, the expression of the classical Treg marker CD25 was analysed. This marker was not up- but rather down-regulated on both Treg populations after FV infection (Figure 4. 12 A and B) and this down-regulation was more pronounced for Vβ5$^-$ Tregs compared to Vβ5$^+$ Tregs.

Next the expression of different activation (CD43 and CD11a) and a homing marker (CD103), especially described for Tregs (269), were assessed. Interestingly, the percentages of CD43$^+$ and CD11a$^+$ Vβ5$^+$ Tregs were elevated compared to CD43$^+$ and CD11a$^+$ Vβ5$^-$ Tregs, respectively, for the spleen but not the bone marrow in infected mice. No differences were observed between Vβ5$^+$ and Vβ5$^-$ Tregs from infected mice for CD69, CD44 and CD62L in the spleen or bone marrow (data not shown). Although, the frequency of CD103$^+$ Tregs was not significantly altered between naïve and FV-infected mice (Figure 4. 3 F), when Vβ5$^+$ and Vβ5$^-$ Tregs from infected mice were investigated it was shown that Vβ5$^+$ Tregs expressed higher levels of this marker compared to all other subsets (Figure 4. 13 C). In conclusion, FV infection induced Treg activation and Vβ5$^+$ Tregs from FV-infected mice showed higher levels of activation than Vβ5$^-$ Tregs. For the evaluation of Vβ5$^+$ Treg activation and homing CD43, CD11a and CD103 showed to be most useful.

Next, two co-stimulatory (ICOS and GITR, Figure 4. 14 A and B) and two inhibitory (Lag3 and PD-1, Figure 4. 14 C and D) markers were chosen for the characterisation of Vβ5$^+$ and Vβ5$^-$ Tregs during acute FV infection. No major differences in the frequencies of ICOS$^+$, GITR$^+$, Lag3$^+$ and PD-1$^+$ Vβ5$^+$ Tregs and Vβ5$^-$ Tregs from FV-infected mice were observed in either organ (Figure 4. 14 A – D). Only the frequency of Vβ5$^+$ GITR$^+$ Tregs was significantly higher than the frequency of Vβ5$^-$ GITR$^+$ Tregs in the spleen of FV-infected mice (Figure 4. 14 D, left side). Moreover, Vβ5$^-$ Tregs showed higher percentages of ICOS$^+$ cells in the bone marrow compared to Vβ5$^+$ Tregs (Figure 4. 14 A, right side). In conclusion, the expression of co-stimulatory and

inhibitory markers did not vary significantly between Vβ5$^+$ and Vβ5$^-$ Tregs from FV-infected mice.

Finally, the differentiation and proliferation of Vβ5$^+$ and Vβ5$^-$ Tregs from FV-infected mice were investigated. Vβ5$^+$ Tregs from FV-infected mice were more terminally differentiated compared to Vβ5$^-$ Tregs in the bone marrow (CD127^{low} and KLRG1^{high}) and spleen (KLRG1^{high}) (Figure 4. 15 A and B). Furthermore, Vβ5$^+$ Tregs from FV-infected mice proliferated significantly more than Vβ5$^-$ Tregs in the spleen (BrdU and Ki67) and the bone marrow (Ki67) (Figure 4. 15 C and D).

Overall, it was determined that Vβ5$^+$ Tregs showed the phenotype of highly activated, short-lived effector cells, with higher levels of activation, differentiation and proliferation than Vβ5$^-$ Tregs during acute FV infection.

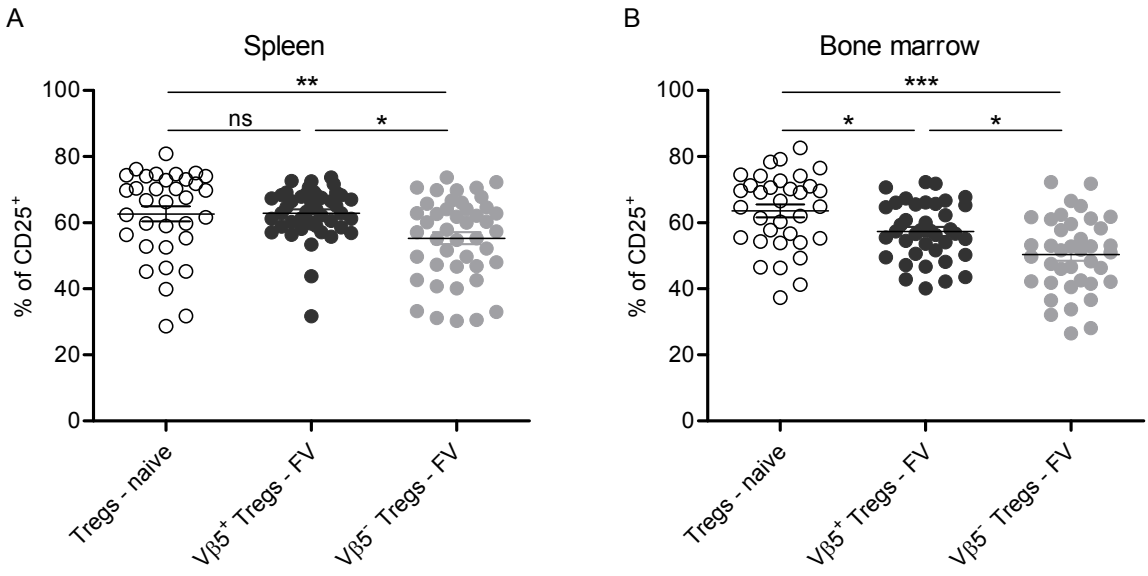

Figure 4. 12 **Expression of CD25 on Vβ5$^+$ and Vβ5$^-$ Tregs during the acute phase of FV infection.** B6 mice were infected i.v. with 20,000 SFFU FV or left un-infected and the expression of CD25 on CD4$^+$Foxp3$^+$ Tregs from naïve mice and Vβ5$^+$ or Vβ5$^-$ Tregs (CD4$^+$Foxp3$^+$) from 12 dpi mice were measured using flow cytometry for **(A)** spleen and **(B)** bone marrow cells. Multiple independent experiments were carried out, with each dot representing a single mouse. Bars indicate the mean and SEM. Data sets following a Gaussian distribution were analysed using a one-way ANOVA with Bonferroni's multiple comparison post-test. Data sets not following a Gaussian distribution were tested using Kruskal-Wallis-test with Dunn's multiple comparison post-test. Statistical significance is indicated by asterisks (ns not significant and * < 0.05, ** < 0.005, *** < 0.0005).

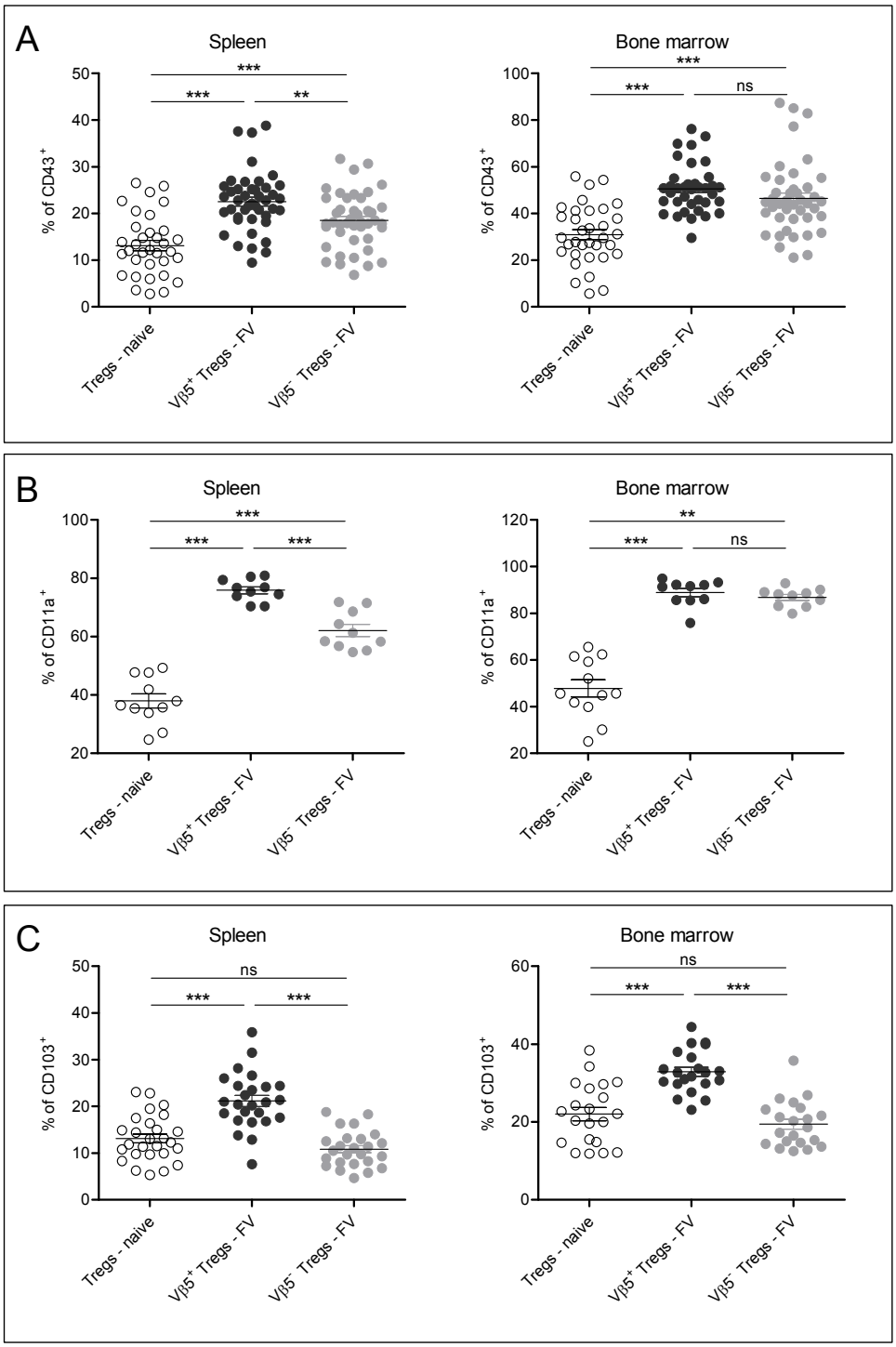

Figure 4. 13 **Expression of activation and homing markers on Vβ5$^+$ and Vβ5$^-$ Tregs during the acute phase of FV infection.** B6 mice were infected i.v. with 20,000 SFFU FV or left un-infected. The expression of various activation markers on CD4$^+$Foxp3$^+$ Tregs from the spleen and bone marrow of naïve mice or Vβ5$^+$ and Vβ5$^-$ Tregs (CD4$^+$Foxp3$^+$) from infected mice (12 dpi) were measured using flow cytometry. The markers investigated were: **(A)** CD43, **(B)** CD11a and **(C)** CD103. Multiple independent experiments were carried out, with each dot representing a single mouse. The bars indicate the mean and SEM. Data sets following a Gaussian distribution were analysed using a one-way ANOVA with Bonferroni's multiple comparison post-test. Data sets not following a Gaussian distribution were tested using Kruskal-Wallis-test with Dunn's multiple comparison post-test. Statistical significance is indicated by asterisks (ns not significant, * < 0.05, ** < 0.005 and *** < 0.0005).

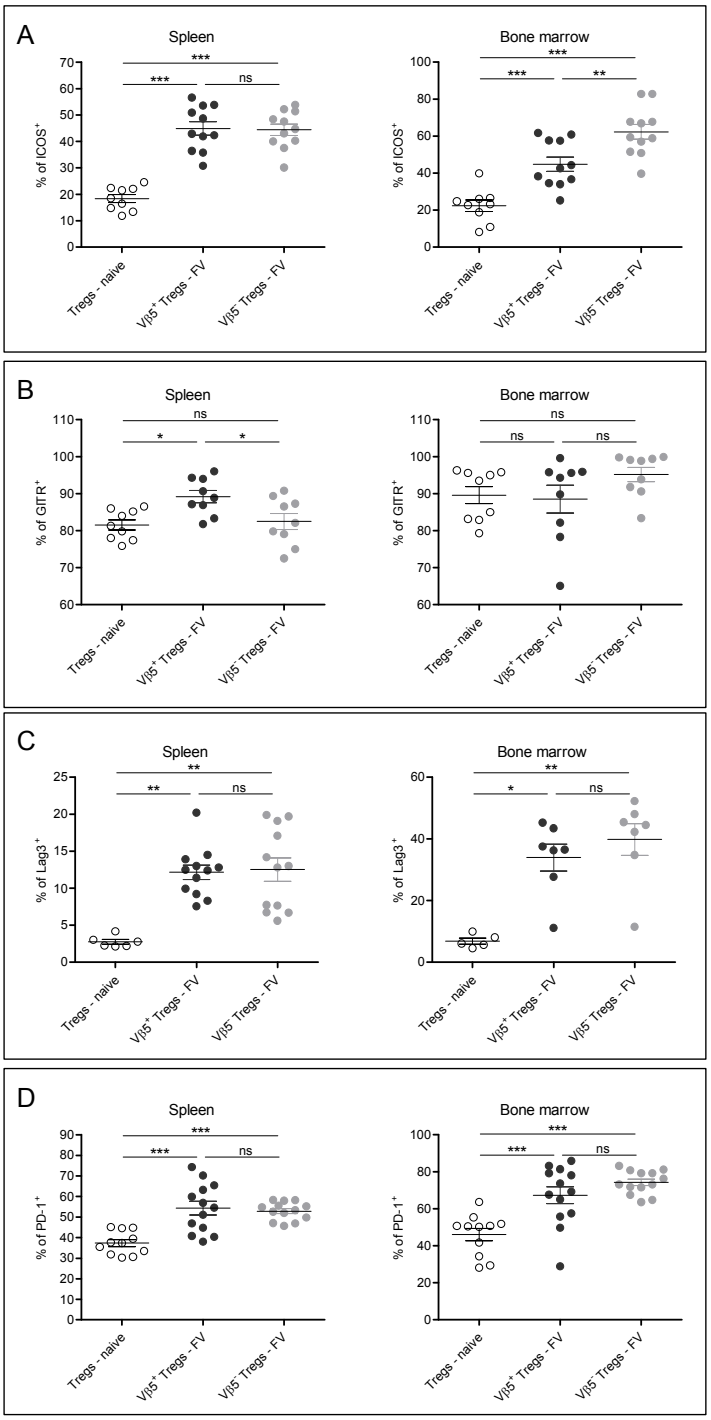

Figure 4. 14 **Expression of co-stimulatory markers and inhibitory receptors on Vβ5$^+$ and Vβ5$^-$ Tregs during FV infection.** B6 mice were infected i.v. with 20,000 SFFU FV or left un-infected and the expression of various co-stimulatory and inhibitory markers on CD4$^+$Foxp3$^+$ Tregs from the spleen and bone marrow in naïve mice or Vβ5$^+$ and Vβ5$^-$ Tregs (CD4$^+$Foxp3$^+$) from infected mice (12 dpi) were measured using flow cytometry. The markers investigated were: **(A)** ICOS, **(B)** GITR, **(C)** Lag3 and **(D)** PD-1. Multiple independent experiments were carried out, with each dot representing a single mouse. Bars indicate the mean and SEM. Data sets following a Gaussian distribution were analysed using a one-way ANOVA with Bonferroni's multiple comparison post-test. Data sets not following a Gaussian distribution were tested using Kruskal-Wallis-test with Dunn's multiple comparison post-test. Statistical significance is indicated by asterisks (ns not significant, * < 0.05, ** < 0.005 and *** < 0.0005).

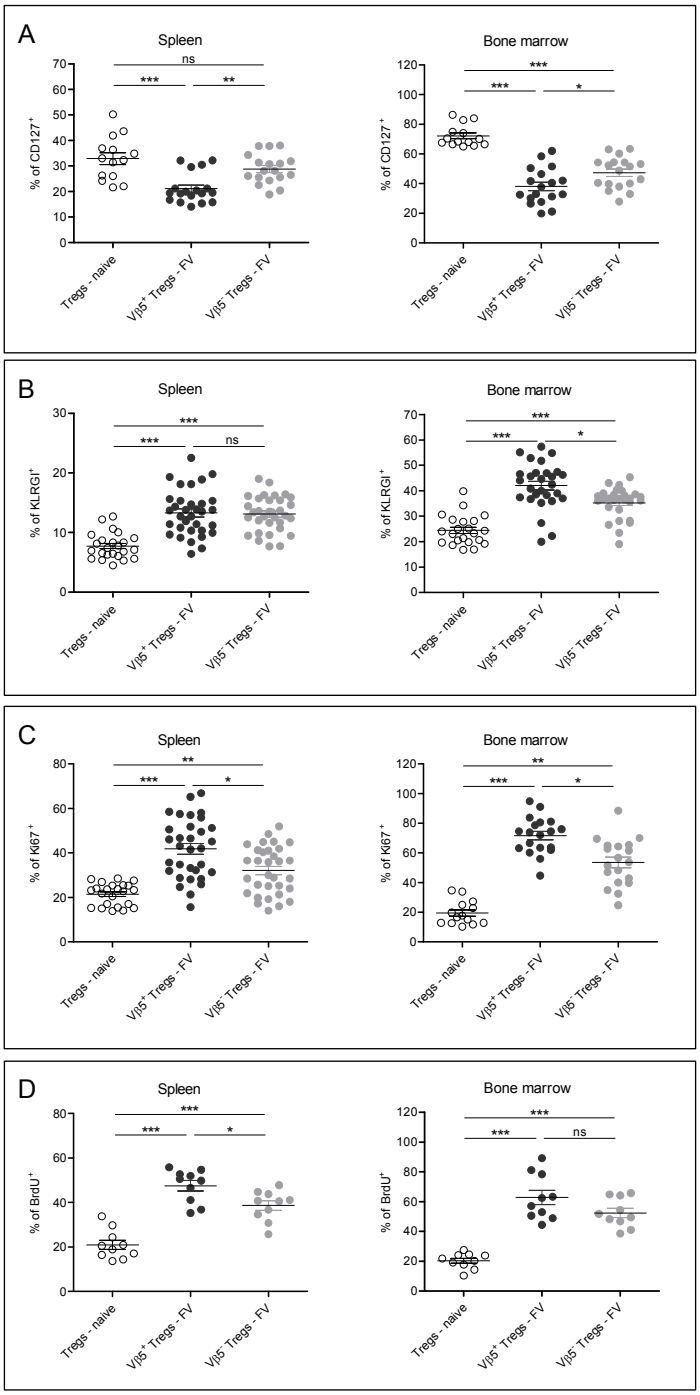

Figure 4. 15 **Expression of differentiation and proliferation markers on Vβ5$^+$ and Vβ5$^-$ Tregs during FV infection.** B6 mice were infected i.v. with 20,000 SFFU of FV or left un-infected. All mice were fed with BrdU in their drinking water for three days before sacrifice. The expression of differentiation: **(A)** CD127 and **(B)** KLRG1; and proliferation: **(C)** Ki67 and **(D)** BrdU markers of CD4$^+$Foxp3$^+$ Tregs from the spleen or bone marrow of naïve mice or Vβ5$^+$ and Vβ5$^-$ Tregs (CD4$^+$Foxp3$^+$) from infected mice (12 dpi) were measured using flow cytometry. Multiple independent experiments were carried out, with each dot representing a single mouse. The bars indicate the mean and SEM. Data sets following a Gaussian distribution were analysed using a one-way ANOVA with Bonferroni's multiple comparison post-test. Data sets not following a Gaussian distribution were tested using Kruskal-Wallis-test with Dunn's multiple comparison post-test. Statistical significance is indicated by asterisks (ns not significant, * < 0.05, ** < 0.005 and *** < 0.0005).

4.7 Vβ5$^+$ Tregs show a higher level of TCR-activation than Vβ5$^-$ Tregs after FV infection

After determining that Vβ5$^+$ Tregs display a phenotype of highly activated, short-lived effector cells, it was important to investigate the nature of the TCR signal they had received. As Vβ5$^+$ Tregs were Sag stimulated (238), it was hypothesised that they had received a very strong TCR signal due to the Sag. Nur77-GFP mice were used to test this as these mice express GFP dependent on the strength signal received by the TCR of T cells. Nur77-GFP mice were infected with FV for 12 days and the GFP signal expressed by Tcon, Vβ5$^+$ Tregs and Vβ5$^-$ Tregs was investigated. As expected, a higher TCR signal strength (MFI of GFP/Nur77) was detected for Vβ5$^+$ Tregs from infected mice in comparison to Vβ5$^-$ Tregs in the spleen (Figure 4. 16 A) and bone marrow (Figure 4. 16 B). Interestingly, the MFI of GFP/Nur77 was higher for Tregs in comparison to Tcon, indicating that Tregs received stronger TCR signals than Tcon during FV infection.

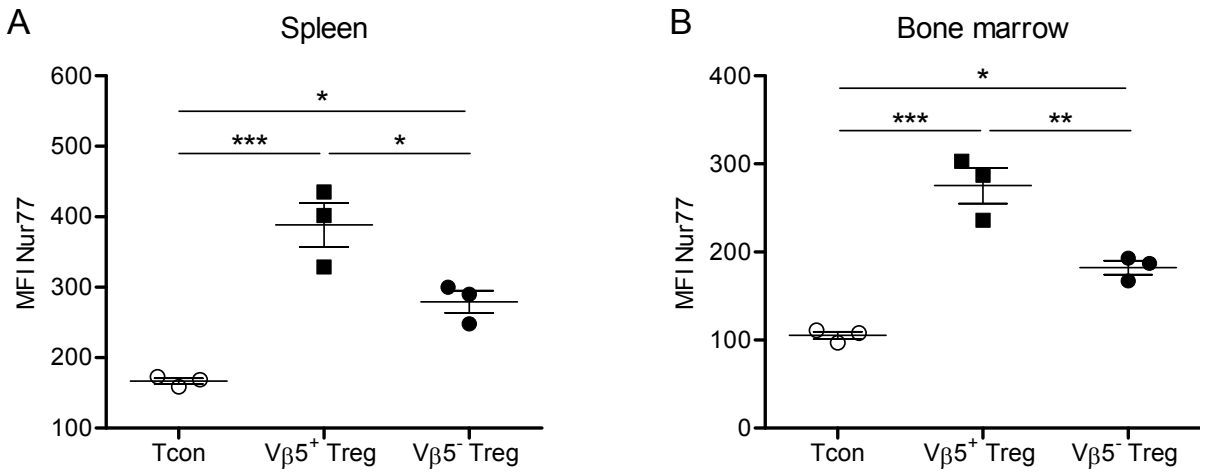

Figure 4. 16 **Expression of Nur77 in Tcon, Vβ5$^+$ and Vβ5$^-$ Tregs from FV-infected mice.** Nur77-GFP transgenic mice were infected i.v. with 20,000 SFFU FV for 12 days and **(A)** the spleen and **(B)** bone marrow were analysed for the MFI of Nur77-GFP expression in total CD4$^+$Foxp3$^-$ Tcon, CD4$^+$Foxp3$^+$Vβ5$^+$ Tregs and CD4$^+$Foxp3$^+$Vβ5$^-$ Tregs. Three mice per group were analysed and bars indicate the mean and SEM. For statistical analysis a one-way ANOVA with Bonferroni's multiple comparison post-test was carried out (* < 0.05, ** < 0.005 and *** < 0.0005).

4.8 The expansion of Vβ5$^-$ Tregs is dependent on signals produced by effector CD4$^+$ T cells

It has been shown in a model of bone marrow pathology induced by FV that virus-specific Tcon from CD4 TCR^{tg} mice induced expansion of Tregs (12). To determine what cell subset is responsible for the expansion of Vβ5$^+$ or Vβ5$^-$ Tregs a similar model was utilised. In this experiment FV-infected mice (CD45.1$^-$) received additional CD4$^+$ T cells (CD45.1$^+$) at 4 dpi by adoptive T cell transfer. These additional CD4$^+$ T cells were isolated from CD4 TCR^{tg} mice (EVα3-tg, FV-specific Tcon) or CD4 TCR^{wt} mice (EVα3-wt). The spleens of the recipient mice were investigated at 7 dpi, which is a time point where almost no expansion of endogenous Tregs is detectable (340) (Figure 4. 1). This early time point was chosen to ensure that only the transferred, and not endogenous, CD4$^+$ T cells could trigger Treg expansion. As control for the effective transfer, the numbers of virus-specific MHC class II tetramer$^+$ (TetrII$^+$) donor CD4$^+$ T cells were quantified in the spleens of the recipient mice and significantly higher numbers were detected in mice that received FV-specific TCR^{tg} CD4$^+$ T cells compared to mice that received TCR^{wt} CD4$^+$ T cells (Figure 4. 17 A). Interestingly, the frequency of Vβ5$^-$, but not Vβ5$^+$, endogenous Tregs were significantly increased for mice that received TCR^{tg} CD4$^+$ T cells in comparison to mice that received TCR^{wt} CD4$^+$ T cells (Figure 4. 17 B).

The factor that was produced by the activated TCR^{tg} CD4$^+$ and that most likely drove Vβ5$^-$ Treg expansion was IL2, which was expressed by a large number of transferred TCR^{tg} CD4$^+$ T cells (Figure 4. 17 C). In contrast, the IL2 production by endogenous CD4$^+$ or CD8$^+$ T cells was unaffected by the adoptive transfer (Figure 4. 17 D and E). In summary, these results suggest that the IL2 required for expansion of Vβ5$^-$ Tregs (212) was produced by virus-specific Tcon, which did not trigger the expansion of Vβ5$^+$ Tregs.

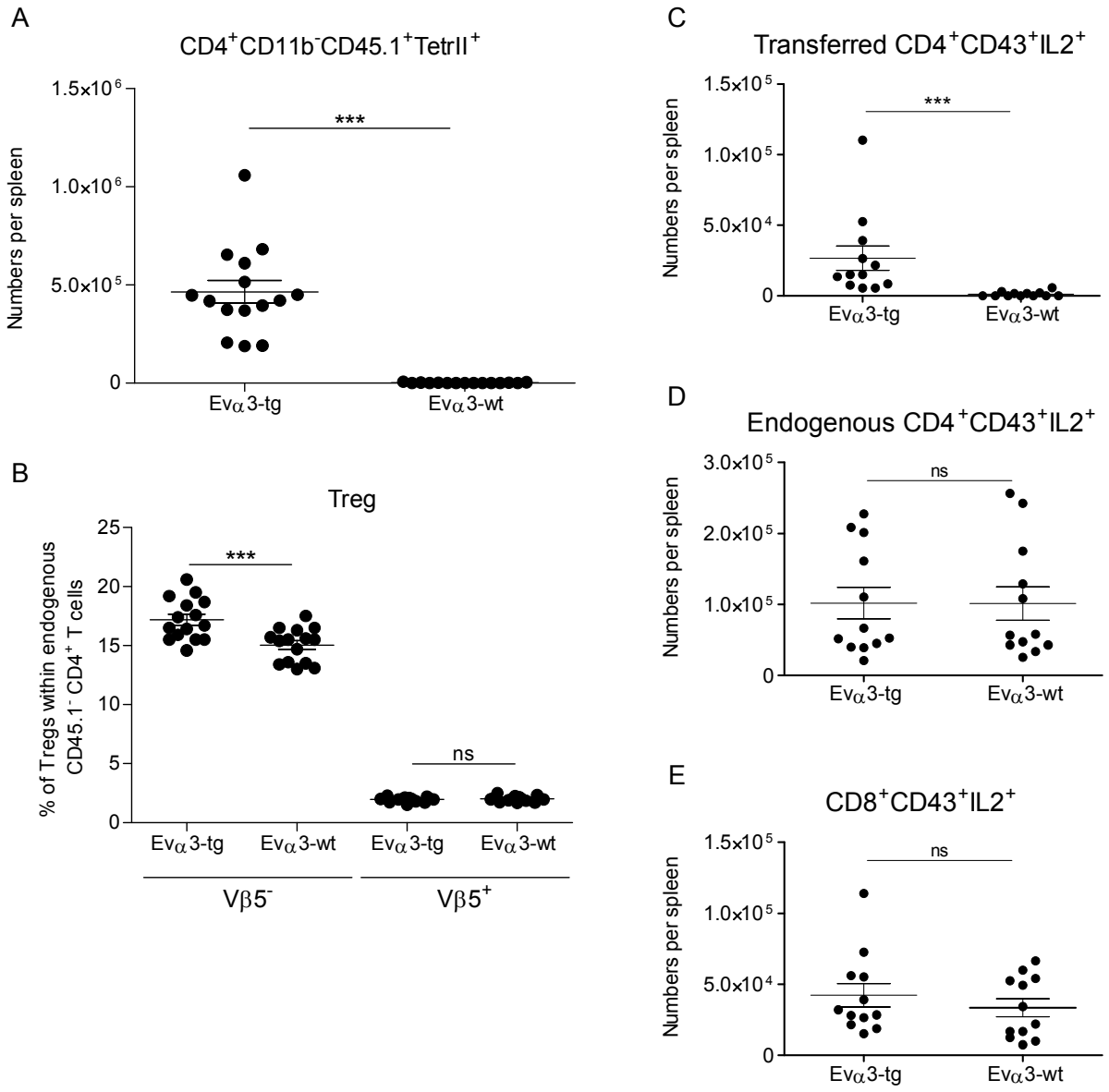

Figure 4. 17 **Expansion of Treg subsets after adoptive transfer of virus-specific CD4$^+$ T cells.** CD45.1$^-$ B6 mice were infected i.v. with 20,000 SFFU FV for 7 days. 5x10^6 magnetic bead isolated naïve CD4$^+$ T cells from either CD45.1$^+$ x EVα3-tg (FV-specific CD4$^+$ T cells) or CD45.1$^+$ x EVα3-wt mice were transferred into FV-infected CD45.1$^-$ mice at 4 dpi and the spleens were analysed at 7 dpi using flow cytometry. **(A)** The numbers of MHC class II tetramer$^+$ CD4$^+$CD11b$^-$ transferred (CD45.1$^+$) cells in the spleen were determined and are displayed in the graph. **(B)** The relative expansion of Vβ5$^+$ and Vβ5$^-$ endogenous (CD45.1$^-$) Tregs when either virus specific or non-specific cells were transferred was evaluated and is shown. The numbers of IL2 expressing **(C)** activated transferred CD4$^+$ T cells, **(D)** activated endogenous CD4$^+$ T cells or **(E)** activated CD8$^+$ T cells were measured after unspecific *in vitro* re-stimulation and are displayed in the graphs. Mice from three independent experiments were pooled and each dot represents an individual mouse. The bars represent the mean and SEM. For statistical analysis a Student's t-test was used (ns not significant and *** < 0.0005).

4.9 The expansion of Vβ5$^+$ Tregs is dependent on activated CD8$^+$ T cells

As shown in previous sections, Vβ5$^+$ Tregs expand disproportionally during acute FV infection in the spleens of B6 mice (Figure 4. 18 A). To find the factor or cell type involved in this expansion, different transgenic mouse strains bred on a B6 background or NK/NKT cell depleted mice were investigated.

B cells are APCs capable of presenting the Sag required for TCR-stimulation of Vβ5$^+$ Tregs (74). When two B cell deficient mouse strains were used: JH mice (Figure 4. 18 B) and μMT mice (Figure 4. 18 C); no differences in Vβ5$^+$ Treg expansion compared to B6 mice were observed. Granzyme B is an important molecule mainly produced by CD8$^+$ T cells during acute FV infection (338). However, GzmB-KO mice also showed a disproportional Vβ5$^+$ Treg expansion (Figure 4. 18 D). When NK cells, which also become activated during FV infection (183) were depleted, also no effect on the magnitude of Vβ5$^+$ Treg expansion was observed (Figure 4. 18 E). These results suggested that neither B cells nor NK cells were involved in the expansion of Vβ5$^+$ Tregs and that GzmB was also not required.

CD8$^+$ T cells play a prominent role in eliminating viral loads during acute FV infection and become highly activated by FV (84, 339, 340). Thus, it was of interest to investigate their influence on Tregs, especially Vβ5$^+$ Treg expansion, during acute FV infection. When CD8$^+$ T cell deficient mice were infected with FV, a lack of Vβ5$^+$ Treg expansion was discovered in the spleen at 12 dpi (Figure 4. 19 A). Moreover, when CD8$^+$ T cells were depleted in FV-infected mice during the acute phase of infection, the expansion of Vβ5$^+$ Tregs was abolished in the spleen (Figure 4. 19 B). Interestingly, the overall number of Foxp3$^+$ Tregs in the spleen of infected CD8$^+$ T cell depleted mice did not change compared to only FV-infected mice (Figure 4. 19 C), most likely because the expansion of Vβ5$^-$ Tregs was still present even in the absence of CD8$^+$ T cells (Figure 4. 19 D). The same effect was also seen in CD8$^+$ T cell deficient mice (data not shown). Interestingly, since CD8$^+$ T cell deficient and CD8$^+$ T cell depleted mice exhibited higher viral loads compared to wild type mice with CD8$^+$ T cells, the expansion of Vβ5$^+$ Tregs was clearly not driven by virus replication (data not shown). Thus, CD8$^+$ T cells were identified as the major player driving Vβ5$^+$ Treg expansion but not the expansion of the Vβ5$^-$ Treg subpopulation during acute FV infection.

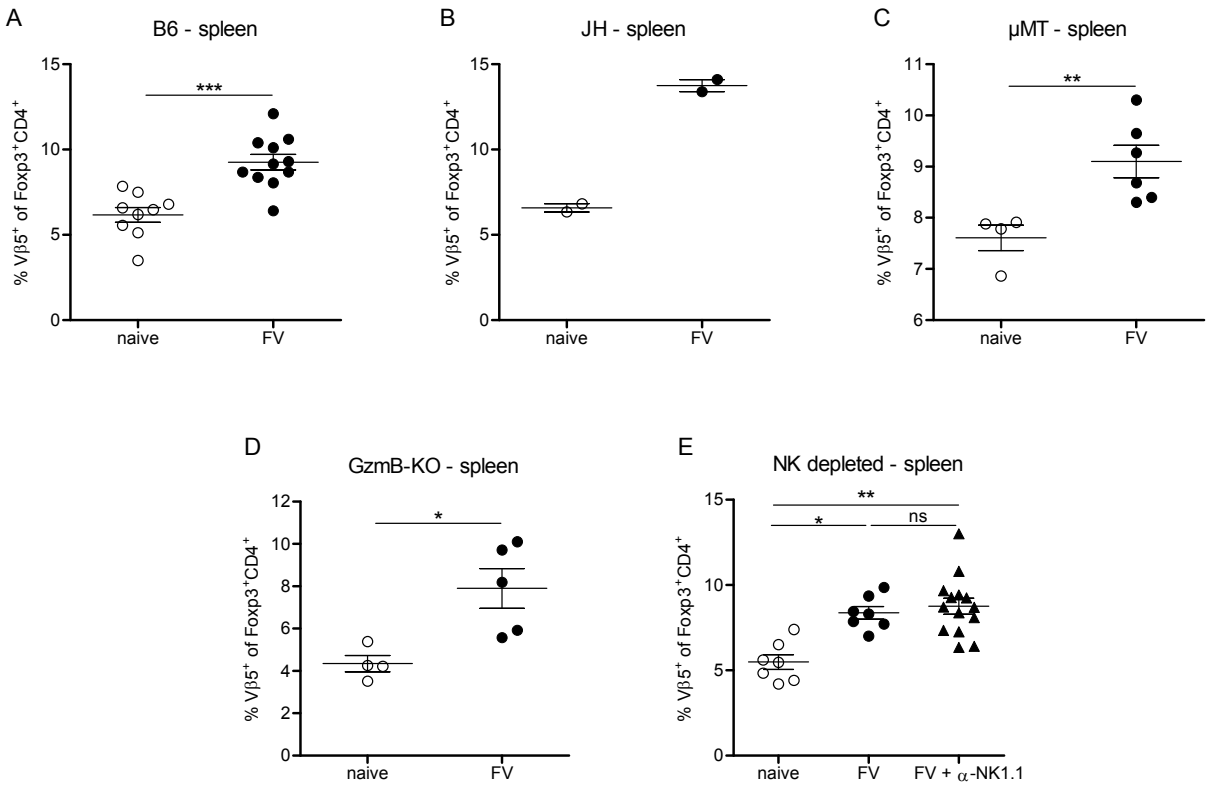

Figure 4. 18 **Expansion of Vβ5$^+$ Tregs in different knockout mouse strains or NK/NKT cell depleted mice during acute FV infection. (A)** Wild type B6 mice **(B)** JH-mice (B cell deficient), **(C)** μMT-mice (B cell deficient), **(D)** GzmB-KO mice and (E) NK/NKT cell depleted (four times α-NK1.1, 300μL) or non-depleted wild type B6 mice were infected i.v. with 20,000 SFFU FV (FV) or left uninfected (naïve). The percentages of Vβ5$^+$ were investigated in the spleens using flow cytometry at 12 dpi and are shown in the graphs. At least one experiment per mouse strain was performed with each dot representing a single mouse. Bars indicate the mean and SEM. For statistical analysis a Student's t-test was utilised (ns not significant, ** < 0.005 and *** < 0.0005). For analysis of more than two groups a Kruskal-Wallis-test with Dunn's multiple comparison post-test was carried out (ns not significant, * <0.05 and ** < 0.005).

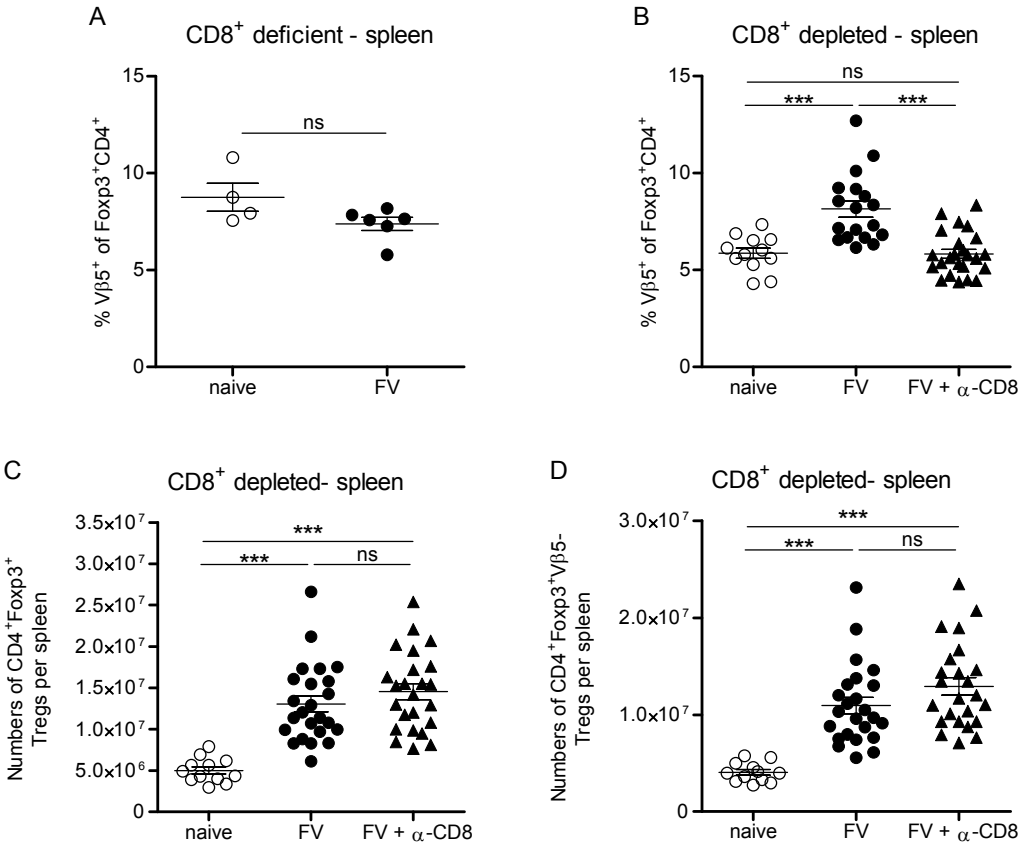

Figure 4. 19 **Expansion of Vβ5$^+$ Tregs in CD8$^+$ T cell deficient mice during acute FV infection.** CD8$^+$ T cell deficient, wild type B6 mice and B6 mice depleted for CD8$^+$ T cells (FV + four times α-CD8, 500 µL) were infected i.v. with 20,000 SFFU FV (FV). As controls CD8$^+$ T cell deficient or B6 mice were left uninfected (naïve). The percentages of Vβ5$^+$ Tregs in the spleen were investigated using flow cytometry between 8 and 16 dpi in: **(A)** CD8$^+$ T cell deficient (12 dpi) and **(B)** CD8$^+$ T cell depleted (8 to 16 dpi) mice. The numbers of **(C)** total CD4$^+$Foxp3$^+$ Tregs or **(D)** CD4$^+$Foxp3$^+$Vβ5$^-$ Tregs were calculated per spleen for naïve and FV-infected (8 to 16 dpi) mice with or without CD8$^+$ T cell depletion. Bars indicate the mean and SEM. **(A)** For CD8$^+$ T cell deficient mice at least four mice per group were analysed. For statistical analysis a Student's t-test was used (ns not significant). **(B - D)** For CD8$^+$ T cell depleted mice multiple independent experiments were performed with each dot representing a single mouse. Data sets following a Gaussian distribution were analysed using a one-way ANOVA with Bonferroni's multiple comparison post-test. Data sets not following a Gaussian distribution were tested using Kruskal-Wallis-test with Dunn's multiple comparison post-test. Statistical significance is indicated by asterisks (ns not significant and *** < 0.0005).

4.10 Vβ5$^+$ Tregs expand via mbTNFα on CD8$^+$ T cells that binds to TNFRII on these Tregs

CD8$^+$ T cells become activated during acute FV infection and produce different cytotoxic molecules and cytokines like Gzms, IFNγ, IL2 and TNFα (84, 341). In the previous section it was shown that GzmB and IL2 were not required for Vβ5$^+$ Treg

expansion (see Figure 4. 17 B and E, and Figure 4. 18 D). Furthermore, IFNγ has been shown to be ineffective in inducing Vβ5$^+$ Treg expansion during FV infection (Kim Hasenkrug, personal communication). However, CD8$^+$ T cells produce substantial amounts of intracellular TNFα (icTNFα) during acute FV infection when re-stimulated *in vitro* (Figure 4. 20 A). icTNFα was measured first, as this gives an indication about the potential of CD8$^+$ T cells to produce this cytokine before it is secreted. icTNFα is then transported to the surface of the CD8$^+$ T cell as mbTNFα and becomes subsequently cleaved from the surface by TACE and released as solTNFα (5, 198, 273).

When FV-specific CD8^{tg} T cells were stimulated *in vitro* with peptide loaded bone marrow-derived DCs, presenting their cognate antigen, a strong up-regulation of mbTNFα was observed 6 hours after stimulation (MFI = 1812) in comparison to control cultures without the epitope peptide (MFI = 665) (Figure 4. 20 B). This high surface expression of TNFα was substantially decreased after 24 hours of stimulation (data not shown), most likely due to shedding of mbTNFα induced by the cleaving enzyme TACE (5, 198, 273).

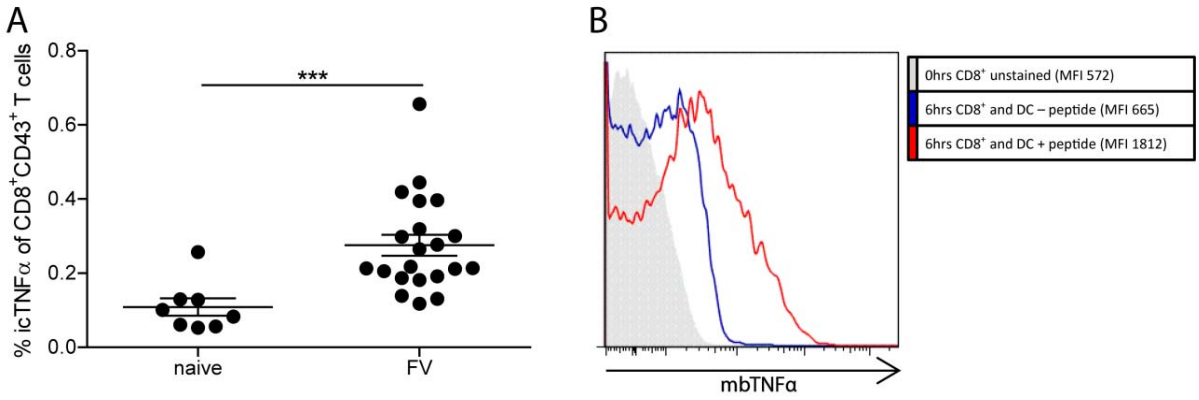

Figure 4. 20 **Production of intracellular and membrane-bound TNFα by FV-specific CD8$^+$ T cells. (A)** B6 mice were infected i.v. with 20,000 SFFU FV or left uninfected and the percentage of icTNFα from activated CD8$^+$ T cells (CD8$^+$CD43$^+$) was evaluated for spleen cells at 10 dpi using flow cytometry. icTNFα was measured after *ex vivo* unspecific re-stimulation. Mice from four independent experiments were pooled and each dot represents an individual mouse. The bars represent the mean and SEM. For statistical analysis a Student's t-test was used (*** < 0.0005). **(B)** CD8$^+$ T cells were bead isolated from CD8^{tg} mice and stimulated with bone marrow-derived DCs loaded or not with the cognate antigen. After six hours of culture, the CD8$^+$ T cells were subject to TNFα surface analysis using flow cytometry. The legend indicates the sample and the MFI of mbTNFα on TNFα$^+$ CD8$^+$ T cells. One representative experiment from three is shown.

TNFα can bind two different surface receptors, TNFRI and TNFRII. It has been shown that TNFRI preferentially binds soluble TNFα, whereas TNFRII has a much higher affinity for mbTNFα (120, 121). To analyse if Tregs selectively express either receptor during FV infection, Tregs were stained for TNFRI and TNFRII and analysed using flow cytometry. TNFRI was only expressed on very few Tregs from the spleen of naïve mice (less than 2.5%) and this percentage was not enhanced after FV infection for either Treg subset, $V\beta5^+$ and $V\beta5^-$ Tregs (Figure 4. 21 A). Furthermore, when the MFI of the TNFRI expression was compared between the few cells positive for TNFRI no difference was observed between $V\beta5^+$ and $V\beta5^-$ Tregs and both subsets showed rather down-regulation compared to Tregs from naïve mice (Figure 4. 21). In a stark contrast, TNFRII was present on approximately 35% of all Tregs from the spleen of naïve mice, which increased significantly to over 55% after FV infection. Strikingly, there was a significantly higher percentage of $TNFRII^+V\beta5^+$ Tregs compared to $TNFRII^+V\beta5^-$ Tregs in FV-infected mice (Figure 4. 21 C). Additionally, the MFI for TNFRII expression was significantly increased after FV infection for both Treg subsets (Figure 4. 21 D).

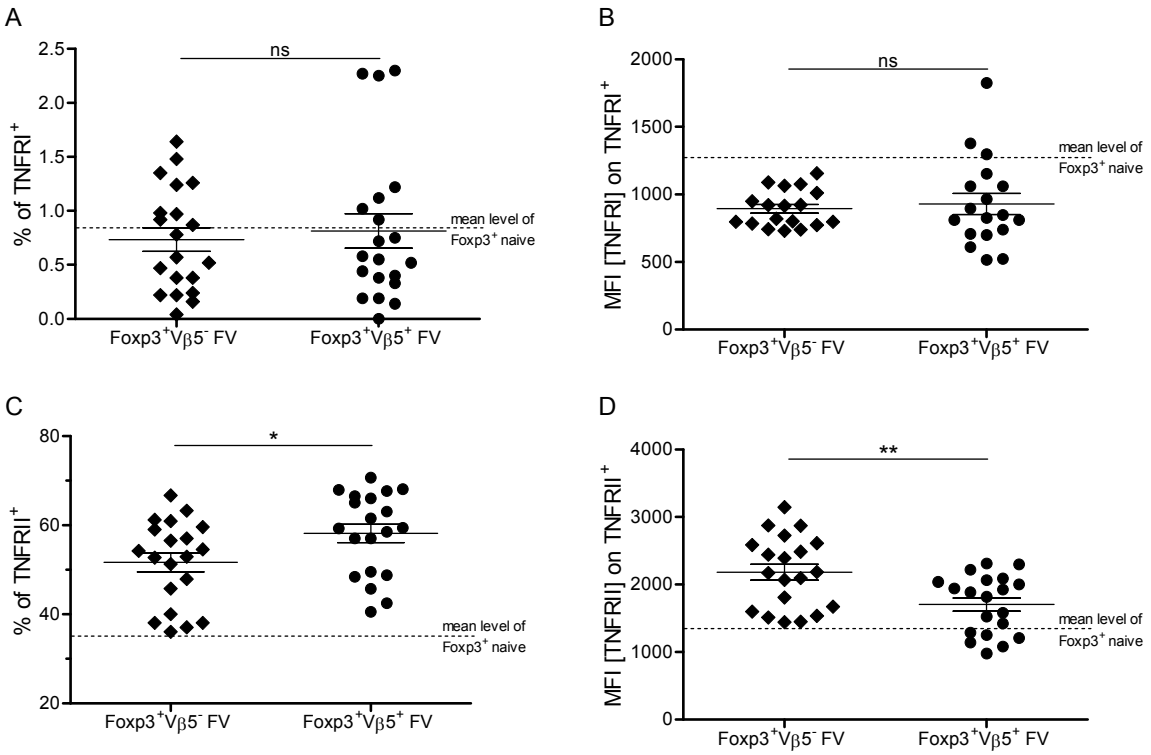

Figure 4. 21 **Expression of TNFRI and TNFRII on $V\beta5^+$ and $V\beta5^-$ Tregs during FV infection.** B6 mice were infected i.v. with 20,000 SFFU FV and the expression of TNFRI and TNFRII was measured on $V\beta5^+$ and $V\beta5^-$ Tregs from the spleen at 12 dpi using flow cytometry. **(A)** The percentages of Treg subsets positive for TNFRI are shown. **(B)** Graph

showing the MFI for TNFRI expression on TNFRI$^+$ Tregs. **(C)** The percentages of Treg subsets positive for TNFRII are shown. **(D)** Graph showing the MFI for TNFRII expression on TNFRII$^+$ Tregs. The TNFR expression levels of all Tregs (CD4$^+$Foxp3$^+$) from naïve mice are shown by the dotted line. Six independent experiments were carried out, with each dot representing a single mouse. Bars indicate the mean and SEM. For statistical analysis a Student's t-test was used (ns not significant, * < 0.005 and ** < 0.005).

These results imply that TNFRII, which is relatively selective for mbTNFα, is critically involved in Treg and especially Vβ5$^+$ Treg expansion during acute FV infection. To test this hypothesis, transgenic mice lacking either TNFRI or both TNFRs were analysed for the expansion of Vβ5$^+$ Tregs during FV infection. Bead isolated and genetically-labelled (CD45.1$^-$) naïve CD4$^+$ T cells, containing Tregs, from either TNFRI-KO or TNFRI+II-KO mice were transferred into FV-infected wild type mice (6 dpi) (CD45.1$^+$). As a control naïve CD4$^+$ T cells from wild type B6 mice were used. This resulted in an expansion of the donor wild type Vβ5$^+$ Treg population in the recipient mice at 12 dpi (Figure 4. 22 A). The transfer of Vβ5$^+$ Tregs from TNFRI-KO mice resulted in a similar expansion, whereas Vβ5$^+$ Tregs from TNFRI+II-KO did not expand (Figure 4. 22 A). A control experiment showed that the transfer of CD4$^+$ T cells did not interfere with the expansion of the endogenous Vβ5$^+$ Tregs (Figure 4. 22 B). Taken together this data suggests that TNFRII is the critical receptor involved in Vβ5$^+$ Treg expansion during acute FV infection.

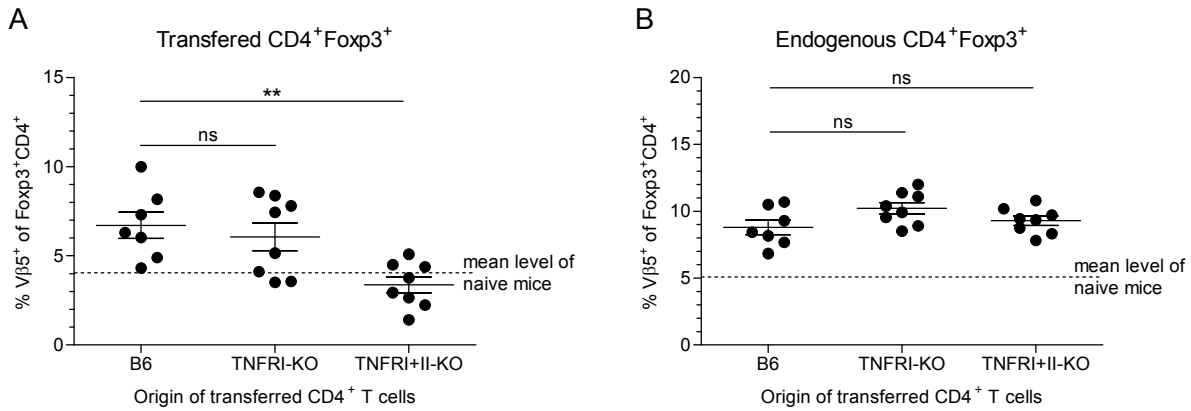

Figure 4. 22 **Transfer of TNFRI-KO and TNFRI+II-KO CD4$^+$ T cells into FV-infected mice and their effect on Vβ5$^+$ Treg expansion.** CD45.1$^+$ B6 mice were infected i.v. with 20,000 SFFU of FV. On day 6 post infection 3-5x10^6 magnetic bead isolated CD4$^+$ T cells of either naïve B6, TNFRI-KO or TNFRI+II-KO origin (all CD45.1$^-$ mice) were transferred i.v. and left to proliferate for an additional six days. The mice were sacrificed at 12 dpi and the spleen cells analysed using flow cytometry. **(A)** The percentage of Vβ5$^+$ Tregs of the transferred (CD45.1$^-$) CD4$^+$Foxp3$^+$ Tregs is shown. The dotted line indicates the mean level of Vβ5$^+$ Tregs in the spleen of naïve mice. **(B)** The percentage of endogenous Vβ5$^+$ Tregs

(CD45.1$^+$CD4$^+$Foxp3$^+$) in mice that received CD4$^+$ T cells of different origin is displayed. The dotted line indicates the mean level of Vβ5$^+$ Tregs in naive mice. For statistical analysis a Dunnett's multiple comparison test was used with B6 as reference group (ns not significant, ** < 0.005).

TNFRII has a strong affinity for mbTNFα, a molecule that is expressed on the surface of activated FV-specific CD8$^+$ T cells *in vitro,* as shown above (Figure 4. 20 B). To better understand the role of mbTNFα for Vβ5$^+$ Treg expansion, iRhom2-KO mice were utilised. These mice lack the expression of the rhomboid family member iRhom2 which is critical for the expression of TACE on hematopoietic cells and therefore the cleavage and liberation of mbTNFα (5, 198, 273). When iRhom2-WT and iRhom2-KO CD8$^+$ T cells were stimulated *in vitro* with α-CD3/α-CD28 T cell stimulator beads, both cell populations up-regulated mbTNFα 6 hours after stimulation, with CD8$^+$ T cells of iRhom2-KO mice (MFI = 1619) showing a higher signal than CD8$^+$ T cells of iRhom2-WT mice (MFI = 1076) (Figure 4. 23).

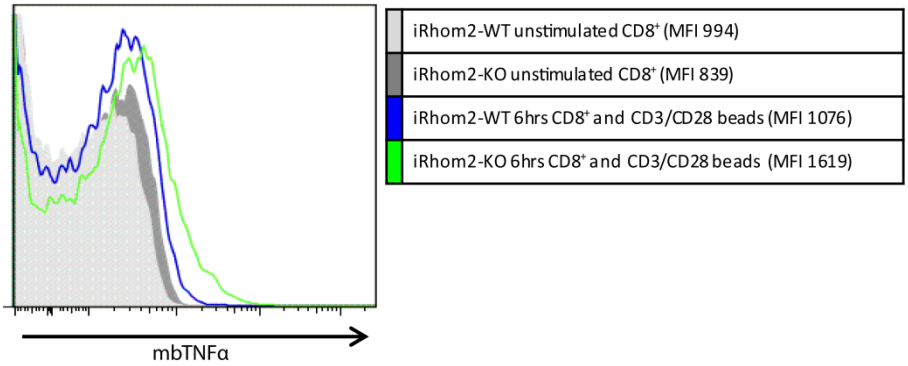

Figure 4. 23 **Expression of membrane-bound TNFα on stimulated iRhom2-WT and iRhom2-KO CD8$^+$ T cells.** For the evaluation of mbTNFα, CD8$^+$ T cells of iRhom2-WT or iRhom2-KO mice were unspecifically re-stimulated *in vitro* or left unstimulated. After six hours the CD8$^+$ T cells were subject to TNFα surface analysis by flow cytometry. The legend indicates the sample and the MFI of mbTNFα on mbTNFα$^+$ CD8$^+$ T cells. One representative example is shown.

To show that mbTNFα is the important factor for Vβ5$^+$ Treg expansion on CD8$^+$ T cells, bead isolated CD8$^+$ T cells from either iRhom2-WT or iRhom2-KO mice were transferred into FV-infected CD8$^+$ T cell deficient mice, which do not show a disproportionate expansion of Vβ5$^+$ Tregs after FV infection because of their lack in CD8$^+$ T cells (Figure 4. 19 A). As expected, the increased levels of mbTNFα on the surface of iRhom2-KO CD8$^+$ T cells resulted in significantly enhanced Vβ5$^+$ Treg expansion in the recipient mice compared to mice that received iRhom2-WT CD8$^+$ T

cells (Figure 4. 24 A). No such difference was seen for the expansion of Vβ5$^-$ Tregs (Figure 4. 24 B).

Furthermore, when the proliferation (Figure 4. 24 C) and the activation (Figure 4. 24 D) of the two Treg populations were analysed from mice that received iRhom2-WT or iRhom2-KO cells, it was found that the endogenous Vβ5$^+$ Treg populations showed higher activation and proliferation in recipients of iRhom2-KO than of iRhom2-WT CD8$^+$ T cells. No such effect was seen on Vβ5$^-$ Treg proliferation and activation. Taken together these data indicate that mbTNFα expressed on activated CD8$^+$ T cells provides an important signal required for the activation and expansion of Vβ5$^+$ Tregs, whereas Vβ5$^-$ Tregs were obviously only dependent on IL2 stimulation.

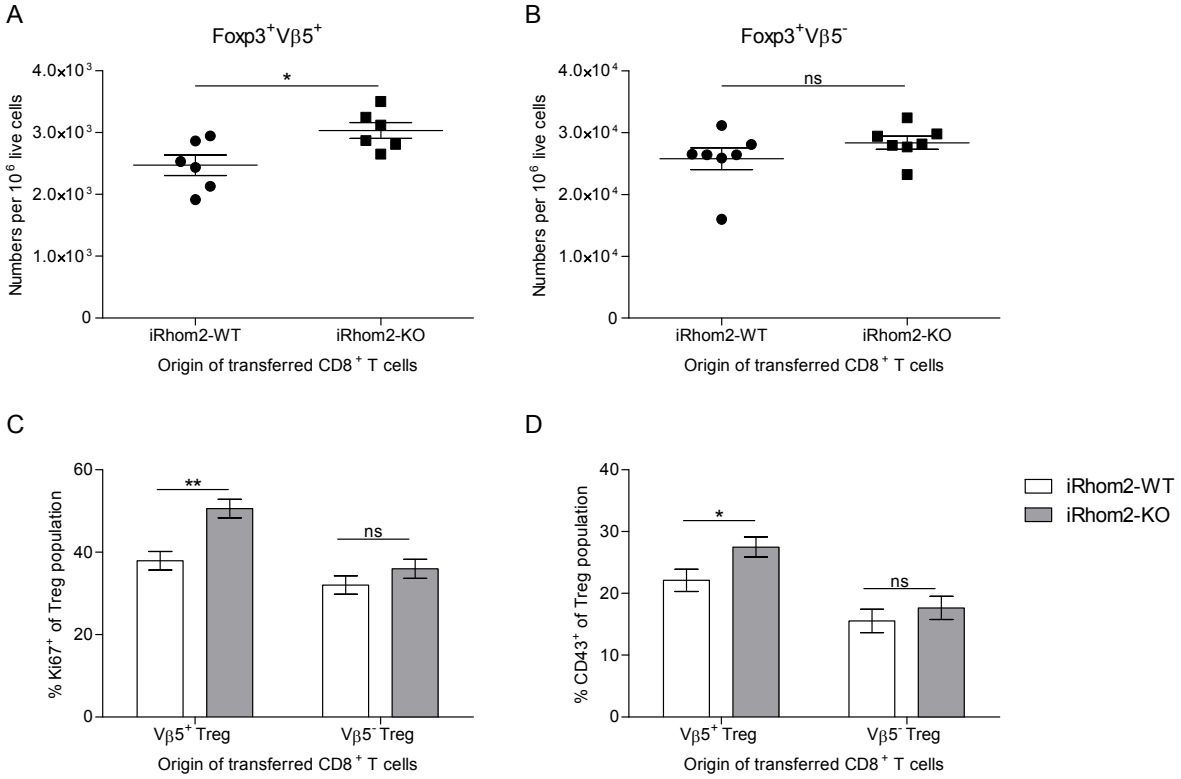

Figure 4. 24 **Transfer of iRhom2-WT and iRhom2-KO CD8$^+$ T cells into CD8$^+$ T cell deficient mice to trigger Vβ5$^+$ Treg expansion during FV infection.** CD8$^+$ T cell deficient mice were infected i.v. with 20,000 SFFU FV. Five dpi, 7-8x10^6 magnetic bead isolated CD8$^+$ T cells from either naïve iRhom2-WT or iRhom2-KO mice were transferred via i.v. injection into infected CD8$^+$ T cell deficient mice. On day 10 post infection the spleen cells were analysed using flow cytometry and the numbers of **(A)** Vβ5$^+$ Tregs and **(B)** Vβ5$^-$ Tregs per million live cells were assessed. The frequency of Vβ5$^+$ or Vβ5$^-$ Tregs as: **(C)** Ki67$^+$ or **(D)** CD43$^+$ in mice that received iRhom2-WT-CD8$^+$ or iRhom2-KO-CD8$^+$ T cells are shown. The results of two independent experiments are shown. Bars indicate the mean and SEM. For statistical analysis a Student's t-test was used (ns not significant, * < 0.05 and ** < 0.005).

4.11 Expansion of Vβ5$^+$ Tregs with a synthetic TNFRII-ligand in the absence of infection

To analyse if the intercellular communication between Vβ5$^+$ Tregs and activated CD8$^+$ T cells can be bypassed, a complexed TNFα nonamer (compTNFα) was used which can only bind to TNFRII. As a control recombinant human soluble TNFα, which can only bind mouse TNFRI, was used (180). Naïve mice were treated twice i.p. with the different forms of TNFα. The solTNFα did not expand Vβ5$^+$ Tregs in naïve mice, nor did it influence their proliferation (Figure 4. 25 A and B). Strikingly, the compTNFα was able to significantly increase the number of Vβ5$^+$ Tregs per one million spleen cells and their proliferation measured by Ki67 expression analysis (Figure 4. 25 A and B). This expansion of Vβ5$^+$ Tregs was dependent on the presence of TNFRII as shown by the lack of expansion and proliferation in TNFRII-KO mice treated with the compTNFα (Figure 4. 25 A and B). In conclusion, this data provides clear evidence that Vβ5$^+$ Tregs, which receive a strong TCR signal by the constitutively expressed *mtv-9* Sag, require TNFRII mediated secondary signalling for their efficient activation and expansion.

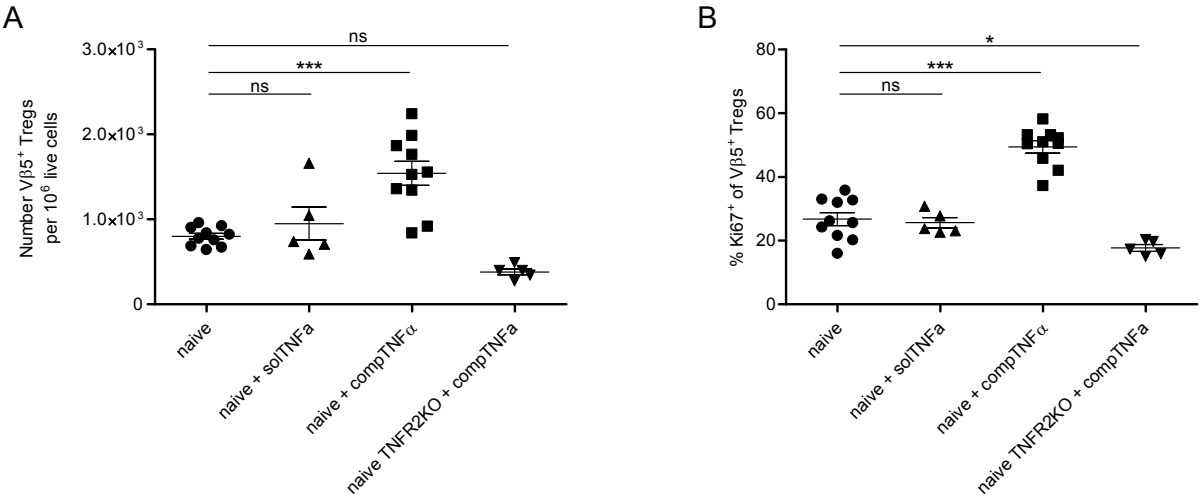

Figure 4. 25 **Induction of Vβ5$^+$ Treg expansion with soluble human TNFα or complexed mouse TNFα nonamer.** Naïve B6 were treated twice (day 0 and day 2) i.p. with 1 ng human solTNFα or 25 µg of mouse compTNFα. As a control TNFRII-KO mice were treated with compTNFα. Four days after the start of the treatment the animals were sacrificed and the spleen cells analysed using flow cytometry. **(A)** The numbers of Vβ5$^+$ Tregs per million live spleen cells and **(B)** the frequency of Ki67$^+$ cells of Vβ5$^+$ Tregs are shown. Multiple independent experiments were carried out, with each dot representing a single mouse. Bars indicate the mean and SEM. For statistical analysis a Dunnett's multiple comparison test was performed with the naïve group as reference (ns not significant, ** < 0.005).

4.12 Depletion of Vβ5$^+$ T cells augments CD8$^+$ T cell function but does not result in reduced viral loads

In the previous sections it has been shown that Vβ5$^+$ Tregs are highly activated during acute FV infection. Furthermore, they expand in response to TNFα presented on the surface of activated virus-specific CD8$^+$ T cells. Therefore the biological importance of the Vβ5$^+$ Treg subset during FV infection was of great interest. To test this Vβ5$^+$ T cells were depleted by antibody treatment and the effector phenotype of CD8$^+$ T cells was subsequently determined. The depletion efficiency of the Vβ5 depletion-antibody was more than 98% for Vβ5$^+$ Tregs and Tcon in the spleen (Figure 4. 26 A). Importantly, the depletion of Vβ5$^+$ T cells also affected the subset of CD8$^+$Vβ5$^+$ T cells, which resulted in a mean of 14.75%±4.06% of all activated CD8$^+$ T cells depleted (Figure 4. 26 B). However, despite this reduction in numbers of activated CD8$^+$ T cells, no significant loss of activated virus-specific (CD43$^+$TetrI$^+$) CD8$^+$ T cells (Figure 4. 27 A) was detected. In contrast, higher frequencies of activated GzmB producing (CD43$^+$GzmB$^+$) CD8$^+$ T cells and virus-specific GzmB producing (TetrI$^+$GzmB$^+$) CD8$^+$ T cells were observed after Vβ5 depletion compared to the non-depleted FV-infected control group (Figure 4. 27 B and C). This showed that the Vβ5$^+$ Treg subpopulation played a significant role in suppressing CD8$^+$ T cell function during acute FV infection. Surprisingly, despite the elevated cytotoxic CD8$^+$ T cell response in Vβ5$^+$ T cell depleted mice, there was no significant difference in the viral loads in the spleen of Vβ5$^+$ T cell depleted versus control mice detectable at 12 dpi (Figure 4. 28).

Overall, the depletion of Vβ5$^+$ Tregs augmented the cytotoxic activity of FV-specific CD8$^+$ T cells but at the same time reduced the total numbers of activated CD8$^+$ T cells, which might explain why no changes in viral loads were observed after Vβ5$^+$ T cell depletion.

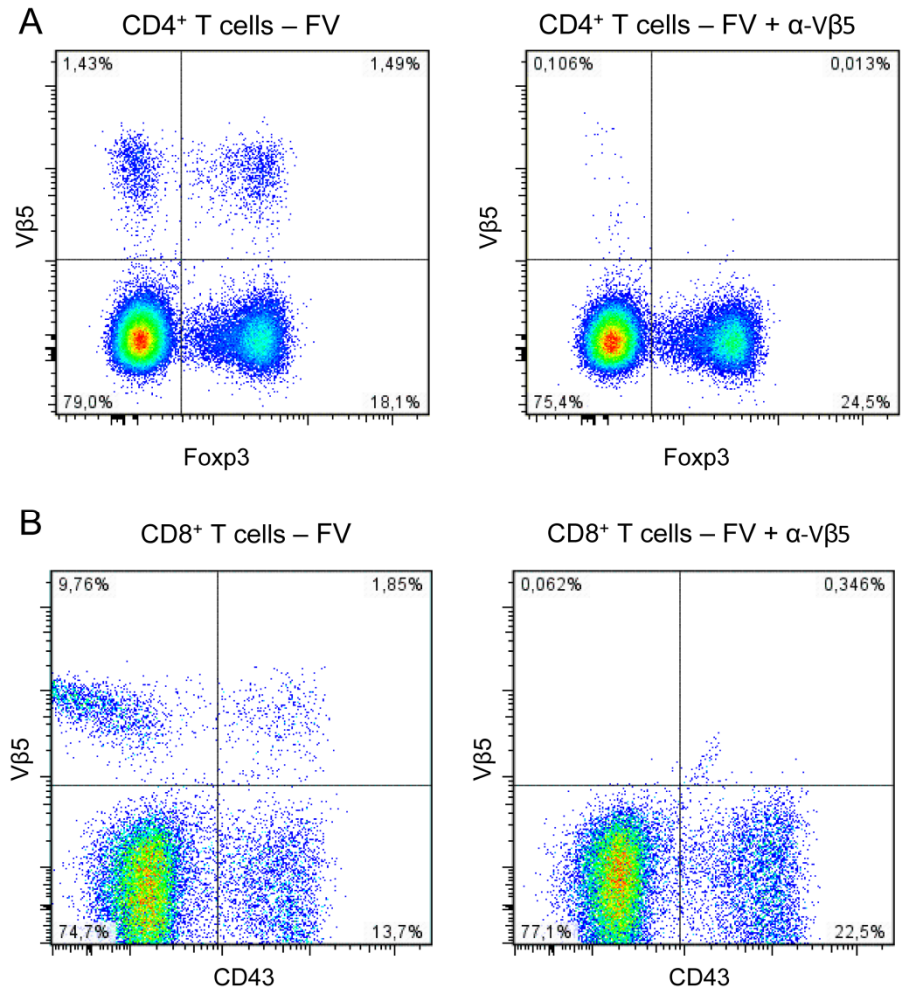

Figure 4. 26 **Vβ5 depletion efficiency of a α-Vβ5 MAb in the spleen of FV-infected mice.** B6 mice were infected i.v. with 20,000 SFFU FV and one group was treated i.p. with 300 µg of α-Vβ5 depletion MAb on day 4 post infection. To check for the depletion efficiency, spleen samples were stained for analysis by flow cytometry at 12 dpi. The depletion efficiency for **(A)** Tcon ($CD4^+Foxp3^-$) and Treg ($CD4^+Foxp3^+$) and **(B)** activated ($CD43^+$) $CD8^+$ T cells are shown as representative dot blots (left – non-depleted, right – depleted). The percentages in each gate are displayed in the corners of each quadrant.

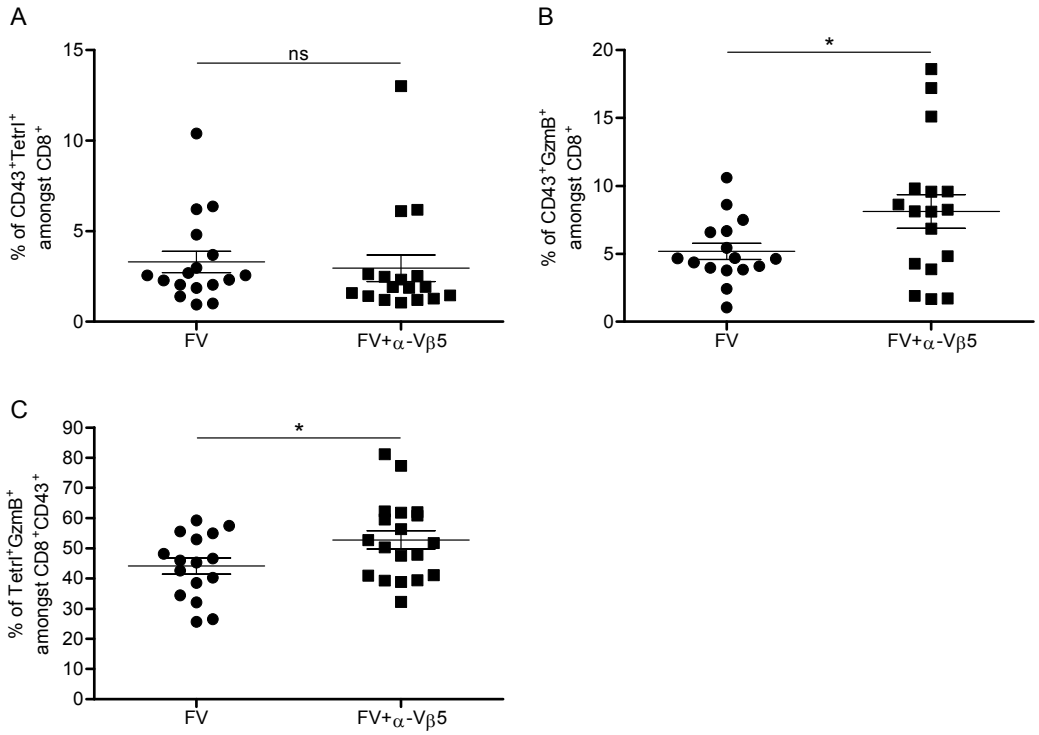

Figure 4. 27 **The CD8$^+$ T cell response in Vβ5-depleted mice.** B6 mice were infected i.v. with 20,000 SFFU FV and one group was treated i.p. with 300 µg of α-Vβ5 depletion MAb on day 4 post infection. The CD8$^+$ T cell response was investigated in the spleen at 12 dpi for the frequencies of **(A)** activated virus-specific (CD43$^+$TetrI$^+$), **(B)** activated GzmB producing (CD43$^+$GzmB$^+$) and **(C)** activated virus-specific GzmB$^+$ (CD43$^+$TetrI$^+$GzmB$^+$) CD8$^+$ cells using flow cytometry. Four independent experiments were carried out with each dot representing a single mouse. Bars indicate the mean and SEM. For statistical analysis a Student's t-test was used (ns not significant and * < 0.05).

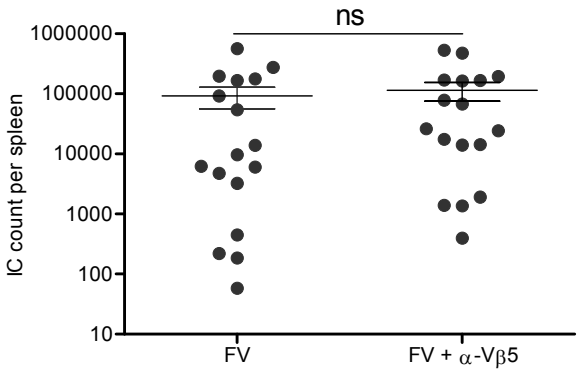

Figure 4. 28 **Viral loads in Vβ5-depleted FV-infected mice.** B6 mice were infected i.v. with 20,000 SFFU FV and one group was treated i.p. with 300 µg of α-Vβ5 depletion MAb on day 4 post infection. An IC assay was performed and the counts of infectious centres per total spleens were calculated. Four independent experiments were analysed with each dot representing a single mouse. Bars indicate the mean and SEM. For statistical analysis a Student's t-test was used (ns not significant and * < 0.05).

4.13 Expression of immune-suppression associated enzymes on Tregs during acute FV infection

After demonstrating that Tregs have a suppressive effect on $CD8^+$ T cells during FV infection, it was of interest to determine the molecular mechanism of Tregs mediated suppression. Various mechanisms for the suppressive activity of Tregs have been described. Thus far, no mechanism for Treg-induced immune suppression in FV infection has been defined, but a few possibilities can be excluded. These include IL10 (Dittmer U et al., 2004;Iwashiro M et al., 2001) and TGFβ (Robertson S J et al., 2006) and also CTLA-4 played only a minor role in Treg mediated suppression (Iwashiro M et al., 2001). However, Robertson *et al.* showed that Tregs suppress FV-specific $CD8^+$ T cells in a cell-contact dependent, APC-independent manner.

GzmB is a serine protease that can, with the help of perforin, kill cells in close proximity and has been shown to be produced by Tregs in a FV *in vivo* tumour model (Akhmetzyanova I et al., 2013). $CD8^+$ T cells are potent producers of GzmB during FV infection (Zelinskyy G et al., 2006) and $CD4^+$ T cells are also able to produce low amounts of this cytokine (195). It was therefore possible that Tregs might induce suppression by GzmB-mediated killing of effector T cells. In addition, TNFα can mediate apoptosis in adjacent cells and is also produced by $CD8^+$ T cells and Tcon during FV infection. However, for both molecules no production by Tregs could be detected during acute FV infection (data not shown).

Recently, two molecules that can mediate immune suppression have been described: CD73 (ecto-5'-nucleotidase) and CD39 (ecto-nucleoside triphosphate diphosphohydrolase 1). These enzymes work in a subsequent reaction in which ATP is metabolised to adenosine. Adenosine can then bind to the A2A receptor and mediate T cell suppression (34, 78, 162). To determine if this mechanism is involved in $CD8^+$ T cell suppression by Tregs during FV infection, the expression of CD73 and CD39 on Tregs from naïve and infected mice was investigated. In the spleen of naïve and FV-infected mice, Tregs were almost entirely positive for either CD39 (Figure 4. 29 A, left side) or CD73 (Figure 4. 29 A, right side), but a significant up-regulation of CD39 could still be demonstrated after infection. The frequency of Tcon positive for CD39 and CD73 was much lower compared to Tregs and CD39 was also up-regulated upon infection (Figure 4. 29 B).

For an effective suppressive function using this enzyme cascade, the expression of both molecules on a single cell is important. Most Tregs were positive for both CD39 and CD73 in the spleen of naïve mice and this percentage significantly increased in FV-infected mice. Tcon showed a low percentage of double positive cells in naïve mice and this increased only marginally in FV-infected mice (Figure 4. 29 C). Similar results were also obtained for the bone marrow (data not shown). In summary, it was found that more than 75% of all Tregs express both CD39 and CD73 on their surface in naïve and FV-infected mice, which suggests that this pathway might play a role in $CD8^+$ T cell suppression during acute FV infection.

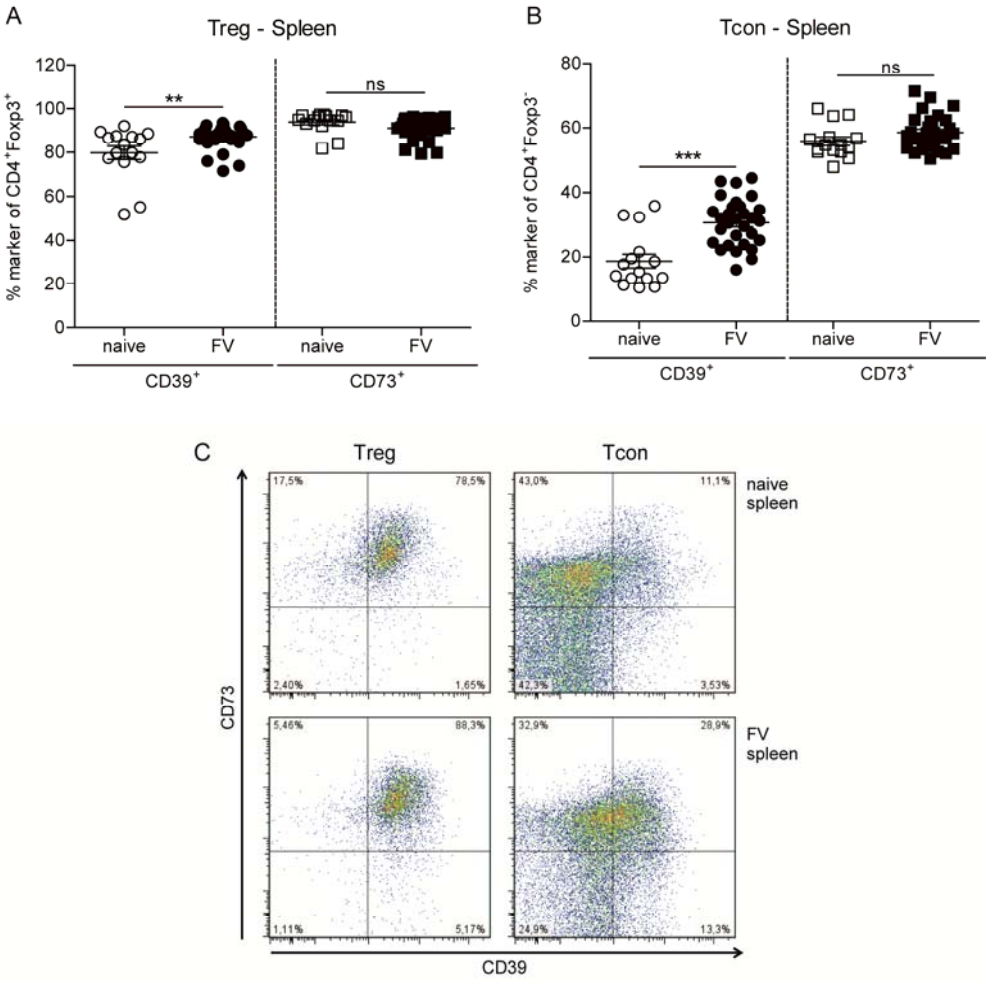

Figure 4. 29 **Expression of CD39 and CD73 on Tregs in the spleen of naïve or FV-infected mice.** B6 mice were infected i.v. with 20,000 SFFU FV or left un-infected and the expression of CD39 and CD73 on spleen cells was measured using flow cytometry on **(A)** Tregs ($CD4^+Foxp3^+$) and **(B)** Tcon ($CD4^+Foxp3^-$) at 12 dpi. Multiple independent experiments were carried out, with each dot representing a single mouse. Bars indicate the mean and SEM. For statistical analysis a Student's t-test was used (ns not significant, ** < 0.005 and *** < 0.0005). **(C)** Representative dot blots are shown for the dual expression of CD39 and CD73 on Tregs and Tcon from naïve and infected mice (12 dpi).

4.14 Effects of blocking CD73 on T cell responses during acute FV infection

Firstly, the down-stream enzyme, CD73, was tested for its role in Treg mediated suppression during FV infection. CD73 was blocked with a small molecule, AMPCP, via i.p. injection into FV-infected mice. This methodology for blocking CD73 enzymatic activity with AMPCP is specific and has been proven effective in mouse tumour models (334, 344). To evaluate the effect of this molecular blocking on the expression of both enzymes, the numbers of $CD39^+$ and $CD73^+$ Tregs of mice in the acute phase of FV infection were investigated. The block of CD73, did not change the numbers of $CD39^+$, $CD73^+$ or $CD39^+CD73^+$ Tregs per million spleen cells (Figure 4. 30), and similar results were obtained for the bone marrow (data not shown). Furthermore, no alteration of activation and proliferation markers such as Ki67, KLRG1 or Helios, were observed on Tregs after AMPCP injection (data not shown). However, the used dose has been shown to be effective in blocking CD73 enzymatic activity (personal communication Svetlana Karakhanova, Department of Dermatology, University of Heidelberg, Germany). Thus the Treg phenotype or activation status was not altered, but the suppressive function of the Tregs may still be affected by blocking CD73.

To determine any effects on the *in vivo* suppressive activity of treated Tregs the $CD8^+$ and $CD4^+$ T cell response was evaluated in FV-infected mice. $CD4^+$ T cells did not increase activation ($CD43^+CD62L^-$) in AMPCP treated mice, nor did they show any signs of enhanced cytokine production ($IFN\gamma^+$, $IL2^+$ or $TNF\alpha^+$) in the spleen (Figure 4. 31 A and Figure 4. 32 A) or bone marrow (data not shown) compared to only FV-infected mice.

$CD8^+$ T cells also did not become more activated in treated compared to un-treated mice ($CD43^+CD62L^-$), and there were no higher frequencies of activated virus specific ($CD43^+TetrI^+$), cytotoxin producing ($CD43^+GzmB^+$) or $CD8^+$ T cells showing signs of recent degranulation ($CD43^+CD107a^+$) in the spleen (Figure 4. 31 B) or bone marrow (data not shown). Furthermore, when $CD8^+$ T cells were investigated for cytokine ($IFN\gamma^+$, $IL2^+$ or $TNF\alpha^+$) production, no differences between FV-infected and the infected AMPCP treated mice were found in the spleen (Figure 4. 32 B) or bone marrow (data not shown).

Finally, the viral loads in FV-infected and infected AMPCP treated mice were investigated and no reduction was seen in the spleen (Figure 4. 33) or bone marrow (data not shown). Thus overall, the block of CD73 with AMPCP does not influence adaptive T cell immune responses or the viral load during acute FV infection.

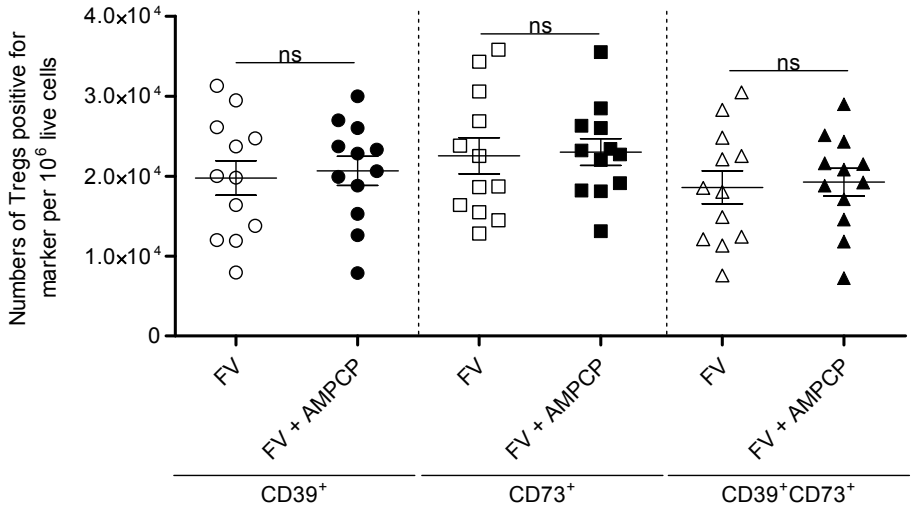

Figure 4. 30 **The numbers of CD39$^+$ and CD73$^+$ Tregs after AMPCP treatment.** B6 mice were infected i.v. with 20,000 SFFU FV for 12 days and one group was treated i.p. three times every other day with 200 µg AMPCP starting from 6 dpi. The numbers of CD39$^+$, CD73$^+$ and CD39$^+$CD73$^+$ Tregs in the spleen were measured using flow cytometry and a comparison between non-treated infected mice (FV) and AMPCP treated infected mice (FV + AMPCP) was carried out. Three independent experiments were done, with each dot representing a single mouse. Bars indicate the mean and SEM. For statistical analysis a Student's t-test was used (ns not significant).

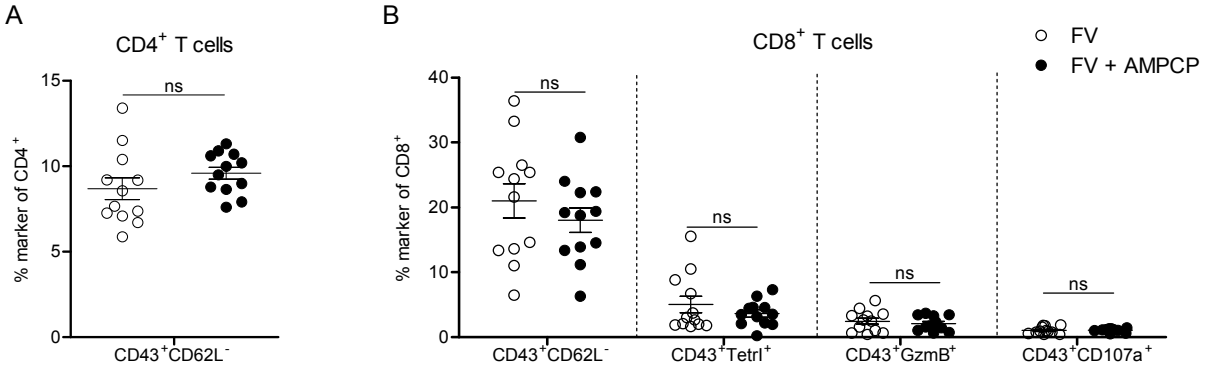

Figure 4. 31 **Treatment of FV-infected mice with AMPCP and the effect on activation and production of cytotoxic molecules from CD4$^+$ and CD8$^+$ T cells.** B6 mice were infected i.v. with 20,000 SFFU FV for 12 days and one group was treated i.p. three times every other day with 200 µg AMPCP starting from 6 dpi. **(A)** CD4$^+$ T cells and **(B)** CD8$^+$ T cells from the spleen were assessed for their phenotype. The percentage of activated cells

($CD43^+CD62L^-$), activated virus-specific cells ($CD43^+TetrI^+$), production of the cytotoxic molecule GzmB by activated cells ($CD43^+GzmB^+$) and activated cells that recently de-granulated ($CD43^+CD107a^+$) were measured using flow cytometry. A comparison between untreated infected mice (FV) and AMPCP treated infected mice (FV + AMPCP) is shown. Three independent experiments were conducted, with each dot representing a single mouse. Bars indicate the mean and SEM. For statistical analysis a Student's t-test was used (ns not significant).

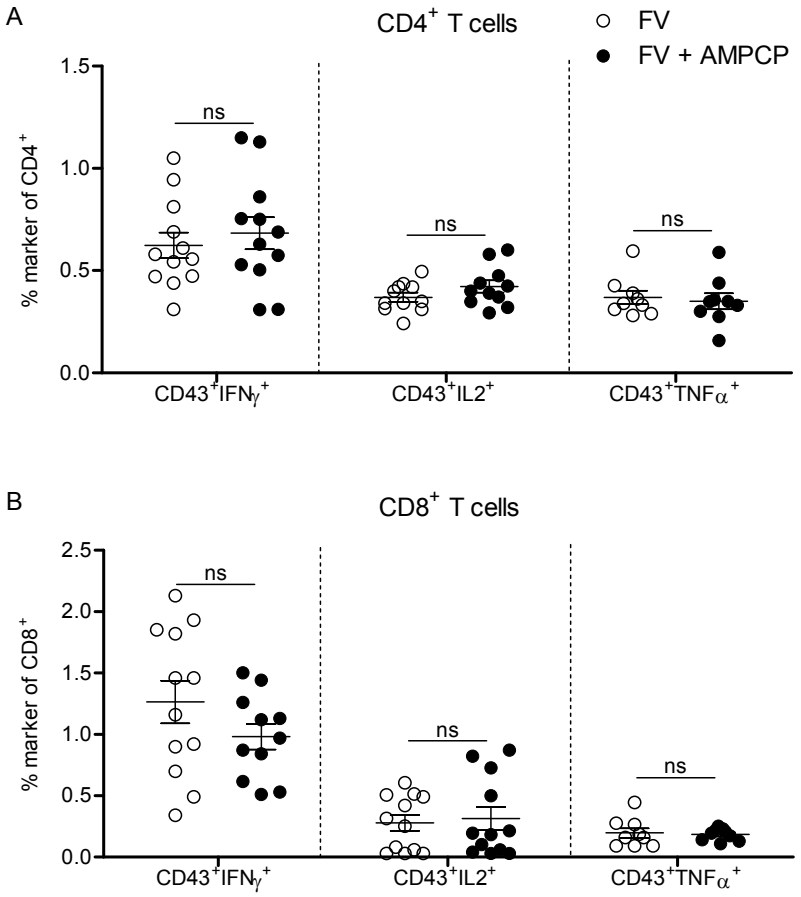

Figure 4. 32 **Treatment of FV-infected mice with AMPCP and the effect on cytokine production from $CD4^+$ and $CD8^+$ T cells.** B6 mice were infected i.v. with 20,000 SFFU FV for 12 days and one group was treated i.p. three times every other day with 200 µg AMPCP starting from 6 dpi. Before staining for FACS analysis the cells were unspecifically re-stimulated *ex vivo*. The percentage of activated cells producing different cytokines ($CD43^+IFN\gamma^+$, $CD43^+IL2^+$, $CD43^+TNF\alpha^+$) was measured by flow cytometry and a comparison between untreated acutely infected mice (FV) and AMPCP treated acutely infected mice (FV + AMPCP) is shown for the spleen for **(A)** $CD4^+$ and **(B)** $CD8^+$ T cells. Three independent experiments were conducted, with each dot representing a single mouse. Bars indicate the mean and SEM. For statistical analysis a Student's t-test was used (ns not significant).

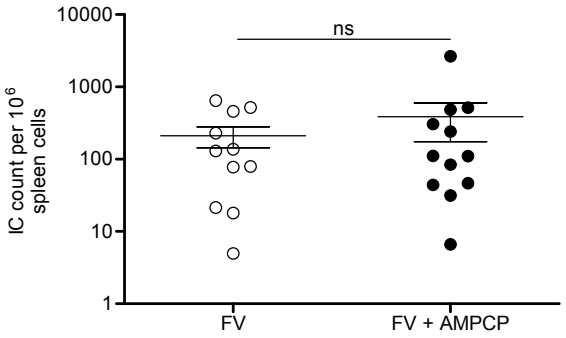

Figure 4. 33 **Virus titres after AMPCP treatment of FV-infected mice.** B6 mice were infected i.v. with 20,000 SFFU FV for 12 days and one group was treated i.p. three times every other day with 200 µg AMPCP starting from 6 dpi. An IC assay was carried out and the count of infectious centres per $1x10^6$ spleen cells is shown for untreated infected mice (FV) and AMPCP treated infected mice (FV + AMPCP). Three independent experiments were conducted with each dot representing a single mouse. Bars indicate the mean and SEM. For statistical analysis a Student's t-test was used (ns not significant).

4.15 CD73 knock-out mice show an only slightly enhanced cytotoxic $CD8^+$ T cell response during FV infection

To verify the results from the biochemical blockage experiment, antiviral immune responses to FV infection were investigated in CD73-KO mice. Treg cell numbers in CD73-KO and CD73-WT mice were normal compared to B6-WT mice and were also indistinguishable between FV-infected CD73-WT and CD73-KO mice (data not shown).

For effector T cell responses, no differences in activation of $CD4^+$ T cells ($CD43^+CD62L^-$; Figure 4. 34 A) or cytokine production (TNFα, IL2 and IFNγ; data not shown) were found between FV-infected CD73-KO and WT mice. $CD8^+$ T cells play a more dominant role for controlling acute FV infection and are therefore more susceptible to Treg induced suppression. There was a minor, albeit significant, increase in the frequency of activated ($CD43^+CD62L^-$) and GzmB-producing ($CD43^+GmzB^+$) $CD8^+$ T cells in the spleens of FV-infected CD73-KO mice compared to WT mice (Figure 4. 34 B). However, no differences for virus-specific ($CD43^+TetrI^+$), degranulated ($CD43^+CD107a^+$) (Figure 4. 34 B) or cytokine producing (TNFα, IL2 and IFNγ; data not shown) $CD8^+$ T cells were seen between CD73-KO and CD73-WT mice. Similar results were obtained for $CD4^+$ and $CD8^+$ T cells in the bone marrow.

Even though $CD8^+$ T cells from CD73-KO mice were slightly more activated and a higher frequency were $CD43^+GzmB^+$ compared to CD73-WT mice, this had no effect on the viral load assessed in the spleen (Figure 4. 35) or bone marrow (data not shown) at 10 dpi. In summary, CD73 does not play a major role in Treg mediated suppression of $CD4^+$ and $CD8^+$ T cell responses; although a small effect on $CD8^+$ T cell activation was found.

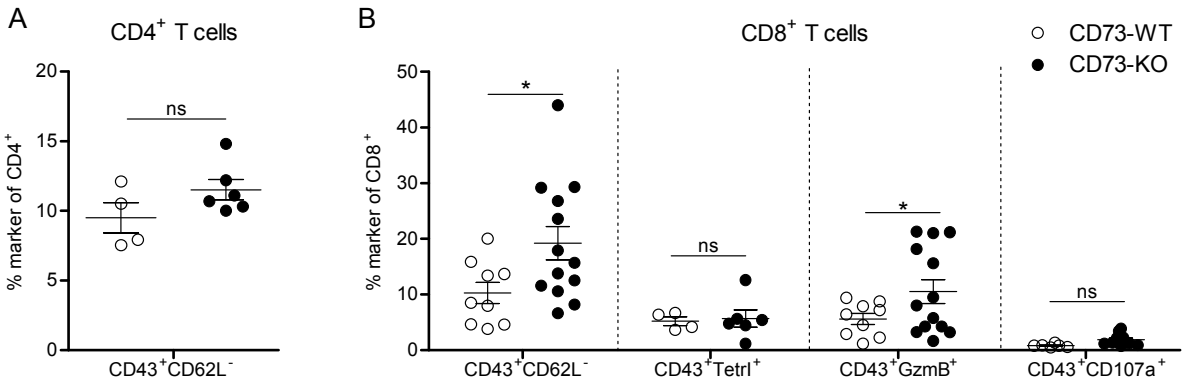

Figure 4. 34 **The effect of CD73-KO on activation and production of cytotoxic molecules from $CD4^+$ and $CD8^+$ T cells in FV-infected mice.** CD73-WT and CD73-KO mice were infected i.v. with 20,000 SFFU FV for 10 days and **(A)** $CD4^+$ T cells and **(B)** $CD8^+$ T cells from the spleen were analysed. The frequency of activated cells ($CD43^+CD62L^-$), activated virus-specific cells ($CD43^+TetrI^+$)**,** activated cells producing GzmB ($CD43^+GzmB^+$) and cell that had recently de-granulated ($CD43^+CD107a^+$) were measured using flow cytometry and are shown. One to three independent experiments with at least four mice per group were analysed. Bars indicate the mean and SEM. For statistical analysis a Student's t-test was used (ns not significant and * < 0.05).

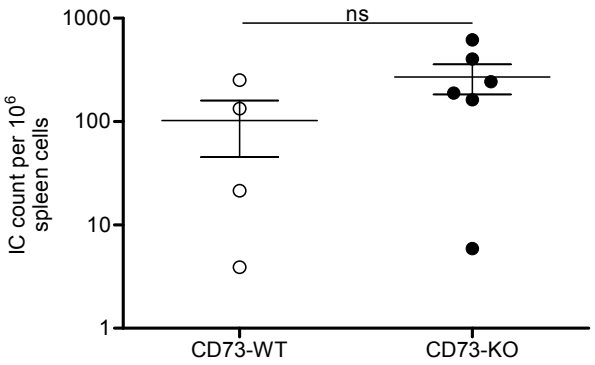

Figure 4. 35 **Virus titres of FV-infected CD73-KO mice.** CD73-WT and CD73-KO mice were infected i.v. with 20,000 SFFU FV for 10 days and an IC assay was performed with splenocytes. The count of infectious centres per $1x10^6$ spleen cells was calculated and is shown in the graph. At least four mice per group were analysed. Bars indicate the mean and SEM. For statistical analysis a Student's t-test was used (ns not significant).

4.16 CD39 knock-out mice show an augmented T cell response during acute FV infection without altering viral loads

After analysing the role of CD73 during FV infection, the role of CD39 was also investigated in a knockout mouse model. CD39 is the rate limiting enzyme in the cascade of Treg-mediated suppression via CD39 and CD73. To evaluate the role of CD39, CD39-KO and CD39-WT mice were infected with FV for 10 days and the same immunological parameters as for the CD73-KO/WT mice were analysed. Again the CD39 knockout had no influence on the numbers of Tregs in the spleen when compared to CD39-WT or B6-WT mice in infected animals (Figure 4. 36 A). In contrast, there was a significant increase in Treg numbers in the bone marrow of infected CD39-KO mice compared to infected CD39-WT mice (Figure 4. 36 B).

To investigate if the lack of CD39 has an effect on the suppressive function of Tregs, the production of cytokines and cytotoxic molecules in $CD4^+$ and $CD8^+$ T cells from FV-infected CD39-KO and CD39-WT mice was assessed. After 10 dpi there were no significant differences in the activation ($CD43^+CD62L^-$) or cytokine production (TNFα, IL2 and IFNγ) of $CD4^+$ T cells between CD39-WT and CD39-KO mice in the spleen (Figure 4. 37 A and Figure 4. 38 A) or bone marrow (data not shown). However, a lack of CD39 led to an increased frequency of activated ($CD43^+CD62L^-$), virus specific ($CD43^+TetrI^+$) and GzmB producing ($CD43^+GzmB^+$) $CD8^+$ T cells in the spleen (Figure 4. 37 B) and bone marrow of infected mice (data not shown). No changes in frequencies of recently de-granulated ($CD43^+CD107a^+$) $CD8^+$ T cells were detected due to the CD39 knockout (Figure 4. 37 B). Interestingly, for cytokine responses, an increase in the frequencies of activated IFNγ producing $CD8^+$ T cells was seen in the spleen (Figure 4. 38 B) and bone marrow (data not shown) of CD39-KO compared to CD39-WT mice. No change in the frequencies of $CD43^+TNFα^+$ and $CD43^+IL2^+$ $CD8^+$ T cells were found in the spleen (Figure 4. 38 B) or bone marrow (data not shown) of FV-infected CD39-KO mice compared to infected CD39-WT mice.

Finally, as knockout of CD39 increased activated virus-specific, cytotoxin and IFNγ producing $CD8^+$ T cell numbers, it was of interest to assess the viral loads in FV-infected CD39-KO compared to infected CD39-WT mice. No differences in viral loads were observed in the spleen (Figure 4. 39) or bone marrow (data not shown);

however, a trend towards lower viral loads was seen in CD39-KO compared to CD39-WT mice. In conclusion, it was shown that $CD8^+$ T cells from CD39-KO mice show a higher activation and production of GzmB and IFNγ compared to CD39-WT mice, however this had no effect on viral loads during the acute phase of infection.

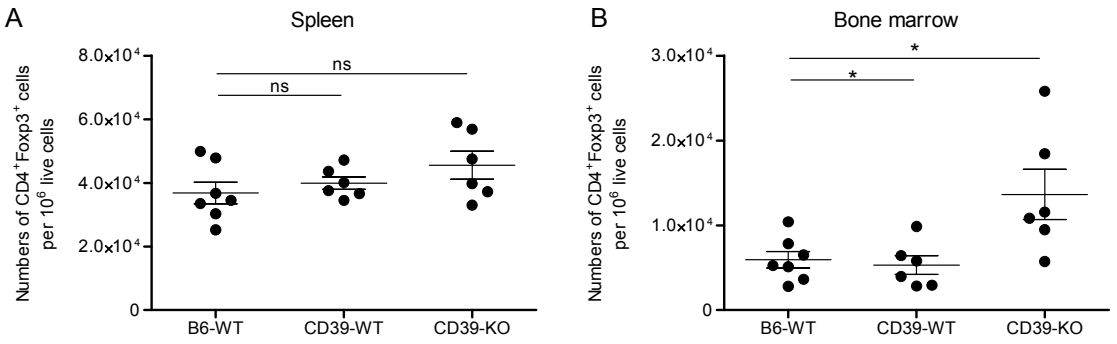

Figure 4. 36 **Numbers of Tregs in FV-infected CD39-KO, and CD39-WT mice.** CD39-KO, CD39-WT and B6-WT mice were infected i.v. with FV for 10 days and the numbers of $CD4^+Foxp3^+$ Tregs per $1x10^6$ cells were assessed using flow cytometry for spleen and bone marrow cells. A comparison of infected CD39-KO, CD39-WT and B6-WT mice is shown: **(A)** for the spleen and **(B)** the bone marrow. Each dot represents a single mouse. The bars indicate the mean and SEM. For statistical analysis a Dunnett's multiple comparison test was carried out with B6-WT as a reference (ns not significant, * < 0.05).

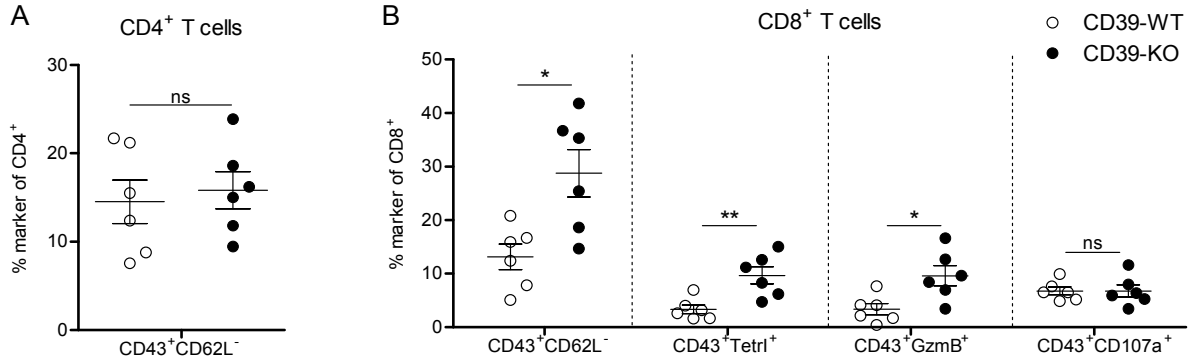

Figure 4. 37 **The effect of CD39-KO on activation and production of cytotoxic molecules from $CD4^+$ and $CD8^+$ T cells in FV-infected mice.** CD39-WT and CD39-KO mice were infected i.v. with 20,000 SFFU FV for 10 days and **(A)** $CD4^+$ T cells and **(B)** $CD8^+$ T cells from the spleen were analysed. The frequency of activated ($CD43^+CD62L^-$), virus-specific cells ($CD43^+TetrI^+$), cells producing GzmB ($CD43^+GzmB^+$) and cells that recently de-granulated ($CD43^+CD107a^+$) were measured using flow cytometry and are shown. At least six mice per group were analysed. The bars indicate the mean and SEM. For statistical analysis a Student's t-test was used (ns not significant, * < 0.05, ** < 0.005).

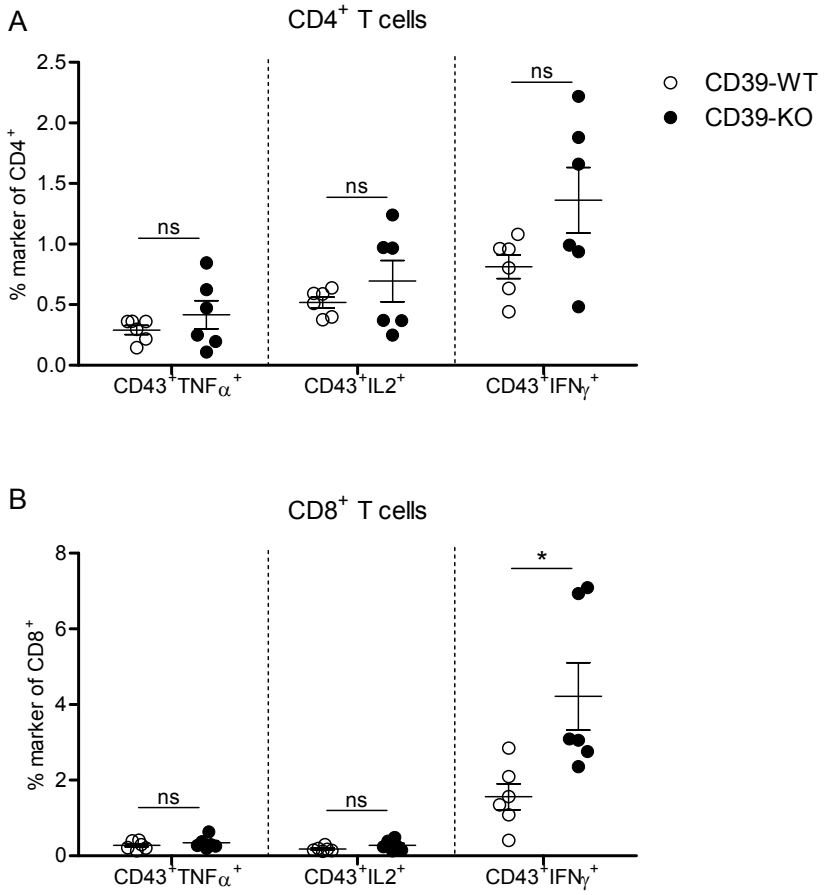

Figure 4. 38 **Cytokine production in CD4$^+$ and CD8$^+$ T cells from FV-infected CD39-KO and CD39-WT mice.** CD39-WT and CD39-KO mice were infected i.v. with 20,000 SFFU FV for 10 days and the frequency of activated cells producing different cytokines (CD43$^+$TNFα $^+$, CD43$^+$IL2$^+$, CD43$^+$IFNγ $^+$) were measured using flow cytometry. Before staining for FACS analysis the cells were unspecifically re-stimulated *ex vivo.* The cytokine profiles for: **(A)** CD4$^+$ and **(B)** CD8$^+$ T cells in the spleen are shown. At least six mice per group were analysed. Bars indicate the mean and SEM. For statistical analysis a Student's t-test was used (ns not significant, * < 0.05).

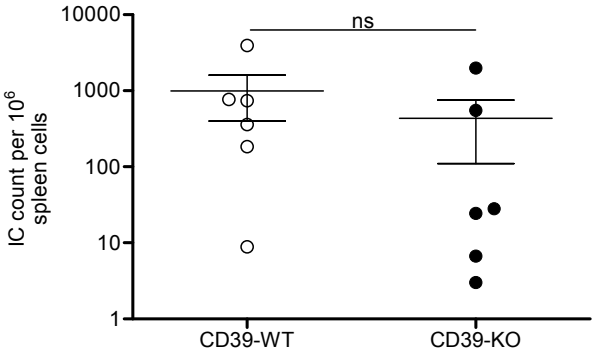

Figure 4. 39 **Virus titres of FV-infected CD39-KO mice.** CD39-WT and CD39-KO mice were infected i.v. with 20,000 SFFU FV for 10 days and an IC assay was conducted. The count of infectious centres per 1x10^6 spleen cells was calculated and is shown. At least four mice per group were analysed. The bars indicate the mean and SEM. For statistical analysis a Student's t-test was used (ns not significant).

4.17 Investigation into the activation profile of human Tregs during HIV-1 infection and the influence of HAART

Tregs play an important role in suppressing anti-viral immune responses in HIV-1 infection (251). While HIV-1 is a complex retrovirus, from the lentivirus genus, and FV is a simple retrovirus, both induce the expansion of Tregs during chronic infection of their host. To determine if human Tregs show similar characteristics of activation compared to mouse Tregs, the activation of human Tregs *in vitro* and *ex vivo* was investigated. Four markers, KLRG1, TNFRII, CD25 and CD127, were chosen based on the observations made in the FV infection model. To establish if these markers could be used to monitor activation of human Tregs, PBMCs from healthy donors were TCR stimulated and the levels of marker expression on Tregs were measured. Human Tregs were characterised as $CD4^+Foxp3^+$, based on the gating strategy shown in Figure 3. 4. Three markers (KLRG1, TNFRII and CD25) became significantly up-regulated on the stimulated compared to the non-stimulated Tregs. CD127 expression was down-regulated, although no significance was detected (Figure 4. 40).

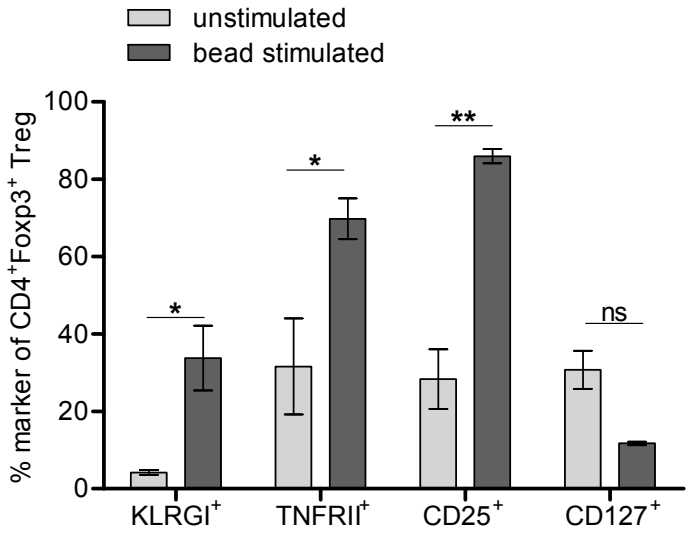

Figure 4. 40 **The effect of bead-stimulation on the activation of human Tregs.** Isolated human PBMCs from healthy donors were plated and either not stimulated or stimulated with α-CD3/α-CD28 coated human stimulation beads. The cells were then stained and analysed using flow cytometry. The percentage of different markers on $CD4^+Foxp3^+$ Tregs is displayed. The experiment was performed three times and the results were pooled. Bars indicate the mean and SEM. For statistical analysis a Student's t-test was used (ns not significant, * < 0.05 and ** < 0.005).

Next the expression of these markers was investigated on non-stimulated cells from HIV-1 infected individuals. The selected patients were part of a clinical trial studying the effect of a specific HAART regime on previously untreated, chronically HIV-1 positive individuals (non-treated, NT) (for more detail see page 50, 2.10.2 HIV-1 infected volunteers). Sex and age matched healthy volunteers (healthy control, HC) were also enrolled in this study. No significant differences were observed for KLRG1, TNFRII and CD25 expression on Tregs between HIV-1 infected individuals and healthy controls, although a tendency towards higher expression of TNFRII and CD25 was seen in non-treated HIV-1 infected individuals. However, CD127 expression was significantly reduced from HC to NT, indicating activation of Tregs in HIV-1 infected individuals (Figure 4. 41).

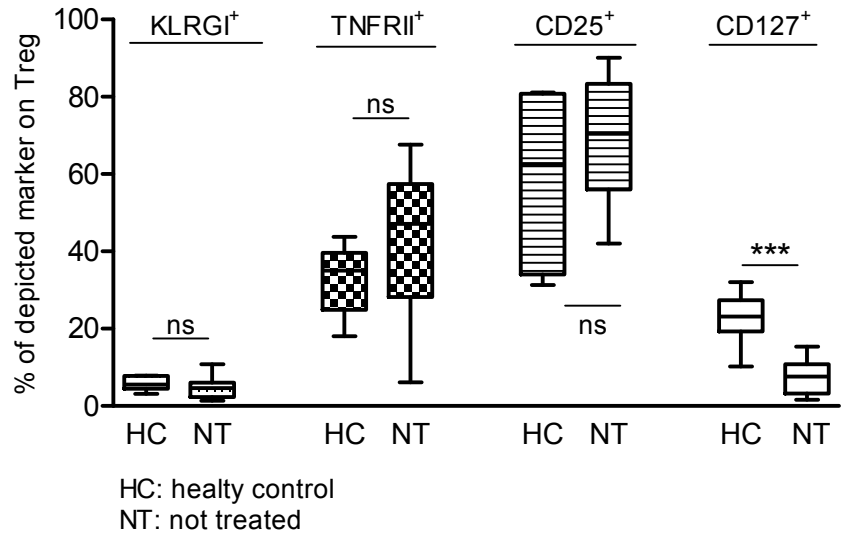

Figure 4. 41 **Markers on Tregs from healthy and untreated HIV-1 infected individuals.** Isolated human PBMCs of healthy individuals (n=6) (HC) and untreated HIV-1 positive individuals (n=8) (NT) were stained and analysed using flow cytometry. The percentage of different markers on $CD4^+Foxp3^+$ Tregs is displayed. Boxplots indicate the minimum, median, maximum and range. For statistical analysis a Student's t-test was used (ns not significant and ** < 0.005).

As mentioned earlier, the enrolled patients were part of a clinical trial, where all patients received the same regime of antiretroviral drugs. The blood samples were drawn at set time points after the start of HAART (4, 8 and 24 weeks). Interestingly, at the time point prior to treatment (0), these individuals displayed a significant increase in Treg percentages in the peripheral blood compared to healthy controls,

which was lost as the patients began HAART (4, 6 and 24 weeks post HAART) (Figure 4. 42).

To evaluate the activation level of Tregs during HAART, the frequencies of KLRG1$^+$, TNFRII$^+$, CD25$^+$ and CD127$^+$ Tregs in PBMCs from infected individuals were analysed and compared to PBMCs from HC. There were no differences in the expression of KLRG1, TNFRII or CD25 detected between HC and HIV-1 infected patients receiving HAART (Figure 4. 43). Only the frequency of CD127$^+$ Tregs displayed a significant decrease from HC to patients that were untreated or treated (Figure 4. 43). In summary, human Tregs can be activated *in vitro* but the defined activation markers (KLRG1, TNFRII and CD25) were not significantly up-regulated on Tregs during HIV-1 infection.

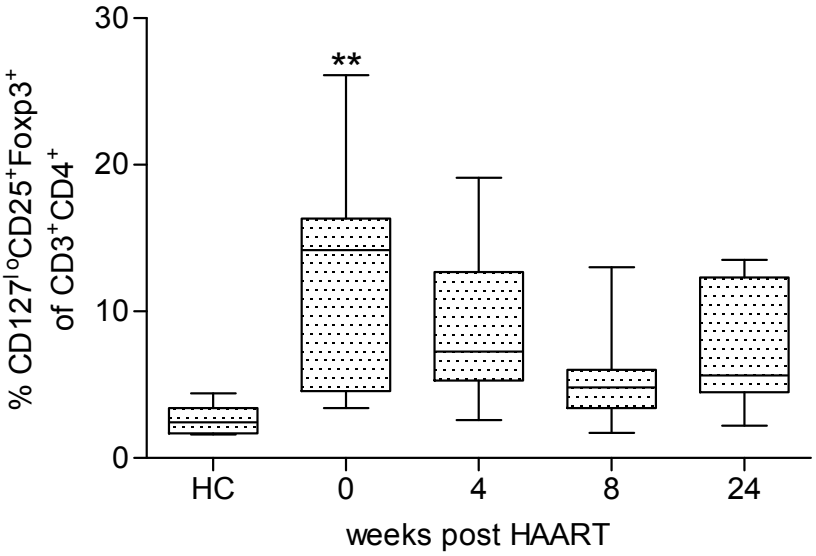

Figure 4. 42 **Percentages of Tregs during HAART of HIV-1 positive individuals.** Isolated PBMCs from healthy donors (n=6) (HC) and chronically HIV-1 positive individuals (n=8) from different time points post HAART (0, 4, 8 and 24 weeks) were stained and analysed using flow cytometry. The percentage of CD4$^+$CD25^{hi}CD127^{lo}Foxp3$^+$ Tregs of CD3$^+$CD4$^+$ T cells is displayed. Boxplots indicate the minimum, median, maximum and range. Statistical analysis was done using a Dunnett's multiple comparison test with the group of healthy individuals as reference (** < 0.005).

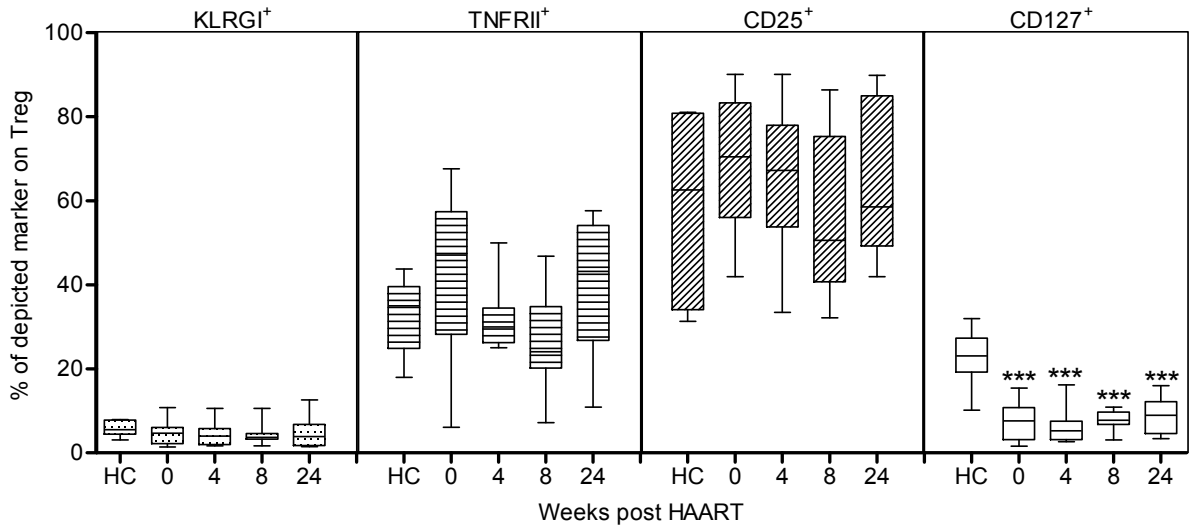

Figure 4. 43 **Markers on Tregs from HIV-1 infected individuals before and during HAART.** Isolated PBMCs of healthy individuals (n=6) (HC) and HIV-1 infected individuals (n=8) at different times post HAART initiation (x-axis) were stained and analysed using flow cytometry. The percentage of markers on $CD4^+Foxp3^+$ Tregs is displayed (marker name at the top). Boxplots indicate the minimum, median, maximum and range. Statistical analysis was done using a Dunnett's multiple comparison test with the group of healthy individuals as reference (*** < 0.0005).

4.18 Investigation of the suppressive activity of Tregs from HIV-1 infected patients

After determining the activation status of Tregs during HIV-1 infection it was of interest to analyse the functional activity of these Tregs. In HIV-1 infection it has been shown that Tregs have both beneficial and detrimental effects. On the one hand they can limit chronic immune activation, thereby limiting immune response mediated damage and disease progression, and on the other hand this leads to an ineffective anti-viral immune response and chronic infection (206).

To investigate the protective effect of Tregs during HIV-1 infection a model of mucosal virus encounter was chosen. For this, human bead-isolated $CD14^+$ cells were cultured with IL4 and GM-CSF to differentiate them into monocyte derived DCs (MoDCs). These were then infected with HIV-1 JRFL-iGFP and SIV_{mac}-VLPs for three days. A productive infection of MoDCs with HIV-1 can be demonstrated via the Amnis ImageStream technology detecting the iGFP signal of HIV-1 particles (Figure 4. 44 A). To analyse the spread of HIV-1 infection, $CD4^+$ T cells were co-cultured with

the infected MoDCs. The $CD4^+$ T cells were defined as Tcon ($CD4^+CD8^-CD25^{lo}CD127^{hi}$, labelled with violet tracker (VT)) and Treg ($CD4^+CD8^-CD25^{hi}CD127^{lo}$, labelled with $CD25^+$-BV785) and the formation of clusters was investigated (Figure 4. 44 B).

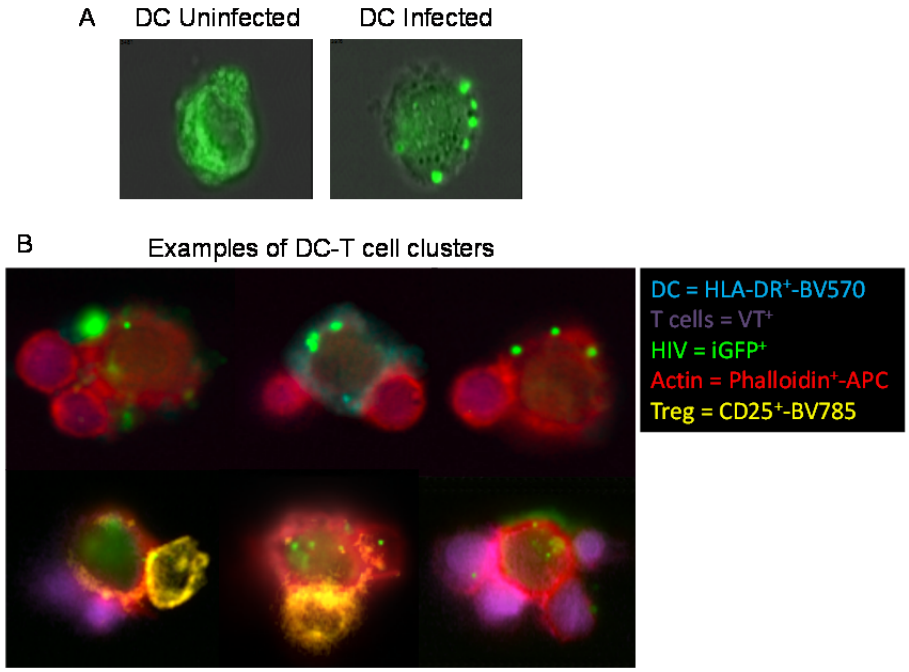

Figure 4. 44 ***In vitro* HIV-1 JRFL-iGFP infected MoDC:$CD4^+$ T cell clusters.** MoDCs were cultured and infected with HIV-1 JRFL-iGFP and SIV_{mac}-VLPs. The infection of MoDCs was measured with the Amnis ImageStream technology and a representative example of **(A)** an uninfected (left) and an infected MoDC (right) is shown. **(B)** HIV-1 JRFL-iGFP and SIV_{mac}-VLP infected MoDCs were co-cultured with $CD4^+CD8^-CD25^{lo}CD127^{hi}$ Tcon and $CD4^+CD8^-CD25^{hi}CD127^{lo}$ Tregs from the same donor. After 36 hours of co-culture the samples were stained as indicated (right panel – pseudo colour scheme) and measured with the Amnis ImageStream imaging flow cytometer.

To measure the spread of the infection into different cell populations after 36 hours of *in vitro* co-culture, the iGFP signal was investigated for: clusters of MoDCs and $CD4^+$ T cells (clusters), MoDCs (DC) and $CD4^+$ T cells (CD4). The highest percentage of infection was found in the $CD4^+$ T cell:DC clusters, whereas much lower levels were found in single MoDCs or single $CD4^+$ T cells (Figure 4. 45 A). This indicated that cluster formation was important to mediate the spread of HIV-1 into $CD4^+$ T cells.

The influence of $CD4^+$ Tregs on cluster formation was investigated, as the inhibition of this cluster formation could be a mechanism for Tregs to prevent $CD4^+$ T cell infection with HIV-1 via cell-to-cell contacts to DCs. No differences in cluster formation were found when Tregs were cultured with infected MoDCs (infDC) and

Tcon (plus Treg) in comparison to only infDC+Tcon co-cultures. Furthermore, addition of Treg inhibitors: ddADA, α-CTLA-4 and α-TGFβ; to inhibit an array of Treg suppression mechanisms, also did not have an effect on cluster formation (Figure 4. 45 B). This data indicated that Tregs did not directly inhibit the formation of clusters between MoDCs and Tcon.

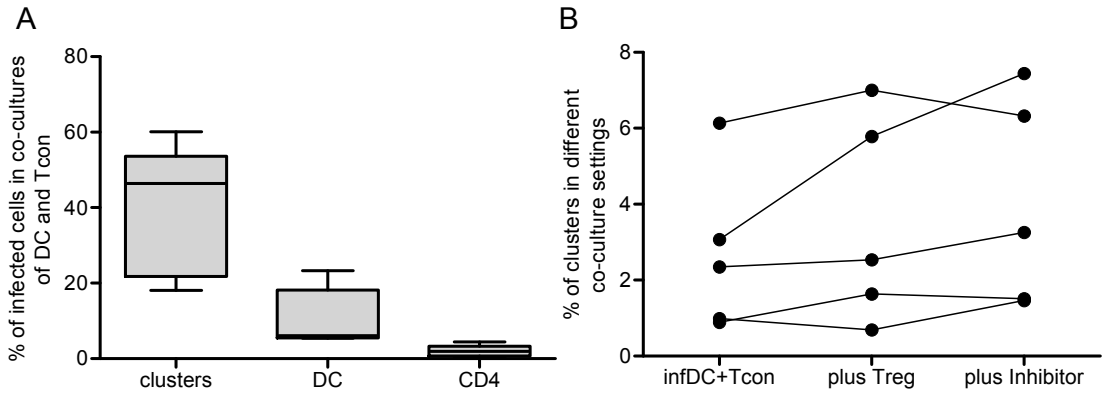

Figure 4. 45 **Investigation of HIV-1 infection in *in vitro* co-cultures and the influence of Tregs on cluster formation.** Infected MoDCs were co-cultured with Tcon and Treg from the same donor. After 36 hours of co-culture the samples were stained and measured with the Amnis ImageStream imaging flow cytometer for **(A)** the presence of HIV-1 JRFL-iGFP infection in either MoDC:$CD4^+$ T cell clusters (clusters), MoDCs (DC) or $CD4^+$ Tcon (CD4). Five different donors were investigated. Boxplots indicate the minimum, median, maximum and range. **(B)** To investigate the cluster formation in different co-culture settings infected MoDCs and Tcon (infDC+Tcon), infected MoDCs, Tcon and Tregs (plus Treg) or infected MoDCs, Tcon, Tregs with the addition of the inhibitors ddADA, α-CTLA-4 and α-TGFβ (plus Inhibitor), were co-cultured and the percentage of clusters forming in the co-culture is shown for five different PBMC donors.

It has been shown that Tregs can inhibit the infection of Tcon with HIV-1 in such MoDC:$CD4^+$ T cell clusters (Moreno-Fernandez, submitted). The stability of the clusters was not influenced by Tregs and can now be excluded as a mechanism of Treg-mediated limitation of HIV-1 infection spread. Another possible mechanism for Treg mediated suppression of Tcon infection could be the suppression of the actin cytoskeleton of DCs and/or Tcon. The intracellular movement of HIV-1 is dependent on the cytoskeleton and its suppression could have an influence on the virus spread to other cells (Moreno-Fernandez, submitted). Based on this, the actin polymerisation at the immunological synapse in co-cultures of HIV-1 infected MoDCs and $CD4^+$ T cells was investigated using the iGFP signal-localisation and phalloidin (actin) staining. The data revealed a correlation between actin and HIV-1 particles at the immunological synapse in co-cultures of HIV-1 infected MoDCs with Tcon (Figure 4.

46 A). Most interestingly, this correlation was less strong when Tregs were added to the co-cultures, which indicates that Tregs are able to suppress the transport of viral particles along the actin cytoskeleton (Figure 4. 46 B).

In summary, it was shown that Tregs did not inhibit cluster formation between HIV-1 infected MoDCs and Tcon, but the presence of Tregs decreased the actin polymerisation in MoDCs and the presence of HIV-1 at the immunological synapse between Tcon and HIV-1 infected MoDCs. This is a potential mechanism of Treg mediated suppression of DC to Tcon transmission of HIV-1 infection, however the molecular basis for this remains to be defined.

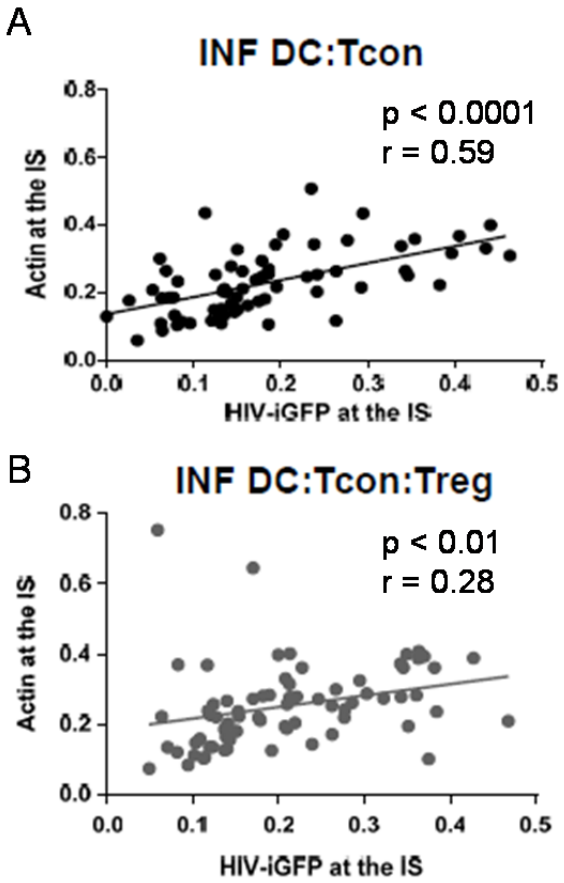

Figure 4. 46 **HIV-1 JRFL-iGFP localization in MoDC:Tcon clusters in the presence or absence of Tregs.** Infected MoDCs were co-cultured with **(A)** $CD4^+CD8^+CD25^{lo}CD127^{hi}$ Tcon (INF DC:Tcon) or **(B)** with the addition of $CD4^+CD8^+CD25^{hi}CD127^{lo}$ Tregs (INF DC:Tcon:Treg) from the same donor. After 24 hours of co-cultivation the samples were stained and measured with the Amnis ImageStream imaging flow cytometer. The amount of phalloidin signal for actin (y-axis: actin at the immunological synapse (IS)) and GFP signal for HIV-1 JRFL-iGFP (x-axis: HIV-iGFP at the IS) in DC:Tcon clusters was measured in **(A)** the absence and **(B)** presence of Tregs. For statistical analysis these two parameters were correlated and the p- and r-value are shown.

5. Discussion

Regulatory T cells play an important role in retroviral infections. The effect of Tregs on infection can be both beneficial for the host, in limiting immune pathology, and detrimental, by promoting the establishment of a chronic infection. Both of these effects have been described for Tregs in retroviral infections of humans and mice. Currently the precise mechanism(s) of Treg expansion and their functional properties during retroviral infections remain to be elucidated (23). This knowledge could provide important information to alter Treg responses and induce an improved immune response to infection with limited immune pathology.

Overall, the work presented in this thesis has elucidated the influence of effector T cells on Treg expansion during FV infection. Tregs become activated during the acute phase of FV infection and remain activated in chronic infection. During acute FV infection the expanding Treg population was shown to consist of nTregs with a subset of IL2-dependent Vβ5$^-$ Tregs and a highly activated subset of TNFα-dependent Vβ5$^+$ Tregs. The discovery of different Treg populations during retroviral infection can have important implications for further research in this field.

5.1 The phenotype of Tregs during retroviral infections.

One of the main aims of this thesis was to characterise the phenotype of Tregs during FV infection. It was shown that Tregs were expanded in the spleen and bone marrow during acute FV infection, they proliferated (Figure 4. 1) and displayed an activated and differentiated phenotype (Figure 4. 3 and Figure 4. 5). It was thought for a long time that Tregs were anergic and did not proliferate in response to stimulation. However, this was only established using *in vitro* models, and *in vivo* studies have clearly shown that Tregs do proliferate in response to stimulation. Haribhai *et al.* demonstrated that Tregs proliferate after immunisation of mice and can control the magnitude of primary effector T cell response to a foreign antigen. In this model, Treg expansion and contraction paralleled that of Tcon (128). The same effect has also been seen during FV infection (340).

The activation and differentiation of Tregs during infection has been described for many viruses such as: HIV-1 infection of humans (236), Influenza A virus infection of mice (22) or infection of cats with feline immunodeficiency virus (201). Despite a few

exceptions like Influenza, the activation and expansion of Tregs has mainly been shown in chronic human infections, such as HIV-1, HBV and HSV (reviewed in (247)). In the chronic phase of FV infection Treg numbers remained elevated, showing an activated phenotype with no proliferation (Figure 4. 6 and Figure 4. 7). Similar results were obtained when studying the expansion and activation of Tregs in chronic HIV-1 infection. Here, Tregs were expanded and activated in chronically, untreated HIV-1 infected individuals (Figure 4. 41 and Figure 4. 42). However, there has been conflicting data showing different frequencies of Tregs in patients in distinct phases of HIV infection. These discrepancies are likely due to a number of factors including: isolation of Tregs from different lymphoid tissues (like blood, lymph nodes or GALT), differences in the length of infection, utilisation of different Treg markers and the utilisation of different methods to assess Treg numbers (frequencies or actual cell numbers) (143). The main targets of HIV-1 are $CD4^+$ T cells which are most abundant in lymphoid organs like the lymph nodes and GALT. This results in higher viral loads than in the blood and therefore a more pronounced immune response. In these organs higher levels of Tregs are detectable, which correlated with the increase in viral load (10, 89, 222).

Co-stimulatory markers were also expressed on Tregs during FV infection (Figure 4. 4). One of these markers was ICOS (Figure 4. 4 B). $ICOS^+$ Tregs have been shown to be highly suppressive, highly proliferative and less prone to cell-death (60, 282). Furthermore, it was also shown that ICOS is critical for homeostasis and functional stability of $Foxp3^+$ Tregs (166). This could indicate that the $ICOS^+$ Tregs have similar functional abilities in FV infection, although this point requires further investigation.

Another co-stimulatory marker expressed on Tregs during FV infection was GITR (Figure 4. 4 G). GITR is predominantly expressed on $CD4^+CD25^+$ Tregs in mice (271) and has been associated with the expansion of T cells and Tregs upon stimulation, although with a loss of Treg suppressive activity (250, 303). Furthermore, it has also been shown that GITR stimulation of Tregs results in a decrease in Treg lineage stability and subsequently reduced Treg mediated suppression (250, 260). Moreover, the stimulation of Tregs with GITR agonistic antibody abrogated Treg mediated suppression in a dose-dependent manner (271). When the same antibody was used to treat chronically FV infected mice, transferred FV-specific $CD8^+$ T cells were no longer suppressed by Tregs (84). Concluding from this, GITR expression on

Tregs and stimulation with agonists could provide an inhibitory mechanism for Tregs, and could be beneficial in situations where Treg suppression is detrimental.

The expression of inhibitory molecules on Tregs during acute FV infection was also investigated (Figure 4. 4). Strikingly, an up-regulation was seen for all the investigated markers (TIM3, PD-1 and PD-L1, Lag3) during FV infection. The detection of elevated levels of these inhibitory molecules on Tregs argues towards a role in their function. In a systemic model of murine acute myeloid leukaemia, Treg-mediated suppression of $CD8^+$ T cells was dependent on the expression of PD-1 on Tregs (343). Furthermore, it has been shown that Tregs expressing PD-1 and TIM3 are highly suppressive (256). In contrast, it was reported in chronic HCV infection that Treg proliferation was inhibited by PD-1 signalling (239), arguing towards Treg suppression by inhibitory receptors. PD-L1 expression was also up-regulated on Tregs during FV infection (Figure 4. 4 F). It has been shown that Tregs are able to suppress auto-reactive B cells via PD-L1 (116) and blocking of this molecule was found to inhibit the suppressive activity of Tregs towards $CD4^+CD25^-$ Tcon (159).

Lag3 has been shown to interfere with TCR signalling and thereby T cell activation (127) and expansion (328). However, the expression of Lag3 is a marker for Tregs with potent suppressive activity (139). Lag3 was up-regulated on Tregs during acute FV infection (Figure 4. 4 C), which could be an indicator of their suppressive activity.

Wakamatsu *et al.* demonstrated that Tcon and Treg responded to the same co-stimulatory and inhibitory signals (CD28, CTLA-4, ICOS, PD-1, BLA and CD80) but this induced different clusters of genes (314). Another study has shown that CD28, CTLA-4 and PD-L1 differentially control interaction of Tregs or Tcon with APCs, resulting in different outcomes for activation (82). This highlights the role of co-stimulatory and inhibitory receptors for Tregs and provides evidence that they might not only represent molecules important for the suppressive mechanisms of Tregs, but also implicates that Tregs could be limited in their stimulation and activation by these receptors. Due to the expression of different co-stimulatory markers and inhibitory receptors Tregs can therefor integrate multiple signals for their own stimulation and induction of suppressor functions.

5.2 The mechanism(s) of Treg-mediated suppression in retroviral infection.

It is of great importance to define the major mechanisms of Treg-mediated suppression in retroviral infections, as this could provide a viable target for future immune-based therapies. Multiple mechanisms have been described for Treg-mediated immune suppression and they are not mutually exclusive. However, dominant mechanisms of Treg mediated suppression do exist, depending on a number of immunological parameters.

It has been shown in FV infection that Tregs suppress effector T cell responses in a contact-dependent manner (248), and that CTLA-4 could have a minor role in mediating this suppression (whereas TGFβ or IL10 individually were not involved) (144). Interestingly, though, when multiple mechanisms were blocked at the same time (CTLA-4, TGFβ and IL10), the reduction in Treg suppressive activity was increased (144). This provides evidence for multiple Treg-mediated mechanisms of suppression, and that there may be some level of functional redundancy.

In other disease models, it has been shown that Tregs suppress via adenosine production by the enzymes CD39 and CD73 (78, 94, 162). Interestingly, mouse Tregs have been shown to be mostly positive for CD39 and CD73, suggesting adenosine production may be a general mechanism used by mouse Tregs. Encouragingly, this same phenotype of $CD39^+CD73^+$ Tregs was observed in FV infection (Figure 4. 29). To establish if this enzymatic cascade could play a role in Treg-mediated immune suppression during FV infection, the influence of CD39 and CD73 deficiency on anti-viral immune responses was investigated. CD39, the upstream enzyme of the cascade, did play a role, and $CD8^+$ T cell responses were elevated in CD39-KO mice (Figure 4. 37 and Figure 4. 38). CD39 has been shown to be important in HIV-1 infection, where Tregs need CD39 for their suppressive activity (207). The effect of CD39 seen in FV infection was not as dramatic as expected and is thus unlikely to be the only immune-suppression pathway involved. It has been shown that both enzymes act in a cascade to generate the immunosuppressive adenosine which binds to the A2A receptor on Tcon, causing suppression (34, 78, 162). Interestingly, CD73, which catalyses the production of adenosine, did not play a clear role in Treg mediated suppression of either $CD4^+$ or $CD8^+$ T cells in FV infection (Figure 4. 31 to Figure 4. 35), leaving a puzzling observation that requires further

investigation. Interestingly, CD73 down-regulation on $CD8^+$ T cells was associated with immune activation and disease progression during HIV-1 infection. Also a functional impairment of the $CD8^+CD73^-$ T cells compared with $CD8^+CD73^+$ T cells was detected (305). This argues for an important role of CD73 in $CD8^+$ T cells during retroviral infection and may have influenced the outcome of these experiments in FV-infected CD73-knockout mice. However, it is possible that the effect seen in FV infection is solely mediated by the reduction of extracellular ATP levels by CD39, resulting in less immune activation.

During HIV-1 infection Tregs can have beneficial effects in the early phase of infection by suppressing the transfer of virus from infected DCs to $CD4^+$ T cells. This effect is most likely mediated by Treg-induced suppression of the actin cytoskeleton, which is important for the transport of HIV-1 particles to the immunological synapse, and thus the cell-to-cell transfer of virus (43). It was shown that Tregs were able to decrease the actin polymerisation at the immunological synapse between DCs and $CD4^+$ T cells, without disrupting the cluster formation among these cells (Moreno-Fernandez, accepted and Figure 4. 45). Furthermore, Tregs abolished the positive correlation of HIV-1 particles and actin accumulation at the interface between DCs and Tcon (Figure 4. 46), suggesting Treg-mediated suppression of DCs and/or Tcon. However, these results should be regarded as preliminary, and more work is required to establish the exact mechanisms behind these observations.

5.3 The mechanism(s) of Treg expansion during FV infection

It has been demonstrated in multiple virus infections that iTregs can be induced by viral antigen. In influenza A virus infection of mice matrix-1 specific Tregs were found to expand (233). Moreover, in infections with chronic viruses like HCV, EBV and HIV, virus-specific Tregs were shown to exist (86, 247). In contrast, the $CD4^+$ T cell repertoire of FV-specific $CD4^+$ TCR^{tg} mice was determined to be devoid of FV-specific Tregs during FV infection (12). Furthermore, no FV-specific $CD4^+$ T cell expressing Foxp3 were found using the MHCII tetramer technology (148). This suggested that FV infection does not induce expansion of virus-specific Tregs and prompts the question about the origin of these expanding Tregs.

Tregs expanding during FV infection were shown to express markers of nTregs (CD25, CTLA-4, GITR, CD62L and Nrp1) (Figure 4. 2, Figure 4. 3, Figure 4. 4, Figure

4. 8 and Figure 4. 9). Since Nrp1 is the most accepted marker for nTregs, this marker was used and the expansion of Nrp1$^+$ Tregs was demonstrated to be dominant (Figure 4. 8 and Figure 4. 9). This indicated that the main subset of Tregs expanding during FV infection consisted of nTregs. This observation is strengthened by the fact that no conversion of FV-specific CD4$^+$ T cells into Tregs during FV infection was observed (212). Thus in conclusion, a pre-existing pool of nTregs expands during FV infection, which is caused by activation and proliferation of these presumably self-specific Tregs. Indeed, nTregs, which arise directly from the thymus, are usually self-reactive and recognise self-antigens (44, 73, 75, 175). Therefore, nTregs are constantly exposed to their specific antigen in circulation and are thus consistently activated, albeit at a low level (154). However, no self-antigen had been described to play a role in the expansion of Tregs during FV infection.

To gain further insight into the Treg repertoire, the Vβ usage of Tregs was analysed during FV infection and a disproportionate expansion of Vβ5$^+$ Tregs was found (Figure 4. 10 and Figure 4. 11) (212). LCMV clone 13 infection of mice was also found to preferentially expand Vβ5$^+$ Tregs (238). This shows that viruses from different families (LCMV belongs to the family of *Arenaviridae)* are able to induce the disproportionate Vβ5$^+$ Treg proliferation. The expansion of Vβ5$^+$ T cells was restricted to Tregs and not observed for peripheral CD4$^+$ Tcon or CD8$^+$ T cells (unpublished data and (238)). These results argue for a Treg-specific and immune system-mediated mechanism of Vβ5$^+$ Treg expansion, independent of exogenous viral antigens.

Many ERVs are present in the genome of mice and the *mtv* ERV family contain a Sag in the 3'-LTR open reading frame of the provirus (4, 64). From previous studies it is known that the *mtv-9* Sag binds to the Vβ5 chain of the TCR, thereby crosslinking the TCR with an MHC class II molecule displayed by APCs (3, 324, 326). During thymic development this leads to clonal deletion of Vβ5$^+$ T cells in the thymus or anergy of T cells in the periphery (27, 151, 152, 277). Despite expressing the *mtv-9* Sag, B6 mice show weak deletion of Vβ5$^+$ T cells in the thymus, due to a lack of expression of MHC class II IE molecules, which bind to Sags with high avidity (28). This equates to a substantial amount of CD8$^+$ and CD4$^+$ T cells positive for Vβ5 in the periphery of adult B6 mice (unpublished data). Additionally, Tregs are relatively resistant to clonal depletion by endogenous Sags in the thymus in general (230).

Punkosdy *et al.* could directly show that the LCMV clone 13 induced expansion of Vβ5$^+$ Tregs in the periphery was dependent on the expression of *mtv-9* (238). In this thesis, it was shown that Vβ5$^+$ Tregs receive a stronger TCR signal than Vβ5$^-$ Tregs (Figure 4. 16), which fits with the results mentioned above. In addition, Punkosdy *et al.* showed that this expansion is MHC class II dependent but CD4$^+$ independent. Finally, by utilising CD11c-DTR mice they found that this expansion requires DCs, which is in line with the model using Sag stimulation (238). It was also shown that the absence of B cells, another subset presenting Sags (157), was not able to abolish Vβ5$^+$ Treg expansion (Figure 4. 18), a phenomenon also demonstrated for LCMV (238). Interestingly, Punkosdy *et al.* showed that infection with LCMV clone 13 up-regulated the mRNA expression of *mtv-8* and *mtv-9* Sag in DCs (238). This finding was the basis for their interpretation that Sag expression levels are critical for the magnitude of Vβ5$^+$ Treg expansion. In contrast Myers *et al.* did not observe such changes in mRNA expression for *mtv-9* Sag in either DCs or B cells after FV infection (212). This argues for a more constitutive signal provided to the Vβ5$^+$ Tregs in the periphery by Sag presentation and a dependence of these Tregs on a secondary signal for complete expansion.

One possible co-factor that was known to stimulate Tregs was IL2 (77, 103, 224). However, IL2 was not involved in expanding Vβ5$^+$ Tregs, as neutralisation of this cytokine did not have an effect on Vβ5$^+$ Treg numbers (212). Furthermore, transfer of IL2 producing FV-specific CD4$^+$ T cells did not result in expansion of Vβ5$^+$ Tregs (Figure 4. 17). This IL2-independent effect is possibly due to a specific activation triggered by the Sag stimulation (13, 42, 337). Moreover, it has been shown that bacterial Sags are able to stimulate T cell expansion in the absence of IL2 (147).

Depletion experiments showed that activated CD8$^+$ T cells were critical for Vβ5$^+$ but not Vβ5$^-$ Treg expansion (Figure 4. 19and (212)) and multiple factors produced by these cells were investigated. GzmB, IFNγ, and perforin were excluded as second signals for Vβ5$^+$ Treg expansion based on the data obtained (Figure 4. 18 and unpublished observations). Furthermore, when CD8$^+$ T cells were absent (depleted or in CD8$^+$ knockout mice) during FV infection, the viral loads increased drastically (data not shown and (212)), showing that viral loads were not a factor involved in the expansion. In support of this data, increasing numbers of virus-specific CD8$^+$ T cells added via adoptive transfer increased the magnitude of Vβ5$^+$ Treg expansion (212).

These results provide evidence for the important role of activated $CD8^+$ T cells in the expansion of $V\beta5^+$ Tregs. In LCMV clone 13 infection, depletion of $CD11c^+$ DCs resulted in a loss of $V\beta5^+$ Treg expansion, indicating the importance of this subset for $V\beta5^+$ Treg expansion (238). However, DCs are crucially important for the priming of CTLs during LCMV infection (237) and the depletion of DCs would also restrict $CD8^+$ T cell expansion and activation. This indicated an indirect effect of DCs for the expansion of $V\beta5^+$ Tregs in LCMV clone 13 infection of mice.

Activated $CD8^+$ T cells produce substantial amounts of TNFα during FV infection (Figure (212)). The neutralisation of TNFα led to a decreased frequency and activation of $V\beta5^+$ Tregs but not $V\beta5^-$ Tregs during infection (212). TNFα is a pleiotropic cytokine that exists as a soluble (solTNFα) or a membrane-bound (mbTNFα) form. There are two receptors for TNFα, TNFRI and TNFRII. TNFRI binds to both forms, however solTNFα binds with a higher affinity (121). TNFRII only has a high affinity for mbTNFα (120). In contrast to TNFRI, which mediates mainly pro-apoptotic pathways, TNFRII does not possess a death domain and promotes anti-apoptotic signals (66, 155, 156).

In this thesis it was shown that Tregs did not express TNFRI, however a high percentage of $V\beta5^+$ Tregs expressed TNFRII (Figure 4. 21). Interestingly, both human and mouse Tregs constitutively express TNFRII (57, 214, 308), but it was shown that FV infection could further up-regulate TNFRII expression (Figure 4. 21). The expansion of $V\beta5^+$ Tregs during FV infection was dependent on the expression of TNFRII but not TNFRI on these Tregs (Figure 4. 22). Chen *et al.* were the first to show that the interaction of TNFα with TNFRII on Tregs was beneficial for their expansion and function (56), and that TNFRII is critical for a stable Treg phenotype in inflammatory environments (58). Others have also reported that the expansion of Tregs could be invoked using TNFα via a TNFRII-dependent pathway (65, 122, 160, 227).

It was shown that FV-specific activated $CD8^+$ T cells expressed high levels of mbTNFα when they were stimulated with their cognate antigen (Figure 4. 20). Furthermore, $CD8^+$ T cells of iRhom2-KO mice, which only express mbTNFα induced higher numbers of activated $V\beta5^+$ Tregs than $CD8^+$ T cells from wild type mice (Figure 4. 24). Grindberg-Bleyer *et al.* have demonstrated that in a model of

autoimmune diabetes the activated Tcon were able to induce the proliferation of Tregs in a TNFα-dependent manner (122). This proved that the activated immune system is able to trigger Treg expansion using TNFα. However, no study so far has shown that mbTNFα produced during an ongoing immune response is the central mediator of Treg expansion.

Rauert *et al.* engineered a TNFα construct mimicking the membrane-bound form of TNFα and showed that this Flag-TNC-scTNF(143N/145R) was able to specifically bind to human TNFRII (and not human TNFRI), inducing the alternative NF-κB signalling pathway, implicated in T cell proliferation and survival (240). In this thesis, the same construct, but specific for mouse TNFRII (unpublished) was utilised. It was shown here that the intercellular communication between $CD8^+$ T cells expressing mbTNFα during FV infection and $TNFRII^+V\beta5^+$ Tregs could be bypassed by this synthetic TNFRII-ligand given to naïve wild type mice but not TNFRII-KO mice (Figure 4. 25). This data set has highlighted a role for the interaction of mbTNFα and TNFRII expressed on $V\beta5^+$ Tregs in the expansion and activation of this Treg subset.

The effect of TNFα on Treg function remains a controversial area of research. Valencia *et al.* and Nie *et al.* found that TNFα down-modulates the suppressive function of $CD4^+CD25^+$ Tregs in patients with active rheumatic arthritis, which was also shown in a mouse arthritis model (29). When they blocked TNFα, the Treg suppressive activity was restored (221, 308), and this effect was shown to be TNFRII dependent (214). Another study has demonstrated that TNFα partially abrogated Treg mediated suppression of HBV specific T cell responses (280). However, TNFRII expressing Tregs have been described in different infections associated with Treg expansion, and this correlated with the suppression of pathogen-specific immune responses (316) and a strong suppressive activity of $TNFRII^+$ Tregs (203). Furthermore, high $TNFRII^+$ expression levels on Tregs were found in type I diabetes (252) and in acute myeloid leukaemia where they correlated with low effector T cell responses (119). Also, in an experimental metastasis mouse model, Treg expansion was TNFRII-dependent and after treatment with TNFα resulted in enhanced metastasis (65). Thus the effect of TNFα on Treg expansion and activation is likely to be disease and immune-context dependent.

Some of the conflicting results may be explained by the nature of the Tregs in the different models. Housley *et al.* showed that nTreg mediated suppression was dependent on TNFα, whereas iTregs generated in the presence of TGFβ were not (137). Furthermore, the duration and strength of TNFα signalling in Tregs could have important implications, as it was reported that longer exposure to TNFα restored Treg suppressive effects, whereas short term exposure was inhibitory (56).

Interestingly, Vβ5$^+$ Tregs from an FV-infected mouse showed higher activation, differentiation and proliferation compared to Vβ5$^-$ Tregs from the same mouse (Figure 4. 13, Figure 4. 15 and (212)). This stark activation of Vβ5$^+$ Tregs was also demonstrated in the LCMV infection model (238). Stimulation by Sags has been reported to induce and activate Tregs in other models (297). This could provide an explanation for the higher activation of Vβ5$^+$ Tregs in FV-infected mice.

The mechanisms of Treg expansion have only been partially elucidated in general. While iTregs are converted by triggers like IL10, TGFβ, foreign antigen or other stimuli, nTreg expansion is thought to be triggered mainly by IL2. IL2 is an important survival factor for Tregs and other T cells, but is not produced by Tregs (20, 192, 261). It was shown that the Vβ5$^-$ Tregs require IL2 for their proliferation during FV infection (212). These results were confirmed in this thesis and it was demonstrated that the IL2 driving the Vβ5$^-$ Treg activation and expansion is produced by virus-specific CD4$^+$ Tcons (Figure 4. 17). On the one side, the production of IL2 has beneficial effects for the anti-viral immune response as it is an important survival factor for Tcons and CD8$^+$ T cells (171). However on the other side, IL2 also drives activation and expansion of Tregs, which in turn suppress anti-viral immune responses. Furthermore, it has been reported that IL2, IL2Rα, and IL2Rβ deficient mice develop a strong lymphoproliferative syndrome and suffer from severe autoimmunity due to impaired Treg responses rather than immune dysfunction, due to activation deficiency of Tcons (253, 292, 323).

Overall, it has been shown that the Tregs expanding during FV infection consist of two different subsets. These subsets exhibit differences in their phenotype and their stimuli requirements during infection. This raises questions about the effect of multiple different Treg subsets in human viral infections on immune suppression, and their contributions to the specific disease.

Humans also harbour many ERV (HERV) sequences in their genome, some of which have been shown to have Sag properties. There have been suggestions that HERV-K18 *env* causes stimulation of Vβ7$^+$ T cells in humans (72) and in mice (294). Furthermore, the expression of HERV-K18 can be induced by infection with different herpes viruses (289, 295, 307).

Aside from Sag expression, HERVs have the potential to express viral proteins which could have an influence on innate and adaptive immune responses. It has been shown that HIV-1 infection leads to the expression of HERVs and that a HERV-specific CD8$^+$ T cell response is induced, which inversely correlates with HIV-1 plasma viral loads (107, 296). Individuals who did not receive HAART but were able to control HIV-1 viremia had stronger and broader HERV-specific T cell responses than patients on HAART/progressors/non-controllers or healthy individuals (265). Furthermore, HERV-K specific antibodies were detectable during HIV-1 infection, with high titres in elite controllers (200). Interestingly, HIV-1 exposed, seronegative individuals showed enhanced HIV-1- and HERV-specific CD4$^+$ T cell responses in the GALT compared to the blood (266). This shows that HERV antigens are able to prime T cell responses which can have an influence on the outcome of infection with an exogenous virus. However, to date, no such priming has been shown for Tregs during infection.

In certain cancers, the expression of endogenous retroviral products on tumour cells can specifically activate Tregs and subsequently mediate local expansion of Treg populations. These Treg populations then function to suppress effector T cell responses against the tumour. As an example, it has been shown in a melanoma tumour mouse model that ERV expression in melanoma cells was necessary for a Treg-mediated immune escape for the tumour (194). However, the authors did not look for a direct involvement of ERV-specific Tregs in immunosuppression, although it remains possible that this could be a mechanism of immune escape for tumours or viral infections by triggering ERV expression (193). Alternatively, ERV antigens could provide a TCR signal which is then completed during the immune response by a secondary signal to induce full activation and expansion of Treg subpopulations, as has been described in this thesis. Overall, (H)ERV antigens could play a more important role in shaping the Treg response than is currently appreciated.

6. Summary

The infection of mice with Friend retrovirus (FV) induces the expansion and activation of regulatory T cells (Tregs) during acute infection, which remain active throughout chronic infection. Tregs are responsible for the suppression of FV-specific $CD8^+$ T cell responses, which is associated with the establishment of a chronic infection. In this thesis it was shown that the Tregs expanding during FV infection were natural nTregs rather than induced iTregs. Furthermore, these Tregs possessed the phenotype of activated and differentiated effector T cells, both in acute and chronic FV infection.

In a search of Treg specificity, the disproportionate expansion of T cell receptor $V\beta5^+$ Tregs in acutely FV-infected mice was observed. It was known that these $V\beta5^+$ Tregs are specific for an endogenous retroviral superantigen of the mouse mammary tumour virus 9. Investigation of this subset of $V\beta5^+$ Tregs showed that they were highly activated and suppressive and that their expansion was surprisingly independent of IL2. $V\beta5^+$ Treg expansion was induced by activated effector $CD8^+$ T cells that expressed TNFα.

TNFα is a pleiotropic cytokine present in two forms, a soluble (solTNFα) and membrane-bound form (mbTNFα), which both preferentially bind to two different TNF receptors (TNFR). It was shown that TNFRII but not TNFRI became significantly up-regulated on $V\beta5^+$ Tregs during acute FV infection. Also, the expansion of $V\beta5^+$ Tregs was directly dependent on the presence of TNFRII, but not TNFRI, on the surface of these Tregs. FV-specific $CD8^+$ T cells produce substantial amounts of mbTNF after stimulation, providing the important factor that binds to TNFRII on $V\beta5^+$ Tregs and induces activation and proliferation. The use of $CD8^+$ T cells of iRhom2-knockout mice, which only express mbTNFα, but no solTNFα, revealed a substantial increase in $V\beta5^+$ Treg expansion and activation.

Finally, treatment of naïve mice with solTNFα did not induce expansion of $V\beta5^+$ Tregs, whereas the treatment of naïve mice with a synthetic TNFRII ligand did, indicating that the intercellular communication between Treg and $CD8^+$ T cells can be bypassed by direct stimulation of the TNFRII.

In an attempt to clarify the mechanism of Treg mediated suppression of effector T cell responses during FV infection the CD39/CD73 pathway was investigated. Here, mice that were deficient for either one of these ADP converting enzymes were infected with FV. These experiments revealed that the loss of the rate limiting enzyme CD39 had a positive effect on effector $CD4^+$ and $CD8^+$ T cell responses, whereas no effect could not be demonstrated for the down-stream enzyme CD73.
In a translational approach Tregs were characterised in the blood of untreated chronically HIV-1 infected individuals and shown to be expanded and activated in these patients compared to healthy individuals.

Moreover, a possible mechanism of how Tregs help to prevent the transfer of HIV-1 from infected dendritic cells to conventional $CD4^+$ T cells was investigated. This showed that Tregs were able to interfere with the co-localisation of HIV-1 particles and actin, as part of the cytoskeleton of cells, at the interface between DCs and T cells.

7. Zusammenfassung

Die Infektion mit dem Friend Retrovirus (FV) induziert die Expansion und Aktivierung von regulatorischen T Zellen (Tregs) während der akuten und chronischen Infektion. Tregs verursachen die Suppression von FV-spezifischen $CD8^+$ T Zellen was mit der Etablierung einer chronischen Infektion assoziiert ist. In der vorliegenden Arbeit konnte gezeigt werden, dass es während der FV Infektion zu einer Expansion von natürlichen nTregs kommt und eher nicht zur Expansion von induzierten iTregs. Weiterhin besaßen diese Tregs den Phänotyp aktivierter und differenzierter Effektor T Zellen in der akuten sowie in der chronischen Infektion.

Auf der Suche nach der Treg Spezifität wurde die disproportionale Expansion von T Zell Rezeptor $V\beta5^+$ Tregs während der akuten FV Infektion entdeckt. Es war bereits bekannt, dass diese $V\beta5^+$ Tregs spezifisch für das Superantigen des endogenen mouse mammary tumour virus 9 sind. Die Untersuchung der $V\beta5^+$ Tregs zeigte, dass diese Zellen aktiviert und suppressiv waren. Außerdem besaßen diese Tregs die ungewöhnliche Eigenschaft unabhängig von IL2 in ihrer Expansion zu sein. Die Expansion von $V\beta5^+$ Tregs war abhängig von aktivierten Effektor $CD8^+$ T Zellen die TNFα produzierten.

TNFα ist ein pleiotropisches Zytokin, welches in zwei Formen vorkommt, eine lösliche (solTNFα) und eine membrangebundene (mbTNFα) Form, und diese binden mit unterschiedlichen Präferenzen an zwei TNF Rezeptoren (TNFR). Es konnte gezeigt werden, dass TNFRII, aber nicht TNFRI, während der akuten FV Infektion signifikant auf $V\beta5^+$Tregs hoch reguliert wurde. Die Expansion der $V\beta5^+$ Tregs war direkt abhängig von der Expression von TNFRII aber nicht TNFRI auf ihrer Oberfläche.

FV-spezifische $CD8^+$ T Zellen produzieren mbTNFα nach Stimulation, welches an TNFRII auf $V\beta5^+$ Tregs bindet und das wichtige Signal für die Expansion und Aktivierung dieser Zellen bietet. Durch den Einsatz von $CD8^+$ T Zellen aus iRhom2-Knockout Mäusen, welche nur mbTNFα aber nicht solTNFα exprimieren, konnte eine substantielle Expansion und Aktivierung von $V\beta5^+$ Tregs gezeigt werden.

Letztendlich konnte gezeigt werden, dass die Behandlung von Mäusen mit solTNFα nicht zu einer Expansion von Vβ5$^+$ Tregs führte, wohingegen die Behandlung mit einem synthetischen TNFRII Liganden die Expansion von Vβ5$^+$ Tregs verursachen konnte. Hierdurch konnte gezeigt werden, dass es möglich ist die Kommunikation zwischen Tregs und CD8$^+$ T Zellen durch die Stimulation von TNFRII zu umgehen.

In einem Ansatz, um den Mechanismus der Treg vermittelten Suppression von Effektor T Zell Antworten gegen FV zu bestimmen, wurde der CD39/CD73 Weg untersucht. Hierzu wurden Mäuse infizierten die für je eines dieser ADP konvertierenden Enzyme defizient waren. Es wurde gezeigt, dass der Verlust des reaktionslimitierenden Enzyms CD39 einen positiven Effekt auf die Effektorfunktion von CD4$^+$ und CD8$^+$ T Zellen hatte. CD73 hingegen, welches später im Stoffwechselweg auftaucht, hatte keinen Effekt wenn es nicht vorhanden war.

In einem transnationalen Ansatz wurden Tregs von unbehandelten chronisch HIV-1 infizierten Patienten im Blut charakterisiert. Es konnte gezeigt werden, dass die Tregs dieser Patienten im Vergleich zu nicht infizierten Personen expandiert und aktiviert waren. Weiterhin, wurde ein möglicher Mechanismus untersucht bei dem Tregs wichtig sind um den Transfer von Virus aus infizierten dendritischen Zellen zu CD4$^+$ T Zellen zu inhibieren. Dies zeigte, dass Tregs in der Lage waren mit der Ko-lokalisation von HIV-1 Partikeln und Aktin, einem Bestandteil des Zytoskeletts von Zellen, an der Synapse zwischen DCs und T Zellen zu interferieren.

8. References

1. **Aandahl, E. M., J. Michaelsson, W. J. Moretto, F. M. Hecht, and D. F. Nixon.** 2004. Human CD4+ CD25+ regulatory T cells control T-cell responses to human immunodeficiency virus and cytomegalovirus antigens. J Virol **78:**2454-2459.
2. **Acha-Orbea, H.** 1997. The role of superantigens in resistance to retroviral infection. Trends Microbiol **5:**385.
3. **Acha-Orbea, H., L. Scarpellino, A. N. Shakhov, W. Held, and H. R. MacDonald.** 1992. Inhibition of mouse mammary tumor virus-induced T cell responses in vivo by antibodies to an open reading frame protein. J Exp Med **176:**1769-1772.
4. **Acha-Orbea, H., A. N. Shakhov, L. Scarpellino, E. Kolb, V. Muller, A. Vessaz-Shaw, R. Fuchs, K. Blochlinger, P. Rollini, J. Billotte, and et al.** 1991. Clonal deletion of V beta 14-bearing T cells in mice transgenic for mammary tumour virus. Nature **350:**207-211.
5. **Adrain, C., M. Zettl, Y. Christova, N. Taylor, and M. Freeman.** 2012. Tumor necrosis factor signaling requires iRhom2 to promote trafficking and activation of TACE. Science **335:**225-228.
6. **Akhmetzyanova, I., G. Zelinskyy, S. Schimmer, S. Brandau, P. Altenhoff, T. Sparwasser, and U. Dittmer.** 2013. Tumor-specific CD4+ T cells develop cytotoxic activity and eliminate virus-induced tumor cells in the absence of regulatory T cells. Cancer Immunol Immunother **62:**257-271.
7. **Akimova, T., U. H. Beier, L. Wang, M. H. Levine, and W. W. Hancock.** 2011. Helios expression is a marker of T cell activation and proliferation. PLoS One **6:**e24226.
8. **Albritton, L. M., L. Tseng, D. Scadden, and J. M. Cunningham.** 1989. A putative murine ecotropic retrovirus receptor gene encodes a multiple membrane-spanning protein and confers susceptibility to virus infection. Cell **57:**659-666.
9. **Altman, J. D., P. A. Moss, P. J. Goulder, D. H. Barouch, M. G. McHeyzer-Williams, J. I. Bell, A. J. McMichael, and M. M. Davis.** 1996. Phenotypic analysis of antigen-specific T lymphocytes. Science **274:**94-96.
10. **Andersson, J., A. Boasso, J. Nilsson, R. Zhang, N. J. Shire, S. Lindback, G. M. Shearer, and C. A. Chougnet.** 2005. The prevalence of regulatory T cells in lymphoid tissue is correlated with viral load in HIV-infected patients. J Immunol **174:**3143-3147.
11. **Annacker, O., C. Asseman, S. Read, and F. Powrie.** 2003. Interleukin-10 in the regulation of T cell-induced colitis. J Autoimmun **20:**277-279.
12. **Antunes, I., M. Tolaini, A. Kissenpfennig, M. Iwashiro, K. Kuribayashi, B. Malissen, K. Hasenkrug, and G. Kassiotis.** 2008. Retrovirus-specificity of regulatory T cells is neither present nor required in preventing retrovirus-induced bone marrow immune pathology. Immunity **29:**782-794.
13. **Arad, G., R. Levy, I. Nasie, D. Hillman, Z. Rotfogel, U. Barash, E. Supper, T. Shpilka, A. Minis, and R. Kaempfer.** 2011. Binding of superantigen toxins into the CD28 homodimer interface is essential for induction of cytokine genes that mediate lethal shock. PLoS Biol **9:**e1001149.
14. **Atarashi, K., T. Tanoue, T. Shima, A. Imaoka, T. Kuwahara, Y. Momose, G. Cheng, S. Yamasaki, T. Saito, Y. Ohba, T. Taniguchi, K. Takeda, S. Hori, Ivanov, II, Y. Umesaki, K. Itoh, and K. Honda.** 2011. Induction of colonic regulatory T cells by indigenous Clostridium species. Science **331:**337-341.
15. **Bach, J. F., and L. Chatenoud.** 2001. Tolerance to islet autoantigens in type 1 diabetes. Annu Rev Immunol **19:**131-161.
16. **Bagriacik, E. U., M. D. Armstrong, M. Okabe, and J. R. Klein.** 1999. Differential expression of CD43 isoforms on murine T cells and their relationship to acute intestinal graft versus host disease: studies using enhanced-green fluorescent protein transgenic mice. Int Immunol **11:**1651-1662.
17. **Baine, I., S. Basu, R. Ames, R. S. Sellers, and F. Macian.** 2013. Helios induces epigenetic silencing of IL2 gene expression in regulatory T cells. J Immunol **190:**1008-1016.
18. **Barrat, F. J., D. J. Cua, A. Boonstra, D. F. Richards, C. Crain, H. F. Savelkoul, R. de Waal-Malefyt, R. L. Coffman, C. M. Hawrylowicz, and A. O'Garra.** 2002. In vitro generation of interleukin 10-producing regulatory CD4(+) T cells is induced by

immunosuppressive drugs and inhibited by T helper type 1 (Th1)- and Th2-inducing cytokines. J Exp Med **195:**603-616.

19. **Barre-Sinoussi, F., J. C. Chermann, F. Rey, M. T. Nugeyre, S. Chamaret, J. Gruest, C. Dauguet, C. Axler-Blin, F. Vezinet-Brun, C. Rouzioux, W. Rozenbaum, and L. Montagnier.** 1983. Isolation of a T-lymphotropic retrovirus from a patient at risk for acquired immune deficiency syndrome (AIDS). Science **220:**868-871.
20. **Barron, L., H. Dooms, K. K. Hoyer, W. Kuswanto, J. Hofmann, W. E. O'Gorman, and A. K. Abbas.** 2010. Cutting edge: mechanisms of IL-2-dependent maintenance of functional regulatory T cells. J Immunol **185:**6426-6430.
21. **Barry, M., and R. C. Bleackley.** 2002. Cytotoxic T lymphocytes: all roads lead to death. Nat Rev Immunol **2:**401-409.
22. **Bedoya, F., G. S. Cheng, A. Leibow, N. Zakhary, K. Weissler, V. Garcia, M. Aitken, E. Kropf, D. S. Garlick, E. J. Wherry, J. Erikson, and A. J. Caton.** 2013. Viral antigen induces differentiation of Foxp3+ natural regulatory T cells in influenza virus-infected mice. J Immunol **190:**6115-6125.
23. **Belkaid, Y.** 2007. Regulatory T cells and infection: a dangerous necessity. Nat Rev Immunol **7:**875-888.
24. **Bensinger, S. J., A. Bandeira, M. S. Jordan, A. J. Caton, and T. M. Laufer.** 2001. Major histocompatibility complex class II-positive cortical epithelium mediates the selection of CD4(+)25(+) immunoregulatory T cells. J Exp Med **194:**427-438.
25. **Best, S., P. R. Le Tissier, and J. P. Stoye.** 1997. Endogenous retroviruses and the evolution of resistance to retroviral infection. Trends Microbiol **5:**313-318.
26. **Betts, M. R., and R. A. Koup.** 2004. Detection of T-cell degranulation: CD107a and b. Methods Cell Biol **75:**497-512.
27. **Bill, J., V. B. Appel, and E. Palmer.** 1988. An analysis of T-cell receptor variable region gene expression in major histocompatibility complex disparate mice. Proc Natl Acad Sci U S A **85:**9184-9188.
28. **Bill, J., O. Kanagawa, D. L. Woodland, and E. Palmer.** 1989. The MHC molecule I-E is necessary but not sufficient for the clonal deletion of V beta 11-bearing T cells. J Exp Med **169:**1405-1419.
29. **Biton, J., L. Semerano, L. Delavallee, D. Lemeiter, M. Laborie, G. Grouard-Vogel, M. C. Boissier, and N. Bessis.** 2011. Interplay between TNF and regulatory T cells in a TNF-driven murine model of arthritis. J Immunol **186:**3899-3910.
30. **Bluestone, J. A., and A. K. Abbas.** 2003. Natural versus adaptive regulatory T cells. Nat Rev Immunol **3:**253-257.
31. **Bodor, J., T. Bopp, M. Vaeth, M. Klein, E. Serfling, T. Hunig, C. Becker, H. Schild, and E. Schmitt.** 2012. Cyclic AMP underpins suppression by regulatory T cells. Eur J Immunol **42:**1375-1384.
32. **Boettler, T., H. C. Spangenberg, C. Neumann-Haefelin, E. Panther, S. Urbani, C. Ferrari, H. E. Blum, F. von Weizsacker, and R. Thimme.** 2005. T cells with a CD4+CD25+ regulatory phenotype suppress in vitro proliferation of virus-specific CD8+ T cells during chronic hepatitis C virus infection. J Virol **79:**7860-7867.
33. **Bopp, T., C. Becker, M. Klein, S. Klein-Hessling, A. Palmetshofer, E. Serfling, V. Heib, M. Becker, J. Kubach, S. Schmitt, S. Stoll, H. Schild, M. S. Staege, M. Stassen, H. Jonuleit, and E. Schmitt.** 2007. Cyclic adenosine monophosphate is a key component of regulatory T cell-mediated suppression. J Exp Med **204:**1303-1310.
34. **Borsellino, G., M. Kleinewietfeld, D. Di Mitri, A. Sternjak, A. Diamantini, R. Giometto, S. Hopner, D. Centonze, G. Bernardi, M. L. Dell'Acqua, P. M. Rossini, L. Battistini, O. Rotzschke, and K. Falk.** 2007. Expression of ectonucleotidase CD39 by Foxp3+ Treg cells: hydrolysis of extracellular ATP and immune suppression. Blood **110:**1225-1232.
35. **Boyer, O., D. Saadoun, J. Abriol, M. Dodille, J. C. Piette, P. Cacoub, and D. Klatzmann.** 2004. CD4+CD25+ regulatory T-cell deficiency in patients with hepatitis C-mixed cryoglobulinemia vasculitis. Blood **103:**3428-3430.
36. **Breckpot, K., J. L. Aerts, and K. Thielemans.** 2007. Lentiviral vectors for cancer immunotherapy: transforming infectious particles into therapeutics. Gene Ther **14:**847-862.
37. **Brockhaus, M., H. J. Schoenfeld, E. J. Schlaeger, W. Hunziker, W. Lesslauer, and H. Loetscher.** 1990. Identification of two types of tumor necrosis factor receptors on human cell lines by monoclonal antibodies. Proc Natl Acad Sci U S A **87:**3127-3131.

38. **Browne, K. A., E. Blink, V. R. Sutton, C. J. Froelich, D. A. Jans, and J. A. Trapani.** 1999. Cytosolic delivery of granzyme B by bacterial toxins: evidence that endosomal disruption, in addition to transmembrane pore formation, is an important function of perforin. Mol Cell Biol **19:**8604-8615.
39. **Bruder, D., M. Probst-Kepper, A. M. Westendorf, R. Geffers, S. Beissert, K. Loser, H. von Boehmer, J. Buer, and W. Hansen.** 2004. Neuropilin-1: a surface marker of regulatory T cells. Eur J Immunol **34:**623-630.
40. **Brunkow, M. E., E. W. Jeffery, K. A. Hjerrild, B. Paeper, L. B. Clark, S. A. Yasayko, J. E. Wilkinson, D. Galas, S. F. Ziegler, and F. Ramsdell.** 2001. Disruption of a new forkhead/winged-helix protein, scurfin, results in the fatal lymphoproliferative disorder of the scurfy mouse. Nat Genet **27:**68-73.
41. **Buckner, J. H., U. Holzer, E. J. Novak, H. Reijonen, W. W. Kwok, and G. T. Nepom.** 2002. Defining antigen-specific responses with human MHC class II tetramers. J Allergy Clin Immunol **110:**199-208.
42. **Bueno, C., C. D. Lemke, G. Criado, M. L. Baroja, S. S. Ferguson, A. K. Rahman, C. D. Tsoukas, J. K. McCormick, and J. Madrenas.** 2006. Bacterial superantigens bypass Lck-dependent T cell receptor signaling by activating a Galpha11-dependent, PLC-beta-mediated pathway. Immunity **25:**67-78.
43. **Bukrinskaya, A., B. Brichacek, A. Mann, and M. Stevenson.** 1998. Establishment of a functional human immunodeficiency virus type 1 (HIV-1) reverse transcription complex involves the cytoskeleton. J Exp Med **188:**2113-2125.
44. **Cabarrocas, J., C. Cassan, F. Magnusson, E. Piaggio, L. Mars, J. Derbinski, B. Kyewski, D. A. Gross, B. L. Salomon, K. Khazaie, A. Saoudi, and R. S. Liblau.** 2006. Foxp3+ CD25+ regulatory T cells specific for a neo-self-antigen develop at the double-positive thymic stage. Proc Natl Acad Sci U S A **103:**8453-8458.
45. **Cabrera, R., Z. Tu, Y. Xu, R. J. Firpi, H. R. Rosen, C. Liu, and D. R. Nelson.** 2004. An immunomodulatory role for CD4(+)CD25(+) regulatory T lymphocytes in hepatitis C virus infection. Hepatology **40:**1062-1071.
46. **Campbell, I. K., L. J. Roberts, and I. P. Wicks.** 2003. Molecular targets in immune-mediated diseases: the case of tumour necrosis factor and rheumatoid arthritis. Immunol Cell Biol **81:**354-366.
47. **Cao, X., S. F. Cai, T. A. Fehniger, J. Song, L. I. Collins, D. R. Piwnica-Worms, and T. J. Ley.** 2007. Granzyme B and perforin are important for regulatory T cell-mediated suppression of tumor clearance. Immunity **27:**635-646.
48. **Card, C. M., P. J. McLaren, C. Wachihi, J. Kimani, F. A. Plummer, and K. R. Fowke.** 2009. Decreased immune activation in resistance to HIV-1 infection is associated with an elevated frequency of CD4(+)CD25(+)FOXP3(+) regulatory T cells. J Infect Dis **199:**1318-1322.
49. **Carreno, B. M., and M. Collins.** 2002. The B7 family of ligands and its receptors: new pathways for costimulation and inhibition of immune responses. Annu Rev Immunol **20:**29-53.
50. **Carter, J. S., V.** 2007. Virology - Principles and Applications. Whiley.
51. **Cederbom, L., H. Hall, and F. Ivars.** 2000. CD4+CD25+ regulatory T cells down-regulate co-stimulatory molecules on antigen-presenting cells. Eur J Immunol **30:**1538-1543.
52. **Chatila, T. A., F. Blaeser, N. Ho, H. M. Lederman, C. Voulgaropoulos, C. Helms, and A. M. Bowcock.** 2000. JM2, encoding a fork head-related protein, is mutated in X-linked autoimmunity-allergic disregulation syndrome. J Clin Invest **106:**R75-81.
53. **Chen, J., M. Trounstine, F. W. Alt, F. Young, C. Kurahara, J. F. Loring, and D. Huszar.** 1993. Immunoglobulin gene rearrangement in B cell deficient mice generated by targeted deletion of the JH locus. Int Immunol **5:**647-656.
54. **Chen, P., W. Hubner, M. A. Spinelli, and B. K. Chen.** 2007. Predominant mode of human immunodeficiency virus transfer between T cells is mediated by sustained Env-dependent neutralization-resistant virological synapses. J Virol **81:**12582-12595.
55. **Chen, W., H. Qin, B. Chesebro, and M. A. Cheever.** 1996. Identification of a gag-encoded cytotoxic T-lymphocyte epitope from FBL-3 leukemia shared by Friend, Moloney, and Rauscher murine leukemia virus-induced tumors. J Virol **70:**7773-7782.
56. **Chen, X., M. Baumel, D. N. Mannel, O. M. Howard, and J. J. Oppenheim.** 2007. Interaction of TNF with TNF receptor type 2 promotes expansion and function of mouse CD4+CD25+ T regulatory cells. J Immunol **179:**154-161.

57. **Chen, X., J. J. Subleski, R. Hamano, O. M. Howard, R. H. Wiltrout, and J. J. Oppenheim.** 2010. Co-expression of TNFR2 and CD25 identifies more of the functional CD4+FOXP3+ regulatory T cells in human peripheral blood. Eur J Immunol **40:**1099-1106.
58. **Chen, X., X. Wu, Q. Zhou, O. M. Howard, M. G. Netea, and J. J. Oppenheim.** 2013. TNFR2 is critical for the stabilization of the CD4+Foxp3+ regulatory T. cell phenotype in the inflammatory environment. J Immunol **190:**1076-1084.
59. **Chen, Y., V. K. Kuchroo, J. Inobe, D. A. Hafler, and H. L. Weiner.** 1994. Regulatory T cell clones induced by oral tolerance: suppression of autoimmune encephalomyelitis. Science **265:**1237-1240.
60. **Chen, Y., S. Shen, B. K. Gorentla, J. Gao, and X. P. Zhong.** 2012. Murine regulatory T cells contain hyperproliferative and death-prone subsets with differential ICOS expression. J Immunol **188:**1698-1707.
61. **Chesebro, B., M. Bloom, K. Wehrly, and J. Nishio.** 1979. Persistence of infectious Friend virus in spleens of mice after spontaneous recovery from virus-induced erythroleukemia. J Virol **32:**832-837.
62. **Chesebro, B., M. Miyazawa, and W. J. Britt.** 1990. Host genetic control of spontaneous and induced immunity to Friend murine retrovirus infection. Annu Rev Immunol **8:**477-499.
63. **Chesebro, B., and K. Wehrly.** 1979. Identification of a non-H-2 gene (Rfv-3) influencing recovery from viremia and leukemia induced by Friend virus complex. Proc Natl Acad Sci U S A **76:**425-429.
64. **Choi, Y., J. W. Kappler, and P. Marrack.** 1991. A superantigen encoded in the open reading frame of the 3' long terminal repeat of mouse mammary tumour virus. Nature **350:**203-207.
65. **Chopra, M., S. S. Riedel, M. Biehl, S. Krieger, V. von Krosigk, C. A. Bauerlein, C. Brede, A. L. Jordan Garrote, S. Kraus, V. Schafer, M. Ritz, K. Mattenheimer, A. Degla, A. Mottok, H. Einsele, H. Wajant, and A. Beilhack.** 2013. Tumor necrosis factor receptor 2-dependent homeostasis of regulatory T cells as a player in TNF-induced experimental metastasis. Carcinogenesis **34:**1296-1303.
66. **Chung, J. Y., Y. C. Park, H. Ye, and H. Wu.** 2002. All TRAFs are not created equal: common and distinct molecular mechanisms of TRAF-mediated signal transduction. J Cell Sci **115:**679-688.
67. **Cmarik, J., and S. Ruscetti.** 2010. Friend Spleen Focus-Forming Virus Activates the Tyrosine Kinase sf-Stk and the Transcription Factor PU.1 to Cause a Multi-Stage Erythroleukemia in Mice. Viruses **2:**2235-2257.
68. **Cobbold, S. P., A. Jayasuriya, A. Nash, T. D. Prospero, and H. Waldmann.** 1984. Therapy with monoclonal antibodies by elimination of T-cell subsets in vivo. Nature **312:**548-551.
69. **Coffin, J., A. Haase, J. A. Levy, L. Montagnier, S. Oroszlan, N. Teich, H. Temin, K. Toyoshima, H. Varmus, P. Vogt, and et al.** 1986. Human immunodeficiency viruses. Science **232:**697.
70. **Coffin, J., S. Hughes, and H. Varmus (ed.).** 1997. Retroviruses. Cold Spring Harbor Laboratory Press, Cold Spring Harbor (NY).
71. **Collison, L. W., C. J. Workman, T. T. Kuo, K. Boyd, Y. Wang, K. M. Vignali, R. Cross, D. Sehy, R. S. Blumberg, and D. A. Vignali.** 2007. The inhibitory cytokine IL-35 contributes to regulatory T-cell function. Nature **450:**566-569.
72. **Conrad, B., R. N. Weissmahr, J. Boni, R. Arcari, J. Schupbach, and B. Mach.** 1997. A human endogenous retroviral superantigen as candidate autoimmune gene in type I diabetes. Cell **90:**303-313.
73. **Coquet, J. M., J. C. Ribot, N. Babala, S. Middendorp, G. van der Horst, Y. Xiao, J. F. Neves, D. Fonseca-Pereira, H. Jacobs, D. J. Pennington, B. Silva-Santos, and J. Borst.** 2013. Epithelial and dendritic cells in the thymic medulla promote CD4+Foxp3+ regulatory T cell development via the CD27-CD70 pathway. J Exp Med **210:**715-728.
74. **Corley, R. B., and F. E. Lund.** 1991. Who's zooming who? Curr Biol **1:**278-280.
75. **Coutinho, A., I. Caramalho, E. Seixas, and J. Demengeot.** 2005. Thymic commitment of regulatory T cells is a pathway of TCR-dependent selection that isolates repertoires undergoing positive or negative selection. Curr Top Microbiol Immunol **293:**43-71.
76. **Curotto de Lafaille, M. A., and J. J. Lafaille.** 2009. Natural and adaptive foxp3+ regulatory T cells: more of the same or a division of labor? Immunity **30:**626-635.

77. **Curotto de Lafaille, M. A., A. C. Lino, N. Kutchukhidze, and J. J. Lafaille.** 2004. CD25- T cells generate CD25+Foxp3+ regulatory T cells by peripheral expansion. J Immunol **173:**7259-7268.
78. **Deaglio, S., K. M. Dwyer, W. Gao, D. Friedman, A. Usheva, A. Erat, J. F. Chen, K. Enjyoji, J. Linden, M. Oukka, V. K. Kuchroo, T. B. Strom, and S. C. Robson.** 2007. Adenosine generation catalyzed by CD39 and CD73 expressed on regulatory T cells mediates immune suppression. J Exp Med **204:**1257-1265.
79. **DeFranco, A. L., R.; Robertson, M.** 2007. Immunity: The Immune Response to Infectious and Inflammatory Disease. Oxford University Press, USA.
80. **Denton, P. W., and J. V. Garcia.** 2012. Mucosal HIV-1 transmission and prevention strategies in BLT humanized mice. Trends Microbiol **20:**268-274.
81. **Dietze, K. K., G. Zelinskyy, K. Gibbert, S. Schimmer, S. Francois, L. Myers, T. Sparwasser, K. J. Hasenkrug, and U. Dittmer.** 2011. Transient depletion of regulatory T cells in transgenic mice reactivates virus-specific CD8+ T cells and reduces chronic retroviral set points. Proc Natl Acad Sci U S A **108:**2420-2425.
82. **Dilek, N., N. Poirier, P. Hulin, F. Coulon, C. Mary, S. Ville, H. Vie, B. Clemenceau, G. Blancho, and B. Vanhove.** 2013. Targeting CD28, CTLA-4 and PD-L1 Costimulation Differentially Controls Immune Synapses and Function of Human Regulatory and Conventional T-Cells. PLoS One **8:**e83139.
83. **Dittmer, U., D. M. Brooks, and K. J. Hasenkrug.** 1999. Requirement for multiple lymphocyte subsets in protection by a live attenuated vaccine against retroviral infection. Nat Med **5:**189-193.
84. **Dittmer, U., H. He, R. J. Messer, S. Schimmer, A. R. Olbrich, C. Ohlen, P. D. Greenberg, I. M. Stromnes, M. Iwashiro, S. Sakaguchi, L. H. Evans, K. E. Peterson, G. Yang, and K. J. Hasenkrug.** 2004. Functional impairment of CD8(+) T cells by regulatory T cells during persistent retroviral infection. Immunity **20:**293-303.
85. **Dittmer, U., B. Race, K. E. Peterson, I. M. Stromnes, R. J. Messer, and K. J. Hasenkrug.** 2002. Essential roles for CD8+ T cells and gamma interferon in protection of mice against retrovirus-induced immunosuppression. J Virol **76:**450-454.
86. **Ebinuma, H., N. Nakamoto, Y. Li, D. A. Price, E. Gostick, B. L. Levine, J. Tobias, W. W. Kwok, and K. M. Chang.** 2008. Identification and in vitro expansion of functional antigen-specific CD25+ FoxP3+ regulatory T cells in hepatitis C virus infection. J Virol **82:**5043-5053.
87. **Elahi, S., W. L. Dinges, N. Lejarcegui, K. J. Laing, A. C. Collier, D. M. Koelle, M. J. McElrath, and H. Horton.** 2011. Protective HIV-specific CD8+ T cells evade Treg cell suppression. Nat Med **17:**989-995.
88. **Enjyoji, K., J. Sevigny, Y. Lin, P. S. Frenette, P. D. Christie, J. S. Esch, 2nd, M. Imai, J. M. Edelberg, H. Rayburn, M. Lech, D. L. Beeler, E. Csizmadia, D. D. Wagner, S. C. Robson, and R. D. Rosenberg.** 1999. Targeted disruption of cd39/ATP diphosphohydrolase results in disordered hemostasis and thromboregulation. Nat Med **5:**1010-1017.
89. **Epple, H. J., C. Loddenkemper, D. Kunkel, H. Troger, J. Maul, V. Moos, E. Berg, R. Ullrich, J. D. Schulzke, H. Stein, R. Duchmann, M. Zeitz, and T. Schneider.** 2006. Mucosal but not peripheral FOXP3+ regulatory T cells are highly increased in untreated HIV infection and normalize after suppressive HAART. Blood **108:**3072-3078.
90. **Erickson, S. L., F. J. de Sauvage, K. Kikly, K. Carver-Moore, S. Pitts-Meek, N. Gillett, K. C. Sheehan, R. D. Schreiber, D. V. Goeddel, and M. W. Moore.** 1994. Decreased sensitivity to tumour-necrosis factor but normal T-cell development in TNF receptor-2-deficient mice. Nature **372:**560-563.
91. **Fallarino, F., U. Grohmann, K. W. Hwang, C. Orabona, C. Vacca, R. Bianchi, M. L. Belladonna, M. C. Fioretti, M. L. Alegre, and P. Puccetti.** 2003. Modulation of tryptophan catabolism by regulatory T cells. Nat Immunol **4:**1206-1212.
92. **Fazilleau, N., H. Bachelez, M. L. Gougeon, and M. Viguier.** 2007. Cutting edge: size and diversity of CD4+CD25high Foxp3+ regulatory T cell repertoire in humans: evidence for similarities and partial overlapping with CD4+CD25- T cells. J Immunol **179:**3412-3416.
93. **Ferencík, M. R., J.; Matha, V.; Herold, M.** 2004. Kompendium der Immunologie - Grundlagen und Klinik. SpringerWienNewYork.

94. **Fletcher, J. M., R. Lonergan, L. Costelloe, K. Kinsella, B. Moran, C. O'Farrelly, N. Tubridy, and K. H. Mills.** 2009. CD39+Foxp3+ regulatory T Cells suppress pathogenic Th17 cells and are impaired in multiple sclerosis. J Immunol **183:**7602-7610.
95. **Fontenot, J. D., M. A. Gavin, and A. Y. Rudensky.** 2003. Foxp3 programs the development and function of CD4+CD25+ regulatory T cells. Nat Immunol **4:**330-336.
96. **Fontenot, J. D., J. P. Rasmussen, M. A. Gavin, and A. Y. Rudensky.** 2005. A function for interleukin 2 in Foxp3-expressing regulatory T cells. Nat Immunol **6:**1142-1151.
97. **Fontenot, J. D., J. P. Rasmussen, L. M. Williams, J. L. Dooley, A. G. Farr, and A. Y. Rudensky.** 2005. Regulatory T cell lineage specification by the forkhead transcription factor foxp3. Immunity **22:**329-341.
98. **Freeman, G. J., J. M. Casasnovas, D. T. Umetsu, and R. H. DeKruyff.** 2010. TIM genes: a family of cell surface phosphatidylserine receptors that regulate innate and adaptive immunity. Immunol Rev **235:**172-189.
99. **Freeman, G. J., A. J. Long, Y. Iwai, K. Bourque, T. Chernova, H. Nishimura, L. J. Fitz, N. Malenkovich, T. Okazaki, M. C. Byrne, H. F. Horton, L. Fouser, L. Carter, V. Ling, M. R. Bowman, B. M. Carreno, M. Collins, C. R. Wood, and T. Honjo.** 2000. Engagement of the PD-1 immunoinhibitory receptor by a novel B7 family member leads to negative regulation of lymphocyte activation. J Exp Med **192:**1027-1034.
100. **Friend, C.** 1957. Cell-free transmission in adult Swiss mice of a disease having the character of a leukemia. J Exp Med **105:**307-318.
101. **Fulton, R. B., D. K. Meyerholz, and S. M. Varga.** 2010. Foxp3+ CD4 regulatory T cells limit pulmonary immunopathology by modulating the CD8 T cell response during respiratory syncytial virus infection. J Immunol **185:**2382-2392.
102. **Fung-Leung, W. P., M. W. Schilham, A. Rahemtulla, T. M. Kundig, M. Vollenweider, J. Potter, W. van Ewijk, and T. W. Mak.** 1991. CD8 is needed for development of cytotoxic T cells but not helper T cells. Cell **65:**443-449.
103. **Furtado, G. C., M. A. Curotto de Lafaille, N. Kutchukhidze, and J. J. Lafaille.** 2002. Interleukin 2 signaling is required for CD4(+) regulatory T cell function. J Exp Med **196:**851-857.
104. **Gallatin, W. M., I. L. Weissman, and E. C. Butcher.** 1983. A cell-surface molecule involved in organ-specific homing of lymphocytes. Nature **304:**30-34.
105. **Gallo, R. C., P. S. Sarin, E. P. Gelmann, M. Robert-Guroff, E. Richardson, V. S. Kalyanaraman, D. Mann, G. D. Sidhu, R. E. Stahl, S. Zolla-Pazner, J. Leibowitch, and M. Popovic.** 1983. Isolation of human T-cell leukemia virus in acquired immune deficiency syndrome (AIDS). Science **220:**865-867.
106. **Garin, M. I., C. C. Chu, D. Golshayan, E. Cernuda-Morollon, R. Wait, and R. I. Lechler.** 2007. Galectin-1: a key effector of regulation mediated by CD4+CD25+ T cells. Blood **109:**2058-2065.
107. **Garrison, K. E., R. B. Jones, D. A. Meiklejohn, N. Anwar, L. C. Ndhlovu, J. M. Chapman, A. L. Erickson, A. Agrawal, G. Spotts, F. M. Hecht, S. Rakoff-Nahoum, J. Lenz, M. A. Ostrowski, and D. F. Nixon.** 2007. T cell responses to human endogenous retroviruses in HIV-1 infection. PLoS Pathog **3:**e165.
108. **Gavin, M. A., J. P. Rasmussen, J. D. Fontenot, V. Vasta, V. C. Manganiello, J. A. Beavo, and A. Y. Rudensky.** 2007. Foxp3-dependent programme of regulatory T-cell differentiation. Nature **445:**771-775.
109. **Gerdes, J., U. Schwab, H. Lemke, and H. Stein.** 1983. Production of a mouse monoclonal antibody reactive with a human nuclear antigen associated with cell proliferation. Int J Cancer **31:**13-20.
110. **Gershon, R. K., and K. Kondo.** 1970. Cell interactions in the induction of tolerance: the role of thymic lymphocytes. Immunology **18:**723-737.
111. **Gershon, R. K., and K. Kondo.** 1971. Infectious immunological tolerance. Immunology **21:**903-914.
112. **Goldsby, R. A. K. T. J. K., J.; Osborne, B.A.** 2002. Immunology, 5th ed.
113. **Gondek, D. C., L. F. Lu, S. A. Quezada, S. Sakaguchi, and R. J. Noelle.** 2005. Cutting edge: contact-mediated suppression by CD4+CD25+ regulatory cells involves a granzyme B-dependent, perforin-independent mechanism. J Immunol **174:**1783-1786.
114. **Gonzalez, A., I. Andre-Schmutz, C. Carnaud, D. Mathis, and C. Benoist.** 2001. Damage control, rather than unresponsiveness, effected by protective DX5+ T cells in autoimmune diabetes. Nat Immunol **2:**1117-1125.

115. **Goodchild, N. L., D. A. Wilkinson, and D. L. Mager.** 1993. Recent evolutionary expansion of a subfamily of RTVL-H human endogenous retrovirus-like elements. Virology **196:**778-788.
116. **Gotot, J., C. Gottschalk, S. Leopold, P. A. Knolle, H. Yagita, C. Kurts, and I. Ludwig-Portugall.** 2012. Regulatory T cells use programmed death 1 ligands to directly suppress autoreactive B cells in vivo. Proc Natl Acad Sci U S A **109:**10468-10473.
117. **Gottschalk, R. A., E. Corse, and J. P. Allison.** 2012. Expression of Helios in peripherally induced Foxp3+ regulatory T cells. J Immunol **188:**976-980.
118. **Goujon, C., L. Jarrosson-Wuilleme, J. Bernaud, D. Rigal, J. L. Darlix, and A. Cimarelli.** 2006. With a little help from a friend: increasing HIV transduction of monocyte-derived dendritic cells with virion-like particles of SIV(MAC). Gene Ther **13:**991-994.
119. **Govindaraj, C., P. Tan, P. Walker, A. Wei, A. Spencer, and M. Plebanski.** 2014. Reducing TNF Receptor 2+ Regulatory T Cells via the Combined Action of Azacitidine and the HDAC Inhibitor, Panobinostat for Clinical Benefit in Acute Myeloid Leukemia Patients. Clin Cancer Res.
120. **Grell, M., E. Douni, H. Wajant, M. Lohden, M. Clauss, B. Maxeiner, S. Georgopoulos, W. Lesslauer, G. Kollias, K. Pfizenmaier, and P. Scheurich.** 1995. The transmembrane form of tumor necrosis factor is the prime activating ligand of the 80 kDa tumor necrosis factor receptor. Cell **83:**793-802.
121. **Grell, M., H. Wajant, G. Zimmermann, and P. Scheurich.** 1998. The type 1 receptor (CD120a) is the high-affinity receptor for soluble tumor necrosis factor. Proc Natl Acad Sci U S A **95:**570-575.
122. **Grinberg-Bleyer, Y., D. Saadoun, A. Baeyens, F. Billiard, J. D. Goldstein, S. Gregoire, G. H. Martin, R. Elhage, N. Derian, W. Carpentier, G. Marodon, D. Klatzmann, E. Piaggio, and B. L. Salomon.** 2010. Pathogenic T cells have a paradoxical protective effect in murine autoimmune diabetes by boosting Tregs. J Clin Invest **120:**4558-4568.
123. **Grossman, W. J., J. W. Verbsky, B. L. Tollefsen, C. Kemper, J. P. Atkinson, and T. J. Ley.** 2004. Differential expression of granzymes A and B in human cytotoxic lymphocyte subsets and T regulatory cells. Blood **104:**2840-2848.
124. **Grosso, J. F., C. C. Kelleher, T. J. Harris, C. H. Maris, E. L. Hipkiss, A. De Marzo, R. Anders, G. Netto, D. Getnet, T. C. Bruno, M. V. Goldberg, D. M. Pardoll, and C. G. Drake.** 2007. LAG-3 regulates CD8+ T cell accumulation and effector function in murine self- and tumor-tolerance systems. J Clin Invest **117:**3383-3392.
125. **Groux, H., A. O'Garra, M. Bigler, M. Rouleau, S. Antonenko, J. E. de Vries, and M. G. Roncarolo.** 1997. A CD4+ T-cell subset inhibits antigen-specific T-cell responses and prevents colitis. Nature **389:**737-742.
126. **Hahm, K., B. S. Cobb, A. S. McCarty, K. E. Brown, C. A. Klug, R. Lee, K. Akashi, I. L. Weissman, A. G. Fisher, and S. T. Smale.** 1998. Helios, a T cell-restricted Ikaros family member that quantitatively associates with Ikaros at centromeric heterochromatin. Genes Dev **12:**782-796.
127. **Hannier, S., M. Tournier, G. Bismuth, and F. Triebel.** 1998. CD3/TCR complex-associated lymphocyte activation gene-3 molecules inhibit CD3/TCR signaling. J Immunol **161:**4058-4065.
128. **Haribhai, D., W. Lin, L. M. Relland, N. Truong, C. B. Williams, and T. A. Chatila.** 2007. Regulatory T cells dynamically control the primary immune response to foreign antigen. J Immunol **178:**2961-2972.
129. **Hasenkrug, K. J.** 1999. Lymphocyte deficiencies increase susceptibility to friend virus-induced erythroleukemia in Fv-2 genetically resistant mice. J Virol **73:**6468-6473.
130. **Hasenkrug, K. J., D. M. Brooks, and B. Chesebro.** 1995. Passive immunotherapy for retroviral disease: influence of major histocompatibility complex type and T-cell responsiveness. Proc Natl Acad Sci U S A **92:**10492-10495.
131. **Hasenkrug, K. J., D. M. Brooks, and U. Dittmer.** 1998. Critical role for CD4(+) T cells in controlling retrovirus replication and spread in persistently infected mice. J Virol **72:**6559-6564.
132. **Hasenkrug, K. J., and B. Chesebro.** 1997. Immunity to retroviral infection: the Friend virus model. Proc Natl Acad Sci U S A **94:**7811-7816.
133. **Hawrylowicz, C. M., and A. O'Garra.** 2005. Potential role of interleukin-10-secreting regulatory T cells in allergy and asthma. Nat Rev Immunol **5:**271-283.

134. **Hedrick, S. M., R. N. Germain, M. J. Bevan, M. Dorf, I. Engel, P. Fink, N. Gascoigne, E. Heber-Katz, J. Kapp, Y. Kaufmann, and et al.** 1985. Rearrangement and transcription of a T-cell receptor beta-chain gene in different T-cell subsets. Proc Natl Acad Sci U S A **82:**531-535.
135. **Heusel, J. W., R. L. Wesselschmidt, S. Shresta, J. H. Russell, and T. J. Ley.** 1994. Cytotoxic lymphocytes require granzyme B for the rapid induction of DNA fragmentation and apoptosis in allogeneic target cells. Cell **76:**977-987.
136. **Hori, S., T. Nomura, and S. Sakaguchi.** 2003. Control of regulatory T cell development by the transcription factor Foxp3. Science **299:**1057-1061.
137. **Housley, W. J., C. O. Adams, F. C. Nichols, L. Puddington, E. G. Lingenheld, L. Zhu, T. V. Rajan, and R. B. Clark.** 2011. Natural but not inducible regulatory T cells require TNF-alpha signaling for in vivo function. J Immunol **186:**6779-6787.
138. **Hsieh, C. S., Y. Zheng, Y. Liang, J. D. Fontenot, and A. Y. Rudensky.** 2006. An intersection between the self-reactive regulatory and nonregulatory T cell receptor repertoires. Nat Immunol **7:**401-410.
139. **Huang, C. T., C. J. Workman, D. Flies, X. Pan, A. L. Marson, G. Zhou, E. L. Hipkiss, S. Ravi, J. Kowalski, H. I. Levitsky, J. D. Powell, D. M. Pardoll, C. G. Drake, and D. A. Vignali.** 2004. Role of LAG-3 in regulatory T cells. Immunity **21:**503-513.
140. **Hubner, W., P. Chen, A. Del Portillo, Y. Liu, R. E. Gordon, and B. K. Chen.** 2007. Sequence of human immunodeficiency virus type 1 (HIV-1) Gag localization and oligomerization monitored with live confocal imaging of a replication-competent, fluorescently tagged HIV-1. J Virol **81:**12596-12607.
141. **Idoyaga, J., C. Fiorese, L. Zbytnuik, A. Lubkin, J. Miller, B. Malissen, D. Mucida, M. Merad, and R. M. Steinman.** 2013. Specialized role of migratory dendritic cells in peripheral tolerance induction. J Clin Invest **123:**844-854.
142. **Idriss, H. T., and J. H. Naismith.** 2000. TNF alpha and the TNF receptor superfamily: structure-function relationship(s). Microsc Res Tech **50:**184-195.
143. **Imamichi, H., and H. C. Lane.** 2012. Regulatory T cells in HIV-1 infection: the good, the bad, and the ugly. J Infect Dis **205:**1479-1482.
144. **Iwashiro, M., R. J. Messer, K. E. Peterson, I. M. Stromnes, T. Sugie, and K. J. Hasenkrug.** 2001. Immunosuppression by CD4+ regulatory T cells induced by chronic retroviral infection. Proc Natl Acad Sci U S A **98:**9226-9230.
145. **Iwashiro, M., K. Peterson, R. J. Messer, I. M. Stromnes, and K. J. Hasenkrug.** 2001. CD4(+) T cells and gamma interferon in the long-term control of persistent friend retrovirus infection. J Virol **75:**52-60.
146. **Jaffe, H. W., D. J. Bregman, and R. M. Selik.** 1983. Acquired immune deficiency syndrome in the United States: the first 1,000 cases. J Infect Dis **148:**339-345.
147. **Jin, H., D. Gong, D. Adeegbe, A. L. Bayer, C. Rolle, A. Yu, and T. R. Malek.** 2006. Quantitative assessment concerning the contribution of IL-2Rbeta for superantigen-mediated T cell responses in vivo. Int Immunol **18:**565-572.
148. **Joedicke, J. J., K. K. Dietze, G. Zelinskyy, and U. Dittmer.** 2014. The phenotype and activation status of regulatory T cells during Friend retrovirus infection. Virol Sin.
149. **Jordan, M. S., A. Boesteanu, A. J. Reed, A. L. Petrone, A. E. Holenbeck, M. A. Lerman, A. Naji, and A. J. Caton.** 2001. Thymic selection of CD4+CD25+ regulatory T cells induced by an agonist self-peptide. Nat Immunol **2:**301-306.
150. **Jutel, M., and C. A. Akdis.** 2011. T-cell subset regulation in atopy. Curr Allergy Asthma Rep **11:**139-145.
151. **Kappler, J. W., N. Roehm, and P. Marrack.** 1987. T cell tolerance by clonal elimination in the thymus. Cell **49:**273-280.
152. **Kappler, J. W., U. Staerz, J. White, and P. C. Marrack.** 1988. Self-tolerance eliminates T cells specific for Mls-modified products of the major histocompatibility complex. Nature **332:**35-40.
153. **Kataoka, H., S. Takahashi, K. Takase, S. Yamasaki, T. Yokosuka, T. Koike, and T. Saito.** 2005. CD25(+)CD4(+) regulatory T cells exert in vitro suppressive activity independent of CTLA-4. Int Immunol **17:**421-427.
154. **Killebrew, J. R., N. Perdue, A. Kwan, A. M. Thornton, E. M. Shevach, and D. J. Campbell.** 2011. A self-reactive TCR drives the development of Foxp3+ regulatory T cells that prevent autoimmune disease. J Immunol **187:**861-869.

155. **Kim, E. Y., J. J. Priatel, S. J. Teh, and H. S. Teh.** 2006. TNF receptor type 2 (p75) functions as a costimulator for antigen-driven T cell responses in vivo. J Immunol **176:**1026-1035.
156. **Kim, E. Y., and H. S. Teh.** 2001. TNF type 2 receptor (p75) lowers the threshold of T cell activation. J Immunol **167:**6812-6820.
157. **King, L. B., F. E. Lund, D. A. White, S. Sharma, and R. B. Corley.** 1990. Molecular events in B lymphocyte differentiation. Inducible expression of the endogenous mouse mammary tumor proviral gene, Mtv-9. J Immunol **144:**3218-3227.
158. **Kingsley, C. I., M. Karim, A. R. Bushell, and K. J. Wood.** 2002. CD25+CD4+ regulatory T cells prevent graft rejection: CTLA-4- and IL-10-dependent immunoregulation of alloresponses. J Immunol **168:**1080-1086.
159. **Kitazawa, Y., M. Fujino, Q. Wang, H. Kimura, M. Azuma, M. Kubo, R. Abe, and X. K. Li.** 2007. Involvement of the programmed death-1/programmed death-1 ligand pathway in CD4+CD25+ regulatory T-cell activity to suppress alloimmune responses. Transplantation **83:**774-782.
160. **Kleijwegt, F. S., S. Laban, G. Duinkerken, A. M. Joosten, A. Zaldumbide, T. Nikolic, and B. O. Roep.** 2010. Critical role for TNF in the induction of human antigen-specific regulatory T cells by tolerogenic dendritic cells. J Immunol **185:**1412-1418.
161. **Knipe, D. M. H., P.M.; Griffin, D.E.; Lamb, R.A.; Martin, M.A.; Roizman, B.; Straus, S.E.** 2001. Fields Virology, 4th ed.
162. **Kobie, J. J., P. R. Shah, L. Yang, J. A. Rebhahn, D. J. Fowell, and T. R. Mosmann.** 2006. T regulatory and primed uncommitted CD4 T cells express CD73, which suppresses effector CD4 T cells by converting 5'-adenosine monophosphate to adenosine. J Immunol **177:**6780-6786.
163. **Kohm, A. P., P. A. Carpentier, H. A. Anger, and S. D. Miller.** 2002. Cutting edge: CD4+CD25+ regulatory T cells suppress antigen-specific autoreactive immune responses and central nervous system inflammation during active experimental autoimmune encephalomyelitis. J Immunol **169:**4712-4716.
164. **Kollias, G., and D. Kontoyiannis.** 2002. Role of TNF/TNFR in autoimmunity: specific TNF receptor blockade may be advantageous to anti-TNF treatments. Cytokine Growth Factor Rev **13:**315-321.
165. **Koo, G. C., and J. R. Peppard.** 1984. Establishment of monoclonal anti-Nk-1.1 antibody. Hybridoma **3:**301-303.
166. **Kornete, M., E. Sgouroudis, and C. A. Piccirillo.** 2012. ICOS-dependent homeostasis and function of Foxp3+ regulatory T cells in islets of nonobese diabetic mice. J Immunol **188:**1064-1074.
167. **Kozak, C. A., and R. R. O'Neill.** 1987. Diverse wild mouse origins of xenotropic, mink cell focus-forming, and two types of ecotropic proviral genes. J Virol **61:**3082-3088.
168. **Krammer, P. H.** 2000. CD95's deadly mission in the immune system. Nature **407:**789-795.
169. **Krippner-Heidenreich, A., I. Grunwald, G. Zimmermann, M. Kuhnle, J. Gerspach, T. Sterns, S. D. Shnyder, J. H. Gill, D. N. Mannel, K. Pfizenmaier, and P. Scheurich.** 2008. Single-chain TNF, a TNF derivative with enhanced stability and antitumoral activity. J Immunol **180:**8176-8183.
170. **Kronenberg, M., M. Steinmetz, J. Kobori, E. Kraig, J. A. Kapp, C. W. Pierce, C. M. Sorensen, G. Suzuki, T. Tada, and L. Hood.** 1983. RNA transcripts for I-J polypeptides are apparently not encoded between the I-A and I-E subregions of the murine major histocompatibility complex. Proc Natl Acad Sci U S A **80:**5704-5708.
171. **Kryworuchko, M., and J. Theze.** 2006. Interleukin-2: from T cell growth and homeostasis to immune reconstitution of HIV patients. Vitam Horm **74:**531-547.
172. **Lahl, K., C. Loddenkemper, C. Drouin, J. Freyer, J. Arnason, G. Eberl, A. Hamann, H. Wagner, J. Huehn, and T. Sparwasser.** 2007. Selective depletion of Foxp3+ regulatory T cells induces a scurfy-like disease. J Exp Med **204:**57-63.
173. **Lander, M. R., and S. K. Chattopadhyay.** 1984. A Mus dunni cell line that lacks sequences closely related to endogenous murine leukemia viruses and can be infected by ectropic, amphotropic, xenotropic, and mink cell focus-forming viruses. J Virol **52:**695-698.
174. **Lavender, K. J., W. W. Pang, R. J. Messer, A. K. Duley, B. Race, K. Phillips, D. Scott, K. E. Peterson, C. K. Chan, U. Dittmer, T. Dudek, T. M. Allen, I. L. Weissman, and K. J. Hasenkrug.** 2013. BLT-humanized C57BL/6 Rag2-/-gammac-/-CD47-/- mice are

resistant to GVHD and develop B- and T-cell immunity to HIV infection. Blood **122:**4013-4020.

175. **Leavy, O.** 2013. Regulatory T cells: the thymic medulla - a cradle for TReg cell development. Nat Rev Immunol **13:**304.
176. **Lefrancois, L., T. A. Barrett, W. L. Havran, and L. Puddington.** 1994. Developmental expression of the alpha IEL beta 7 integrin on T cell receptor gamma delta and T cell receptor alpha beta T cells. Eur J Immunol **24:**635-640.
177. **Legrand, F. A., D. F. Nixon, C. P. Loo, E. Ono, J. M. Chapman, M. Miyamoto, R. S. Diaz, A. M. Santos, R. C. Succi, J. Abadi, M. G. Rosenberg, M. I. de Moraes-Pinto, and E. G. Kallas.** 2006. Strong HIV-1-specific T cell responses in HIV-1-exposed uninfected infants and neonates revealed after regulatory T cell removal. PLoS One **1:**e102.
178. **Lenschow, D. J., K. C. Herold, L. Rhee, B. Patel, A. Koons, H. Y. Qin, E. Fuchs, B. Singh, C. B. Thompson, and J. A. Bluestone.** 1996. CD28/B7 regulation of Th1 and Th2 subsets in the development of autoimmune diabetes. Immunity **5:**285-293.
179. **Levings, M. K., R. Sangregorio, and M. G. Roncarolo.** 2001. Human cd25(+)cd4(+) t regulatory cells suppress naive and memory T cell proliferation and can be expanded in vitro without loss of function. J Exp Med **193:**1295-1302.
180. **Lewis, M., L. A. Tartaglia, A. Lee, G. L. Bennett, G. C. Rice, G. H. Wong, E. Y. Chen, and D. V. Goeddel.** 1991. Cloning and expression of cDNAs for two distinct murine tumor necrosis factor receptors demonstrate one receptor is species specific. Proc Natl Acad Sci U S A **88:**2830-2834.
181. **Li, S., E. J. Gowans, C. Chougnet, M. Plebanski, and U. Dittmer.** 2008. Natural regulatory T cells and persistent viral infection. J Virol **82:**21-30.
182. **Lieberman, J.** 2003. The ABCs of granule-mediated cytotoxicity: new weapons in the arsenal. Nat Rev Immunol **3:**361-370.
183. **Littwitz, E., S. Francois, U. Dittmer, and K. Gibbert.** 2013. Distinct roles of NK cells in viral immunity during different phases of acute Friend retrovirus infection. Retrovirology **10:**127.
184. **Liu, J., N. Gong, X. Huang, A. D. Reynolds, R. L. Mosley, and H. E. Gendelman.** 2009. Neuromodulatory activities of CD4+CD25+ regulatory T cells in a murine model of HIV-1-associated neurodegeneration. J Immunol **182:**3855-3865.
185. **Liu, W., A. L. Putnam, Z. Xu-Yu, G. L. Szot, M. R. Lee, S. Zhu, P. A. Gottlieb, P. Kapranov, T. R. Gingeras, B. Fazekas de St Groth, C. Clayberger, D. M. Soper, S. F. Ziegler, and J. A. Bluestone.** 2006. CD127 expression inversely correlates with FoxP3 and suppressive function of human CD4+ T reg cells. J Exp Med **203:**1701-1711.
186. **Lombardi, V., A. O. Speak, J. Kerzerho, N. Szely, and O. Akbari.** 2012. CD8alpha(+)beta(-) and CD8alpha(+)beta(+) plasmacytoid dendritic cells induce Foxp3(+) regulatory T cells and prevent the induction of airway hyper-reactivity. Mucosal Immunol **5:**432-443.
187. **Luger, T. A. S., T.** 1993. Epidermal Growth Factors and Cytokines, 1st ed. CRC Press.
188. **Lund, J. M., L. Hsing, T. T. Pham, and A. Y. Rudensky.** 2008. Coordination of early protective immunity to viral infection by regulatory T cells. Science **320:**1220-1224.
189. **MacDonald, A. J., M. Duffy, M. T. Brady, S. McKiernan, W. Hall, J. Hegarty, M. Curry, and K. H. Mills.** 2002. CD4 T helper type 1 and regulatory T cells induced against the same epitopes on the core protein in hepatitis C virus-infected persons. J Infect Dis **185:**720-727.
190. **MacLeod, C. L., K. D. Finley, and D. K. Kakuda.** 1994. y(+)-type cationic amino acid transport: expression and regulation of the mCAT genes. J Exp Biol **196:**109-121.
191. **Maiti, A., G. Maki, and P. Johnson.** 1998. TNF-alpha induction of CD44-mediated leukocyte adhesion by sulfation. Science **282:**941-943.
192. **Malek, T. R.** 2003. The main function of IL-2 is to promote the development of T regulatory cells. J Leukoc Biol **74:**961-965.
193. **Mangeney, M., N. de Parseval, G. Thomas, and T. Heidmann.** 2001. The full-length envelope of an HERV-H human endogenous retrovirus has immunosuppressive properties. J Gen Virol **82:**2515-2518.
194. **Mangeney, M., J. Pothlichet, M. Renard, B. Ducos, and T. Heidmann.** 2005. Endogenous retrovirus expression is required for murine melanoma tumor growth in vivo. Cancer Res **65:**2588-2591.

195. **Manzke, N., I. Akhmetzyanova, K. J. Hasenkrug, M. Trilling, G. Zelinskyy, and U. Dittmer.** 2013. CD4+ T cells develop antiretroviral cytotoxic activity in the absence of regulatory T cells and CD8+ T cells. J Virol **87:**6306-6313.
196. **McCullagh, P. J.** 1970. The transfer of immunological competence to rats tolerant of sheep erythrocytes with lymphocytes from normal rats. Aust J Exp Biol Med Sci **48:**351-367.
197. **McGuirk, P., C. McCann, and K. H. Mills.** 2002. Pathogen-specific T regulatory 1 cells induced in the respiratory tract by a bacterial molecule that stimulates interleukin 10 production by dendritic cells: a novel strategy for evasion of protective T helper type 1 responses by Bordetella pertussis. J Exp Med **195:**221-231.
198. **McIlwain, D. R., P. A. Lang, T. Maretzky, K. Hamada, K. Ohishi, S. K. Maney, T. Berger, A. Murthy, G. Duncan, H. C. Xu, K. S. Lang, D. Haussinger, A. Wakeham, A. Itie-Youten, R. Khokha, P. S. Ohashi, C. P. Blobel, and T. W. Mak.** 2012. iRhom2 regulation of TACE controls TNF-mediated protection against Listeria and responses to LPS. Science **335:**229-232.
199. **Metodiev, K.** 2012. Immunodeficiency.
200. **Michaud, H. A., M. de Mulder, D. Sengupta, S. G. Deeks, J. N. Martin, C. D. Pilcher, F. M. Hecht, J. B. Sacha, and D. F. Nixon.** 2014. Trans-activation, post-transcriptional maturation, and induction of antibodies to HERV-K (HML-2) envelope transmembrane protein in HIV-1 infection. Retrovirology **11:**10.
201. **Miller, M. M., J. E. Fogle, and M. B. Tompkins.** 2013. Infection with feline immunodeficiency virus directly activates CD4+ CD25+ T regulatory cells. J Virol **87:**9373-9378.
202. **Mills, K. H.** 2004. Regulatory T cells: friend or foe in immunity to infection? Nat Rev Immunol **4:**841-855.
203. **Minigo, G., T. Woodberry, K. A. Piera, E. Salwati, E. Tjitra, E. Kenangalem, R. N. Price, C. R. Engwerda, N. M. Anstey, and M. Plebanski.** 2009. Parasite-dependent expansion of TNF receptor II-positive regulatory T cells with enhanced suppressive activity in adults with severe malaria. PLoS Pathog **5:**e1000402.
204. **Moran, A. E., K. L. Holzapfel, Y. Xing, N. R. Cunningham, J. S. Maltzman, J. Punt, and K. A. Hogquist.** 2011. T cell receptor signal strength in Treg and iNKT cell development demonstrated by a novel fluorescent reporter mouse. J Exp Med **208:**1279-1289.
205. **Moreau-Gachelin, F.** 2008. Multi-stage Friend murine erythroleukemia: molecular insights into oncogenic cooperation. Retrovirology **5:**99.
206. **Moreno-Fernandez, M. E., P. Presicce, and C. A. Chougnet.** 2012. Homeostasis and function of regulatory T cells in HIV/SIV infection. J Virol **86:**10262-10269.
207. **Moreno-Fernandez, M. E., C. M. Rueda, L. K. Rusie, and C. A. Chougnet.** 2011. Regulatory T cells control HIV replication in activated T cells through a cAMP-dependent mechanism. Blood **117:**5372-5380.
208. **Morgan, M. E., J. H. van Bilsen, A. M. Bakker, B. Heemskerk, M. W. Schilham, F. C. Hartgers, B. G. Elferink, L. van der Zanden, R. R. de Vries, T. W. Huizinga, T. H. Ottenhoff, and R. E. Toes.** 2005. Expression of FOXP3 mRNA is not confined to CD4+CD25+ T regulatory cells in humans. Hum Immunol **66:**13-20.
209. **Motyka, B., G. Korbutt, M. J. Pinkoski, J. A. Heibein, A. Caputo, M. Hobman, M. Barry, I. Shostak, T. Sawchuk, C. F. Holmes, J. Gauldie, and R. C. Bleackley.** 2000. Mannose 6-phosphate/insulin-like growth factor II receptor is a death receptor for granzyme B during cytotoxic T cell-induced apoptosis. Cell **103:**491-500.
210. **Mucida, D., N. Kutchukhidze, A. Erazo, M. Russo, J. J. Lafaille, and M. A. Curotto de Lafaille.** 2005. Oral tolerance in the absence of naturally occurring Tregs. J Clin Invest **115:**1923-1933.
211. **Murphy, J. T., P. ; Walport, M.** 2008. Janeway's Immunobiology, 7th ed.
212. **Myers, L., J. J. Joedicke, A. B. Carmody, R. J. Messer, G. Kassiotis, J. P. Dudley, U. Dittmer, and K. J. Hasenkrug.** 2013. IL-2-independent and TNF-alpha-dependent expansion of Vbeta5+ natural regulatory T cells during retrovirus infection. J Immunol **190:**5485-5495.
213. **Myers, L., R. J. Messer, A. B. Carmody, and K. J. Hasenkrug.** 2009. Tissue-specific abundance of regulatory T cells correlates with CD8+ T cell dysfunction and chronic retrovirus loads. J Immunol **183:**1636-1643.

214. **Nagar, M., J. Jacob-Hirsch, H. Vernitsky, Y. Berkun, S. Ben-Horin, N. Amariglio, I. Bank, Y. Kloog, G. Rechavi, and I. Goldstein.** 2010. TNF activates a NF-kappaB-regulated cellular program in human CD45RA- regulatory T cells that modulates their suppressive function. J Immunol **184:**3570-3581.
215. **Nair, S. R., G. Zelinskyy, S. Schimmer, N. Gerlach, G. Kassiotis, and U. Dittmer.** 2010. Mechanisms of control of acute Friend virus infection by CD4+ T helper cells and their functional impairment by regulatory T cells. J Gen Virol **91:**440-451.
216. **Nakamura, K., A. Kitani, and W. Strober.** 2001. Cell contact-dependent immunosuppression by CD4(+)CD25(+) regulatory T cells is mediated by cell surface-bound transforming growth factor beta. J Exp Med **194:**629-644.
217. **Nathanson, N. A., R.; Biron, C.A.; Brinton, M.A.; Gonzalez-Scarano, F.; Griffin, D.E.; Holmes, K.V.; Murphy, F.A.; Overbaugh, J.; Richman, D.D.; Robertson, E.S.; Robinson, H.L.** 2007. Viral Pathogenesis and Immunity, vol. 2nd.
218. **Neumann, J.** 2008. Immunbiologie - Eine Einführung. Springer.
219. **Ney, P. A., and A. D. D'Andrea.** 2000. Friend erythroleukemia revisited. Blood **96:**3675-3680.
220. **Ngiow, S. F., M. W. Teng, and M. J. Smyth.** 2011. Prospects for TIM3-Targeted Antitumor Immunotherapy. Cancer Res **71:**6567-6571.
221. **Nie, H., Y. Zheng, R. Li, T. B. Guo, D. He, L. Fang, X. Liu, L. Xiao, X. Chen, B. Wan, Y. E. Chin, and J. Z. Zhang.** 2013. Phosphorylation of FOXP3 controls regulatory T cell function and is inhibited by TNF-alpha in rheumatoid arthritis. Nat Med **19:**322-328.
222. **Nilsson, J., A. Boasso, P. A. Velilla, R. Zhang, M. Vaccari, G. Franchini, G. M. Shearer, J. Andersson, and C. Chougnet.** 2006. HIV-1-driven regulatory T-cell accumulation in lymphoid tissues is associated with disease progression in HIV/AIDS. Blood **108:**3808-3817.
223. **Novembre, F. J., J. de Rosayro, S. Nidtha, S. P. O'Neil, T. R. Gibson, T. Evans-Strickfaden, C. E. Hart, and H. M. McClure.** 2001. Rapid CD4(+) T-cell loss induced by human immunodeficiency virus type 1(NC) in uninfected and previously infected chimpanzees. J Virol **75:**1533-1539.
224. **O'Gorman, W. E., H. Dooms, S. H. Thorne, W. F. Kuswanto, E. F. Simonds, P. O. Krutzik, G. P. Nolan, and A. K. Abbas.** 2009. The initial phase of an immune response functions to activate regulatory T cells. J Immunol **183:**332-339.
225. **O'Neil, S. P., F. J. Novembre, A. B. Hill, C. Suwyn, C. E. Hart, T. Evans-Strickfaden, D. C. Anderson, J. deRosayro, J. G. Herndon, M. Saucier, and H. M. McClure.** 2000. Progressive infection in a subset of HIV-1-positive chimpanzees. J Infect Dis **182:**1051-1062.
226. **Oderup, C., L. Cederbom, A. Makowska, C. M. Cilio, and F. Ivars.** 2006. Cytotoxic T lymphocyte antigen-4-dependent down-modulation of costimulatory molecules on dendritic cells in CD4+ CD25+ regulatory T-cell-mediated suppression. Immunology **118:**240-249.
227. **Okubo, Y., T. Mera, L. Wang, and D. L. Faustman.** 2013. Homogeneous expansion of human T-regulatory cells via tumor necrosis factor receptor 2. Sci Rep **3:**3153.
228. **Ostman, S., C. Rask, A. E. Wold, S. Hultkrantz, and E. Telemo.** 2006. Impaired regulatory T cell function in germ-free mice. Eur J Immunol **36:**2336-2346.
229. **Pacholczyk, R., H. Ignatowicz, P. Kraj, and L. Ignatowicz.** 2006. Origin and T cell receptor diversity of Foxp3+CD4+CD25+ T cells. Immunity **25:**249-259.
230. **Papiernik, M., M. L. de Moraes, C. Pontoux, F. Vasseur, and C. Penit.** 1998. Regulatory CD4 T cells: expression of IL-2R alpha chain, resistance to clonal deletion and IL-2 dependency. Int Immunol **10:**371-378.
231. **Pfeffer, K., T. Matsuyama, T. M. Kundig, A. Wakeham, K. Kishihara, A. Shahinian, K. Wiegmann, P. S. Ohashi, M. Kronke, and T. W. Mak.** 1993. Mice deficient for the 55 kd tumor necrosis factor receptor are resistant to endotoxic shock, yet succumb to L. monocytogenes infection. Cell **73:**457-467.
232. **Pham, C. T., and T. J. Ley.** 1997. The role of granzyme B cluster proteases in cell-mediated cytotoxicity. Semin Immunol **9:**127-133.
233. **Piersma, S. J., J. M. van der Hulst, K. M. Kwappenberg, R. Goedemans, C. E. van der Minne, and S. H. van der Burg.** 2010. Influenza matrix 1-specific human CD4+ FOXP3+ and FOXP3(-) regulatory T cells can be detected long after viral clearance. Eur J Immunol **40:**3064-3074.

234. **Pinkoski, M. J., M. Hobman, J. A. Heibein, K. Tomaselli, F. Li, P. Seth, C. J. Froelich, and R. C. Bleackley.** 1998. Entry and trafficking of granzyme B in target cells during granzyme B-perforin-mediated apoptosis. Blood **92:**1044-1054.
235. **Platt, E. J., M. Bilska, S. L. Kozak, D. Kabat, and D. C. Montefiori.** 2009. Evidence that ecotropic murine leukemia virus contamination in TZM-bl cells does not affect the outcome of neutralizing antibody assays with human immunodeficiency virus type 1. J Virol **83:**8289-8292.
236. **Presicce, P., K. Orsborn, E. King, J. Pratt, C. J. Fichtenbaum, and C. A. Chougnet.** 2011. Frequency of circulating regulatory T cells increases during chronic HIV infection and is largely controlled by highly active antiretroviral therapy. PLoS One **6:**e28118.
237. **Probst, H. C., and M. van den Broek.** 2005. Priming of CTLs by lymphocytic choriomeningitis virus depends on dendritic cells. J Immunol **174:**3920-3924.
238. **Punkosdy, G. A., M. Blain, D. D. Glass, M. M. Lozano, L. O'Mara, J. P. Dudley, R. Ahmed, and E. M. Shevach.** 2011. Regulatory T-cell expansion during chronic viral infection is dependent on endogenous retroviral superantigens. Proc Natl Acad Sci U S A **108:**3677-3682.
239. **Radziewicz, H., R. M. Dunham, and A. Grakoui.** 2009. PD-1 tempers Tregs in chronic HCV infection. J Clin Invest **119:**450-453.
240. **Rauert, H., A. Wicovsky, N. Muller, D. Siegmund, V. Spindler, J. Waschke, C. Kneitz, and H. Wajant.** 2010. Membrane tumor necrosis factor (TNF) induces p100 processing via TNF receptor-2 (TNFR2). J Biol Chem **285:**7394-7404.
241. **Regateiro, F. S., S. P. Cobbold, and H. Waldmann.** 2013. CD73 and adenosine generation in the creation of regulatory microenvironments. Clin Exp Immunol **171:**1-7.
242. **Ren, X., F. Ye, Z. Jiang, Y. Chu, S. Xiong, and Y. Wang.** 2007. Involvement of cellular death in TRAIL/DR5-dependent suppression induced by CD4(+)CD25(+) regulatory T cells. Cell Death Differ **14:**2076-2084.
243. **Ring, S., S. Karakhanova, T. Johnson, A. H. Enk, and K. Mahnke.** 2010. Gap junctions between regulatory T cells and dendritic cells prevent sensitization of CD8(+) T cells. J Allergy Clin Immunol **125:**237-246 e231-237.
244. **Robertson, M. N., M. Miyazawa, S. Mori, B. Caughey, L. H. Evans, S. F. Hayes, and B. Chesebro.** 1991. Production of monoclonal antibodies reactive with a denatured form of the Friend murine leukemia virus gp70 envelope protein: use in a focal infectivity assay, immunohistochemical studies, electron microscopy and western blotting. J Virol Methods **34:**255-271.
245. **Robertson, M. N., G. J. Spangrude, K. Hasenkrug, L. Perry, J. Nishio, K. Wehrly, and B. Chesebro.** 1992. Role and specificity of T-cell subsets in spontaneous recovery from Friend virus-induced leukemia in mice. J Virol **66:**3271-3277.
246. **Robertson, S. J., C. G. Ammann, R. J. Messer, A. B. Carmody, L. Myers, U. Dittmer, S. Nair, N. Gerlach, L. H. Evans, W. A. Cafruny, and K. J. Hasenkrug.** 2008. Suppression of acute anti-friend virus CD8+ T-cell responses by coinfection with lactate dehydrogenase-elevating virus. J Virol **82:**408-418.
247. **Robertson, S. J., and K. J. Hasenkrug.** 2006. The role of virus-induced regulatory T cells in immunopathology. Springer Semin Immunopathol **28:**51-62.
248. **Robertson, S. J., R. J. Messer, A. B. Carmody, and K. J. Hasenkrug.** 2006. In vitro suppression of CD8+ T cell function by Friend virus-induced regulatory T cells. J Immunol **176:**3342-3349.
249. **Roncador, G., P. J. Brown, L. Maestre, S. Hue, J. L. Martinez-Torrecuadrada, K. L. Ling, S. Pratap, C. Toms, B. C. Fox, V. Cerundolo, F. Powrie, and A. H. Banham.** 2005. Analysis of FOXP3 protein expression in human CD4+CD25+ regulatory T cells at the single-cell level. Eur J Immunol **35:**1681-1691.
250. **Ronchetti, S., O. Zollo, S. Bruscoli, M. Agostini, R. Bianchini, G. Nocentini, E. Ayroldi, and C. Riccardi.** 2004. GITR, a member of the TNF receptor superfamily, is costimulatory to mouse T lymphocyte subpopulations. Eur J Immunol **34:**613-622.
251. **Rouse, B. T., P. P. Sarangi, and S. Suvas.** 2006. Regulatory T cells in virus infections. Immunol Rev **212:**272-286.
252. **Ryba, M., N. Marek, L. Hak, K. Rybarczyk-Kapturska, M. Mysliwiec, P. Trzonkowski, and J. Mysliwska.** 2011. Anti-TNF rescue CD4+Foxp3+ regulatory T cells in patients with type 1 diabetes from effects mediated by TNF. Cytokine **55:**353-361.
253. **Sadlack, B., H. Merz, H. Schorle, A. Schimpl, A. C. Feller, and I. Horak.** 1993. Ulcerative colitis-like disease in mice with a disrupted interleukin-2 gene. Cell **75:**253-261.

254. **Sakaguchi, S., N. Sakaguchi, M. Asano, M. Itoh, and M. Toda.** 1995. Immunologic self-tolerance maintained by activated T cells expressing IL-2 receptor alpha-chains (CD25). Breakdown of a single mechanism of self-tolerance causes various autoimmune diseases. J Immunol **155:**1151-1164.
255. **Sakaguchi, S., N. Sakaguchi, J. Shimizu, S. Yamazaki, T. Sakihama, M. Itoh, Y. Kuniyasu, T. Nomura, M. Toda, and T. Takahashi.** 2001. Immunologic tolerance maintained by CD25+ CD4+ regulatory T cells: their common role in controlling autoimmunity, tumor immunity, and transplantation tolerance. Immunol Rev **182:**18-32.
256. **Sakuishi, K., S. F. Ngiow, J. M. Sullivan, M. W. Teng, V. K. Kuchroo, M. J. Smyth, and A. C. Anderson.** 2013. TIM3FOXP3 regulatory T cells are tissue-specific promoters of T-cell dysfunction in cancer. Oncoimmunology **2:**e23849.
257. **Salomon, B., D. J. Lenschow, L. Rhee, N. Ashourian, B. Singh, A. Sharpe, and J. A. Bluestone.** 2000. B7/CD28 costimulation is essential for the homeostasis of the CD4+CD25+ immunoregulatory T cells that control autoimmune diabetes. Immunity **12:**431-440.
258. **Sanchez-Madrid, F., P. Simon, S. Thompson, and T. A. Springer.** 1983. Mapping of antigenic and functional epitopes on the alpha- and beta-subunits of two related mouse glycoproteins involved in cell interactions, LFA-1 and Mac-1. J Exp Med **158:**586-602.
259. **Sarris, M., K. G. Andersen, F. Randow, L. Mayr, and A. G. Betz.** 2008. Neuropilin-1 expression on regulatory T cells enhances their interactions with dendritic cells during antigen recognition. Immunity **28:**402-413.
260. **Schaer, D. A., S. Budhu, C. Liu, C. Bryson, N. Malandro, A. Cohen, H. Zhong, X. Yang, A. N. Houghton, T. Merghoub, and J. D. Wolchok.** 2013. GITR Pathway Activation Abrogates Tumor Immune Suppression Through Loss of Regulatory T cell Lineage Stability. Cancer Immunol Res **1**.
261. **Scheffold, A., J. Huhn, and T. Hofer.** 2005. Regulation of CD4+CD25+ regulatory T cell activity: it takes (IL-)two to tango. Eur J Immunol **35:**1336-1341.
262. **Schepers, K., M. Toebes, G. Sotthewes, F. A. Vyth-Dreese, T. A. Dellemijn, C. J. Melief, F. Ossendorp, and T. N. Schumacher.** 2002. Differential kinetics of antigen-specific CD4+ and CD8+ T cell responses in the regression of retrovirus-induced sarcomas. J Immunol **169:**3191-3199.
263. **Schroder, K., P. J. Hertzog, T. Ravasi, and D. A. Hume.** 2004. Interferon-gamma: an overview of signals, mechanisms and functions. J Leukoc Biol **75:**163-189.
264. **Seddiki, N., B. Santner-Nanan, J. Martinson, J. Zaunders, S. Sasson, A. Landay, M. Solomon, W. Selby, S. I. Alexander, R. Nanan, A. Kelleher, and B. Fazekas de St Groth.** 2006. Expression of interleukin (IL)-2 and IL-7 receptors discriminates between human regulatory and activated T cells. J Exp Med **203:**1693-1700.
265. **SenGupta, D., R. Tandon, R. G. Vieira, L. C. Ndhlovu, R. Lown-Hecht, C. E. Ormsby, L. Loh, R. B. Jones, K. E. Garrison, J. N. Martin, V. A. York, G. Spotts, G. Reyes-Teran, M. A. Ostrowski, F. M. Hecht, S. G. Deeks, and D. F. Nixon.** 2011. Strong human endogenous retrovirus-specific T cell responses are associated with control of HIV-1 in chronic infection. J Virol **85:**6977-6985.
266. **SenGupta, D. R., S.; Michaud, H.; Loh, L.; Tandon, R.; Jones, R.; Garrison, K.; York, V.; Cunha-Neto, E.; Ostrowski, M.; Pilcher, C.; Hecht, F.; Martin, J.; Deeks, S.; Hunt, P.; Nixon, D.** 2013.
267. **Serra, P., A. Amrani, J. Yamanouchi, B. Han, S. Thiessen, T. Utsugi, J. Verdaguer, and P. Santamaria.** 2003. CD40 ligation releases immature dendritic cells from the control of regulatory CD4+CD25+ T cells. Immunity **19:**877-889.
268. **Shein, H. M., and J. F. Enders.** 1962. Transformation induced by simian virus 40 in human renal cell cultures. I. Morphology and growth characteristics. Proc Natl Acad Sci U S A **48:**1164-1172.
269. **Shevach, E. M.** 2002. CD4+ CD25+ suppressor T cells: more questions than answers. Nat Rev Immunol **2:**389-400.
270. **Shevach, E. M.** 2009. Mechanisms of foxp3+ T regulatory cell-mediated suppression. Immunity **30:**636-645.
271. **Shimizu, J., S. Yamazaki, T. Takahashi, Y. Ishida, and S. Sakaguchi.** 2002. Stimulation of CD25(+)CD4(+) regulatory T cells through GITR breaks immunological self-tolerance. Nat Immunol **3:**135-142.

272. **Shimizu, T., H. Uenishi, Y. Teramura, M. Iwashiro, K. Kuribayashi, H. Tamamura, N. Fujii, and H. Yamagishi.** 1994. Fine structure of a virus-encoded helper T-cell epitope expressed on FBL-3 tumor cells. J Virol **68:**7704-7708.
273. **Siggs, O. M., N. Xiao, Y. Wang, H. Shi, W. Tomisato, X. Li, Y. Xia, and B. Beutler.** 2012. iRhom2 is required for the secretion of mouse TNFalpha. Blood **119:**5769-5771.
274. **Simon, M. A., S. J. Brodie, V. G. Sasseville, L. V. Chalifoux, R. C. Desrosiers, and D. J. Ringler.** 1994. Immunopathogenesis of SIVmac. Virus Res **32:**227-251.
275. **Simpson, T. R., S. A. Quezada, and J. P. Allison.** 2010. Regulation of CD4 T cell activation and effector function by inducible costimulator (ICOS). Curr Opin Immunol **22:**326-332.
276. **Sperling, A. I., J. M. Green, R. L. Mosley, P. L. Smith, R. J. DiPaolo, J. R. Klein, J. A. Bluestone, and C. B. Thompson.** 1995. CD43 is a murine T cell costimulatory receptor that functions independently of CD28. J Exp Med **182:**139-146.
277. **Sprent, J., E. K. Gao, and S. R. Webb.** 1990. T cell reactivity to MHC molecules: immunity versus tolerance. Science **248:**1357-1363.
278. **Starborg, M., K. Gell, E. Brundell, and C. Hoog.** 1996. The murine Ki-67 cell proliferation antigen accumulates in the nucleolar and heterochromatic regions of interphase cells and at the periphery of the mitotic chromosomes in a process essential for cell cycle progression. J Cell Sci **109 (Pt 1):**143-153.
279. **Steinmetz, M., K. Minard, S. Horvath, J. McNicholas, J. Srelinger, C. Wake, E. Long, B. Mach, and L. Hood.** 1982. A molecular map of the immune response region from the major histocompatibility complex of the mouse. Nature **300:**35-42.
280. **Stoop, J. N., A. M. Woltman, P. J. Biesta, J. G. Kusters, E. J. Kuipers, H. L. Janssen, and R. G. van der Molen.** 2007. Tumor necrosis factor alpha inhibits the suppressive effect of regulatory T cells on the hepatitis B virus-specific immune response. Hepatology **46:**699-705.
281. **Strauch, U. G., F. Obermeier, N. Grunwald, S. Gurster, N. Dunger, M. Schultz, D. P. Griese, M. Mahler, J. Scholmerich, and H. C. Rath.** 2005. Influence of intestinal bacteria on induction of regulatory T cells: lessons from a transfer model of colitis. Gut **54:**1546-1552.
282. **Strauss, L., C. Bergmann, M. J. Szczepanski, S. Lang, J. M. Kirkwood, and T. L. Whiteside.** 2008. Expression of ICOS on human melanoma-infiltrating CD4+CD25highFoxp3+ T regulatory cells: implications and impact on tumor-mediated immune suppression. J Immunol **180:**2967-2980.
283. **Stromnes, I. M., U. Dittmer, T. N. Schumacher, K. Schepers, R. J. Messer, L. H. Evans, K. E. Peterson, B. Race, and K. J. Hasenkrug.** 2002. Temporal effects of gamma interferon deficiency on the course of Friend retrovirus infection in mice. J Virol **76:**2225-2232.
284. **Sudo, T., S. Nishikawa, N. Ohno, N. Akiyama, M. Tamakoshi, and H. Yoshida.** 1993. Expression and function of the interleukin 7 receptor in murine lymphocytes. Proc Natl Acad Sci U S A **90:**9125-9129.
285. **Sugimoto, K., F. Ikeda, J. Stadanlick, F. A. Nunes, H. J. Alter, and K. M. Chang.** 2003. Suppression of HCV-specific T cells without differential hierarchy demonstrated ex vivo in persistent HCV infection. Hepatology **38:**1437-1448.
286. **Sugimoto, N., T. Oida, K. Hirota, K. Nakamura, T. Nomura, T. Uchiyama, and S. Sakaguchi.** 2006. Foxp3-dependent and -independent molecules specific for CD25+CD4+ natural regulatory T cells revealed by DNA microarray analysis. Int Immunol **18:**1197-1209.
287. **Sun, C. M., J. A. Hall, R. B. Blank, N. Bouladoux, M. Oukka, J. R. Mora, and Y. Belkaid.** 2007. Small intestine lamina propria dendritic cells promote de novo generation of Foxp3 T reg cells via retinoic acid. J Exp Med **204:**1775-1785.
288. **Sun, L., J. Wu, F. Du, X. Chen, and Z. J. Chen.** 2013. Cyclic GMP-AMP synthase is a cytosolic DNA sensor that activates the type I interferon pathway. Science **339:**786-791.
289. **Sutkowski, N., B. Conrad, D. A. Thorley-Lawson, and B. T. Huber.** 2001. Epstein-Barr virus transactivates the human endogenous retrovirus HERV-K18 that encodes a superantigen. Immunity **15:**579-589.
290. **Suvas, S., A. K. Azkur, B. S. Kim, U. Kumaraguru, and B. T. Rouse.** 2004. CD4+CD25+ regulatory T cells control the severity of viral immunoinflammatory lesions. J Immunol **172:**4123-4132.

291. **Suvas, S., U. Kumaraguru, C. D. Pack, S. Lee, and B. T. Rouse.** 2003. CD4+CD25+ T cells regulate virus-specific primary and memory CD8+ T cell responses. J Exp Med **198:**889-901.
292. **Suzuki, H., G. S. Duncan, H. Takimoto, and T. W. Mak.** 1997. Abnormal development of intestinal intraepithelial lymphocytes and peripheral natural killer cells in mice lacking the IL-2 receptor beta chain. J Exp Med **185:**499-505.
293. **Swain, S. L., K. K. McKinstry, and T. M. Strutt.** 2012. Expanding roles for CD4(+) T cells in immunity to viruses. Nat Rev Immunol **12:**136-148.
294. **Tai, A. K., M. Lin, F. Chang, G. Chen, F. Hsiao, N. Sutkowski, and B. T. Huber.** 2006. Murine Vbeta3+ and Vbeta7+ T cell subsets are specific targets for the HERV-K18 Env superantigen. J Immunol **177:**3178-3184.
295. **Tai, A. K., J. Luka, D. Ablashi, and B. T. Huber.** 2009. HHV-6A infection induces expression of HERV-K18-encoded superantigen. J Clin Virol **46:**47-48.
296. **Tandon, R., D. SenGupta, L. C. Ndhlovu, R. G. Vieira, R. B. Jones, V. A. York, V. A. Vieira, E. R. Sharp, A. A. Wiznia, M. A. Ostrowski, M. G. Rosenberg, and D. F. Nixon.** 2011. Identification of human endogenous retrovirus-specific T cell responses in vertically HIV-1-infected subjects. J Virol **85:**11526-11531.
297. **Taylor, A. L., and M. J. Llewelyn.** 2010. Superantigen-induced proliferation of human CD4+CD25- T cells is followed by a switch to a functional regulatory phenotype. J Immunol **185:**6591-6598.
298. **Thoma, B., M. Grell, K. Pfizenmaier, and P. Scheurich.** 1990. Identification of a 60-kD tumor necrosis factor (TNF) receptor as the major signal transducing component in TNF responses. J Exp Med **172:**1019-1023.
299. **Thomas, H. E., J. A. Trapani, and T. W. Kay.** 2010. The role of perforin and granzymes in diabetes. Cell Death Differ **17:**577-585.
300. **Thompson, L. F., H. K. Eltzschig, J. C. Ibla, C. J. Van De Wiele, R. Resta, J. C. Morote-Garcia, and S. P. Colgan.** 2004. Crucial role for ecto-5'-nucleotidase (CD73) in vascular leakage during hypoxia. J Exp Med **200:**1395-1405.
301. **Thornton, A. M., P. E. Korty, D. Q. Tran, E. A. Wohlfert, P. E. Murray, Y. Belkaid, and E. M. Shevach.** 2010. Expression of Helios, an Ikaros transcription factor family member, differentiates thymic-derived from peripherally induced Foxp3+ T regulatory cells. J Immunol **184:**3433-3441.
302. **Tomonari, K.** 1997. Viral Superantigens. CRC Press LLC.
303. **Tone, M., Y. Tone, E. Adams, S. F. Yates, M. R. Frewin, S. P. Cobbold, and H. Waldmann.** 2003. Mouse glucocorticoid-induced tumor necrosis factor receptor ligand is costimulatory for T cells. Proc Natl Acad Sci U S A **100:**15059-15064.
304. **Torheim, E. A., L. C. Ndhlovu, F. O. Pettersen, T. L. Larsen, A. R. Jha, K. M. Torgersen, D. Kvale, D. F. Nixon, K. Tasken, and E. M. Aandahl.** 2009. Interleukin-10-secreting T cells define a suppressive subset within the HIV-1-specific T-cell population. Eur J Immunol **39:**1280-1287.
305. **Toth, I., A. Q. Le, P. Hartjen, A. Thomssen, V. Matzat, C. Lehmann, C. Scheurich, C. Beisel, P. Busch, O. Degen, A. W. Lohse, T. Eiermann, G. Fatkenheuer, D. Meyer-Olson, M. Bockhorn, J. Hauber, J. van Lunzen, and J. Schulze Zur Wiesch.** 2013. Decreased frequency of CD73+CD8+ T cells of HIV-infected patients correlates with immune activation and T cell exhaustion. J Leukoc Biol **94:**551-561.
306. **Trowbridge, I. S., J. Lesley, R. Schulte, R. Hyman, and J. Trotter.** 1982. Biochemical characterization and cellular distribution of a polymorphic, murine cell-surface glycoprotein expressed on lymphoid tissues. Immunogenetics **15:**299-312.
307. **Turcanova, V. L., B. Bundgaard, and P. Hollsberg.** 2009. Human herpesvirus-6B induces expression of the human endogenous retrovirus K18-encoded superantigen. J Clin Virol **46:**15-19.
308. **Valencia, X., G. Stephens, R. Goldbach-Mansky, M. Wilson, E. M. Shevach, and P. E. Lipsky.** 2006. TNF downmodulates the function of human CD4+CD25hi T-regulatory cells. Blood **108:**253-261.
309. **Verhagen, J., and D. C. Wraith.** 2010. Comment on "Expression of Helios, an Ikaros transcription factor family member, differentiates thymic-derived from peripherally induced Foxp3+ T regulatory cells". J Immunol **185:**7129; author reply 7130.
310. **Vignali, D. A., L. W. Collison, and C. J. Workman.** 2008. How regulatory T cells work. Nat Rev Immunol **8:**523-532.

311. **Voehringer, D., C. Blaser, P. Brawand, D. H. Raulet, T. Hanke, and H. Pircher.** 2001. Viral infections induce abundant numbers of senescent CD8 T cells. J Immunol **167:**4838-4843.
312. **Voehringer, D., M. Koschella, and H. Pircher.** 2002. Lack of proliferative capacity of human effector and memory T cells expressing killer cell lectinlike receptor G1 (KLRG1). Blood **100:**3698-3702.
313. **Wajant, H., K. Pfizenmaier, and P. Scheurich.** 2003. Tumor necrosis factor signaling. Cell Death Differ **10:**45-65.
314. **Wakamatsu, E., D. Mathis, and C. Benoist.** 2013. Convergent and divergent effects of costimulatory molecules in conventional and regulatory CD4+ T cells. Proc Natl Acad Sci U S A **110:**1023-1028.
315. **Walker, M. R., D. J. Kasprowicz, V. H. Gersuk, A. Benard, M. Van Landeghen, J. H. Buckner, and S. F. Ziegler.** 2003. Induction of FoxP3 and acquisition of T regulatory activity by stimulated human CD4+CD25- T cells. J Clin Invest **112:**1437-1443.
316. **Wammes, L. J., A. E. Wiria, C. G. Toenhake, F. Hamid, K. Y. Liu, H. Suryani, M. M. Kaisar, J. J. Verweij, E. Sartono, T. Supali, H. H. Smits, A. J. Luty, and M. Yazdanbakhsh.** 2013. Asymptomatic plasmodial infection is associated with increased tumor necrosis factor receptor II-expressing regulatory T cells and suppressed type 2 immune responses. J Infect Dis **207:**1590-1599.
317. **Wang, H. Y., D. A. Lee, G. Peng, Z. Guo, Y. Li, Y. Kiniwa, E. M. Shevach, and R. F. Wang.** 2004. Tumor-specific human CD4+ regulatory T cells and their ligands: implications for immunotherapy. Immunity **20:**107-118.
318. **Waring, P., and A. Mullbacher.** 1999. Cell death induced by the Fas/Fas ligand pathway and its role in pathology. Immunol Cell Biol **77:**312-317.
319. **Wei, W. Z., G. P. Morris, and Y. C. Kong.** 2004. Anti-tumor immunity and autoimmunity: a balancing act of regulatory T cells. Cancer Immunol Immunother **53:**73-78.
320. **Weiss, J. M., A. M. Bilate, M. Gobert, Y. Ding, M. A. Curotto de Lafaille, C. N. Parkhurst, H. Xiong, J. Dolpady, A. B. Frey, M. G. Ruocco, Y. Yang, S. Floess, J. Huehn, S. Oh, M. O. Li, R. E. Niec, A. Y. Rudensky, M. L. Dustin, D. R. Littman, and J. J. Lafaille.** 2012. Neuropilin 1 is expressed on thymus-derived natural regulatory T cells, but not mucosa-generated induced Foxp3+ T reg cells. J Exp Med **209:**1723-1742, S1721.
321. **Weiss, L., V. Donkova-Petrini, L. Caccavelli, M. Balbo, C. Carbonneil, and Y. Levy.** 2004. Human immunodeficiency virus-driven expansion of CD4+CD25+ regulatory T cells, which suppress HIV-specific CD4 T-cell responses in HIV-infected patients. Blood **104:**3249-3256.
322. **Wildin, R. S., F. Ramsdell, J. Peake, F. Faravelli, J. L. Casanova, N. Buist, E. Levy-Lahad, M. Mazzella, O. Goulet, L. Perroni, F. D. Bricarelli, G. Byrne, M. McEuen, S. Proll, M. Appleby, and M. E. Brunkow.** 2001. X-linked neonatal diabetes mellitus, enteropathy and endocrinopathy syndrome is the human equivalent of mouse scurfy. Nat Genet **27:**18-20.
323. **Willerford, D. M., J. Chen, J. A. Ferry, L. Davidson, A. Ma, and F. W. Alt.** 1995. Interleukin-2 receptor alpha chain regulates the size and content of the peripheral lymphoid compartment. Immunity **3:**521-530.
324. **Woodland, D. L., and M. A. Blackman.** 1993. How do T-cell receptors, MHC molecules and superantigens get together? Immunol Today **14:**208-212.
325. **Woodland, D. L., and M. A. Blackman.** 1992. Retroviral super-antigens and T cells. Int Rev Immunol **8:**311-325.
326. **Woodland, D. L., M. P. Happ, K. J. Gollob, and E. Palmer.** 1991. An endogenous retrovirus mediating deletion of alpha beta T cells? Nature **349:**529-530.
327. **Woodland, D. L., R. Wen, and M. A. Blackman.** 1997. Why do superantigens care about peptides? Immunol Today **18:**18-22.
328. **Workman, C. J., and D. A. Vignali.** 2003. The CD4-related molecule, LAG-3 (CD223), regulates the expansion of activated T cells. Eur J Immunol **33:**970-979.
329. **Workman, C. J., and D. A. Vignali.** 2005. Negative regulation of T cell homeostasis by lymphocyte activation gene-3 (CD223). J Immunol **174:**688-695.
330. **Wu, L., and V. N. KewalRamani.** 2006. Dendritic-cell interactions with HIV: infection and viral dissemination. Nat Rev Immunol **6:**859-868.
331. **Yadav, M., C. Louvet, D. Davini, J. M. Gardner, M. Martinez-Llordella, S. Bailey-Bucktrout, B. A. Anthony, F. M. Sverdrup, R. Head, D. J. Kuster, P. Ruminski, D.**

Weiss, D. Von Schack, and J. A. Bluestone. 2012. Neuropilin-1 distinguishes natural and inducible regulatory T cells among regulatory T cell subsets in vivo. J Exp Med **209:**1713-1722, S1711-1719.

332. **Yadav, M., S. Stephan, and J. A. Bluestone.** 2013. Peripherally induced tregs - role in immune homeostasis and autoimmunity. Front Immunol **4:**232.
333. **Yamaguchi, S., M. Hasegawa, T. Suzuki, H. Ikeda, S. Aizawa, K. Hirokawa, and M. Kitagawa.** 2003. In vivo distribution of receptor for ecotropic murine leukemia virus and binding of envelope protein of Friend Murine leukemia virus. Arch Virol **148:**1175-1184.
334. **Yegutkin, G. G., F. Marttila-Ichihara, M. Karikoski, J. Niemela, J. P. Laurila, K. Elima, S. Jalkanen, and M. Salmi.** 2011. Altered purinergic signaling in CD73-deficient mice inhibits tumor progression. Eur J Immunol **41:**1231-1241.
335. **Yokoyama, W. M., F. Koning, P. J. Kehn, G. M. Pereira, G. Stingl, J. E. Coligan, and E. M. Shevach.** 1988. Characterization of a cell surface-expressed disulfide-linked dimer involved in murine T cell activation. J Immunol **141:**369-376.
336. **Young, G. R., M. J. Ploquin, U. Eksmond, M. Wadwa, J. P. Stoye, and G. Kassiotis.** 2012. Negative selection by an endogenous retrovirus promotes a higher-avidity CD4+ T cell response to retroviral infection. PLoS Pathog **8:**e1002709.
337. **Zamoyska, R.** 2006. Superantigens: supersignalers? Sci STKE **2006:**pe45.
338. **Zelinskyy, G., S. Balkow, S. Schimmer, T. Werner, M. M. Simon, and U. Dittmer.** 2007. The level of friend retrovirus replication determines the cytolytic pathway of CD8+ T-cell-mediated pathogen control. J Virol **81:**11881-11890.
339. **Zelinskyy, G., K. Dietze, T. Sparwasser, and U. Dittmer.** 2009. Regulatory T cells suppress antiviral immune responses and increase viral loads during acute infection with a lymphotropic retrovirus. PLoS Pathog **5:**e1000406.
340. **Zelinskyy, G., K. K. Dietze, Y. P. Husecken, S. Schimmer, S. Nair, T. Werner, K. Gibbert, O. Kershaw, A. D. Gruber, T. Sparwasser, and U. Dittmer.** 2009. The regulatory T-cell response during acute retroviral infection is locally defined and controls the magnitude and duration of the virus-specific cytotoxic T-cell response. Blood **114:**3199-3207.
341. **Zelinskyy, G., A. R. Kraft, S. Schimmer, T. Arndt, and U. Dittmer.** 2006. Kinetics of CD8+ effector T cell responses and induced CD4+ regulatory T cell responses during Friend retrovirus infection. Eur J Immunol **36:**2658-2670.
342. **Zelinskyy, G., S. J. Robertson, S. Schimmer, R. J. Messer, K. J. Hasenkrug, and U. Dittmer.** 2005. CD8+ T-cell dysfunction due to cytolytic granule deficiency in persistent Friend retrovirus infection. J Virol **79:**10619-10626.
343. **Zhou, Q., M. E. Munger, S. L. Highfill, J. Tolar, B. J. Weigel, M. Riddle, A. H. Sharpe, D. A. Vallera, M. Azuma, B. L. Levine, C. H. June, W. J. Murphy, D. H. Munn, and B. R. Blazar.** 2010. Program death-1 signaling and regulatory T cells collaborate to resist the function of adoptively transferred cytotoxic T lymphocytes in advanced acute myeloid leukemia. Blood **116:**2484-2493.
344. **Zhou, X., X. Zhi, P. Zhou, S. Chen, F. Zhao, Z. Shao, Z. Ou, and L. Yin.** 2007. Effects of ecto-5'-nucleotidase on human breast cancer cell growth in vitro and in vivo. Oncol Rep **17:**1341-1346.
345. **Ziegler, S. F.** 2006. FOXP3: of mice and men. Annu Rev Immunol **24:**209-226.

9. Appendix

9.1 List of Abbreviations

A	
α	Anti
AB	Antibody
ADP	Adenosine diphosphate
AEC	3-amino-9-ethylcarbazole
AF	Alexa Flour
AICD	Activation-induced cell death
AIDS	Acquired immunodeficiency syndrome
AMP	Adenosine monophosphate
AMPCP	Adenosine 5'-(α,β-methylene)diphosphate
ANOVA	Analysis of variance between groups
APC	Allophycocyanin
APC	Antigen presenting cell
ATP	Adenosine triphosphate
B	
β-ME	β-mercaptoethanol
B6	C57BL/6
BFA	Brefeldin A
BLT	Bone marrow-liver-thymus
BrdU	Bromodeoxyuridine
BSA	Bovine serum albumin
BV	Brilliant Violet
C	
°C	Celsius
CA	Capsid
cAMP	Cyclic adenosine diphosphate
CCR5	C-C chemokine receptor type 5
CD	Cluster of differentiation
cGAS	Cyclic-guanosine monophosphate-adenosine monophosphate synthase
CLIP	Class II-associated invariant chain peptide
CO	Colorado
CO_2	Carbon dioxide
compTNFα	Complexed tumour necrosis factor α
CTL	Cytotoxic $CD8^+$ T cell
CTLA-4	Cytotoxic T lymphocyte antigen-4
CXCR4	C-X-C chemokine receptor type 4
Cy	Cyanine
D	
DC	Dendritic Cell
ddADA	2',5'-DiDeoxyadenosine
DEREG	Depletion of Regulatory T cells
DMEM	Dulbecco´s modified Eagle medium

DMSO	Dimethylsulfoxid
DNA	Deoxyribonucleic acid
dpi	Days post infection
DR5	Death receptor 5
dsDNA	Double-stranded deoxyribonucleic acid
dsRNA	Double-stranded ribonucleic acid
DT	Diphtheria toxin
E	
EDTA	Ethylendiaminetetraacetic acid
eF	eFlour
ELISA	Enzyme-linked immunosorbent assay
ENTPD1	Ectonucleotide triphosphate diphosphohydrolase
Env	Envelope
ERV	Endogenous retroviruses
F	
FACS	Fluorescence-activated cell sorting
FC	Fragment, crystallisable
FCS	Foetal calve serum
FELASA	Federation of European Laboratory Animal Science Association
FELASA	European Laboratory Animal Science Association
FITC	Fluorescein isothiocyanate
F-MuLV	Friend murine leukaemia virus
Foxp3	Forkhead box protein 3
FSC	Forward scatter
Fv	Friend virus susceptibility factors
FV	Friend virus complex
FVD	Fixable viability dye
G	
g	g-force
g	Gramm
G phase	Gap phase
Gag	Group-specific antigen
GALT	Gastro-intestinal associated lymphoid tissue
GFP	Green fluorescent protein
GITR	Glucocorticoid-induced tumour necrosis factor receptor family related gene
GmbH	Gemeinschaft mit beschränkter Haftung
GM-CSF	Granulocyte macrophage colony-stimulating factor
gp	Glycoprotein
GVHD	Graft-versus-host disease
GV-SOLAS	German regulations of the Society for Laboratory Animal Science
Gzm	Granzyme
H	
H_2O	Water
H_2O_2	Hydrogen peroxide
HAART	Highly active antiretroviral therapy
HCV	Hepatitis C virus
HEPES	4-(2-hydroxyethyl)-1-piperazineethanesulfonic acid

HERV	Human endogenous retroviruses
HIV-1	Human immunodeficiency virus-I
HLA-DR	Human leukocyte antigen-DR
hr	Human recombinant
HRP	Horse reddish peroxidase
HSV	Herpes simplex virus
I	
i.p.	Intra peritoneal
i.v.	Intra venous
IC assay	Infectious centre assay
ICER	Inducible cAMP early repressor
ICOS	TCR-inducible co-stimulatory receptor
icTNFα	Intracellular tumour necrosis factor α
IDO	Indolamine 2,3-dioxygenase
IFN	Interferon
Ig	Immunoglobulin
iGFP	Interdomain green fluorescent protein
IL	Interleukin
IL	Illinois
IL2R	IL2 receptor
IN	Integrase
IPEX	Immune dysregulation, polyendocrinopathy, enteropathy, X-linked syndrome
IRB	Institutional Review Board
iTreg	Induced regulatory T cell
K	
kDa	Kilo Dalton
KLRG1	Killer cell lectin-like receptor G1
KO	Knockout
L	
L	Litre
Lag3	Lymphocyte-activation gene 3
LANUV	North Rhine-Westphalia State Agency for Nature, Environment and Consumer Protection
Laser	Light amplification by stimulated emission of radiation
LD Blue	Live/Dead Blue
LDV	Lactate dehydrogenase elevating virus
LTR	Long terminal repeats
Luc	Luciferase
M	
µg	Micrograms
µL	Microlitre
µM	Micromolar
M	Molar
M phase	Mitosis
m^2	Square metres
MA	Matrix
MA	Massachusetts
MAb	Monoclonal antibody

mac	Macaque
Mac1	Macrophage-1 antigen
MACS	Magnetic assisted cell sorting
mbTNFα	Membrane-bound tumour necrosis factor α
mCAT-1	Cationic amino acid transporter
MDA-5	Melanoma Differentiation-Associated protein 5
mg	Milligrams
$MgCl_2$	Magnesium chloride
MHC	Major histocompatibility complex
min	Minutes
MIP	Macrophage inflammatory protein
mL	Millilitres
MLV	Murine leukaemia virus
mM	Milimolar
MMTV	Mouse mammary tumour virus
MN	Maine
MoDC	Monocyte derived dendritic cells
mr	Mouse recombinant
mRNA	Messenger ribonucleic acid
MTA	Material transfer agreement
mtv	Endogenous mouse mammary tumour virus
mu	Murine
MuLV	Murine leukaemia virus
MW	Molecular weight
N	
NaN_3	Sodium azide
NC	Nucleocapsid
NFAT	Nuclear factor of activated T cells
NF-κB	Nuclear factor κB
ng	Nanogramm
NIH	National Institute of Health
NK	Natural killer cell
NKT	Natural T killer cell
nm	Nanometres
Nrp1	Neuropilin 1
ns	Not significant
nt5e	Ecto-5’ nucleotidase
nTreg	Natural regulatory T cell
O	
OH	Ohio
ORF	Open reading frame
P	
p	Plasmid
Pacblue	Pacific Blue
PAMP	Pathogen associated molecular pattern
PBMC	Peripheral blood mononuclear cells
PBMC	Peripheral blood mononuclear cells

pbs	Primer binding site
PBS	Phosphate buffered saline
PCR	Polymerase chain reaction
PD-1	Programmed death 1
pDC	Plasmacytoid DC
PD-L1	Programmed death ligand 1
PE	Phycoerythrin
PenStrep	Penicillin-streptomycin
PerCP	Peridinin-chlorophyll
pH	Potentia Hydrogenii
PhD	Doctor of Philosophy
PIC	Pre-integration complex
PMT	Photomultiplier tube
Pol	Polymerase
ppt	Polypurine tract
PR	Protease
PRR	Pattern recognition receptor
R	
R	Repeated region or short terminal repeats
Rag	Recombination-activating gene
RANTES	Regulation on activation, normal T expressed and secreted
rER	Rough endoplasmic reticulum
Retrovirus	Reverse transcriptase oncovirus
RIG-I	Retinoic acid-inducible gene I
RNA	Ribonucleic acid
RSV	Respiratory syncytial virus
RT	Reverse transcriptase
RTC	Reverse transcription complex
S	
S phase	Synthesis
Sag	Superantigen
sc	Single chain
SEM	Standard error of the mean
SFFU	Spleen focus forming units
SFFV	Spleen focus forming virus
SIV	Simian immunodeficiency virus
solTNFα	Soluble tumour necrosis factor α
spi-1	Spleen focus forming virus proviral integration site-1
SSC	Side scatter
ssRNA	Single-stranded ribonucleic acid
SU	Surface glycoprotein
T	
TACE	Tumour necrosis factor α convertase
TAP	Transporter associated with antigen processing
Tcon	Conventional $CD4^+$ T cells
TCR	T cell receptor
Tfh	T follicular helper cell
tg or TG	Transgene

TGFβ	Transforming growth factor β
Th	Helper T cell
TIM3	T cell immunoglobulin domain and mucin domain 3
TLR	Toll-like receptor
TM	Transmembrane glycoprotein
TM	Trade mark
TNC	Tenascin-C
TNFR	Tumour necrosis factor receptor
TNFRSF	Tumour necrosis factor receptor superfamily
TNFα	Tumour necrosis factor α
TRAIL	Tumour-necrosis-factor-related-apoptosis-inducing ligand
Tregs	Regulatory T cells
tRNA	Transfer ribonucleic acid
U	
U3/5	Unique 3'/5'
UK	United Kingdom
USA	United States of America
UV	Ultra violet
V	
VLP	Virus like particle
VSVg	Vesicular stomatitis virus g
W	
wt or WT	Wild type
X	
X-gal	5-bromo-4-chloro-3-indolyl-β-D-galactopyranoside
XLAAD	X-linked autoimmunity-allergic dysregulation syndrome

9.2 Figure list

9.3 Table list

9.4 List of publications

1. **Interferon-alpha subtype 11 activates NK cells and enables control of retroviral infection.** Gibbert K, **Joedicke JJ**, Meryk A, Trilling M, Francois S, Duppach J, Kraft A, Lang KS, Dittmer U. PLoS Pathog. 2012;8(8):e1002868. doi: 10.1371/journal.ppat.1002868. Epub 2012 Aug 9.

2. **IL-2-Independent and TNF-α-Dependent Expansion of Vβ5+ Natural Regulatory T Cells during Retrovirus Infection.** Myers L, **Joedicke JJ**, Carmody AB, Messer RJ, Kassiotis G, Dudley JP, Dittmer U, Hasenkrug KJ. J Immunol. J Immunol. 2013 Jun 1;190(11):5485-95. doi: 10.4049/jimmunol.1202951. Epub 2013 May 3.

3. **The phenotype and activation status of regulatory T cells during Friend retrovirus infection. Joedicke JJ**, Dietze KK, Zelinskyy G, Dittmer U. Virol Sin. 2014 Feb;29(1):48-60. doi: 10.1007/s12250-014-3396-z. Epub 2014 Jan 20.

4. **$CD8^+$ T cells are essential for controlling acute FV infection in B6 mice. Joedicke JJ**, Zelinskyy G, Dittmer U, Hasenkrug KJ. Comment on "Elimination of Friend Retrovirus in the Absence of $CD8^+$ T cells" Tsuji-Kawahara S, Miyazawa M. J Virol. 2014 Feb;88(3):1854-5. doi: 10.1128/JVI.03271-13. Epub 2013 Nov 13. Submitted

5. **Regulatory T cells control transmission of HIV from dendritic cells to conventional $CD4^+$ T cells.** Moreno-Fernandez ME, **Joedicke JJ**, Chougnet CA. Accepted.

6. **Expanded regulatory T cells in chronically Friend retrovirus infected mice influence the outcome of a primary mCMV infection.** Duppach J, Francois S, Gibbert K, **Joedicke JJ**, Dittmer U, Kraft ARM. Submitted.

7. **Activated $CD8^+$ T cells induce expansion of $V\beta5^+$ regulatory T cells via TNFR2 signaling. Joedicke JJ**, Myers L, Carmody AB, Messer RJ, Wajant H, Lang KS, Lang PA, Mak TW, Hasenkrug KJ, Dittmer U. Submitted.

9.5 Acknowledgements

First and foremost I want to thank Prof. Dr. Ulf Dittmer who made it possible for me to conduct my PhD work in his group at the Institute for Virology. I want to thank him for his guidance throughout all the years and I am grateful for the stimulating conversations we had. Also, I want to thank him for letting me peruse my work in a guided but independent way, which has helped to shape my scientific abilities.

I want to thank all the members of the Institute for Virology for their help and guidance with challenging aspects of my work. Notably, I want to thank everyone in the group of Prof. Dr. Ulf Dittmer, present and past members (Kathrin, Kirsten, Gennadiy, Wibke, Nora, Ilseyar, Inga, Elisabeth, Gosia, Simone, Sonja, Tanja, Sandra).

I am thankful for the DFG stipend provided, which enabled me to conduct my work and has helped me to share my data at scientific conferences. Also, I want to thank all the people in the graduate school (GRK1045) for the stimulating discussions and good times we had. I especially want to thank Daniela Catrini, who became a good friend and was always able to help with different work related issues.

I especially want to thank Kathrin Gibbert, who helped me a lot in the first months (and years) of my PhD work, providing scientific and personal advice as well as help in the lab. She has become a good friend.

I want to thank my friends Anne and Julia for the good times in Essen and an open ear when times were difficult. Furthermore, I want to thank Anni, Martin, Jana and Frieda for the great times we had that made me forget about all the stress.

I want to thank my parents who have always believed in me and made it possible for me to pursue my ambitions to work in academia. They taught me to fight for my dreams.

Last but not least, I want to thank my boyfriend Darren who has helped me through the tough times of my PhD, with lots of good personal and scientific advice. I want to thank him for being immensely supportive.

9.6 Curriculum vitae

Der Lebenslauf ist in der Online-Version aus Gründen des Datenschutzes nicht enthalten.

9.7 Erklärungen

Erklärung:

Hiermit erkläre ich, gem. § 6 Abs. 2, f der Promotionsordnung der Math.-Nat. Fakultäten zur Erlangung der Dr. rer. nat., dass ich das Arbeitsgebiet, dem das Thema **„Titel der Dissertation“** zuzuordnen ist, in Forschung und Lehre vertrete und den Antrag von Jara Johanna Joedicke befürworte.

Essen, den _____ _____

Prof. Dr. Ulf Dittmer

Erklärung:

Hiermit erkläre ich, gem. § 7 Abs. 2, c und e der Promotionsordnung der Math.-Nat. Fakultäten zur Erlangung des Dr. rer. nat., dass ich die vorliegende Dissertation selbständig verfasst und mich keiner anderen als der angegebenen Hilfsmittel bedient habe und alle wörtlich oder inhaltlich übernommenen Stellen als solche gekennzeichnet habe.

Essen, den _____ _____

Jara Johanna Joedicke

Erklärung:

Hiermit erkläre ich, gem. § 7 Abs. 2, d und f der Promotionsordnung der Math.-Nat. Fakultäten zur Erlangung des Dr. rer. nat., dass ich keine anderen Promotionen bzw. Promotionsversuche in der Vergangenheit durchgeführt habe, dass diese Arbeit von keiner anderen Fakultät abgelehnt worden ist, und dass ich die Dissertation nur in diesem Verfahren einreiche.

Essen, den _____ _____

Jara Johanna Joedicke